Earth-Abundant Transition Metal-Catalyzed Electro-Reductive Cross-Electrophile Coupling Reactions and C–H Activation by Cobaltaelectro-Catalysis

Dissertation

for the award of the degree

"Doctor rerum naturalium" (Dr.rer.nat.)

of the Georg-August-Universität Göttingen

within the doctoral program of chemistry

of the Georg-August-Universität School of Science (GAUSS)

Submitted by

Nate Woon Jie Ang

From Singapore

Göttingen, 2021

Thesis Committee

Prof. Dr. Lutz Ackermann, Institute of Organic and Biomolecular Chemistry

Prof. Dr. Shoubhik Das, ORSY Division, Department of Chemistry, Universiteit Antwerpen, Antwerpen, Belgium.

Members of the Examination Board

Reviewer: Prof. Dr. Lutz Ackermann, Institute of Organic and Biomolecular Chemistry, Göttingen

Second Reviewer: Prof. Dr. Shoubhik Das, ORSY Division, Department of Chemistry, Universiteit Antwerpen, Antwerpen, Belgium.

Further members of the Examination Board

Prof. Dr. Dr. h.c.mult. Lutz F. Tietze, Institute of Organic and Biomolecular Chemistry, Göttingen

Prof. Dr. Dietmar Stalke, Institute of Inorganic Chemistry, Göttingen

Dr. Holm Frauendorf, Institute of Organic and Biomolecular Chemistry, Göttingen

Dr. Michael John, Institute of Organic and Biomolecular Chemistry, Göttingen

Date of the Oral Examination: 29.11.2021

Table of Contents

List of Abbreviations

Ac	acetyl
Alk	alkyl
AMLA	ambiphilic metal-ligand activation
AQ	8-aminoquinoline
aq.	aqueous
Ar	aryl
atm	atmospheric pressure
BDEs	bond dissociation energies
BIES	base-assisted internal electrophilic substitution
BINAP	2,2'-bis(diphenylphosphino)-1,1'-binaphthyl
BIPHEP	2,2'-bis(diphenylphosphino)biphenyl
Bn	benzyl
bpy	2,2'-bipyridyl
BQ	1,4-benzoquinone
Bu	butyl
Bz	benzoyl
calc.	calculated
cat.	catalytic
CCE	constant current electrolysis
CCU	carbon capture and utilization
CDC	cross-dehydrogenative coupling
CMD	concerted-metalation-deprotonation
cod	1,5-cyclooctadiene
coe	cyclooctene
conv.	conversion
Cp	cyclopentadienyl
CPE	constant potential electrolysis
Cp*	1,2,3,4,5-pentamethylcyclopenta-1,3-diene
Cy	cyclohexyl
δ	chemical shift
d	doublet
DBN	1,5-diazabicyclo*[4.3.0]*non-5-ene
DBU	1,8-diazabicyclo*[5.4.0]*undec-7-ene
DCE	1,2-dichloroethane
DCIB	dichloro-*iso*-butane

dd	doublet of doublet
DFT	density functional theory
DG	directing group
DME	dimethoxyethane
DMA	*N*,*N*-dimethylacetamide
DMF	*N*,*N*-dimethylformamide
DMI	1,3-dimethyl-2-imidazolidinone
DMPU	1,3-dimethyltetrahydropyrimidin-2(*1H*)-one
DMSO	dimethylsulfoxide
dppBz	1,2-bis(diphenylphosphino)benzene
dppe	1,2-bis(diphenylphosphino)ethane
dppf	1,1'-bis(diphenylphosphino)ferrocene
dppp	1,3-bis(diphenylphosphino)propane
dt	doublet of triplet
d*t*bpy	4,4'-di-*tert*-butyl-2,2'-bipyridine
EI	electron ionization
equiv.	equivalent
ES	electrophilic substitution
ESI	electrospray ionization
Et	ethyl
FG	functional group
g	gram
GC	gas chromatography
GVL	*γ*-valerolactone
h	hour
Hal	halogen
Het	heteroatom
Hept	heptyl
Hex	hexyl
HFIP	1,1,1,3,3,3-hexafluoro-2-propanol
HMDS	hexamethyldisilazane
HMPA	hexamethylphosphoramide
HPLC	high performance liquid chromatography
HR-MS	high resolution mass spectrometry
Hz	Hertz
i	*iso*
IPr▪HCl	1,3-bis-(2,6-diisopropylphenyl) imidazolinium chloride

IR	infrared spectroscopy
IES	internal electrophilic substitution
J	coupling constant
KIE	kinetic isotope effect
L	ligand
m	*meta*
m	multiplet
M	molar
$[M]^+$	molecular ion peak
MALDI	matrix-assisted laser desorption/ionisation
Me	methyl
Mes	mesityl
mg	milligram
MHz	megahertz
min	minute
mL	milliliter
MLCT	metal-ligand charge transfer
mmol	millimole
M.p.	melting point
MPV	membrane pump vacuum
MS	mass spectrometry
m/z	mass-to-charge ratio
NBE	norbornene
NHC	*N*-heterocyclic carbene
NMP	*N*-methylpyrrolidinone
NMR	nuclear magnetic resonance
n.r.	no reaction
o	*ortho*
OPV	oil pump vacuum
p	*para*
PAHs	*polycyclic aromatic hydrocarbons*
Ph	phenyl
Phen	1,10-phenanthroline
PIP	2-(pyridin-2-yl)-*iso*-propyl
Piv	pivaloyl
PPI	proton pump inhibitor
ppm	parts per million

Pr	propyl
Py	pyridyl
Pym	pyrimidine
PyO	2-aminopyridine 1-oxide
q	quartet
Q	quinoline
r.t.	room temperature
s	singlet
sat.	saturated
SCE	saturated calomel electrode
SET	single electron transfer
SPO	secondary phosphine oxides
SPS	solvent purification system
SSRI	selective serotonin reuptake inhibitor
t	*tert*
t	triplet
T	temperature
TBAA	tetrabutylammonium acetate
TBAB	tetrabutylammonium bromide
TBAI	tetrabutylammonium iodide
TBHP	*tert*-butyl hydroperoxide
TEMPO	2,2,6,6-Tetramethylpiperidine-1-oxyl
Tf	triflate
TFE	2,2,2-trifluoroethanol
THF	tetrahydrofuran
TIPS	triisopropylsilyl
TM	transition metal
TMA	tetramethylammonium
TMEDA	*N,N,N',N'*-tetramethylethane-1,2-diamine
TMS	trimethylsilyl
TOF	time-of-flight
Ts	*para*-toluenesulfonyl
TS	transition state

1. Introduction

In the last three decades, worldwide issues such as global warming and depletion of natural resources have prompted scientists from all fields to redirect their focus on developing greener and more sustainable methods for industrial productions. This has indeed influenced a great number of efforts on revolutionizing the way synthetic organic chemistry is conducted. The goal to create novel, sustainable and practical synthetic protocols to improve, *inter alia*, synthetic utility and minimizing chemical waste have been in the hearts of many chemists. Thus, 12 guiding principles of green chemistry[1] were suggested in 1988 by Paul T. Anastas and John C. Warner as the most fundamental code for chemist striving to reduce the amount of detrimental environmental and health impact of chemical production. Organic chemistry arguably represents a vital role for the bottom-up assembly and late-stage diversification of molecular compounds with life-changing applications to such as, *inter alia*, drug development[2] and crop protection.[3] Hence, there is a great desire to introduce and discover greener synthetic methods right from the micro-stage to elevate the quality of chemical research for further utilization.

1.1 Transition Metal-Catalyzed Cross-Coupling Reactions

In the most recent decades, transition metal-catalyzed cross-coupling reactions[4] have dominated the field of synthetic organic chemistry, as they are highly versatile and widely used due to their simplicity. Such developments awed chemists and scientists alike which were exemplified by the award of the Nobel Prize in Chemistry in 2010 to Richard F. Heck, Ei-ichi Negishi and Akira Suzuki.[5] Precious transition metal, such as palladium, was used predominantly in these advancements and the reaction protocols were named, e.g. Mizoroki–Heck,[6] Kumada–Corriu,[7] Sonogashira–Hagihara,[8] Negishi,[9] Migita–Stille,[10] Suzuki–Miyaura[11] and Hiyama[12] coupling reactions (**Figure 1.1.1a**). These established cross-coupling methods for the C–C bond formation have been acknowledged by a variety of applications to material sciences, pharmaceuticals and chemical industries.[13] In relation to these considerable advances,

immense efforts were also directed to the formation of C–Het bonds, since they exist in countless natural products and drug molecular scaffolds. They are namely, Ullman–Goldberg,[14] Buchwald–Hartwig[15] and Chan–Evans–Lam[16] reactions (**Figure 1.1.1b**). Since the 1900s, the first report of the synthesis of symmetrical biaryls using stoichiometric amount of copper by Ullman and co-worker led to a series of discovery that aided the research on the C–Het bond formation.[17] These pioneering works by Ullman, Hurtley and Goldberg paved significant impact in cross-coupling reactions, particularly copper-mediated protocols.[14]

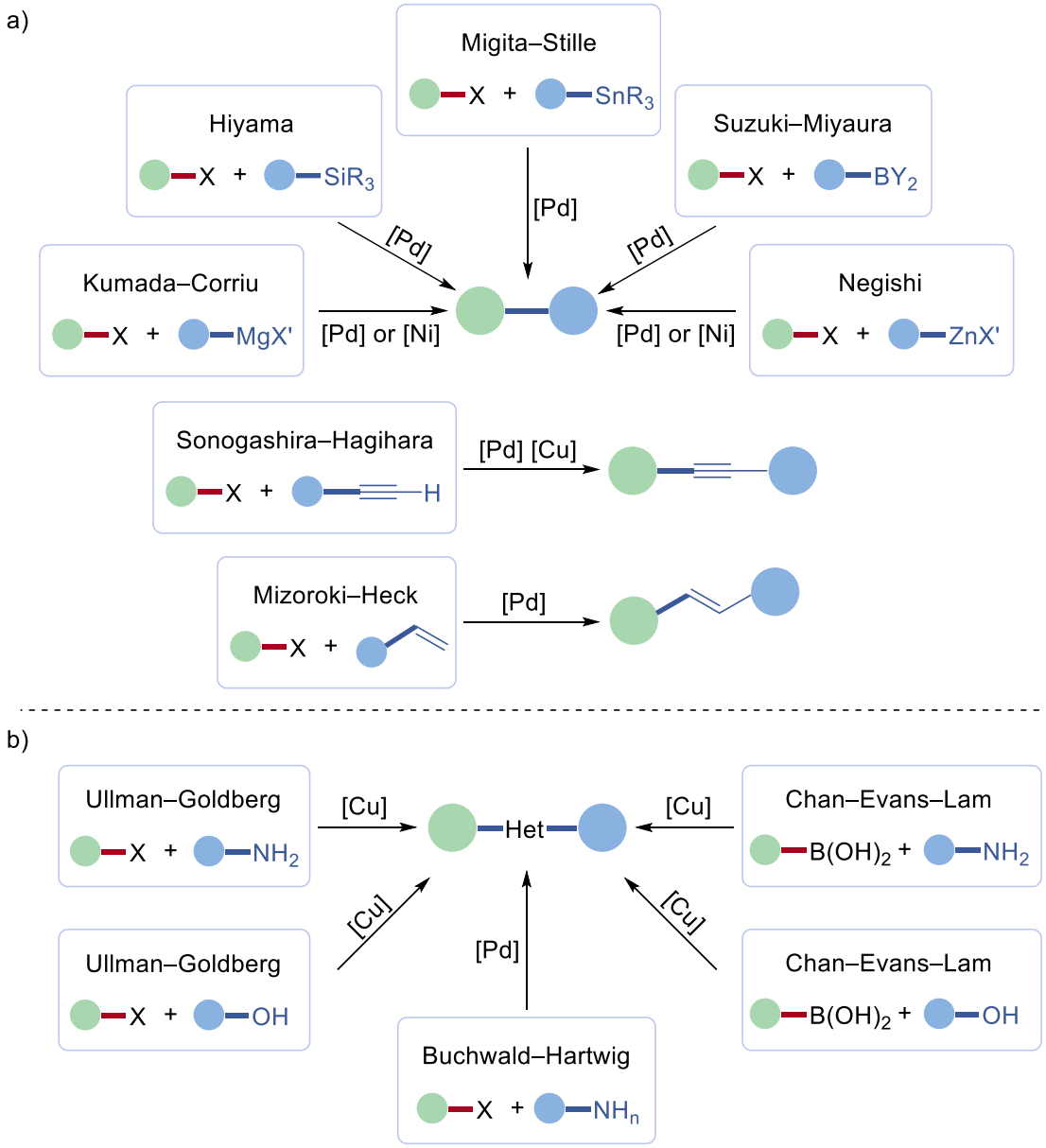

Figure 1.1.1. Transition metal-catalyzed cross-coupling reactions.

The majority of traditional palladium-catalyzed cross-coupling reactions follow a generally accepted reaction mechanism (**Figure 1.1.2**). First an oxidative addition of the electrophile occurs onto the active palladium(0) catalyst **I** forming a palladium(II) complex **II**. Second, transmetallation of the organometallic reagent or nucleophile leads to the formation of the palladium(II) intermediate **III** bearing both substrate fragments. Finally, reductive elimination of the intermediate **III** gives rise to the cross-coupled product and to the regeneration of the active palladium(0) catalyst **I**.

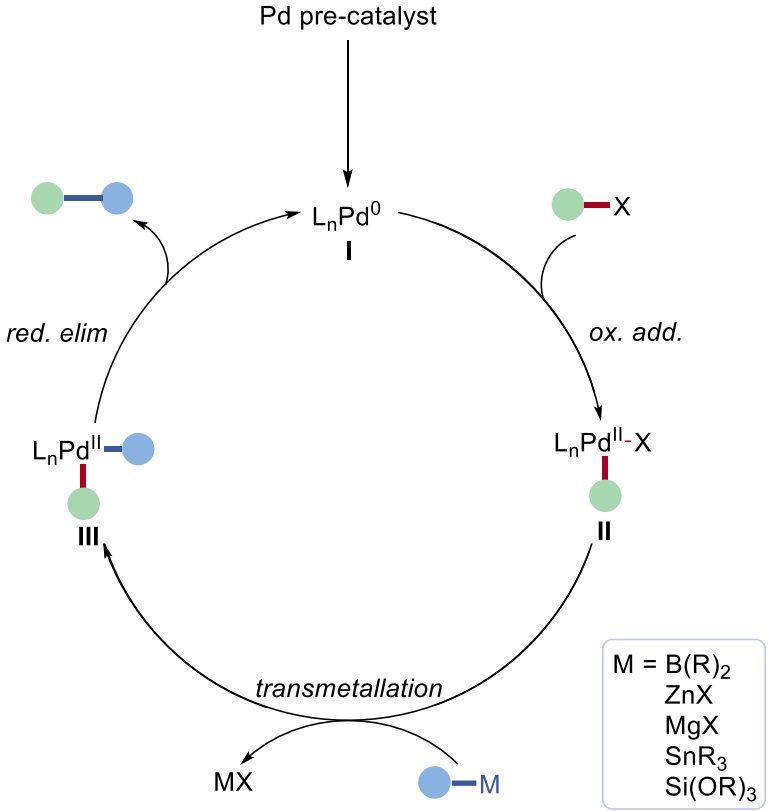

Figure 1.1.2. Traditional palladium-catalyzed cross-coupling reaction mechanism.

Despite all the significant advances in traditional cross-coupling reactions, the major intrinsic drawbacks in association with the reagents involved in these transformations highly compromises their usage in the modern scientific world. This includes the need to pre-functionalize the starting materials, such as organo(pseudo)halides and organometallic coupling partners, e.g. Grignard reagents, organolithium, organostannanes and organozinc compounds. The latter are highly air- and moisture-sensitive reagents, which require multiple step synthesis, that only those who are trained can perform.[18] Notwithstanding, these procedures often produce

stoichiometric amounts of often toxic metallic by-products, which cause chemical waste and hazardous environmental pollution.

1.2 Transition Metal-Catalyzed C–H Activation

Since the impeccable evolution of synthetic organic chemistry with the aid of transition metal-catalyzed cross-coupling reactions (**Figure 1.2.1a**), there is a substantial desire to introduce more atom- and step-economical processes that require lesser pre-functionalization and to minimise the formation of unwanted by-products.[19] Therefore, transition metal-catalyzed site-selective C–H functionalization transformations[20] are extensively more resource economical by a large margin, since pre-functionalization of C–C and C–Het bonds are skipped.[21]

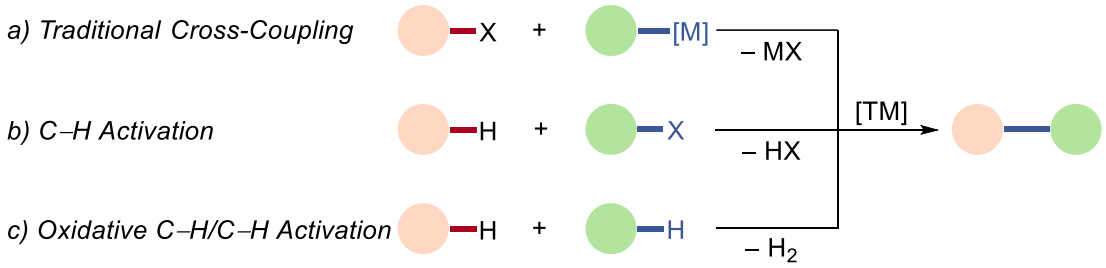

Figure 1.2.1. Contrast between conventional cross-coupling reaction with contemporary oxidative C–H activation and dual oxidative C–H/C–H activation reactions.

Most commonly adopted C–H activation reactions would require one pre-functionalized substrate, as the electrophile typically contain halogen as organic halide or a phenol derivative, which are widely available through industrial synthetical protocols (**Figure 1.2.1b**).[22] The use of direct C–H functionalization eliminates the necessity to use expensive and toxic chemical oxidants, which would otherwise be needed to realize the perfect dual oxidative C–H/C–H activation reactions. Two-fold oxidative C–H activation is one of the most environmentally sustainable mode of reaction (**Figure 1.2.1c**), since molecular hydrogen gas is formed as the sole by-product of the synthesis regime, which is primarily attractive even though costly silver and copper salts are usually employed to facilitate the formation of the product.[23]

The extensive growth of utilizing C–H activation as a sustainable method to achieve shorter synthetic route with little environmental impact relies mainly on the elucidation of its reaction mechanism. Generally, the reaction catalytic cycle (**Figure 1.2.2**) can be described concisely as four elementary steps, first (i) C–H activation of the substrate molecule, second (ii) functionalization of organometallic intermediate, third (iii) reductive elimination of the desired product and lastly (iv) regeneration of the active catalyst.

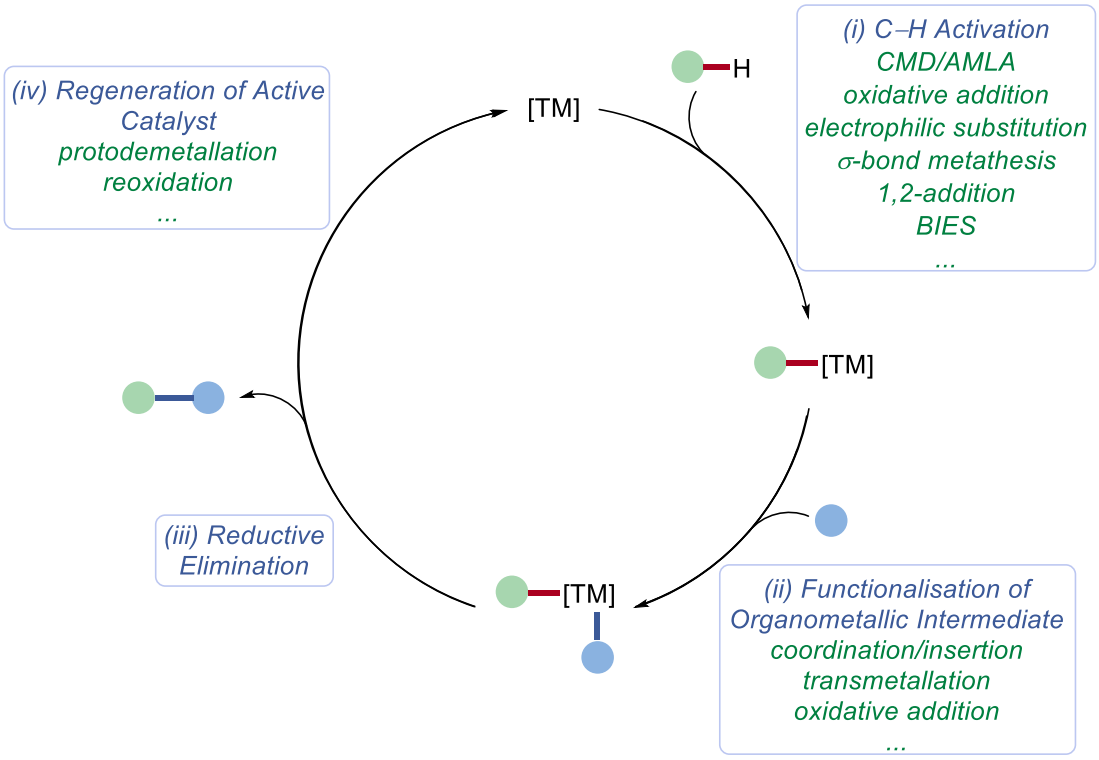

Figure 1.2.2. General catalytic cycle for transition metal-catalyzed C–H activation reactions.

Vast resources have been placed in these studies and a couple of distinctive features on the key C–H activation step were mechanistically identified. The nature of the metal catalyst used and its electronics should also be considered but in general, five main modes of action were proposed.[22c] These excludes examining outer-sphere/radical-type mechanism.[24] Electron-rich late transition metals with low oxidation states frequently adhere to oxidative addition of the C–H bond to the metal centre (**Figure 1.2.3a**).[25] This is not the case for late transition metals with higher oxidation states, as they are more susceptible for electrophilic substitution *via* electrophilic attack of the transition metal center to the carbon (**Figure 1.2.3b**).[26]

a) Oxidative Addition

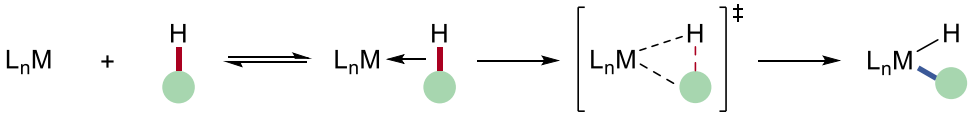

b) Electrophilic Substitution

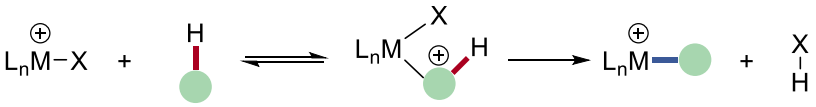

c) σ–Bond Metathesis

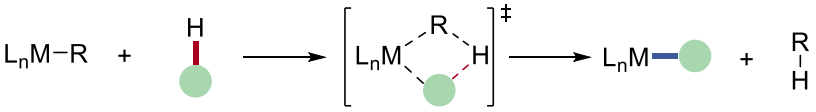

d) 1,2-Addition

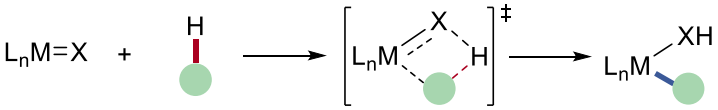

e) Base-assisted Metalation

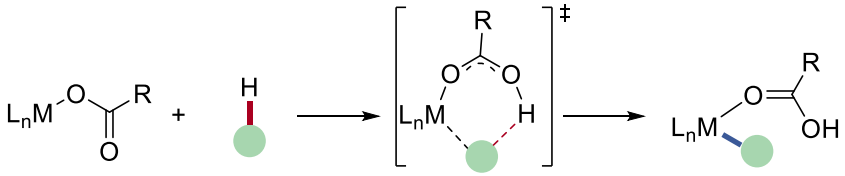

Figure 1.2.3. Mechanistic pathways for the C–H activation step.

Early transition metals, as well as lanthanides and actinides which are difficult to change oxidation states commonly react through σ-bond metathesis (**Figure 1.2.3c**).[27] Complexes with unsaturated M=X bonds, such as group IV metal imido complexes usually undergo 1,2-addition of the C–H bond (**Figure 1.2.3d**).[28] A base-assisted C–H activation process has also been proposed, wherein the cleavage of the C–H bond, as well as the formation of C–M bond occurs almost simultaneously (**Figure 1.2.3e**).[29] The event is known to occur through an electrophilic attack of the metal and deprotonation by carboxylate or carbonate ligands, this is especially prominent in ruthenium-carboxylate complexes.[22c, 30]

More recently, base-assisted C–H activation mechanism has thoroughly unravelled to detail the importance of an internal base for the C–H cleavage step. Within the class

of base-assisted C–H metalation, multiple distinct mechanistic scenarios have been further classified. As a result, four distinctive types of transition states have been mainly described (**Figure 1.2.4**). The first being the concerted metalation-deprotonation (CMD)[31] or ambiphilic metal-ligand activation (AMLA).[32] This proceeds with metalation and deprotonation through a six-membered ring transition state. These are usually found in electron-deficient substrates with significant kinetic C–H acidity. While the last type, base-assisted internal electrophilic substitution (BIES) mechanism proceeds in similar manner *via* an electrophilic substitution-like pathway, but leans more towards electron-rich acetates or carboxylates ligands.[33]

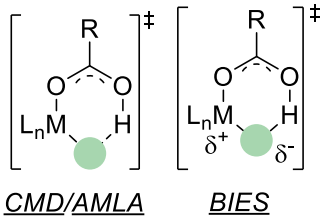

Figure 1.2.4. Transition state models for the C–H cleavage step in base-assisted C–H metalation.

As one of the most step-economical synthesis methods for organic synthesis, C–H activation offers a large avenue of possibilities for greener and more sustainable approach to chemical synthesis. However, its use has been impeded by the abundance of ubiquitous and ambiguous C–H bonds that exist in every organic molecule.[34] Moreover, it is further complicated by similar bond dissociation energies (BDEs) of C–H bonds.[35] The effective discrimination between the C–H bonds is vital for a selective functionalization. Hence, a large part of research is to utilize C–H activation while tackling this challenge. A few strategies have been established that can be employed to circumvent the issue with site selectivity (**Figure 1.2.5**). First, through inherent electronic bias of the chosen substrates, by targeting the lowest pKa or the most acidic C–H provides an efficient way to control site-selectivity (**Figure 1.2.5a**).[22f, 36] The second method (**Figure 1.2.5b**) would be manipulating the steric bias using bulky substituents to effectively block the space adjacent to the C–H bond of interest.

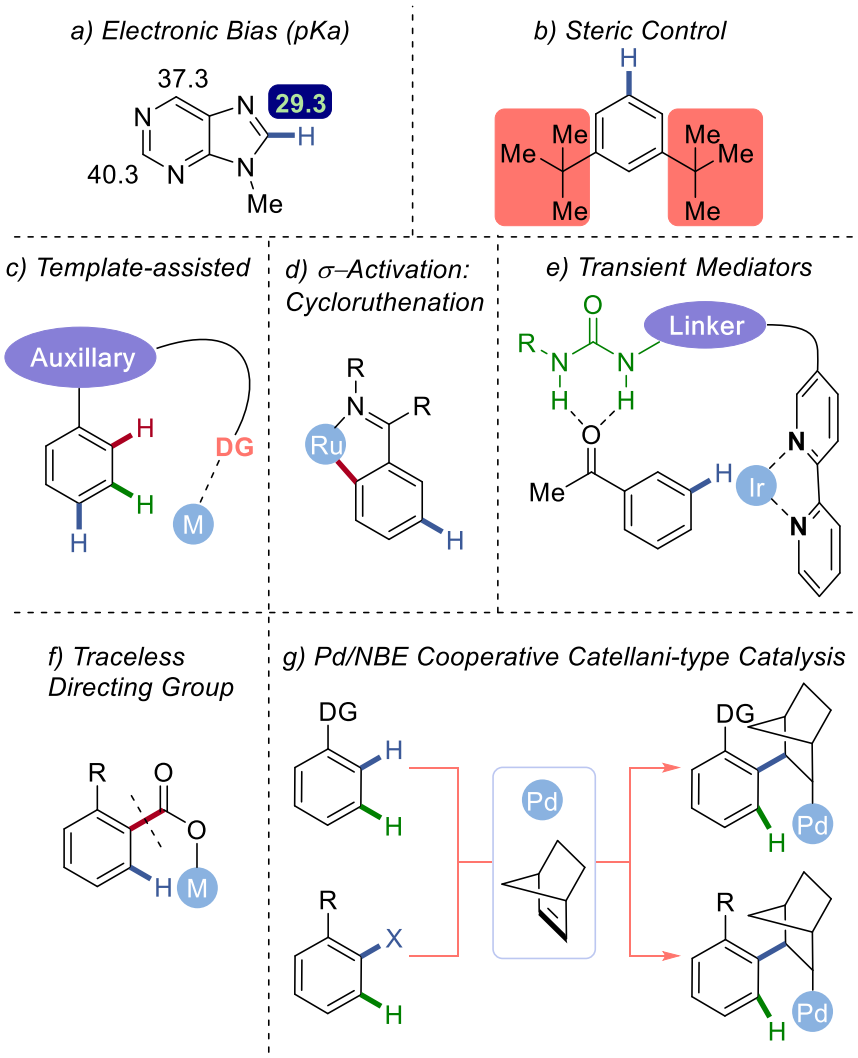

Figure 1.2.5. Several unique strategies for site-selective C–H activation.

It is worth noting that both approaches are inherently limited in terms of applications since they require a specific substrate in order to achieve particular results. This leads to heavily diminished substrate scope and its general applicability. An invested and highly robust approach is the use of directing-groups to control the site selectivity based on the Lewis basic substituents, that binds to the metal centre for facile C–H metalation (**Figure 1.2.5c**).[37] This greatly enhances its usability for a wide range of transformations, restricting the formation of possible side products. Cycloruthenation used specifically with ruthenium catalyst creates an opportunity for σ-activation which provides remote *meta*-selective C–H activation (**Figure 1.2.5d**). This exploits the influence of the electronic properties from the *ortho*-bonded ruthenacycle to the aromatic ring.[35g, 37a] Another particular method is the use of reversible transient

directing group that is bonded with external ligand *in situ* upon catalytic reaction. It coordinates to the metal centre during the reaction, which releases after site-selective C–H activation (**Figure 1.2.5e**).[35e] Traceless directing group, such as carboxylic acid, allows chelation of the metal centre for *meta*-C–H activation and can be removed subsequently after the reaction (**Figure 1.2.5f**). [35h, 38] The merger of norbornene with palladium catalysis creates an avenue for remote *meta*-selective C–H activation by first achieving the *ortho*-C–H activation with norbornene, and then subsequently prompt the adjacent C–H bond in the *meta* position to undergo C–H activation as well (**Figure 1.2.5g**).[35a]

1.3 Cobalt-Catalyzed C–H Activation

One of the Earth-abundant 3d transition metals — cobalt — has gained notable momentum as the transition metal of choice for selective C–H activation reactions.[21b] Due to its relative abundance in the Earth crust and low toxicity, the beginning of its use has propelled vast amount of research on cobalt-catalyzed protocols instead of depending on precious metals such as palladium, rhodium or iridium which are highly expensive and toxic. A myriad of industrial applications have utilized cobalt complexes as their main catalyst since the 1930s, and these include the Fischer–Tropsch process whereby a cobalt complex [$CoH(CO)_4$] was used in the hydrocarbonylation of ethylene to give propanal.[39] Then, cobalt(II) salts were also found to be catalytically feasible for the synthesis of biphenyls from homocoupling reactions of phenylmagnesium bromides.[40] Several years later into the late 1940s, vitamin B_{12} was isolated for the first time, which is essential in biocatalytic processes, such as dehalogenation and methylation transformations in living organisms.[41] Cobalt catalysts have also been found to be extremely versatile and efficient for transformations of π-bond containing substrates, for instances alkynes, allenes or alkenes and this is showcased in various cycloaddition reactions,[42] the Pauson–Khand reaction[43] and the Nicholas reaction.[44] Moreover, cobalt catalysts displayed remarkable catalytic reactivity for cross-coupling reactions that could serve as an alternative to expensive precious metal catalysts.[45]

Regardless, there is a surge on the number of studies that focuses on novel and greener approaches employing cobalt catalytically, such as the aforementioned oxidative C–H activation reaction. Even though progresses in C–H activation started in the last few decades, they were highly limited to precious metals.[24a, 35g, 46] The developments with more sustainable and Earth-abundant 3d metals, such as cobalt were scarce. The nascent report by Kharasch which shed light to the ensuing vast expansion of cobalt-mediated domain in C–H activation reactions illustrating the capability of cobalt catalysis beyond conventional limitations.[40] Needless to say, cobalt-catalyzed C–H activation have tremendously improved and enhanced site-selective C–H transformations, such as annulation reactions, which will be examined into detail in the following section. Broader discussions on cobalt-catalyzed C–H activation developments have been reviewed more comprehensively in reviews articles by Ackermann,[47] Yoshikai,[48] Matsunaga,[49] Ribas[50] and Chatani,[51] among others[52].

1.3.1 Oxidative Cobalt-Catalyzed C–H/N–H Alkyne or Allene Annulations

Oxidative annulation reactions are particularly attractive as cycloaddition reactions provide a wide array of molecules that could be useful in pharmaceuticals and drug developments. In 2014, Daugulis reported the oxidative C–H/N–H annulation reaction of benzamides **1** catalyzed by inexpensive cobalt(II) salts with alkynes **2** (**Figure 1.3.1.1a**).[53] A commonly used directing group, 8-aminoquinoline served as an extra stabiliser for the high-valent cobalt(III) intermediate for the successful annulation to take place. The optimisation of the reaction found that oxygen in the air in conjunction with the use of stoichiometric amount of metal oxidants, such as $Mn(OAc)_2$, efficiently provided the annulated product **3**. Super stoichiometric amounts of carboxylate additives,[22c] like NaOPiv, were reported to be necessary for the C–H/N–H annulation to occur. In addition, the authors were able to synthesize a cyclometalated cobalt(III) complex intermediate **4** with which they were able to prove that it is indeed catalytically involved in the C–H metalation step for the annulation reaction (**Figure 1.3.1.1b**). A plausible reaction pathway of a cobalt(II)/(III)/(I) catalytic manifold

was proposed, based on their first mechanistic investigations (**Figure 1.3.1.1c**). First, an oxidative C–H activation of the benzamide **1** with $Co(OAc)_2$ salt occurs to give the cyclometalated cobalt(III) complex **5**. Second, the insertion of the alkyne **2** to form a seven-membered ring complex intermediate **6**. Last, reductive elimination of the intermediate **6** to generate the desired product **3** and the reduced cobalt(I) complex **7**. Yet, no further studies were performed with regards to the generation of active cobalt(III) species, the nature of the oxidation or the mechanism of the C–H activation step.

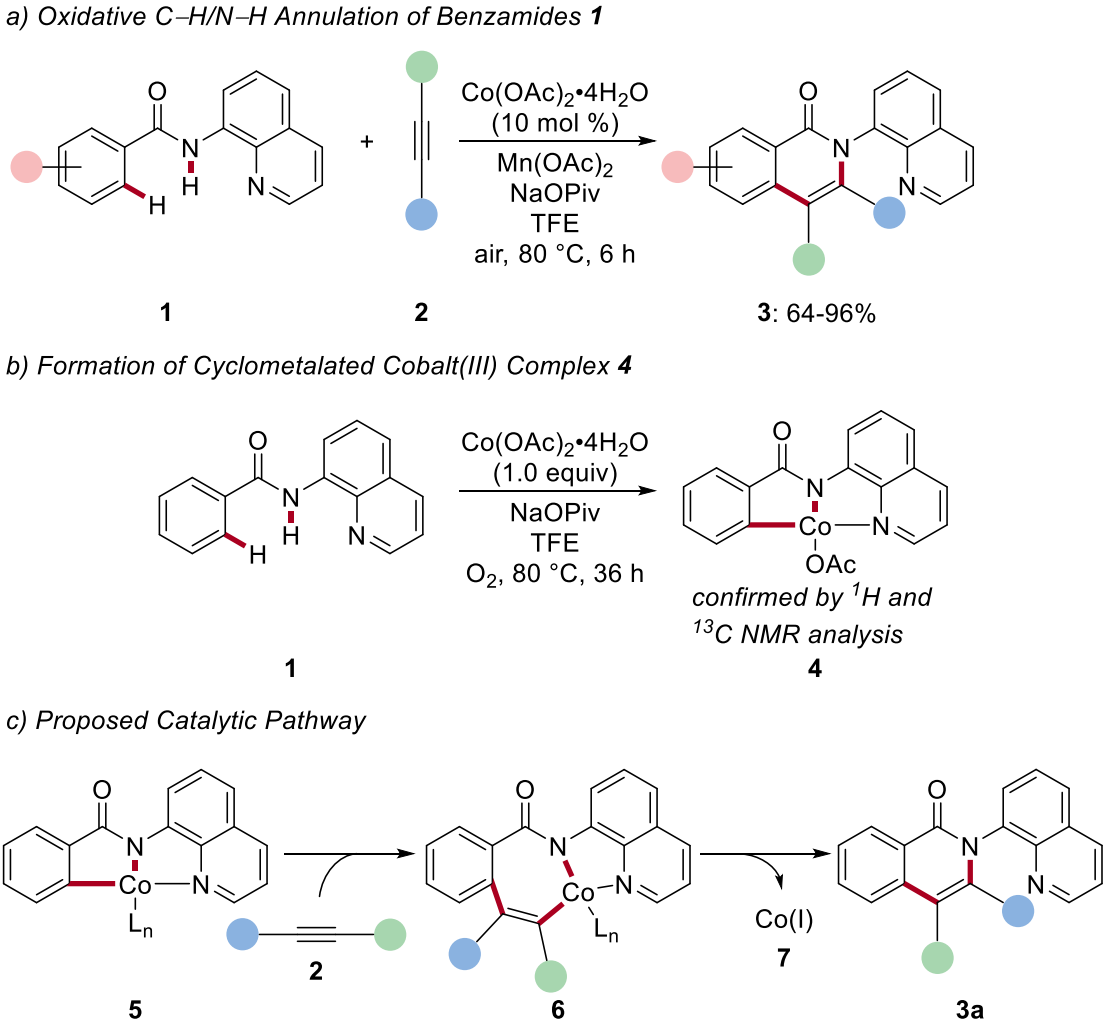

Figure 1.3.1.1. Cobalt-catalyzed C–H/N–H annulation of alkynes **2** with benzamides **1**.

Since the initial success of Daugulis, there have been a myriad of oxidative C–H/N–H annulation reactions with various substrates throughout the years, which demonstrated the catalytic power of cobalt salts for similar transformation.[47a, 50, 54] This is especially the case for cobalt-catalyzed C–H/N–H annulation reactions with alkynes and allenes which will be further focused upon.[52c, 55] Despite of the major impact of the work of

Daugulis in 2014, stoichiometric amounts of metal oxidants were required, which significantly diminished the usability. On the contrary, Ackermann later developed the aerobic cobalt-catalyzed C–H annulation with alkynes for the synthesis of pharmaceutically relevant isoquinolones **9** (**Figure 1.3.1.2a**).[56] This method showcases 2-pyridyl-*N*-oxide as a bidentate directing group with oxygen as the sole oxidant.[57]

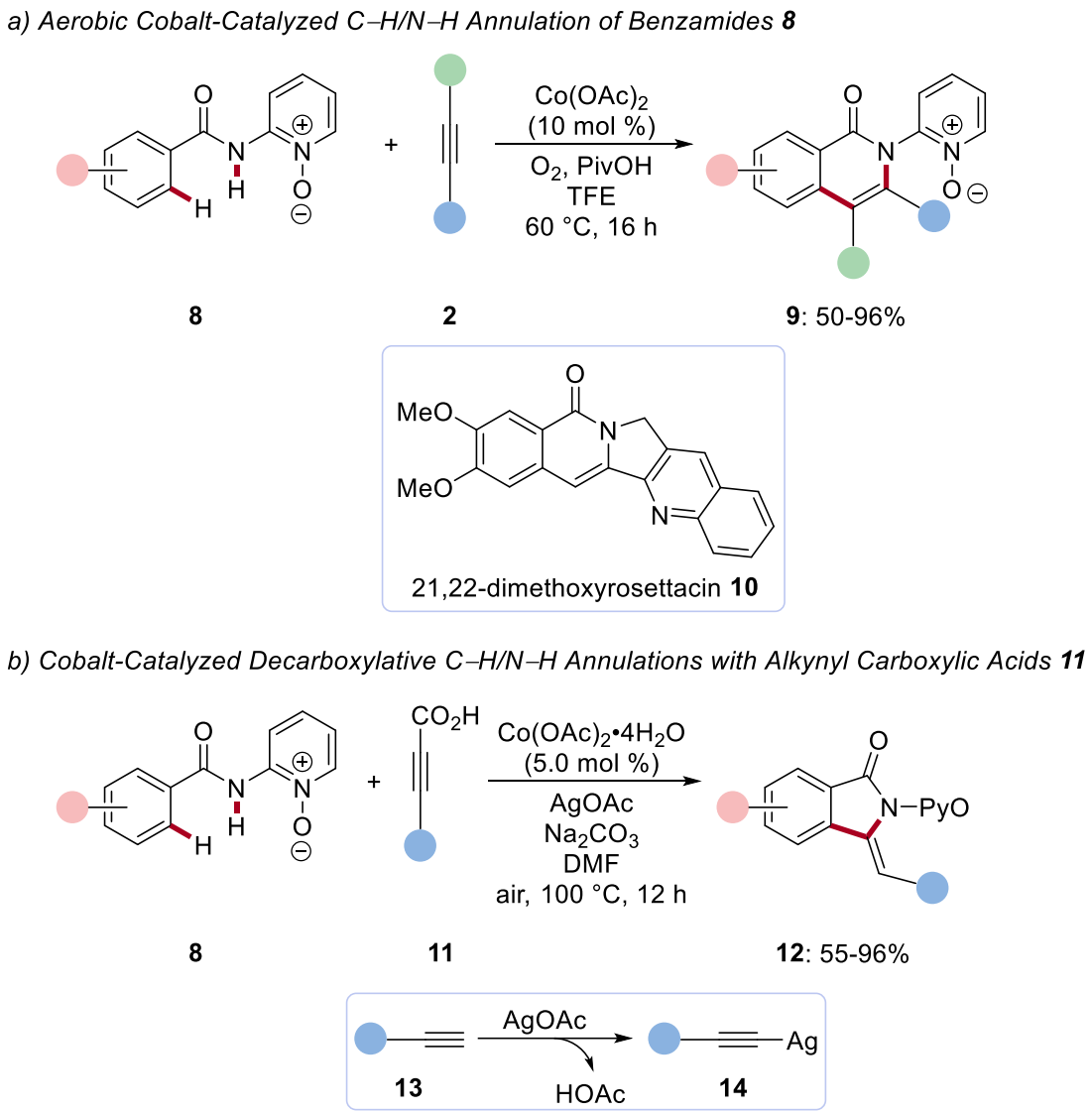

Figure 1.3.1.2. Cobalt-catalyzed C–H/N–H annulation reactions.

The reaction proceeded under mild conditions with TFE as the preferred solvent at 60 °C to achieve a wide substrate scope of differently substituted isoquinolones **9**. This is further pronounced by the successful synthesis of rosettacin derivative **10**, a class of aromathecin alkaloids.[58] Detailed mechanistic investigations including DFT

calculations indicated a cobalt(II)/(III)/(I) catalytic manifold for this transformation. In contrast, Niu and Song reported a similar work also using the bidentate 2-pyridyl-*N*-oxide for the cobalt-catalyzed decarboxylative C–H/N–H annulation reaction with alkynyl carboxylic acids to obtain either isoindolinones or isoquinolones derivatives (**Figure 1.3.1.2b**).[59] The aerobic cobalt catalysis reported earlier did not require the use of silver salt as terminal oxidant as opposed to this work. A silver-acetylide intermediate **14** was proposed by the authors that resulted in the difference in selectivity. This is formed through the decarboxylation of the alkynyl carboxylic acid **11** to form the silver acetylide **14**, which subsequently undergoes homolytic cleavage to give a terminal alkyne radical that facilitate the formation of isoindolinones **12**.

Since then, several directing groups were used to achieve cobalt-catalyzed C–H/N–H annulation reactions (**Figure 1.3.1.3**). This expansion includes outstanding strategies of using the picolinamide directing group by Carretero for the cobalt-catalyzed C–H/N–H activation reaction of benzylamine derivatives **15** to give dihydroisoquinolines **18** (**Figure 1.3.1.3a**).[60] Removable auxiliary directing groups, provide an ample opportunity for further functionalization with improved step-economy of the reaction protocol. Hence, the possibility of using traceless, yet similar picolinamide auxiliary directing group was reported by Cui for the alkyne annulations for the formation of isoquinoline derivatives **19** (**Figure 1.3.1.3b**).[61] The use of a facile removable *N*-2-pyridylhydrazide, an *N*,*N'*-bidentate auxiliary directing group that can be easily eliminated *via* mild traceless reductive nitrogen-nitrogen cleavage was realized by Zhai for the annulation reaction, to achieve the synthesis of isoquinolones **20** (**Figure 1.3.1.3c**).[62] Subsequently, Zhai continued using the same approach with benzamides **16** for the spirocyclisation cascade with maleimides.[63] Later Daugulis showcased alkyne annulations with a peculiar $Co(hfacac)_2$ catalyst using widely available carboxylic acid as an useful directing group to achieve the production of isocoumarins **21** (**Figure 1.3.1.3d**).[64] The authors commented that it goes through a cobalt(II)/(III)/(I) catalytic cycle as well.

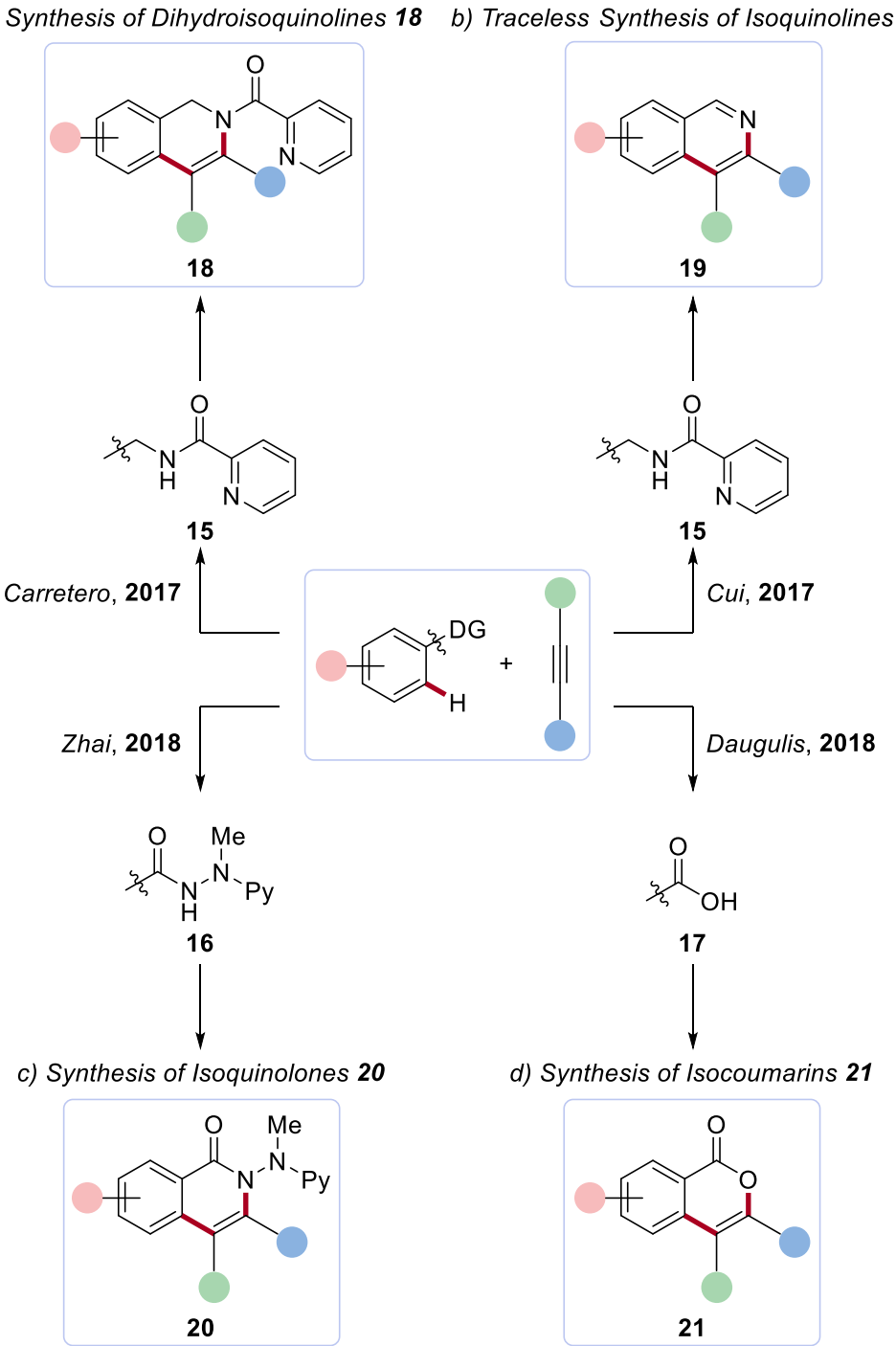

Figure 1.3.1.3. Cobalt-catalyzed C–H/N–H annulation reactions with several different directing groups.

The cobalt-catalyzed C–H/N–H activation for annulation reactions were not limited to alkynes as coupling partner. Nicholls reported a regioselective cobalt-catalyzed annulation process utilizing 1,3-diynes **22** instead and this resulted in the synthesis of non-symmetrical alkynylated isoquinolones **23** (**Figure 1.3.1.4a**).[65] Moreover, this transformation has also been done with C(sp^3)–H bond activation even though most annulation reactions focused on C(sp^2)–H activation. Zhang managed to demonstrate

the useful synthesis of γ-lactams **25** with cobalt-catalyzed C(sp^3)–H annulations with alkynes **13**, albeit under relatively harsh reaction conditions (**Figure 1.3.1.4b**).[66] According to the authors, the combination of additives was essential for the reaction to proceed, this was especially crucial regarding the addition of ammonium salts and pyridine into the reaction mixture to achieve the optimised result. This was supported by the detection of the cyclometallated cobaltacycle **26** using MALDI-TOF mass spectrometry analysis, which identified the coordination of two pyridine molecules and the aromatic solvent.

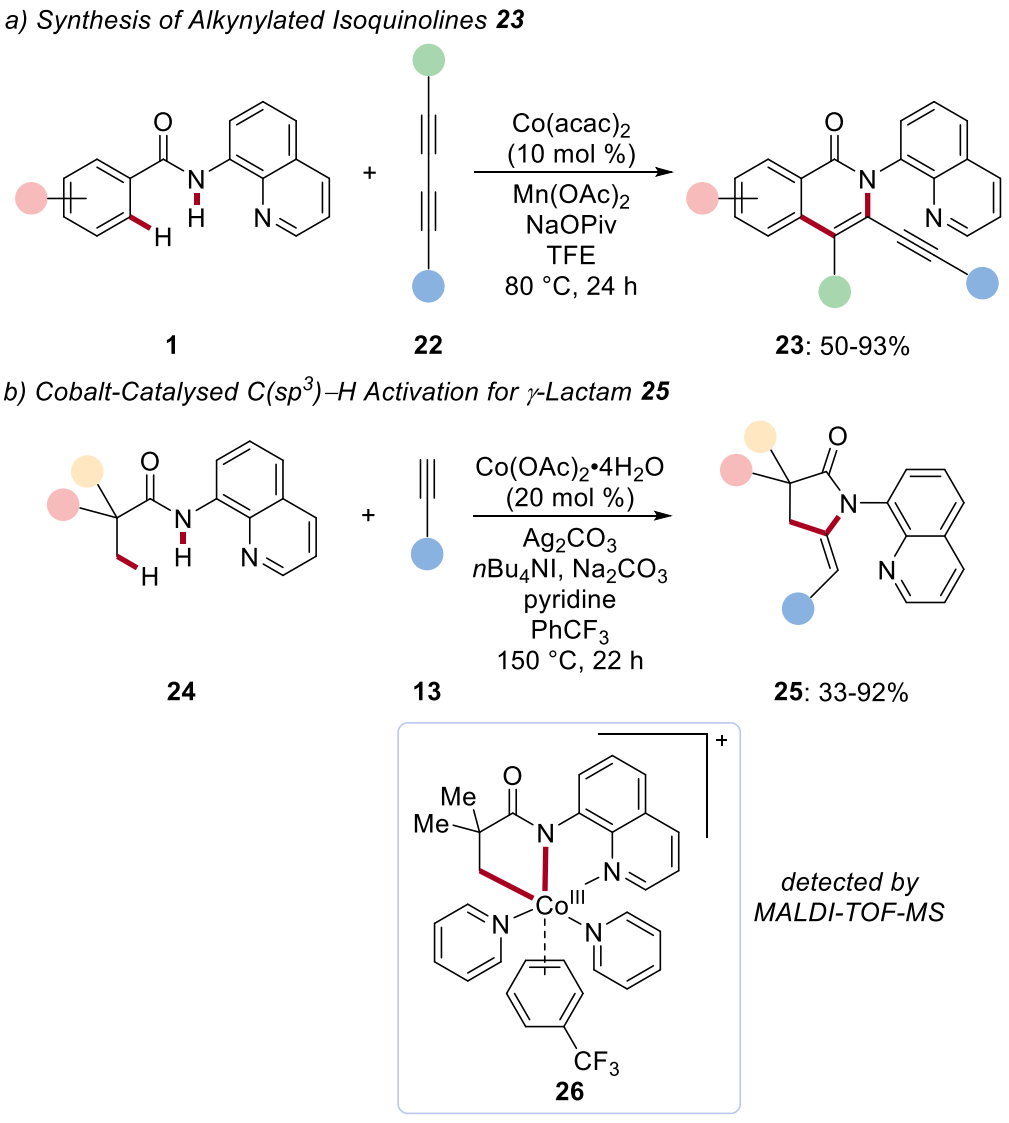

Figure 1.3.1.4. Peculiar 1,3-diynes as substrates and C(sp^3)–H activation.

The development of annulation reactions has also been extended to unsaturated coupling partners, such as allenes, which offer a broad substitution pattern depending

on the substituents.[67] The first report for the cobalt-catalyzed C–H/N–H allene annulation was in 2016 by Volla using bench-stable $Co(acac)_2$ as catalyst (**Figure 1.3.1.5a**).[68] The reaction protocol proceeded under a relatively mild condition that requires both oxygen and $Mn(OAc)_2•2H_2O$ as oxidants. Notably, they were able to obtain two different substitution patterns based on the steric and electronic properties of the allenes used. However, based on precedents for transition metal-catalyzed allene annulation reactions, the regioselectivity and stereoselectivity remains challenging to control.[69]

a) Difference in Substitution Pattern of Different Allenes

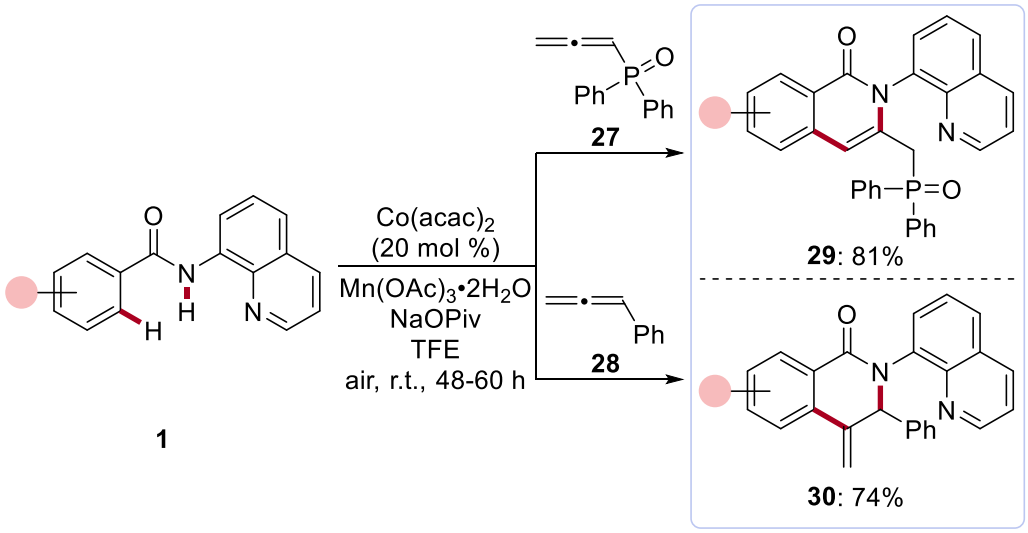

*b) Stoichiometric Reaction for the Synthesis of Cyclometallated Cobalt Species **31***

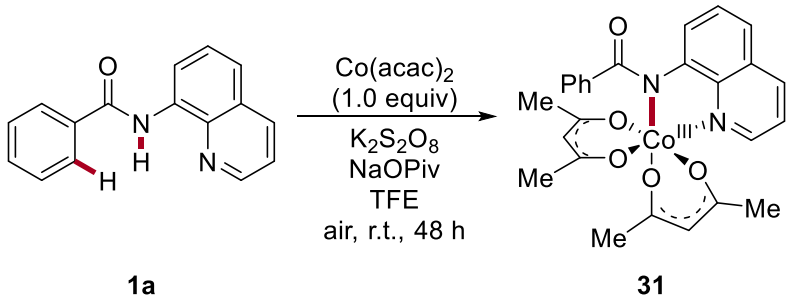

Figure 1.3.1.5. Cobalt-catalyzed C–H/N–H allene annulation.

With relevance to the observed regioselectivity, sterically hindered or electron-deficient allenyl(diphenyl)phosphine oxide **27** gave unsaturated isoquinolone-type products **29**. Whereas, when electron-rich phenylallenes **28** were used, dihydroisoquinolin-1(2*H*)-ones **30** was obtained instead. In addition, the authors were able to synthesize and

characterize the cyclometallated cobaltacycle complex **31** by X-ray crystallography to further elucidate the reaction mechanism (**Figure 1.3.1.5b**). Furthermore, several additional mechanistic results were obtained, such as a low KIE of 1.1 which illustrated a facile C–H cleavage and the preference of electron-rich substrates over electron-poor benzamides **1** was confirmed through competition experiments. Consequently, a catalytic cycle (**Figure 1.3.1.6**) was proposed by the authors in accordance to the obtained mechanistic investigations to further elaborate the change in regioselectivity between the two types of allenes with different electronic properties.

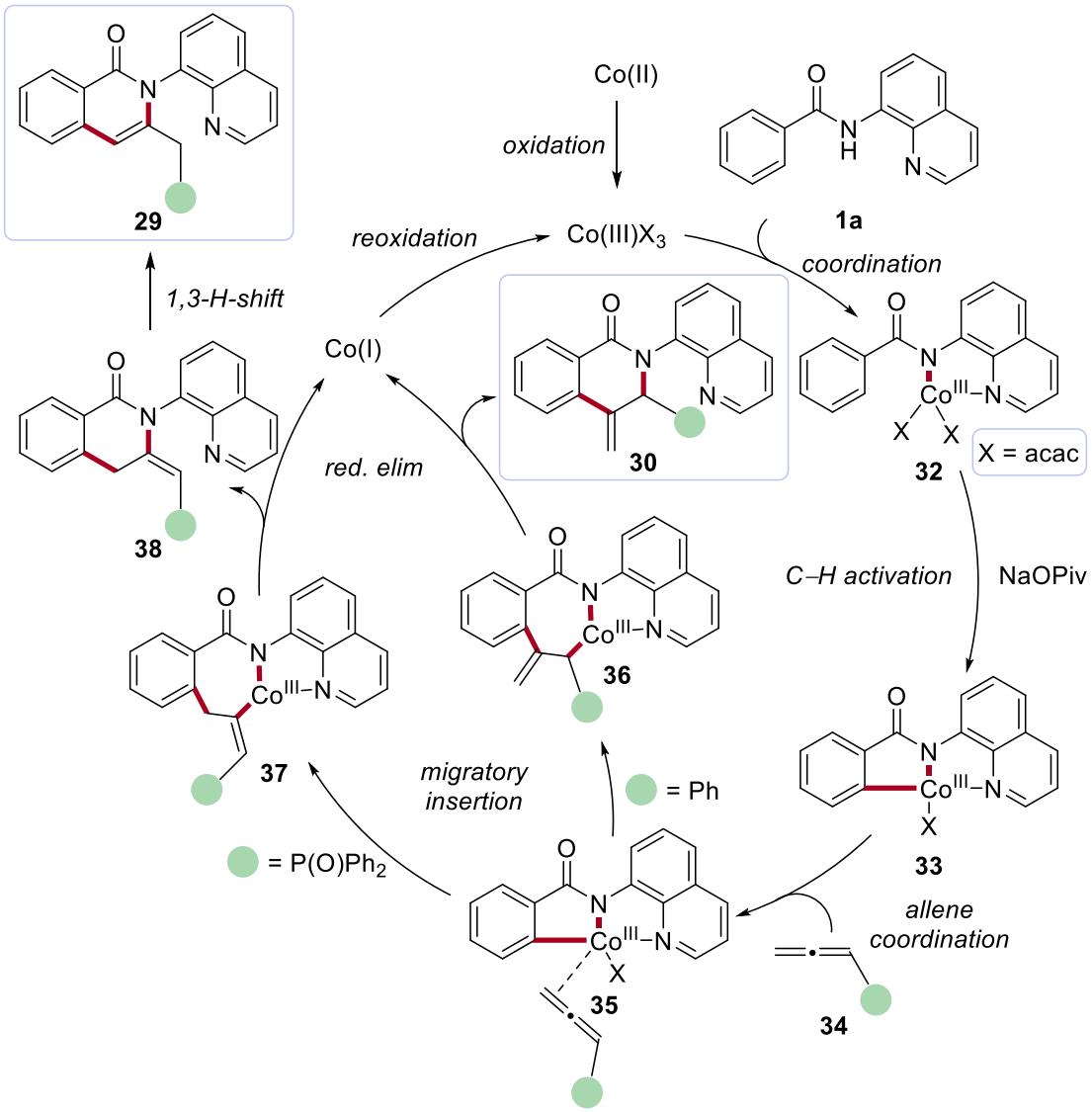

Figure 1.3.1.6. Proposed catalytic cycle.

The authors stated that the catalytic cycle proceeds with an active cobalt(III) catalyst after the oxidation of the bench stable cobalt(II) salt. Subsequently, the coordination of

the cobalt(III) catalyst with benzamide **1a** gives complex intermediate **32** that will further undergo C–H metalation with the aid of NaOPiv base to form the cobalt(III) intermediate **33**. Thereafter, coordination of allene **34** on to the complex **33** leads to the formation of intermediate **35**. From here, migratory insertion occurs giving a seven-membered ring complex intermediate **36** or **37** according to the electronic properties of the subjected allene substrates. Then, a π-allyl-cobalt complex can be formed through the addition of the aryl to the central carbon atom of the allene by carbocobaltation. When electron-rich phenylallene **28** is used, the nature of this substrate favours the formation of σ-allylcobaltacycle complex **36**. Then, the ensuing reductive elimination will result in the formation of the exocyclic product **30**. On the contrary, when electron-poor allenyl(diphenyl)phosphine oxide **27** or sterically hindered substrate are used, a different pathway ensues to give intermediate **37**. Reductive elimination will give compound **38** which undergoes 1,3-hydrogen-shift forming the final endocyclic product **29**. The generated cobalt(I) from both reductive eliminations will be reoxidized to regenerate the catalytically active cobalt(III) catalyst. Major developments were conceived for cobalt-catalyzed C–H/N–H allene annulation in 2017 and 2018, where it was possible to utilize several interesting directing groups for the formation of both endo- and exocyclic isoquinolones. Cheng reported a regioselective allene annulation of 8-aminoquinoline substituted benzamides **1** with 1,3-disubstituted internal allenes to selectively give the endocyclic product **41** with moderate yield (**Figure 1.3.1.7a**).[70] Concurrently, Rao also devised a similar route, where they remarkably obtained both the endocyclic **45** and exocyclic **46** products solely by changing the bases involved in the reaction protocol (**Figure 1.3.1.7e**).[71] This considerable finding supplements the original data (*vide supra*) from Volla regarding the electronic nature of the substituents on the allenes. Subsequently, Rao developed a regioselective oxidative allene annulation with phosphinamides **39** through a cobalt-promoted C–H activation for the synthesis of phosphaisoquinolin-1-ones **42** with possible applications in drug discovery (**Figure 1.3.1.7b**).[72]

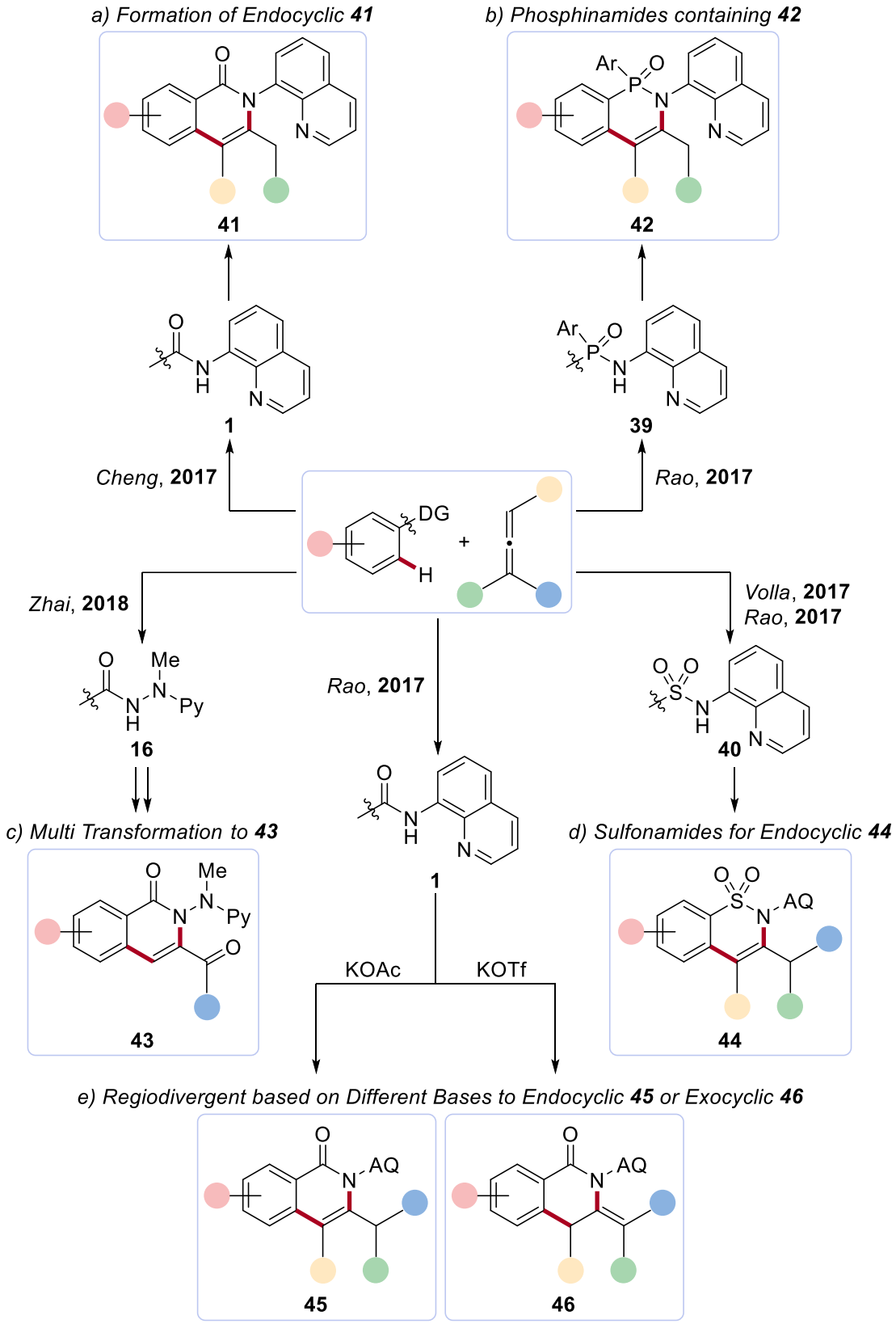

Figure 1.3.1.7. Various reported cobalt-catalyzed C–H/N–H allene annulation strategies.

More recently, Zhai developed a trifunctionalization of allenes to form 3-acylquinoline derivatives **43** with broad functional group tolerance by the inclusion of molecular oxygen (**Figure 1.3.1.7c**).[73] The hydrazide directing group could be easily removed by reductive nitrogen-nitrogen cleavage. Volla and Rao independently reported sulfonamide containing substrates for cobalt-catalyzed allene annulations with moderate to good yields of endocyclic sultam derivatives **44**.[74] This approach is an extremely useful protocol, given the wide sultam scaffolds in drug molecules and biologically active compounds.[75] The mechanistic investigations from previous studies and additional findings from both reports agreed with a cobalt(II)/(III)/(I) catalytic manifold as the general mode of action of this annulation reaction.

1.4 Metalla-Electrocatalysis

Molecular syntheses are conventionally dominated by thermal conditions, and within the last few decades, significant number of more sustainable developments in synthetic organic chemistry have been directed towards the use of other forms of energy source. Intriguing yet innovative platforms, such as photochemistry,[76] mechanochemistry[77] or flow technology,[78] have allowed compelling advancements in organic synthesis. The use of artificial intelligence or machine learning for enhancing productivity of state-of-the-art synthetical protocols and perhaps discovering new reactivity have additionally thrusted the world forward.[79] Yet electroorganic synthesis has considerably rose only in the last decade as it conquers its early limitations as a niche technique only for the specialists.[80] Pioneering works since the 19th century by Volta,[81] Faraday[82] and Kolbe[83] set the stage for the viability of utilizing electricity in organic synthesis. Potentiostatic reactions as hinted first by Hickling were then sought after, since they allow a complete control of the potential minimising the decomposition of substrates involved in the electrolysis.[84] Moreover, electroanalytical tools were subsequently developed, such as cyclic voltammetry, for elucidating transient species or analysing minute changes in oxidation/reduction potential by the relation between current as a function of applied potential.[85] With the aid of this green energy as an indispensable resource, many chemical industries were awed by its simplicity yet innovative and inexpensive nature for large scale synthesis of chemicals, e.g. the Simons fluorination process,[86] the Monsanto adiponitrile processes[87] and the BASF Lysmeral® Lilial synthesis for the fragrance industry.[88] Subsequently, the approach of electroauxiliaries were introduced by Yoshida for reducing the electrochemical potential of molecules of interest.[89] Additionally, there is a rising use of redox mediators which can efficiently aid the electron-transfer by acting as an electron-transfer-shuttle from electrode surfaces to the reaction mixture.[90] Ever since, a vast amount of efforts have been directed to electroorganic synthesis, where these exploitations revolutionised the usefulness of this technique which were advanced by Amatore,[91] Jutand,[92] Schäfer,[93] Little,[90b, 94] Yoshida,[95] Lund[96] and Moeller.[97]

Electrosynthesis for organic chemistry has been recently facing a renaissance owing to the contributions mentioned above, but also due to the need for greener and sustainable synthetic methods to reduce chemical waste and carbon footprints. In this aspect, electrochemistry has emerged as a powerful alternative, since the electrons supplied are considered as traceless redox equivalents, which removes the need to have super-stoichiometric amounts of redox chemicals reducing the generation of by-products.[21a] The resurgence of this technique has also been driven by the vast development of user-friendly electrochemical cells and equipment that are commercially available.[98] Hence, the set-ups are easily accessible and the whole electrolysis process is much more simplified than conventional set-ups. Because of the nature of being able to fine tune the reaction potential under potentiostatic conditions, electrosynthesis provides an exceedingly mild approach, that could improve the overall synthetic utility with increased chemoselectivity as compared to the use of conventional chemical redox reagents.[99]

The aforementioned directed oxidative transition metal-catalyzed C–H activation reactions (*vide supra*) are advantageous for their atom- and step-economy nature. Meanwhile, electrochemistry provides an endless supply of renewable and resource-efficient energy source. As a consequence, the combination of both creates an unparalleled yet innovative method for the continuous development of greener synthetic organic chemistry for the future generations (**Figure 1.4.1**).

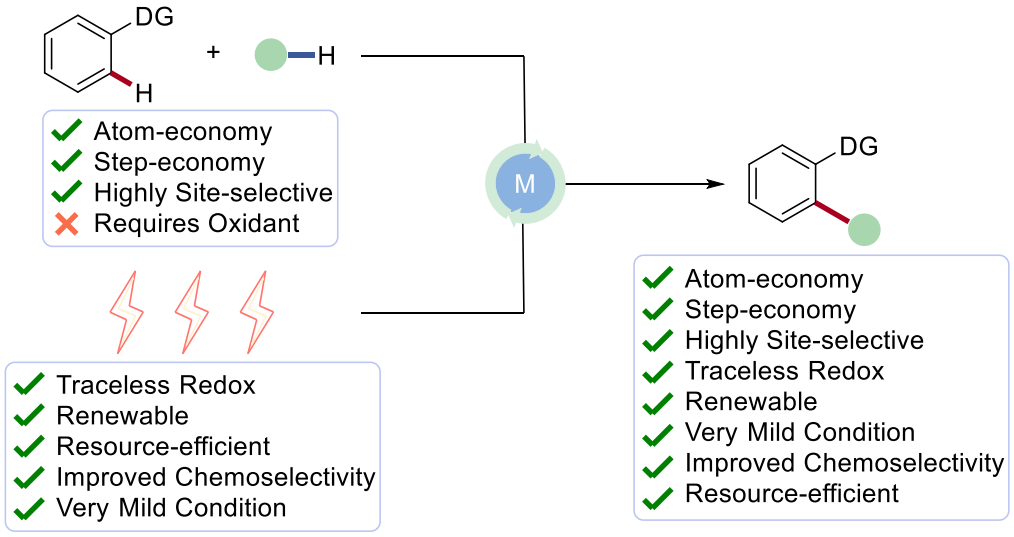

Figure 1.4.1. The merger of electrosynthesis and directed oxidative C–H activation.

Indeed, electrosynthesis has been used with oxidative C–H activation in the last few decades, including the early work by Amatore and Jutand using palladium-catalyzed alkenylation[90d] with the use of benzoquinone redox mediator. With relevance, the electro-modified Fujiwara–Moritani alkenylation was thus accomplished.[100] Even though most of the works were conducted with a palladium catalyst,[101] this groundwork showcased the synergistic combination of the two methods and brought forth opportunities for the expansion of electrocatalyzed C–H activation with Earth-abundant transition metals.[102] Several key contributions have been made to achieve site-selective C–H activation transformations with electrocatalysis, which opens up a new avenue for the development of novel and innovative synthetical protocols, by for example Ackermann,[21a, 21b, 47a, 103] Lei,[104] Xu,[105] and Mei,[106] among others.[107]

1.4.1 Oxidative Cobaltaelectro-Catalysis for C–H Activation

In light of the extensive amount of transition metal-catalyzed electro-oxidative C–H activation reactions, it has been until recently limited to 4d and 5d transition metals. Thus, it is crucial to note that the first cobaltaelectro-catalyzed C–H activation was unravelled in 2017 by Ackermann, an electro-oxidative C–H oxygenation with primary alcohol **47** activated by $Co(OAc)_2•4H_2O$ salts was described (**Figure 1.4.1.1**). The main highlight was the exceedingly mild reaction conditions with the exclusion of silver(I) or copper(II) salts as chemical oxidants at ambient conditions. As a result, the sole by-product of the reaction is molecular hydrogen. The broad substrate scope showcased the robustness of the cobaltelectro-catalyzed C–H oxygenation. Subsequently, the success of utilizing cobalt(II) salts as catalysts were extended to many other C–H activation transformations such as C–C[108] and C–Het bond formation (**Figure 1.4.1.2**).[109] Notwithstanding the fact that cobaltaelectro-catalysis works remarkably well for C–H/N–H annulation reactions that takes the pioneering works (*vide supra*) a step further in terms of sustainability. Whether it is for alkynes,[108d, 108f, 108h] alkenes[108g] or more peculiar coupling partners, such as carbon monoxide or isocyanides,[108c, 108e] this methodology was applied in the synthesis of heterocyclic

scaffolds that could be useful for drug development or natural product synthesis (**Figure 1.4.1.2A–B, D–E, G, J**).

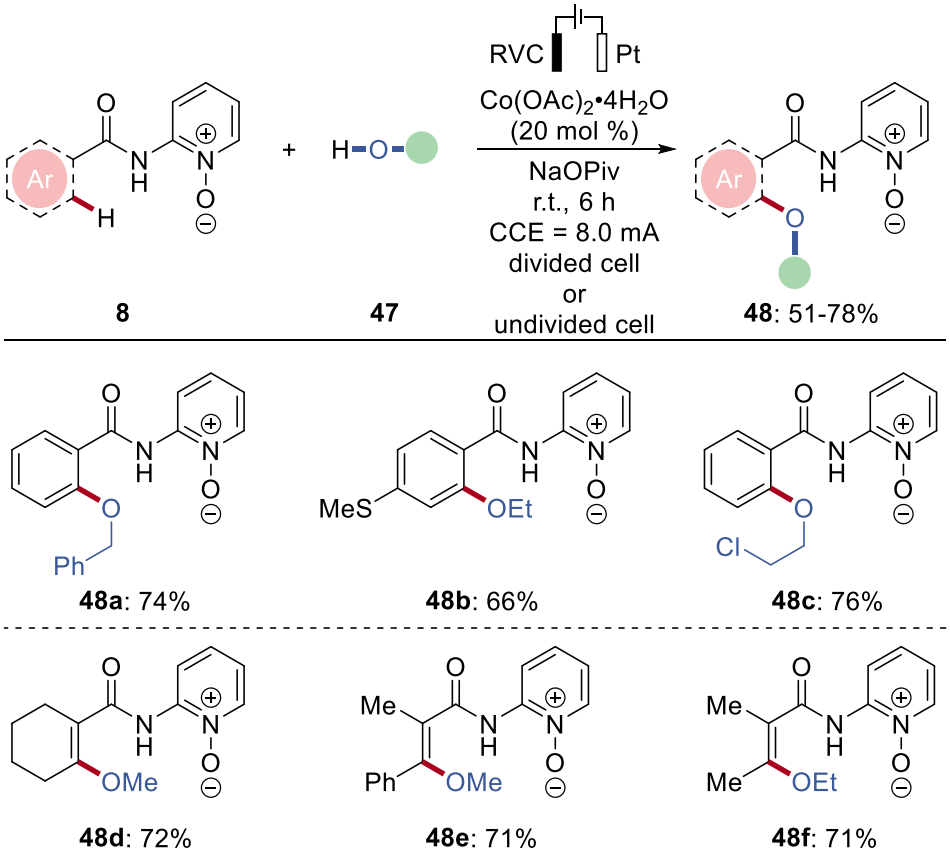

Figure 1.4.1.1. Cobaltaelectro-catalyzed oxidative C–H oxygenation of benzamides **8**.

Most of the successes on cobaltaelectro-catalysis required a bidentate chelation assistance by the directing group. Electrochemically enabled C–H aminations were proven to be viable as well for the C–Het bond formation to give aminated products **52** or **56** with the aid of cobalt catalysis by Ackermann and Lei independently (**Figure 1.4.1.2C, F**).[109b, 109c] These studies provided mechanistic insights into its reaction mechanism. With regard to the formation of C–Het bonds, Ackermann reported the acyloxylation reaction promoted by cobaltaelectro-catalysis in γ-valerolactone (GVL), a biomass-derived solvent, showcasing the capability of cobalt catalysis in more sustainable solvents (**Figure 1.4.1.2I**).[109a] In 2020, cobaltaelectro-catalyzed C–H allylation with unactivated alkenes was also realized by Ackermann with high chemo- and regioselectivity for the formation of products **57** (**Figure 1.4.1.2H**).[108b]

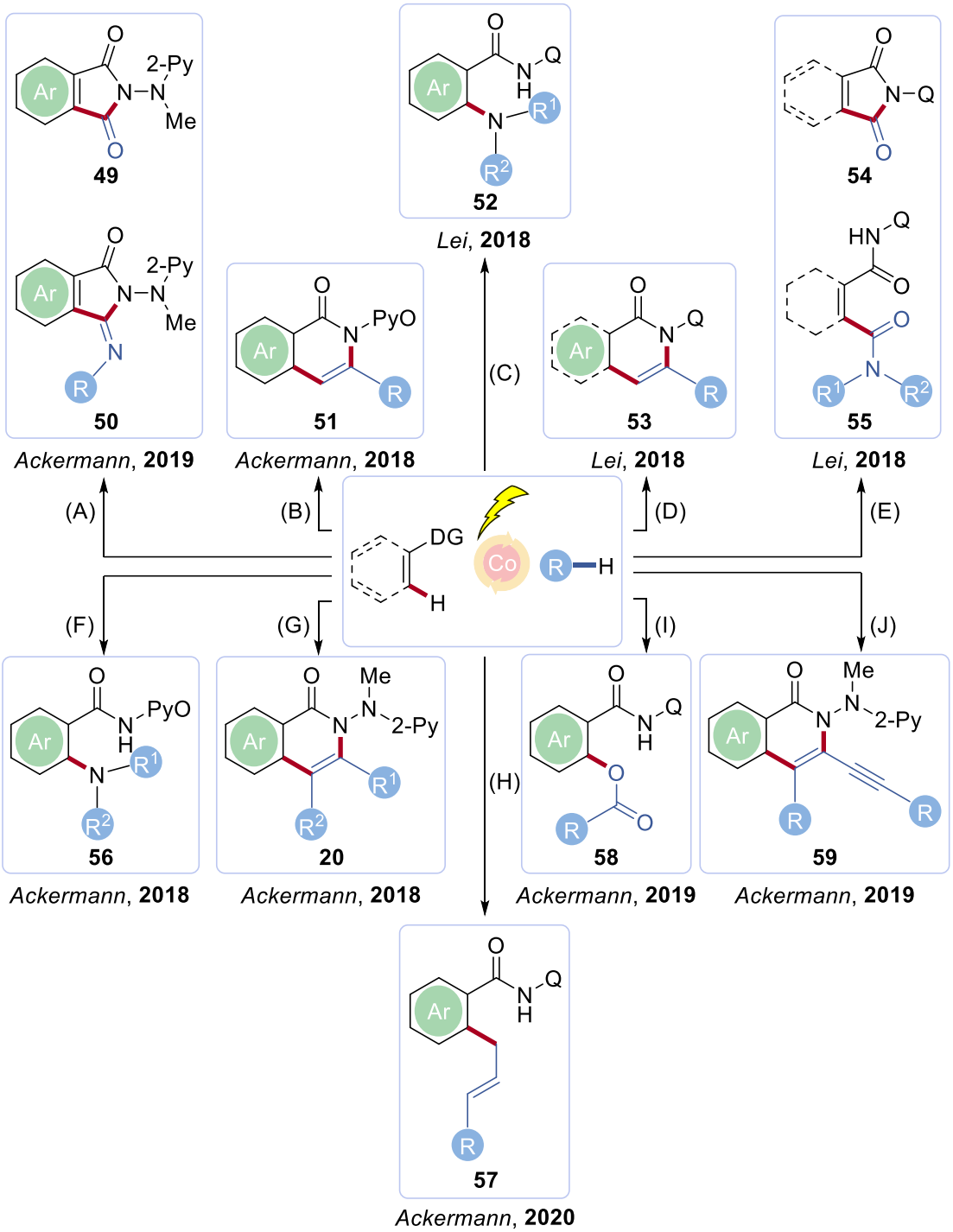

Figure 1.4.1.2. Compilation of cobaltaelectro-catalyzed oxidative C–H activation transformations.

1.5 Reductive Cross-Electrophile Coupling Reactions

The road to minimizing chemical waste and greener approaches in synthetic organic chemistry was simplified by the discovery of cross-coupling reactions and practical C–H activation reactions.[4, 47b] However, carbon nucleophiles are generally far less commercially available than are carbon electrophiles and this affects the step-economy to a certain extent, since preformation of carbon nucleophiles will be essentially needed before the said coupling could happen. Consequently, there is a great desire to streamline synthesis protocols for organometallic reagents and cross-coupling reactions. One of this method is to combine two different carbon electrophiles — or in general two different electrophiles — to achieve the desired cross-coupled product termed as cross-electrophile coupling (**Figure 1.5.1**).[110]

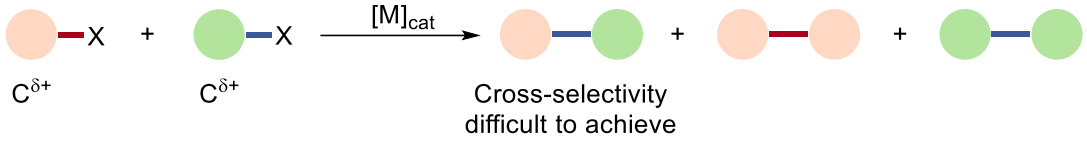

Figure 1.5.1. Cross-electrophile coupling.

The most distinct advantage is that most electrophiles are widely available with a diverse range of substituents, and they are often inherently more stable than are their organometallic counterparts.[111] In addition, most electrophilic reagents such as organohalides, carboxylates and sulfonates, are easily handled and stored in large quantities under moist and aerobic ambient conditions without significant hazardous risks. Whereas, the organometallic derivatives are highly reactive and they often react spontaneously with air and moisture, therefore the handling requirements are more tedious and laborious.[112] As a consequence, more time is required for the pre-formation of the organometallic reagents than is for the actual cross-coupling reaction.[110c]

One of the pioneering studies was the Wurtz reaction, involving the manipulation of Na metal for the reductive dimerization of electrophiles using alkyl halides to achieve longer alkane chain (**Figure 1.5.2a**).[113] The aforementioned Ullman reaction for the synthesis of biaryls by copper and two aryl halides also depicted a cross-electrophile

reaction (**Figure 1.5.2b**).[17] In contrast with its predecessor, the Wurtz–Fittig reaction for making substituted aromatic compounds with Na metal was the first cross-electrophile coupling in which two different electrophiles were utilized, an aryl halide and alkyl halide (**Figure 1.5.2c**).[114] It is noteworthy that the cross-selectivity improves whenever the alkyl halide is more reactive, to form the organosodium bond first and thus act more effectively as a nucleophile towards the aryl halide.

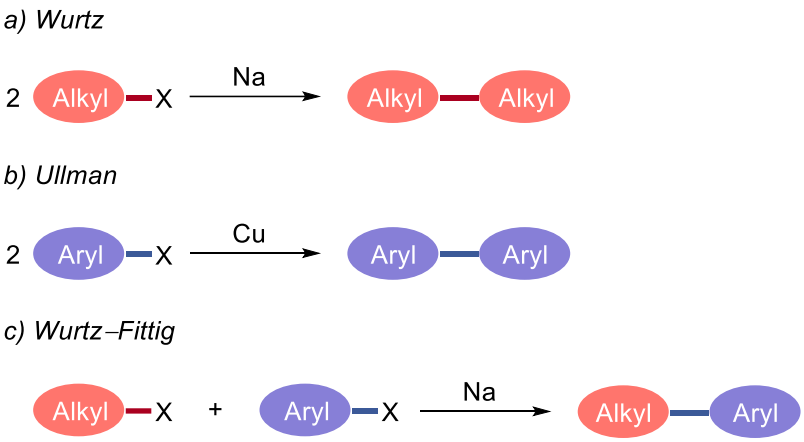

Figure 1.5.2. First reported cross-electrophile systems.

These reactions are heavily limited by the functional group tolerance and the need to use stoichiometric amounts of metallic reagent. Moreover, high loadings of ligands are eventually needed for selectivity and reactivity control, making these methods often impractical for contemporary usage. In the last decade, developments were made possible with catalytic electrochemical method to remove the need of stoichiometric amounts of Na.[92a, 115] However, three main problems persisted which are the imbalanced stoichiometry, high catalyst loadings and the need for a slow addition to suppress dimerization of one substrate. In general, cross-electrophile coupling reactions fail to pick up its momentum through the century to a great extent that it is far behind cross-coupling reactions and C–H functionalizations.

As mentioned before, one of the biggest challenges that impeded the growth of general cross-electrophile coupling is the dimerization of the individual electrophiles. Unlike traditional cross-coupling reactions, the two electrophiles have to compete with each other for the oxidative addition step onto the transition metal catalyst. For structurally akin substrates, the chances of obtaining cross-product are greatly diminished

(**Figure 1.5.3a**). Furthermore, in cases where one electrophile is significantly more reactive than the other electrophile, the first will rapidly undergo symmetrical dimerization with itself and then the latter too, albeit at a much lower rate (**Figure 1.5.3b**).

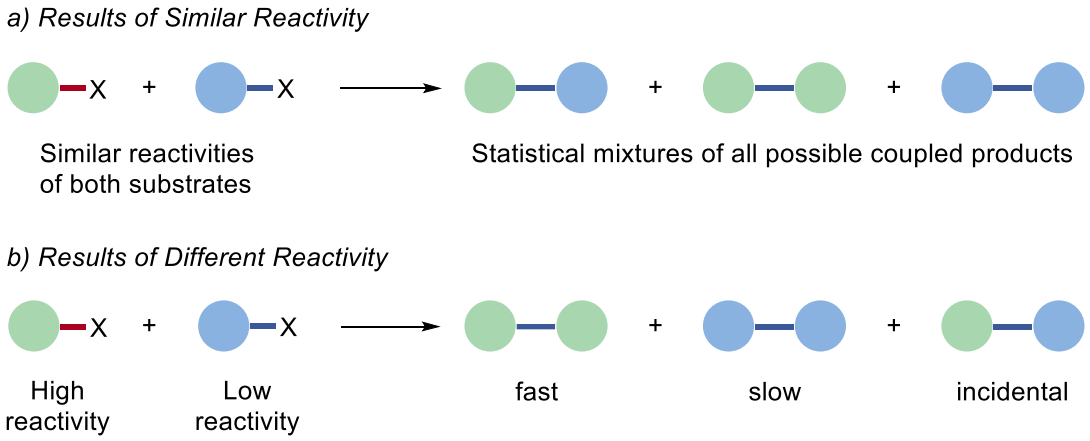

Figure 1.5.3. Outcome of cross-electrophile coupling reactions based on individual reactivities.

In case of similar reactivities of the two electrophiles, increasing the stoichiometry of one substrate can tremendously improve the yield of the cross-coupled product. Needless to say, this method is certainly not economical although feasible on smaller scale. One example is the cross-Ullman-type coupling reaction whereby two different aryl halides react together to give unsymmetrical biaryls (**Figure 1.5.4**).[116] However, a major disadvantage co-exists, since it is obtained as the second yielding product as the excess monomers will combine and give the symmetrical biaryl side-product.

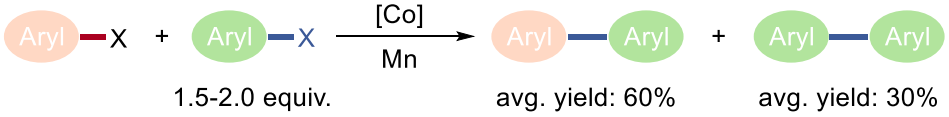

Figure 1.5.4. Cross-Ullman-type coupling reaction.

Ultimately, there is a need to conceive more reaction pathways for cross-electrophile coupling, as it opens up a greener avenue for synthetical usage. Cross-electrophile coupling reactions are thus far termed more for C–C bond formation between two alkyl/aryl halides. Nonetheless, electrophiles, such as CO_2 and heteroatom-containing thiosulfonates, will be considered here (*vide infra*) more in the later discussions.

1.6 Utilization of CO_2 as C-1 Building Block

The tremendous surge in greenhouse gases especially carbon dioxide (CO_2) in the atmosphere is mainly due to combustion of fossil fuels,[117] industrialization of raw material productions,[118] respiration of living organisms and the fermentation of sugars.[119] As such, carbon dioxide, an inert and unconsumed reserve is causing a detrimental effect in global climate change as the adverse rise of atmospheric temperature imbued a semi-permanent note on Earth.[120] It is indisputable that there is an urgent need to address CO_2 emission and construct or invest in competent and dynamic carbon capture and utilization (CCU) systems.[121] Carbon dioxide alongside biomass-derived resources could offer an astounding magnitude of opportunity as opposed to the bulk conventional used carbon resources such as coal, natural gas and crude oil. It is indeed an excellent one-carbon C1 synthon/building block[122] in synthetic organic chemistry through its non-toxicity, availability and abundance nature which illustrated the possibility of manipulating CO_2. Because of this, there have been a substantial number of researches brainstorming on valorisation approaches of CO_2 into value-added synthetical raw materials,[122e, 123] as well as the discovery of CO_2-promoted transformations.[124] Complication arises during the utilization of CO_2 since it is the most oxidized form of carbon which translate into its natural stability as a molecule. CO_2 is thermodynamically stable and kinetically inert, requiring the use of highly reactive species or harsh reaction conditions for the utilization of CO_2.[125] This includes the use of strongly reactive nucleophiles for the formation of C–C bonds with CO_2, such as Grignard or organolithium reagents, which have been exemplified by the rapid advancement of organometallic chemistry.[126] Thus, more efficient and functional-group tolerant protocols that are benign to the environment, which allows transformation of less-activated substrates must be developed for the utilization of CO_2 in organic synthesis. Because effective energy consumed for the fixation of CO_2 should be lower than its production, it is impractical if high energy is consumed for the transformation. In this context, the use of metal catalyst has exceptionally aided approaches using CO_2 as C1 synthon by lowering the activation energy needed.[127]

The key fundamental is to understand the role of the metal catalyst and its interaction with CO_2 in order to efficiently design a feasible synthesis protocol for the inclusion of CO_2 in catalytic processes.

These coordination modes between CO_2 and transition metal centres in general have been extensively investigated through stoichiometric mechanistic studies.[127] CO_2 is known to have two different coordinating atoms, the carbon centre is Lewis-acidic and electrophilic in nature, while the two oxygen atoms are Lewis-basic and weak nucleophiles. This allows various modes of coordination depending also on the specific electronic properties of the transition metal. Ideally speaking, when one molecule of CO_2 reacts with a transition metal centre, five different complexes can exist independently (**Figure 1.6.1**).[128]

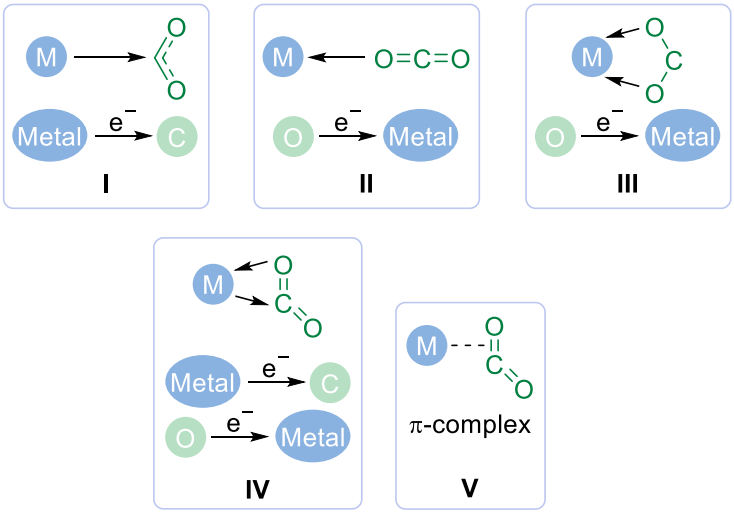

Figure 1.6.1. Different modes of CO_2 coordination with transition metals.

Electron-rich metal centres prefer to coordinate to the electrophilic carbon centre of CO_2 towards electron transfer from the metal centre to the carbon atom to form complex **I**, termed as metallacarboxylate. Coordination from the weakly nucleophilic oxygen atom by one lone pair of electrons to the metal centre to give type **II** adducts is less generally feasible. For electron-poor transition metals, CO_2 can become a bidentate ligand in which both the oxygen atoms donate to the metal centre forming a stable and favourable complex **III** as opposed to adduct **II**. Complex **IV** can also form as an intermediate when electron transfer from the metal centre to the carbon atom

and this causes a follow-up electron donation by one of the oxygen atoms to the electron-spent metal centre. In addition, coordination of CO_2 through the electron-rich unsaturated C–O bond by the metal centre allows the formation of a π-complex **V**. All of these above-mentioned coordination modes can have significant impact on the energy requirement of utilizing CO_2 that can fundamentally improve reactivity and give a better selectivity control during the incorporation of CO_2 in synthetic organic chemistry.[125b]

1.6.1 An Overview of Synthetical Conversions with CO_2

Various synthetic transformations of CO_2 have been developed in the last few decades (**Figure 1.6.1.1**). The most successful transformation utilizing CO_2 as an inexpensive coupling partner is the formation of cyclic carbonates **63** by the insertion of CO_2 into epoxides **62** and the production of polycarbonates **65** through polymerisation of epoxides **62** with CO_2 (**Figure 1.6.1.1a**).[129] These processes have also been industrialised due to their simplicity and high turnover numbers (TONs).[130] Moreover, 100% atom economy have been achieved on ethylene and propylene carbonate synthesis with CO_2 and this feat has a major impact on the fixation of CO_2 which encourages more synthetic routes to be discovered that can be utilized in large scale.[131] Although not industrialised yet, many methods of CO_2 fixation on aziridines **66** have also been devised with good TONs and the mechanistic insights could aid the synthesis of oxazolidinone compounds **67** (**Figure 1.6.1.1a**).[132] Reductive methylation and formylations of amines with CO_2 have also been accomplished to give **70** or **72**, respectively,[133] which depicted the possibility of activating CO_2 by coordinating nitrogen atom to the carbon atom in CO_2 to reduce the energy barrier for the reductive deoxygenation step of CO_2 (**Figure 1.6.1.1b**).[134] It is also proposed that the amine could increase the CO_2 concentration since Lewis bases act by decreasing the hydride affinity which then allows more CO_2 to be freed for a possibly faster rate of reaction.[135] The merger of the C–N bond formation and CO_2 set the stage for the valorisation of CO_2 in a diagonal approach which improves the step-economy and for making useful ingredients.[136]

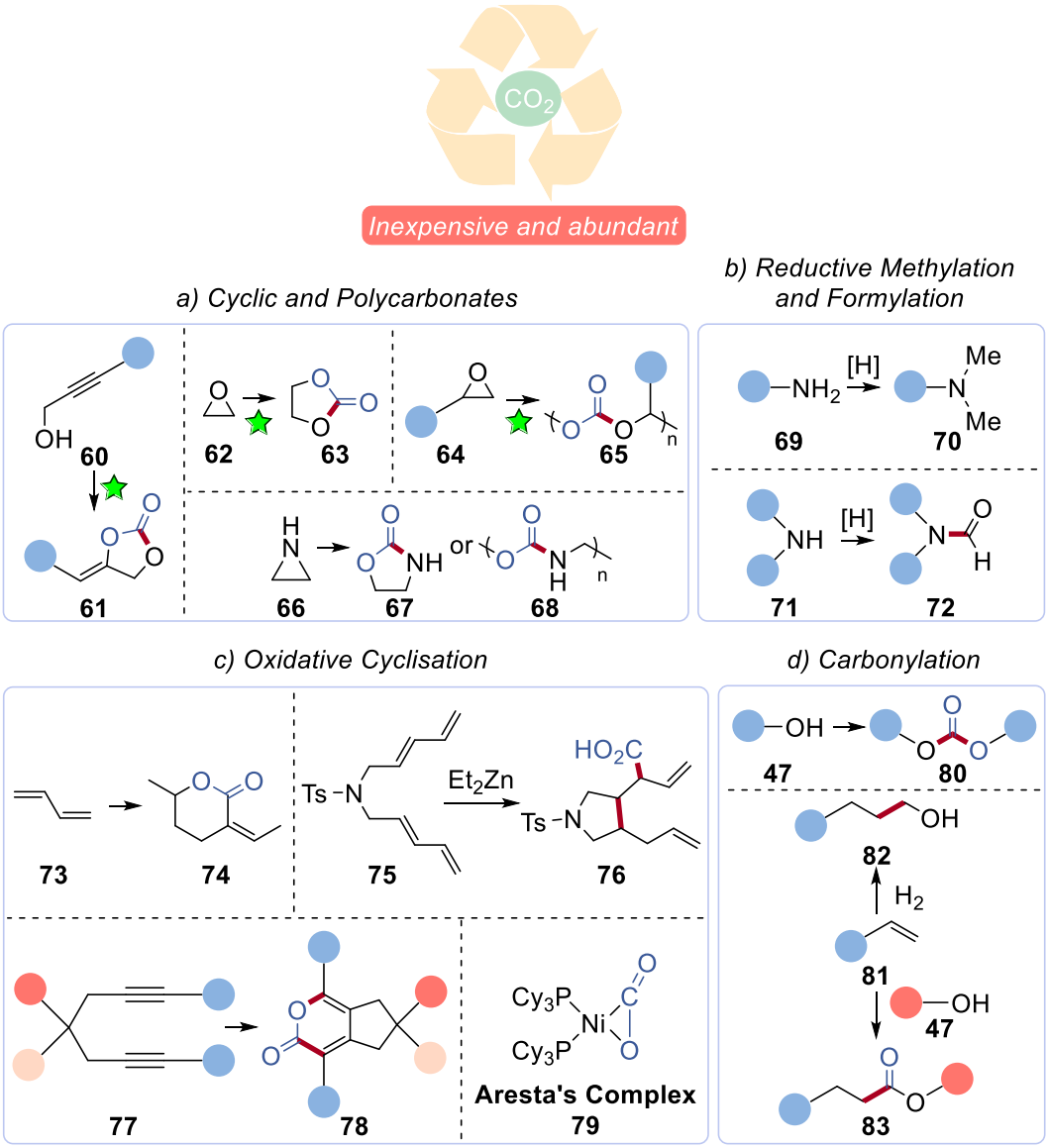

Figure 1.6.1.1. An overview of the utilization of CO_2 as building block. A few transformations have been industrialised which are green starred.

These methodologies for the methylation of amines *via* a six-electron reduction process of CO_2 were greatly improved in terms of sustainability and greener chemistry by the realisation of catalytic methylations with CO_2 and H_2 instead of using hydrosilanes[137] which would in return produce substantial siloxanes waste (**Figure 1.6.1.1b**).[136c, 138]

Transition metals have revolutionised the fixation of CO_2 due to their unique properties. The discovery of low-valent palladium or nickel was pivotal on oxidative coupling reactions of CO_2 as exemplified by the first synthesis of Aresta's complex $[Ni(CO_2)(PCy_3)_2]$ **79** (**Figure 1.6.1.1c**), which was the pioneering metallacycle complex

bound to CO_2.[139] This has indeed allowed a myriad of developments to spawn in the area of oxidative cyclometallation including cross-coupling reactions of CO_2 and organozinc with Aresta's complex as catalyst (**Figure 1.6.1.1c**).[140] Although it has brought forth great advancement, stoichiometric amounts of the transition metals are needed for the generation of distinct metallacycle complexes. In 1983, allylic carboxylate complex intermediate with palladium metal was first observed and reported by Behr which have an extremely important mechanistic impact in allylic carboxylation reactions (*vide infra*). This gave rise to later discoveries of novel and step-economical synthetic protocols.[141]

Due to the odourless, colourless, and toxic nature of carbon monoxide (CO), it is often challenging to handle and to use CO as a carbonylating agent. In addition, even though the valorisation of CO_2 as C1 synthon have been researched upon for various other transformations, its use for the *in situ* generation of CO for carbonylation is still lagging behind. Therefore, copious developments throughout recent years focused more on using CO_2 as CO surrogate for carbonylation reactions because of its practicality and environmentally conscious approach (**Figure 1.6.1.1d**). For many decades, the use of CO as carbonylating agent has a great significance in the large-scale manufacturing of bulk and fine chemicals from widely available feedstocks. For example, the hydroformylation and similar tandem reactions of alkenes produces oxo-products of over 10 million tons every year.[142] Therefore, it is an important quest to utilize massive amount of CO_2 in lieu of CO in order to decrease the concentration of CO_2 in the atmosphere. Furthermore, the large-scale generation of methyl propionate from ethylene through methoxycarbonylation catalyzed by palladium complexes produces more than 3 million tons a year to feed its demand as a key intermediate for the synthesis of methyl methacrylate.[143] As already mentioned regarding the limitations of using CO for carbonylation reactions, the transportation of CO poses a certain hazardous danger making it extremely difficult for large-scale movement of such toxic gaseous substance. Consequently, the *in situ* reduction of CO_2 to CO using the knowledge of reverse water-gas shift (RWGS) reaction (**Figure 1.6.1.2**) could help transit CO_2 into a C1 feedstock for carbonylation reactions.

Figure 1.6.1.2. 'Reverse' water-gas shift reaction. Increasing concentration of CO_2 will shift the equilibrium.

In this regard, the seminal work in 2000 reported by Tominaga and Sasaki was pivotal in the quest for CO_2 fixation through hydroformylation reactions and the reduction of alkenes with the ruthenium $H_4Ru_4(CO)_{12}$ complex as the catalyst (**Figure 1.6.1.3**).[144] Despite the harsh conditions and the low efficiency, this work gave start to solve the problem of CO usage and the reduction of CO_2. The application of hydrogen gas as an efficient reducing agent for CO_2 poses another pitfall for the hydroformylation and hydrocarboxylation of alkenes with CO_2 and H_2 reactions[145] since many of the subsequent carbonylation reactions cannot proceed due to the possible hydrogenation of the substrates.

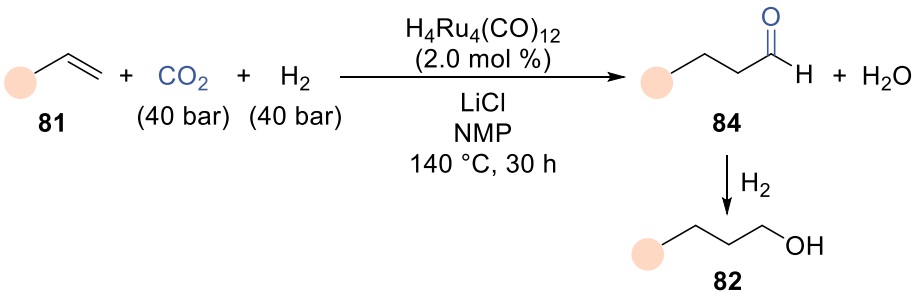

Figure 1.6.1.3. Ruthenium-catalyzed hydroformylation of alkenes with CO_2.

Photocatalysis[146] was subsequently introduced to tackle the reduction of CO_2 more efficiently to, for instance, formic acid.[147] However, since CO_2 is unable to absorb UV-vis light radiation itself, this could be addressed by the addition of a suitable photosensitiser wherein the excited state photosensitiser after absorbance of far-UV and visible light directs an electron to the ligands from the metal centre termed as metal-ligand charge transfer (MLCT). Upon emission from the excited state, the photosensitiser does a single-electron transfer (SET) to the CO_2 molecule for further transformations.[148] The use of photocatalysis in the reduction of CO_2 to CO has evolved based on initial studies by Lehn.[149] Despite of the lack of powerful photocatalyst alternatives that could easily absorb visible light, the advances made

were significant.[150] Several reports that focused on photocatalytic reduction of CO_2 required the use of stoichiometric amount of sacrificial electron donors.[151] Notwithstanding, the possibility of engaging CO_2 as CO surrogate could potentially fundamentally change synthetical protocols for carbonylation reactions for a greener and more sustainable approach.

1.6.2 Carboxylation Reactions with CO_2

In the past few decades, carboxylation reactions were vastly studied, because the formation of thermodynamically and kinetically stable C–C bond is highly desirable. Furthermore, increased utility of value-added compounds, such as carboxylic acid derivatives, are indispensable for bottom-up synthesis approaches, and it is one of the most fundamental building blocks for late-stage diversification. As already mentioned, CO_2 is highly stable and its performance as an electrophile often requires highly reactive nucleophilic reagents, such as organolithium or Grignard compounds **86**, as the coupling partners to furnish the desired carboxylic acid derivatives **88**. The utilization of CO_2 with carbon nucleophiles constitute a major demand in the field of organic synthesis.[127a] The Kolbe-Schmitt carboxylation reaction allows the large-scale synthesis of salicylic acid **90**, which showcases the potential of CO_2 fixation through the formation of C–C bond using carboxylation reaction (**Figure 1.6.2.1**).[152]

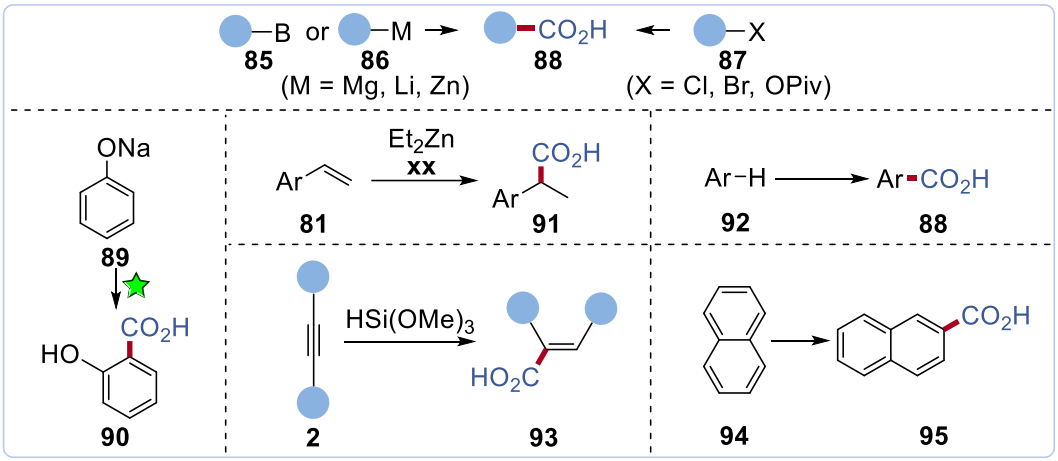

Figure 1.6.2.1. Various carboxylation reactions. Large-scale industrial synthesis of salicylic acid **90** is green starred.

The use of transition metals can significantly lower the activation barrier and promote the C–C bond formation step as a result the strength of the formed carboxylate-complexes by the insertion of CO_2 molecule into C–Metal bonds.[127b] This allows less-nucleophilic reagents, like organo(pseudo)halides **87**, organoborons **85**, unsaturated compounds **2** or **81** and substrates with activated C–H bonds **92** to undergo carboxylation transformations with CO_2. They are often formed through the C–Metal bond intermediate, which is somewhat analogous to conventional transition metal-catalyzed cross-coupling reactions (*vide supra*).[4, 153] Moreover, the carboxylate intermediate can be captured by transition metal and consequently quenched easily to regenerate the catalyst to close a catalytic cycle. Several modern illustrated catalytic methods (**Figure 1.6.2.1**) have been developed for the transition metal-catalyzed carboxylations with CO_2, but more importantly, these pioneering works granted an influx of future greener discoveries for CO_2 fixation by carboxylation.[122d, 145f, 154]

Catalysis with milder nucleophilic organoboron reagents for the carboxylation reaction with CO_2 using organoboron reagents was started by Iwasawa (**Figure 1.6.2.2**),[155] which displayed the enormous potential for replacing the use of organometallic reagents for better functional group tolerance and less demanding ambient requirements. Rhodium was employed in this case catalytically for the first time which was typically used stoichiometrically many decades prior to this discovery.[156] It was proposed that the catalytic use of rhodium is only possible if the active catalyst **98** can be regenerated from the rhodium carboxylates **99**. This is through the high oxophilicity of boron substrates by stimulating the transmetalation step between the rhodium carboxylates **99** and boron carboxylates **101** (**Figure 1.6.2.2**). Notably, subsequent researches for this carboxylation transformation found effectiveness with copper[157] and silver catalysts.[158] Besides organoboron reagents, step-economical direct C–H carboxylation have also been devised for more acidic C–H bonds by the aid of a strong base to give C–Metal bonded complexes *via* deprotonative metalation. This transformation is especially efficient for terminal alkynes.[159]

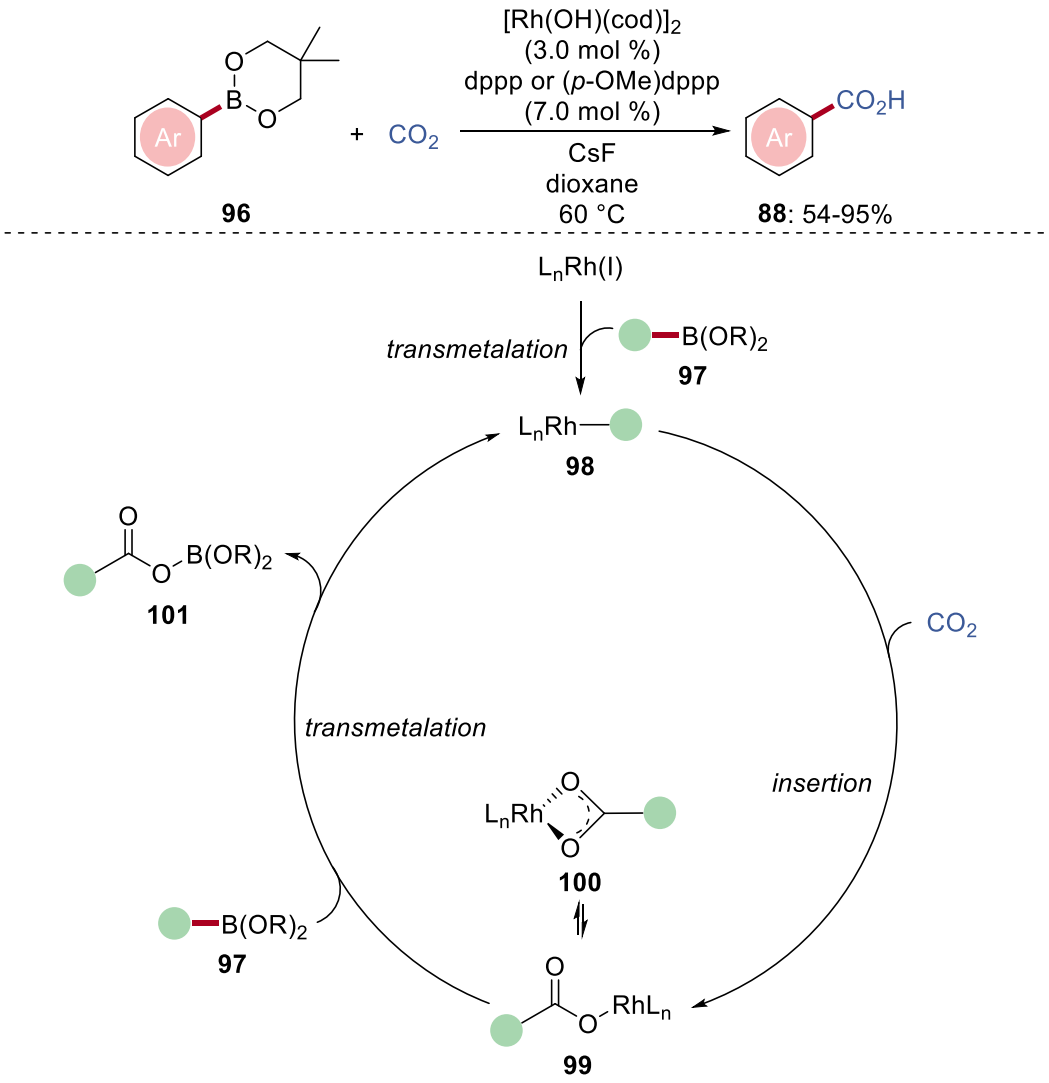

Figure 1.6.2.2. Carboxylation of organoboron substrates with CO_2.

Pioneering studies independently reported by both Gooßen[159d] (**Figure 1.6.2.3a**) and Zhang[159c] (**Figure 1.6.2.3b**) used copper(I) catalysts for the direct C–H carboxylation on terminal alkynes **13**. While Gooßen rather focused on phenanthroline-type copper complex for the successful transformation, the latter used TMEDA or poly-NHC-type ligands. A cooperation between the copper-NHC complex and a free carbene ligand was proposed for the activation of CO_2 to an NHC carboxylate-type intermediate. In 2011, Zhang then developed a metal-free regime utilizing only strong base like Cs_2CO_3 and KO*t*Bu for similar transformations on terminal alkynes with higher CO_2 pressure to achieve carboxylated products with relatively good yield (**Figure 1.6.2.3c**).[159b]

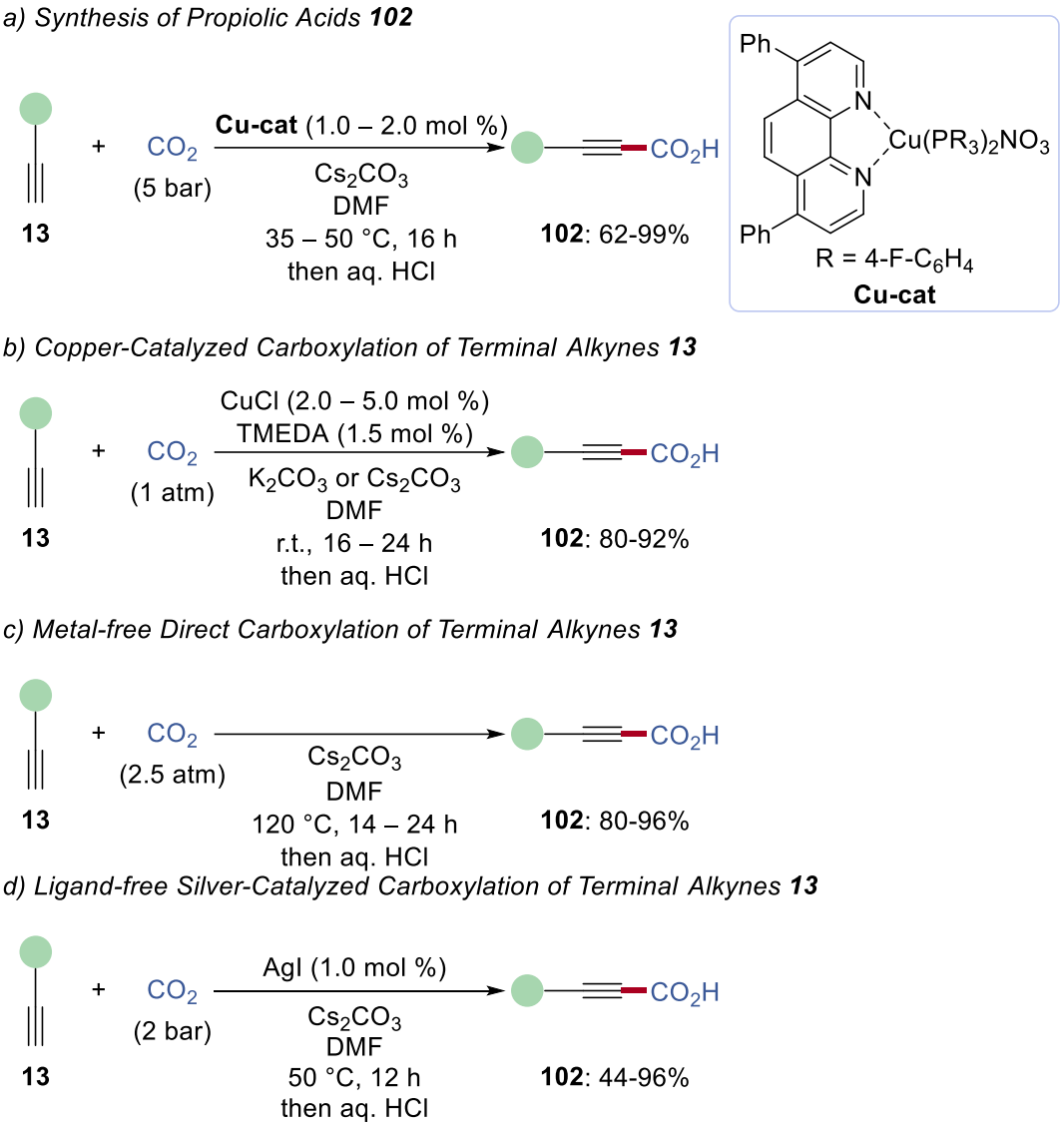

Figure 1.6.2.3. Direct C–H carboxylation of terminal alkynes **13**.

While copper complexes have been mostly employed in the carboxylation of terminal alkynes **13**, silver(I) as well was also exploited by Lu (**Figure 1.6.2.3d**).[159a] Wherein, they reported a ligand-free process with silver(I) as the active catalyst and a low catalytic loading of silver reflects the effectiveness of this transformation. Based on these concurrent progresses on direct C–H carboxylation of terminal alkynes, numerous carboxylation of heteroarenes with relatively acidic C–H bonds utilizing CO_2 have also been developed in which the key essential role of strong bases was amplified.[160]

Seminal work by Iwasawa displayed the possibility of a directing group-aided C–H activation method that could form the C–Metal bond in close proximity for the subsequent carboxylation to happen with CO_2 catalyzed by rhodium complexes (**Figure 1.6.2.4**).[161] Even though this C–H activation regime for carboxylation with CO_2 on arenes requires the use of pyrophoric methylaluminium-based reagents, this concept could be indispensable for a green and step-economical method to make relatively useful aryl carboxylic acid (**Figure 1.6.2.4a**). This approach has also been recently applied to alkenyl C–H bonds by the same group to achieve highly regioselective carboxylations with (*Z*)-selectivities (**Figure 1.6.2.4b**).[161a] The authors have proposed a plausible reaction mechanism with key intermediates on their mechanistic investigations for directed C–H carboxylation transformations (**Figure 1.6.2.4**). First the rhodium(I) chloride reacts with the methylaluminium reagent **109** giving the active methylrhodium(I) catalyst **110**. Subsequently, chelation-assisted C–H bond activation through oxidative addition of the substrate **111** by the active catalyst **110** gives arylrhodium(III) species **112**. Methane is then excluded through reductive elimination to give the key arylrhodium(I) intermediate **113**. This undergoes nucleophilic addition to give rhodium carboxylate **114** with CO_2. Transmetalation of intermediate **114** with another molecule of methylaluminium reagent **109** gives the aluminium carboxylate **115** and regenerates the active methylrhodium(I) catalyst **110**. The final product is obtained through the methylation step by adding $TMSCHN_2$ to give the ester product. The authors observed the methylated side product **116** in both their studies, and this can be accounted for through a C–C forming reductive elimination of the arylrhodium(III) intermediate **112**.

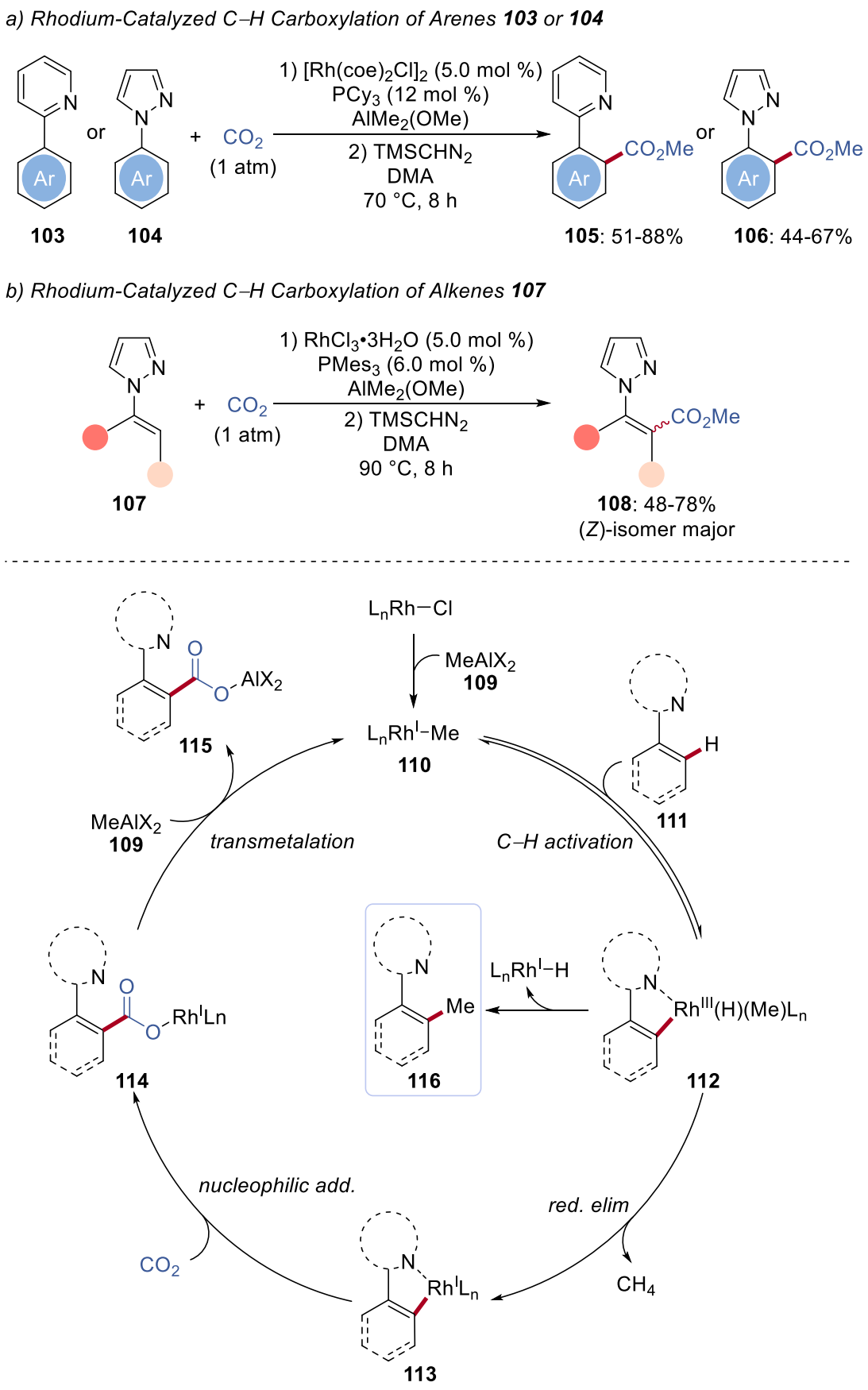

Figure 1.6.2.4. Directing group-assisted C–H carboxylation.

The carboxylation reactions utilizing CO_2 on electrophilic organo(pseudo)halides[162] have been vastly investigated in the last half a century especially in combination with electrochemistry (*vide infra*). The oxidative addition of such organo(pseudo)halides with low-valent transition metals creates a platform for the formation of C–Metal bonds as well. This would then render cross-electrophile coupling (*vide supra*) with CO_2 possible and one such carboxylation reaction with electrophiles instead of the usual nucleophiles was reported by Martin (**Figure 1.6.2.5a**).[163]

a) Palladium-Catalyzed Direct Carboxylation of Bromides

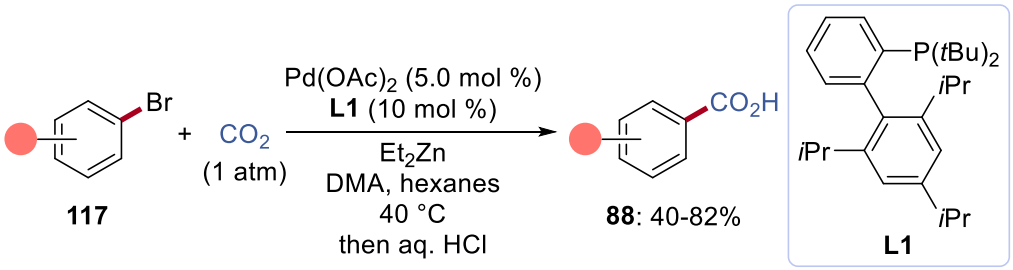

b) Nickel-Catalyzed Carboxylation of Aryl and Alkenyl Chlorides

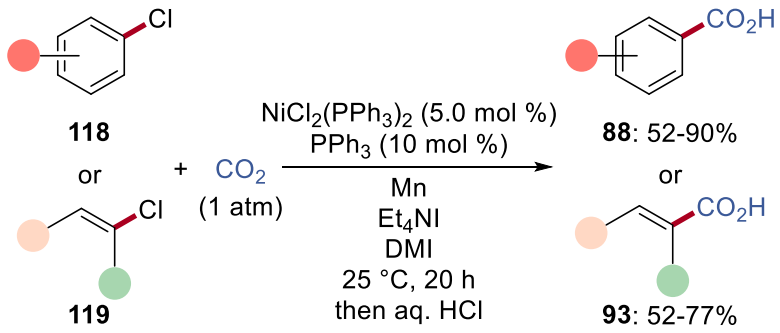

c) Nickel-Catalyzed Carboxylation of Primary, Secondary and Tertiary Alkyl Bromides

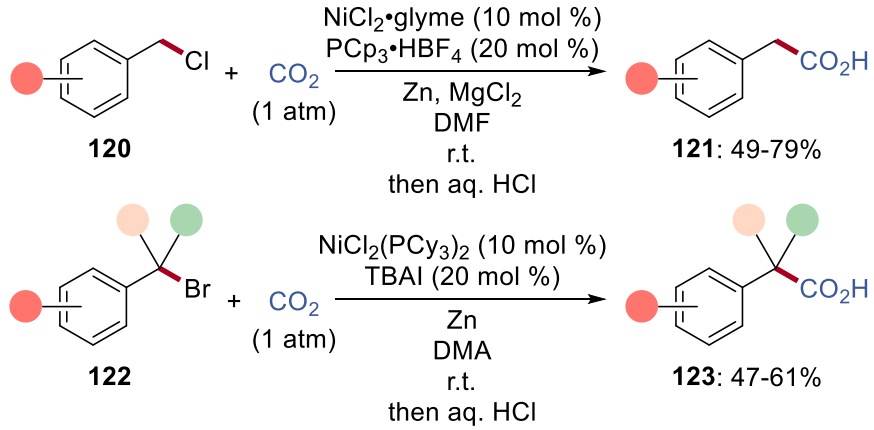

Figure 1.6.2.5. Carboxylation reactions of electrophilic organo(pseudo)halides.

They found that palladium catalysts were capable of the carboxylation of aryl bromides **117** with CO_2 only with the aid of a chemical reductant and in this case, pyrophoric Et_2Zn was utilized. The reductant is essential for the regeneration of the active low-valent palladium(0) catalyst. Thereafter, progresses have been made for using more Earth-abundant transition metals, such as nickel by Tsuji and Fujihara, and Martin independently on carboxylations with aryl chlorides **118** and vinyl chlorides **119** (**Figure 1.6.2.5b**),[164] and primary, secondary and tertiary benzyl halides **122** (**Figure 1.6.2.5c**) respectively.[165]

Among all the carboxylation reactions with organo(pseudo)halides, allylic-containing substrates are especially interesting as they can be further functionalized. Moreover, one can possibly selectively access a stereogenic centre with the right reaction condition.[166] The precise control of the allyl-metal intermediate generated during the course of the reaction defines the regioselectivity of the final carboxylation product. In many cases, the challenge remains for the complete control of one regioisomer. In this aspect, Mita and Sato devised an attractive carboxylation with allylic alcohols **124** or **125**, using a palladium catalyst with Et_2Zn as the reducing agent (**Figure 1.6.2.6a**).[167] The allylic alcohols are activated *via* pyrophoric Et_2Zn metal reductant or possibly through the formation of carbonate with CO_2. The transformation is highly regioselective for the branched product **126**, which makes it valuable. Subsequently, Martin reported site-selective and regio-divergent carboxylation catalyzed by nickel in the expense of high amount of zinc metal reductant (**Figure 1.6.2.6b**).[168] This elegant work switches the regioselective based on the ligand employed. Shortly after, Mei realized a nickel-catalyzed reductive carboxylation with CO_2 using allylic alcohols **129** and propargylic alcohols **60** as coupling partners with the aid of super-stoichiometric amount of manganese metal reductant (**Figure 1.6.2.6c**).[169] This synthesis method paved the way into the synthesis of linear β,γ-unsaturated carboxylic acids **130** with good *E*/*Z* stereoselectivity. Thus, all three synthesis developments granted remarkable control of regioselectivity. These exceptional studies provided the ability to have explicit control over the regioselectivity of the final product but in the heavy expense of utilizing super-stoichiometric metal reductants, which are often pyrophoric and requires

rigorous training for safe handling.

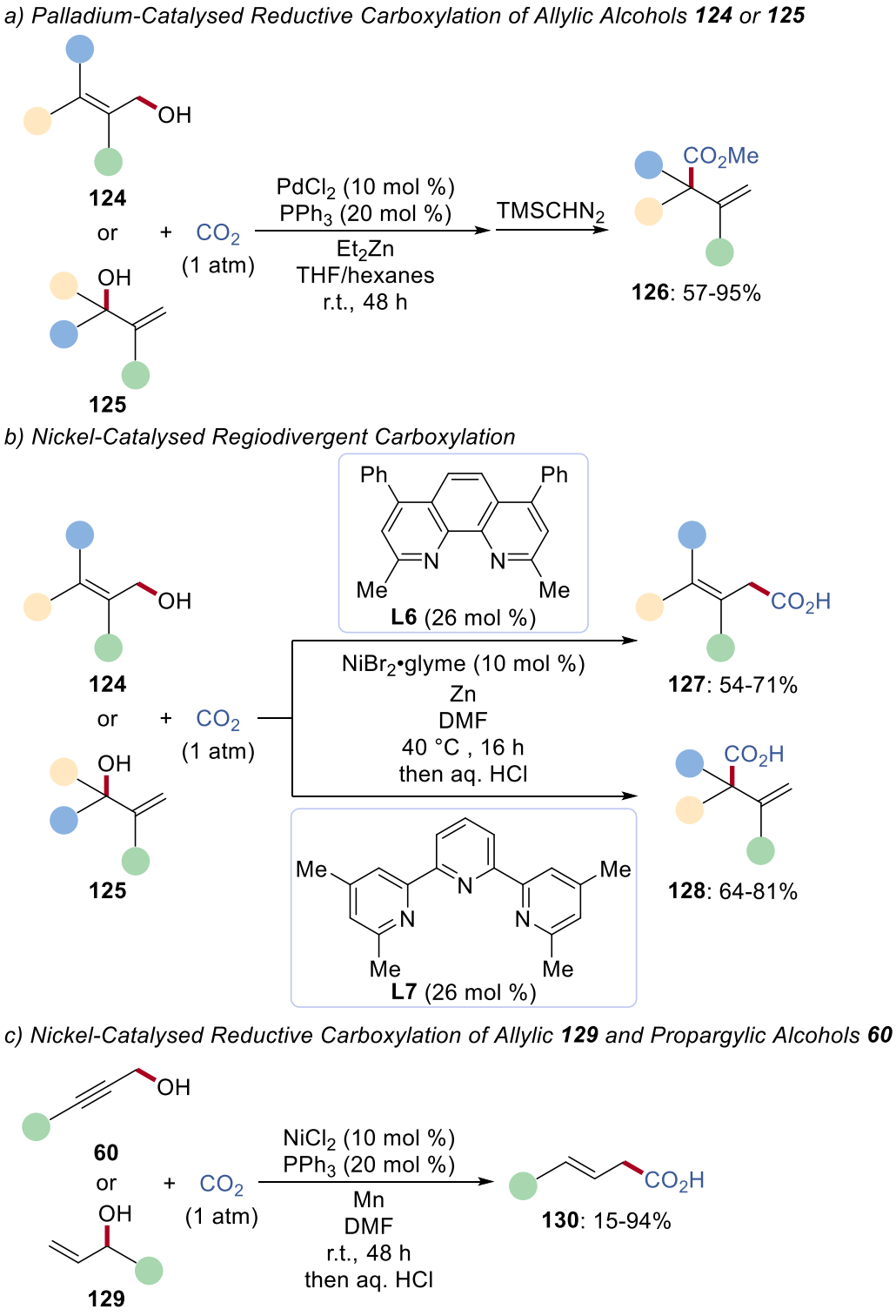

Figure 1.6.2.6. Reductive carboxylation with chemical reductants.

In general, the progress for transition metal-catalyzed carboxylation reactions developed by Yamamoto,[170] Martin,[154a, 163, 168, 171] Tsuji and Fujihara,[172] Daugulis,[173]

He,[174] Sato,[167, 175] Mei[97d, 154b, 169] is considered to be important for future prospects. These examples have aided the evolution of conventional carboxylation of organo(pseudo)halides in the last few decades.[154a, 154b, 154d] Principally, these contemporary usages of CO_2 for carboxylation reactions definitely enhances the functional group tolerance due their milder reaction conditions. However, a major drawback of cross-electrophile coupling with CO_2 is the use of super-stoichiometric amount of metal reductants, some of which are highly pyrophoric that disfavours large-scale synthetical use.

1.6.3 Electro-Reductive Carboxylation

Metalla-electrocatalysis is an important and powerful methodology of providing efficient energy from renewable sources (*vide supra*). It has also been heavily utilized for carboxylation reactions, since the single electron reduction of CO_2 to the radical anion $CO_2^{\bullet-}$ is relatively difficult at E = − 2.21 V *vs.* SCE in DMF[176] and the process is usually irreversible.[177] Transition metal-catalyzed electrocarboxylation using CO_2 provides a promising platform for the synthesis of arenecarboxylic acids from aryl halides.[178] Hence, electrochemical reduction of CO_2 for carboxylation reactions on organo(pseudo)halides were one of the earliest reported successful cross-electrophile coupling reactions with CO_2 in the 1980s, by Perichon and Fauvarque (**Figure 1.6.3.1**).[179] Wherein, a nickel catalyst was able to catalyze the electro-reductive carboxylation of aryl halides with CO_2. The proposed reaction mechanism starts with the oxidative addition of aryl bromide **117** onto the active nickel(0) catalyst **131** to give a nickel(II) complex **132**. This complex would undergo a single electron reduction (SET) to the nickel(I) intermediate **133** and carboxylation with CO_2 to give a nickel(I) arenecarboxylate **134**. Another one-electron reduction regenerates the active nickel(0) catalyst and give the carboxylate **135**. A nickel(III) intermediate has also been proposed by Amatore and Jutand, that can be formed prior to the formation of nickel(I) arenecarboxylate complex **134**.[180]

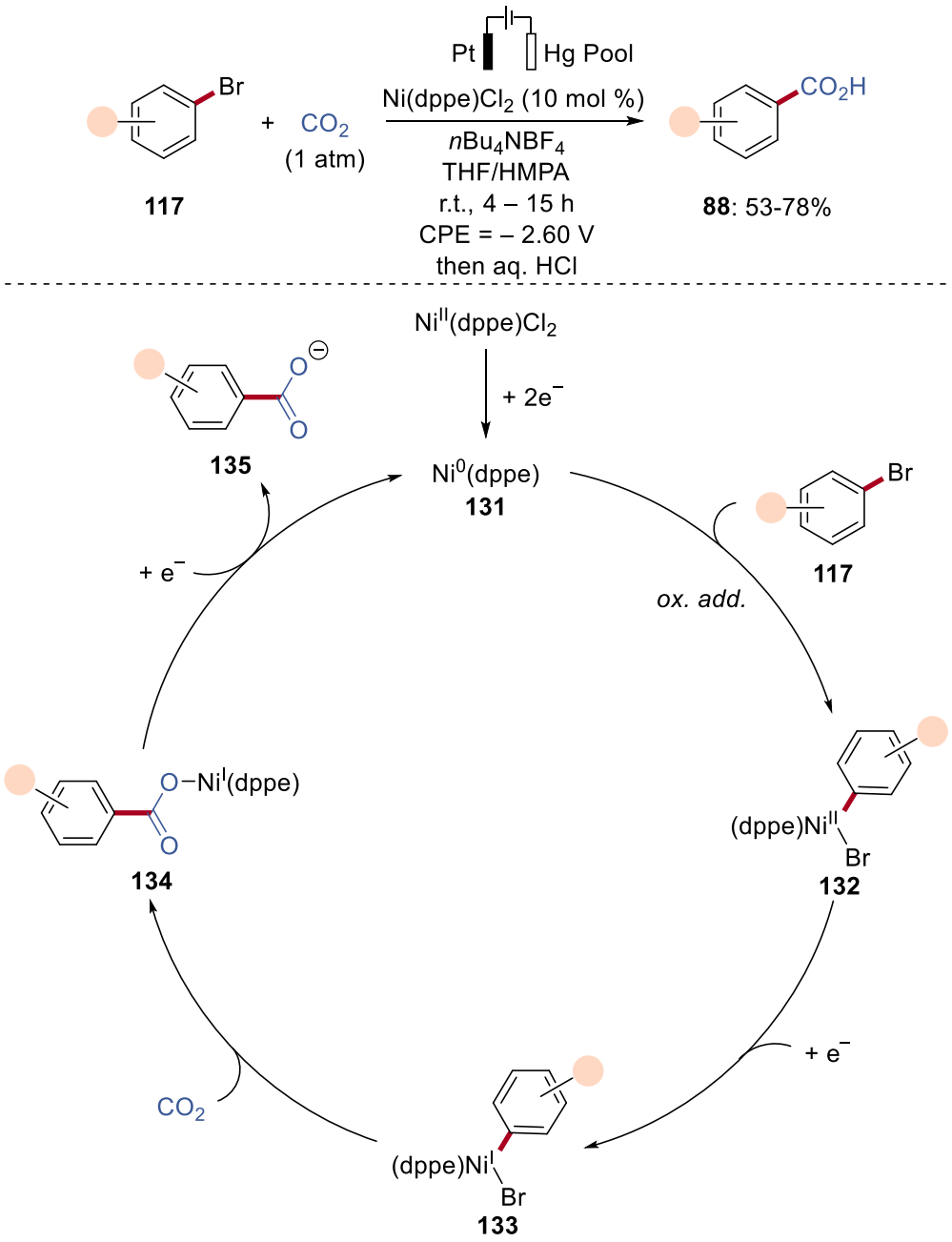

Figure 1.6.3.1. Nickel-catalyzed electrocarboxylation of aryl halides.

Then, Torii and Fauvarque devised a similar carboxylation route with palladium as the catalyst, which have a broader substrate scope than its nickel counterpart (**Figure 1.6.3.2**).[181] They also include the possibility of di-carboxylation on vinyl bromide **136** (**Figure 1.6.3.2b**). Biaryls were not observed as by-products in this case as opposed to metal-free electroreductive carboxylation methods.[182] Subsequently, Jutand showcased the feasibility of using vinyl triflates **139** instead of the usual halogen

leaving groups as coupling partners with CO_2 in a palladium-catalyzed electro-reductive carboxylation (**Figure 1.6.3.2c**).[183]

*a) Palladium-Catalyzed Electro-Reductive Carboxylation on Aryl Halides **87***

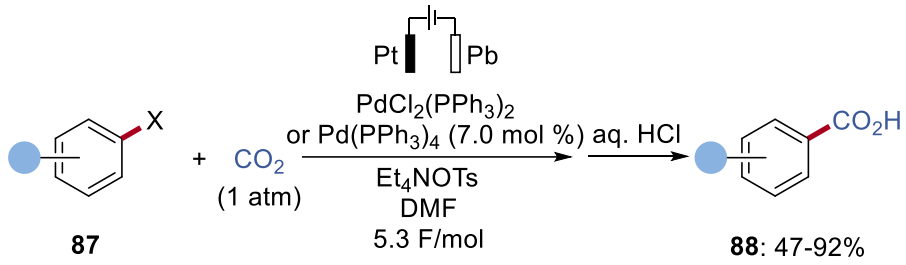

*b) Dual Carboxylations on Vinyl Bromide **136***

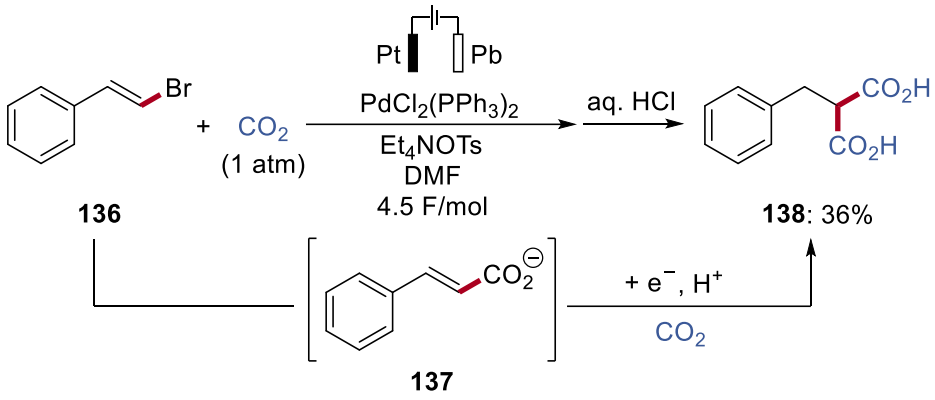

*c) Palladium-Catalyzed Carboxylation of Vinyl Triflates **139***

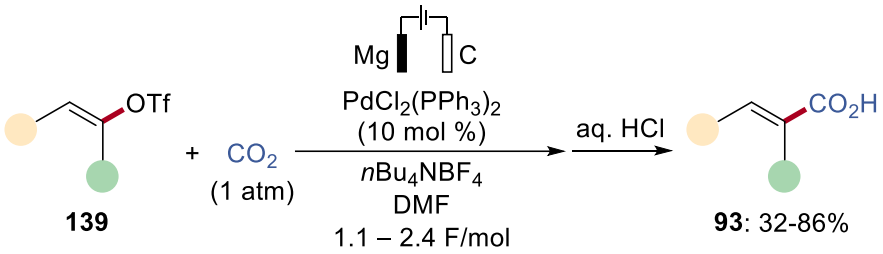

Figure 1.6.3.2. Palladium-catalyzed electro-reductive carboxylation reactions.

One of the earliest well-documented carboxylations on allylic medium with CO_2 was reported by Inoue in 1976 where allylic palladium intermediate was first proposed (**Figure 1.6.3.3a**).[184] First, the formation of π-allylic complex **141** from butadiene **73** with palladium catalyst. Then the insertion of CO_2 to give the carboxylate complex **142**. This would collapse after an intramolecular hydrogen transfer to give carboxylic acid **143a**, which isomerises to compound **143b**. Last, an intramolecular 1,4-addition gives the final five-membered lactone product **140**.

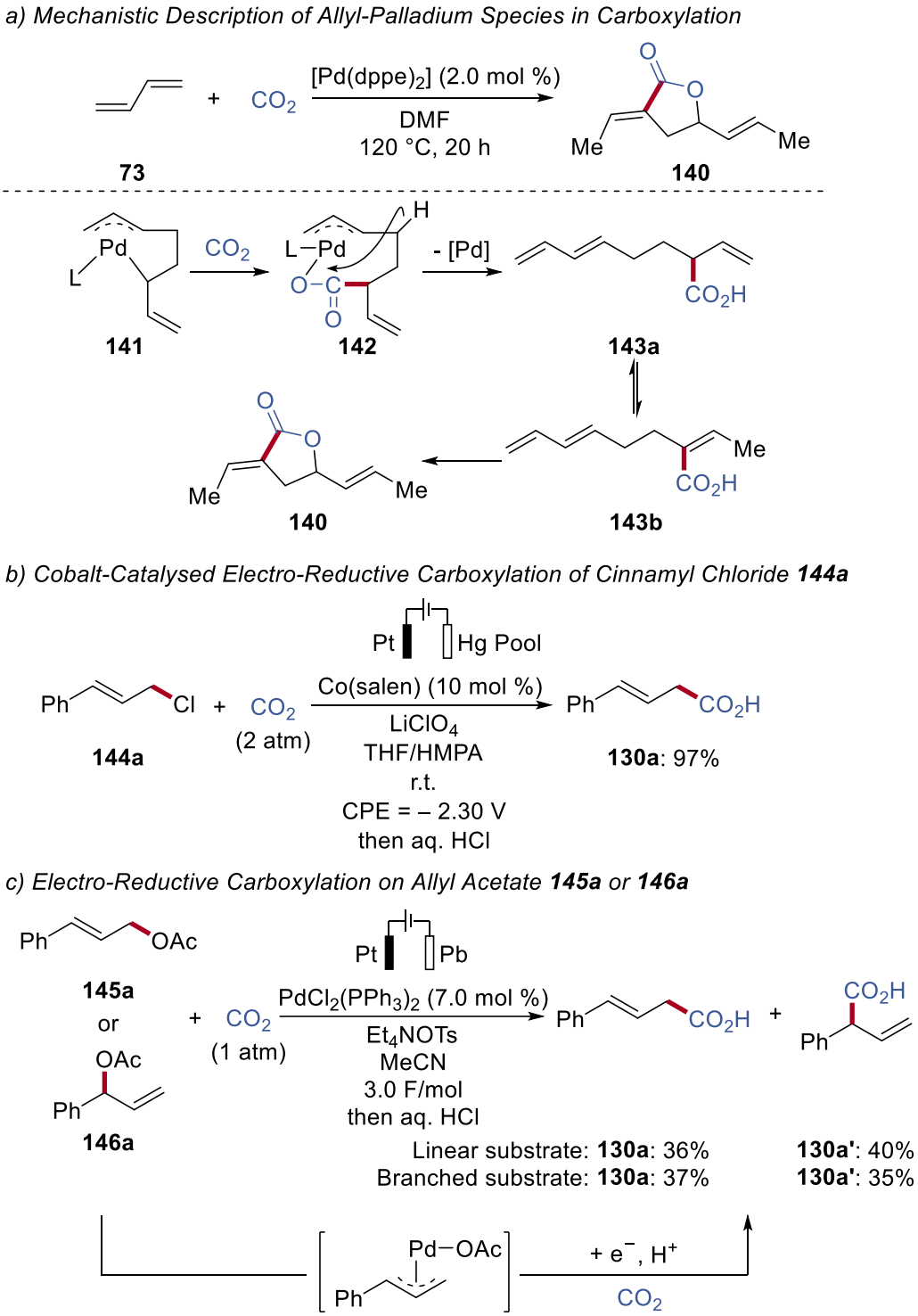

Figure 1.6.3.3. Electro-reductive carboxylations on allylic substrates.

The discovery of the reversible adduct of Co(salen) and CO_2 displayed an intrinsic capability of plausibly delivering the reduced formed of CO_2 through reversible binding.[185] This was exploited by Perichon for the cobalt-catalyzed electro-reductive carboxylation of benzyl chlorides and allylic chloride **144a** but its reaction mechanism

was still underexplored (**Figure 1.6.3.3b**).[186] In the previous report by Torii and Fauvarque, linear allylic acetate **145a** as well as branched allylic acetate **146a** were used with moderate yield for both the regioisomers, showing no significant regioselectivity (**Figure 1.6.3.3c**).[181]

Then, Mei recently reported the reductive electrocarboxylation of allyl esters **145** to give useful carboxylic acids **130'** with moderately good regioselectivity, albeit with precious palladium catalyst (**Figure 1.6.3.4**).[187]

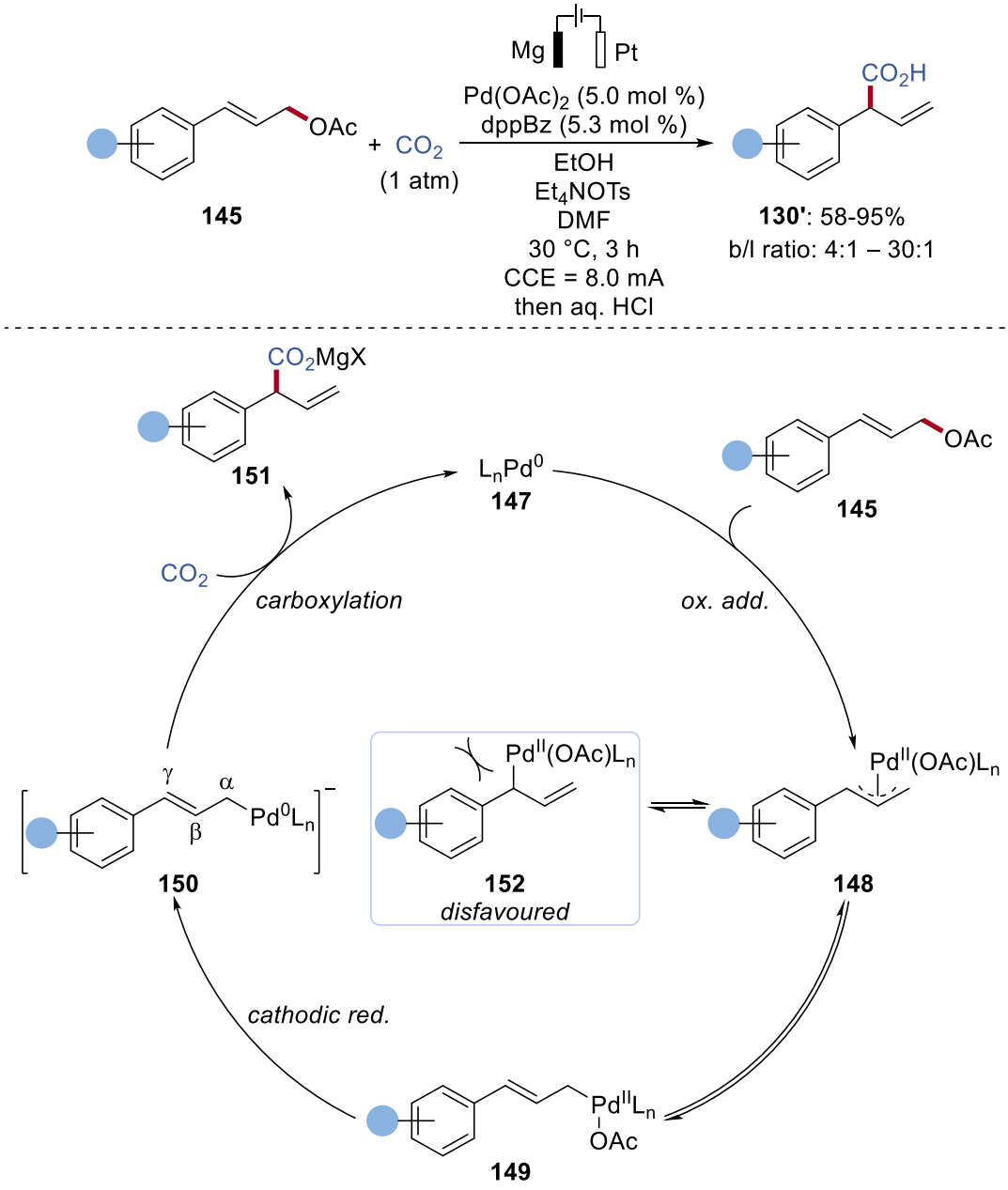

Figure 1.6.3.4. Palladium-catalyzed reductive electrocarboxylation of allyl esters **145**.

A feasible reaction mechanism was proposed by the authors as well. First, oxidative addition of the active palladium(0) catalyst **147** with the allyl ester substrate **145** gives a cationic π-allylpalladium(II) complex **148**, which is in equilibrium with η^1-allylpalladium species **149** and **152**. The branched complex **152** is highly disfavoured due to the significant steric hindrance. Thus, the linear isomer **149** will undergo the ensuing cathodic reduction to anionic η^1-allylpalladium intermediate **150** by an overall two-electron reduction analogous to the studies by Amatore and Jutand on carboxylation of aryl halides.[92a, 178] This intermediate goes through carboxylation with CO_2 at the γ-position to furnish the carboxylate product **151** and regenerate the palladium(0) active catalyst.

1.7 Synthetical Methods for C–S Formation

Sulfur-containing compounds are often perceived as possible therapeutics and they are extensively explored for clinical trials. They are no doubt of utmost contemporary importance towards the dynamic and effective developments of pharmaceuticals and functional materials.[188] As a consequence, an enormous number of resources has been focused on approaches for the formation of C–S bonds in synthetic organic chemistry, which allows simple molecules to be transformed into highly valuable compounds (**Figure 1.7.1**).

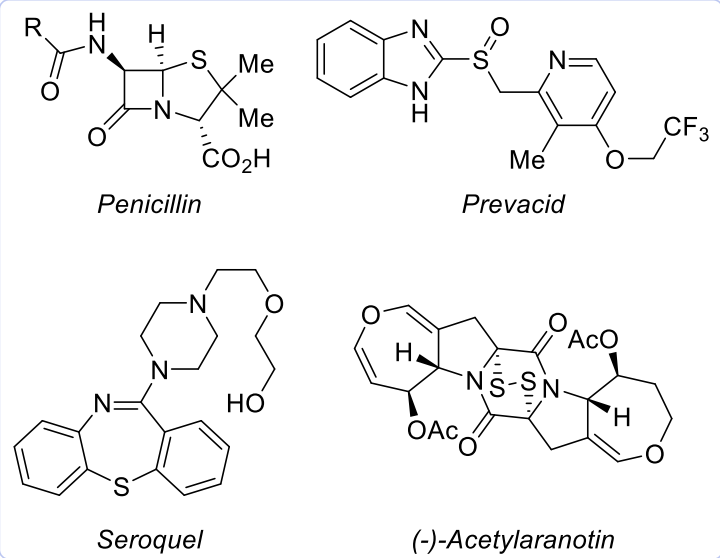

Figure 1.7.1. Selected examples of important therapeutic sulfur-containing compounds.

For example, historically significant and life changing penicillin is one of the most effective sulfur-containing antibiotics for the treatment of syphilis and infections caused by streptococci and staphylococci.[189] Proton-pump inhibitors (PPI) ,such as Prevacid, work efficiently in restricting the production of gastric acid in the stomach.[190] Seroquel, that was approved for the treatment of schizophrenia and bipolar disorder, acts as an atypical antipsychotic drug.[191] This has also since evolved to Seroquel XR which alongside a selective serotonin reuptake inhibitor (SSRI) prove adequate for tackling major depressive disorders.[192] Epipolythiodiketopiperazine alkaloids, like (-)-acetylaranotin, also exhibit many biologically therapeutic properties, e.g. antiviral, antibacterial, antimalarial, antiallergic and cytotoxic characteristics.[193] These

alongside many other medications are important to further improve the efficacy of current and future drugs against strongly-resistant viral or bacterial infections.[194] Hence, there is a need to discover greener and more sustainable methods for the synthesis of sulfur-containing compounds through efficient C–S bond formation.

1.7.1 Conventional Methods for C–S Bond Formation

One of the earliest and most classical protocols for the formation of C–S bonds in alkyl sulfides largely requires harsh alkaline conditions for the substitution reaction of alkyl halides with mercaptans.[195] They suffer, however, from poor yielding reactions and limited substrate scope. The strong and unpleasant odour of mercaptans made the method highly impractical for large-scale synthetic use. Thus, it is highly desirable to develop facile and efficient approaches for the C–S bond formation without compromising the robustness. In the last half a century, transition metal-catalyzed reactions have undoubtedly eased the synthesis of alkyl sulfides akin to many cross-coupling reactions developed through the years (*vide supra*).[196] The traditional cross-coupling reactions of aryl halides or boronic acids with thiols have been well examined, which have been dominated by precious metals, such as palladium and rhodium.[196c, 197]

*a) First Palladium-Catalyzed Cross Coupling of Aryl Halides **87** and Thiols **152** (1978)*

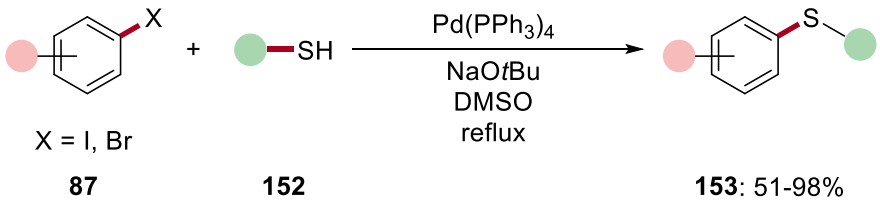

*b) Facile Cross Coupling with Palladium and Ferrocene-based Ligand **L4***

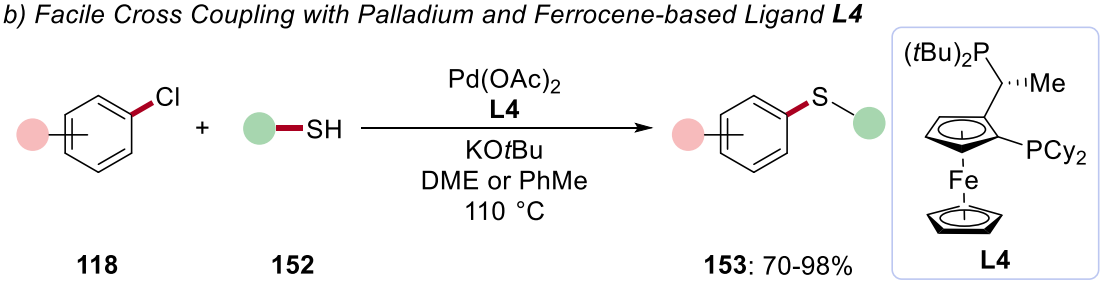

Figure 1.7.1.1. Palladium-catalyzed cross-coupling of aryl halides and thiols.

The first palladium-catalyzed cross-coupling reaction of aryl halides **87** and thiols **152** were presented in 1978 by Migita, where a series of diaryl and arylalkyl sulfides **153** were obtained in good yield (**Figure 1.7.1.1a**).[198] Subsequently, they improved the protocol to obtain higher yields using thiolate anions in EtOH or DMSO solvents.[199] Many years later, Hartwig was able to develop a long-lived catalyst for the palladium-catalyzed coupling of aryl halides **118** and thiols **152** which significantly improved the efficacy from its predecessor (**Figure 1.7.1.1b**).[200] Most of these transformations catalyzed by palladium requires high elevated temperature to ensure efficient transformation. Hence in 2011, Organ reported a low temperature mild palladium-catalyzed C–S bond formation using bulky ligands that encompasses the palladium center (**Figure 1.7.1.2a**).[201] More recently, Morandi reported the C–S formation by single-bond metathesis through reversible arylation, this creates a new pathway of synthesising alkyl sulfides **156** (**Figure 1.7.1.2b**).[202] This was achieved with a palladium-NHC type complex catalyst that promotes the essential C–S metathesis.

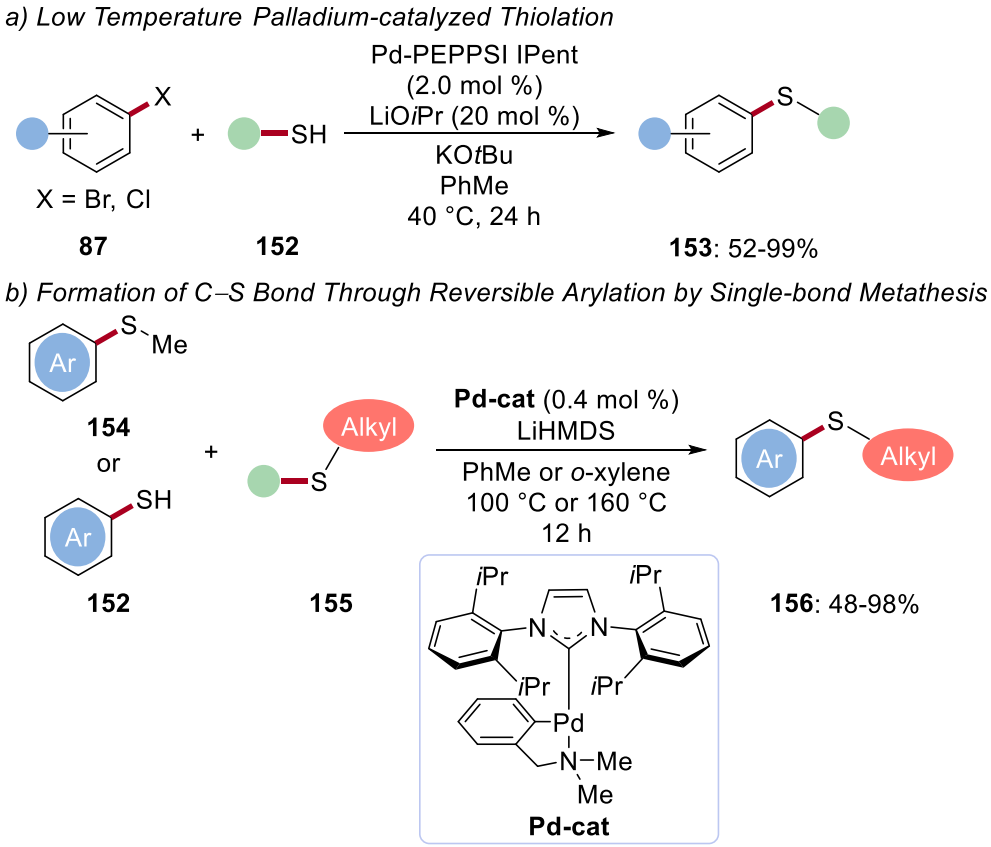

Figure 1.7.1.2. Key developments into palladium-catalyzed C–S bond formation.

The use of rhodium catalysts also expedites the formation of C–S bonds through cross-coupling reactions. In 2008, Yamaguchi was able to show the successful coupling reaction of aryl fluorides **157** and disulfides **158** catalyzed by simple rhodium catalyst (**Figure 1.7.1.3a**).[197c] Subsequently, Lee devised a general rhodium-catalyzed cross-coupling reaction of aryl iodides **159** with thiols **152** using simple triphenylphosphine as the ligand to give diaryl sulfides **153** in good yield (**Figure 1.7.1.3b**).[197b] The C–S cross-coupling reaction was also promoted *via* a well-defined pincer-type rhodium catalyst reported by Ozerov to give diaryl and aryl-alkyl sulfides **153** (**Figure 1.7.1.3c**).[197a]

*a) Rhodium-Catalysed Substitution Reaction of Aryl Fluorides **157** with Disulfides **158***

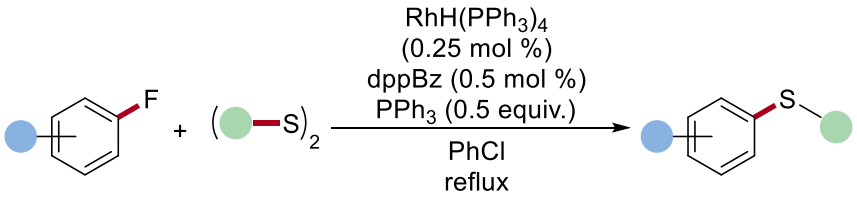

157 **158** **153**: 86-91%

*b) Rhodium-Catalysed Cross-Coupling of Aryl Iodides **159** with Thiols **152***

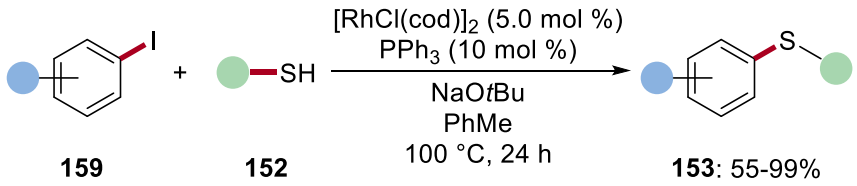

159 **152** **153**: 55-99%

*c) Well-Defined (POCOP)Rh Catalyst for Cross-Coupling of Aryl Halides **87** with Thiols **152***

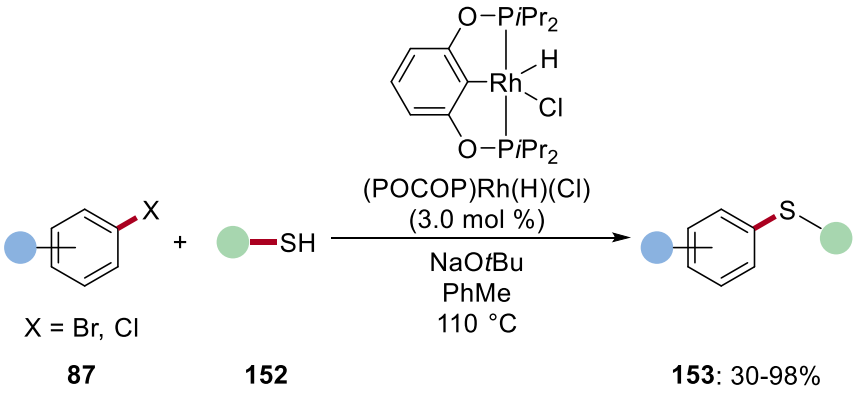

87 **152** **153**: 30-98%

Figure 1.7.1.3. Rhodium-catalyzed C–S formation.

Besides these examples for both palladium and rhodium, gold[203] and silver[204] were also employed as catalysts in several other successful attempts on C(sp^2)–S formation. The use of inexpensive and Earth-abundant 3d transition metals are rising through the

years because of their wide availability as opposed to their precious metal counterparts. In this regard, many synthesis routes for C–S formation were developed with iron,[205] copper,[206] cobalt[207] and manganese.[208] In addition, significant advances were made mostly with nickel as the catalyst which gave impetus and prompted further investigations on the utilization of nickel for C–S bond forming catalysis (**Figure 1.7.1.4**).[209]

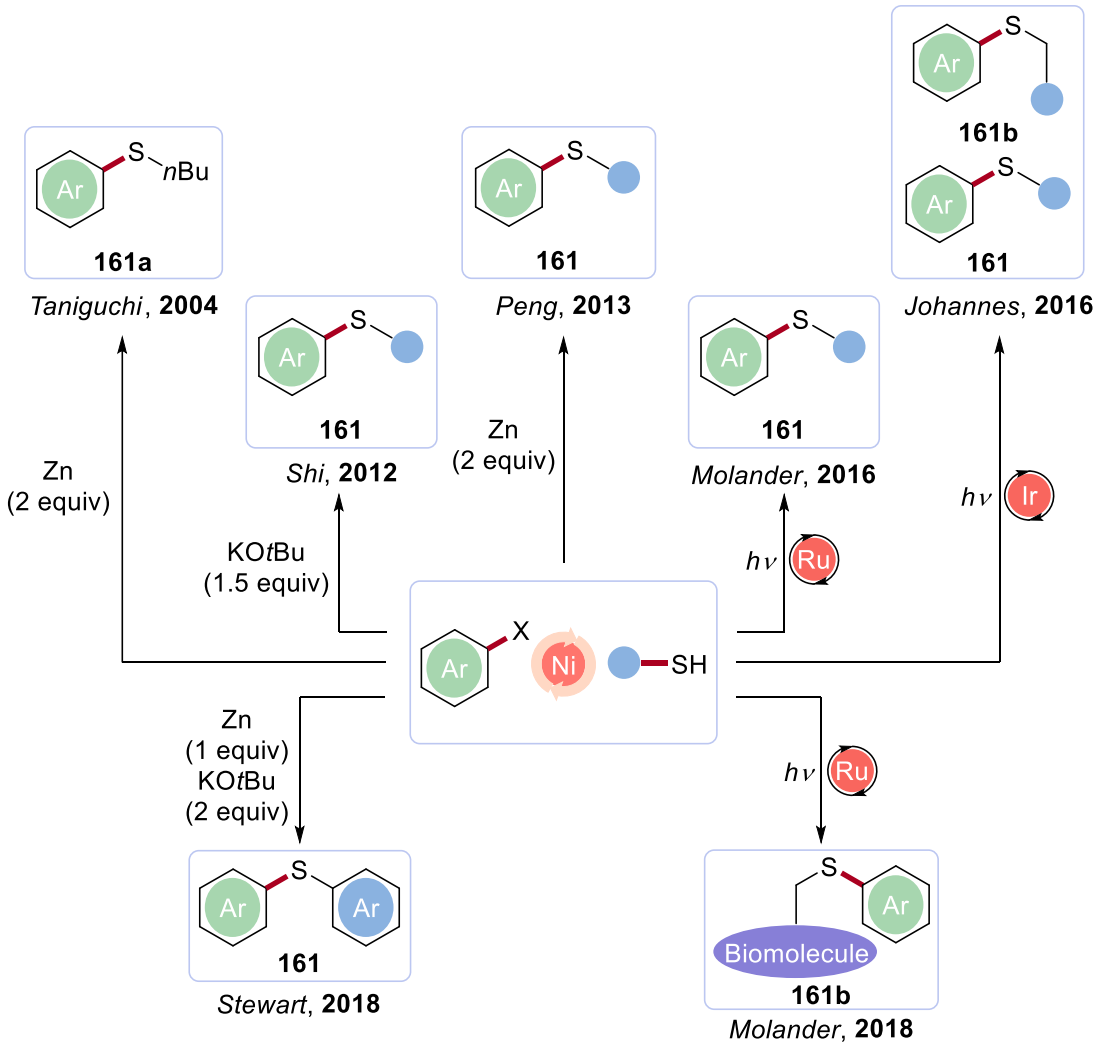

Figure 1.7.1.4. Nickel-catalyzed C–S bond forming reactions.

1.7.2 Contemporary Protocols for C–S Formation

Even though thiols and their oxidized derivatives are commonly used as coupling partners in traditional transition metal-catalyzed C–S forming reactions, they are impractical for large-scale synthesis protocols, since thiols **152** are known to be highly

toxic with foul-smelling odour. This heavily impedes its utilization in modern synthetic organic chemistry. In addition, there is also a lack of availability for alkyl thiols and disulfides which hinders the application and substrate scope. There have been studies on ways to circumvent such limitations, including the use of sulfuration agents, such as KSAc or KSCN, for the synthesis of both symmetrical and unsymmetrical sulfides.[210] Besides these, sulfur powder and $Na_2S_2O_3$ were also successfully employed for the synthesis of aryl and alkyl sulfides which allows alternatives to avoid the use of thiols **152**.[211] The use of electrophilic substrates accentuate the feasibility of cross-electrophile coupling reactions (*vide infra*) for C–S formation, which involves the application of electrophilic benzenesulfonothioates or thiosulfonates. These substrates could be activated by organometallic reagents such as Grignard as reported by Knochel[212] or organolithium compounds (**Figure 1.7.2.1a**).[213] The substrate scope and chemoselectivity are, however, heavily limited due to the harsh reaction conditions.

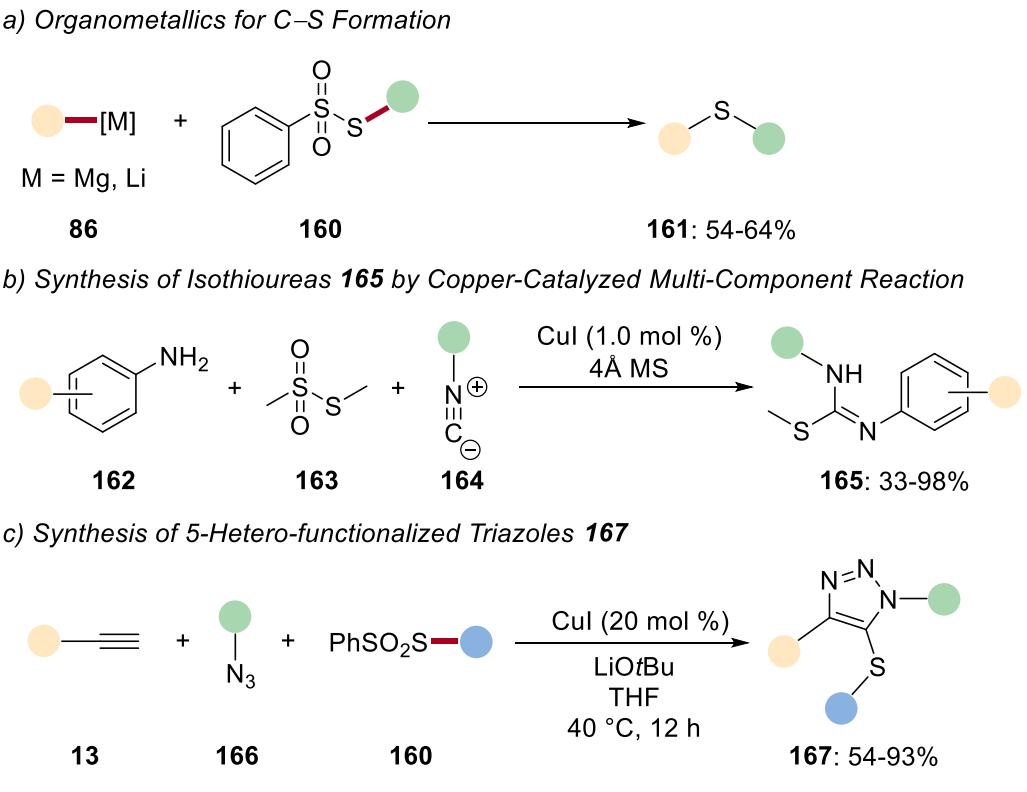

Figure 1.7.2.1. Use of electrophilic thiosulfonates for C–S formation.

Hence, seminal work by Ruijter, Orru and Mae reported a multi-component synthesis of isothioureas **165** using isocyanides **164**, electrophilic thiosulfonates **163** and amines

162 under copper catalysis (**Figure 1.7.2.1b**).[214] Later, Xu devised an elegant multi-component route for making 5-hetero-functionalized triazoles **167** by a copper(I)-catalyzed "interrupted click" reaction using various terminal alkynes **13**, azides **166** and thiosulfonates **160** (**Figure 1.7.2.1c**).[215] More recently, Wang and Ji developed a one-pot multi-component copper-catalyzed reaction for the synthesis of sulfur-containing trisubstituted imidazoles. The use of *S*-aryl benzenesulfonothioate simplified the protocol for a diverse range of substituted imidazoles **170** to be obtained (**Figure 1.7.2.2a**).[216] Around the same time, Wang and Ji also reported a nickel-catalyzed defluorinative reductive cross-electrophile coupling reaction of *gem*-difluoroalkanes **171** with electrophilic thiosulfonates **160** or with selenium sulfonates, which gave access to monofluoroalkanes **172** that could be useful in medicinal chemistry or for drug discovery (**Figure 1.7.2.2b**).[217]

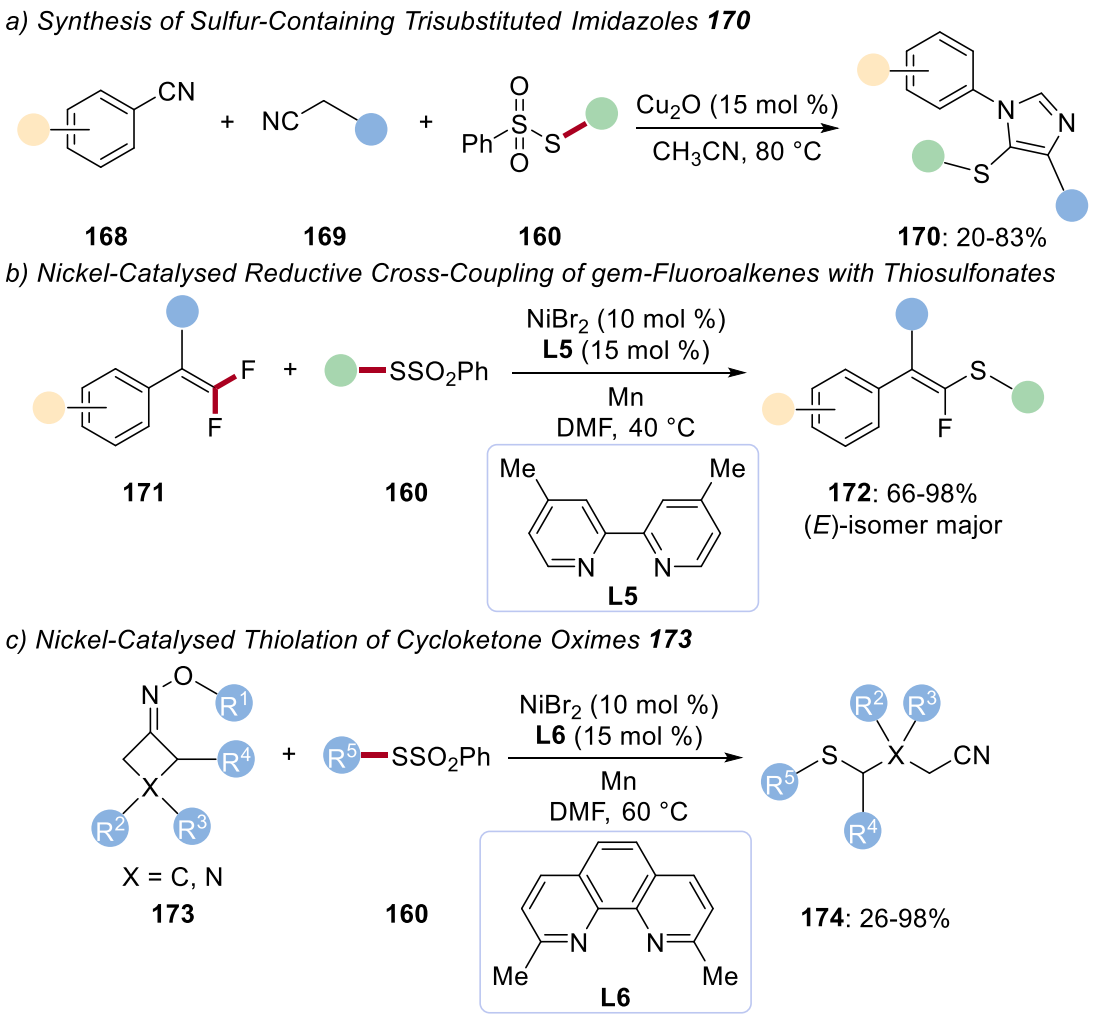

Figure 1.7.2.2. Progress in the utilization of electrophilic thiosulfonates **160**.

In the same context, the reductive thiolation and selenylation of cycloketone oxime **173** catalyzed by nickel were showcased by Wang and Ji as well. The final alkyl sulfide products **174** were obtained through a C–C bond cleavage of cycloketone oxime and then C(sp^3)–S bond formation with the aid of thiosulfonates (**Figure 1.7.2.2c**).[218] Both the above reductive cross-coupling reactions required the undesirable use of super-stoichiometric amount of manganese reductant. A remarkable nickel-catalyzed reductive thiolation and selenylation for the C(sp^3)–S formation with unactivated bromides **175** was first reported by Ackermann, Wang and Ji (**Figure 1.7.2.3**).[219]

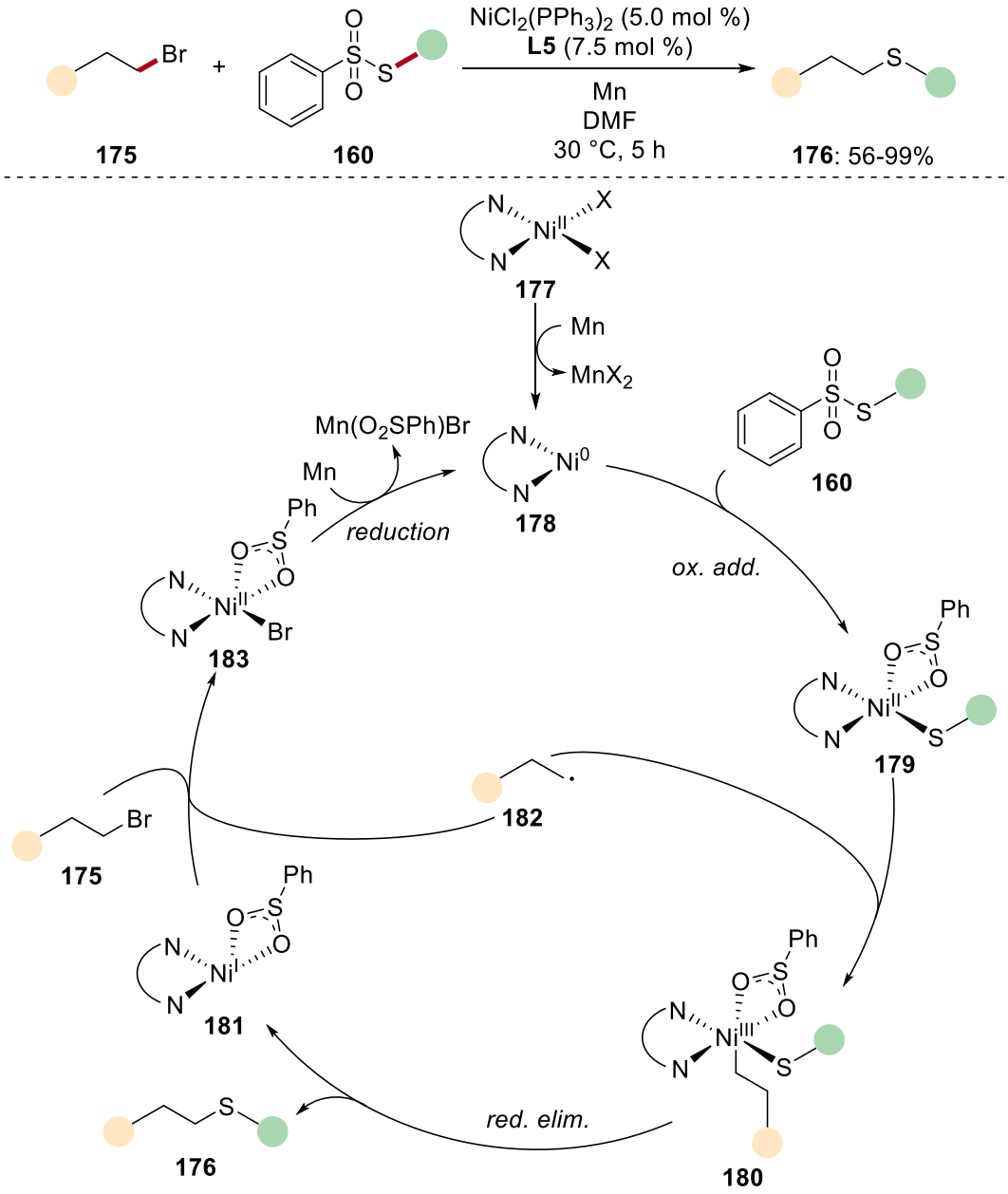

Figure 1.7.2.3. Nickel-catalyzed reductive thiolation with thiosulfonates **160**.

They were able to achieve thiolation on primary and secondary alkyl bromides to access many unsymmetrical aryl-alkyl and alkyl-alkyl sulfides/selenides with excellent chemoselectivity utilizing a simple nickel catalytic regime, though super-stoichiometric amount of chemical metal reductant was still essentially needed. The authors proposed a possible reaction mechanism based on their detailed mechanistic and kinetic investigations (**Figure 1.7.2.3**). First, the *in situ* reduction of nickel(II) **177** to active nickel(0) catalyst **178** by the manganese reductant occurred. Then the oxidative addition of thiosulfonates **160** onto the active nickel(0) catalyst **178** happens generating a nickel(II) intermediate **179**. This would react with an alkyl radical **182** to give a nickel(III) intermediate **180**. Then reductive elimination of this intermediate gave the desired sulfide product **176** and regenerates the nickel(I) complex intermediate **181**, which further reacts with the alkyl bromide **175** to give the alkyl radical **182** and nickel(II) complex **183**. Subsequent reduction of nickel(II) complex **183** regenerates the active nickel(0) catalyst **178** and, thus, closing the catalytic cycle. Most of the examples for C–S formation thus far required large amounts of chemical reductants, which produced major amounts of chemical waste, and, therefore, impeded their usage in large-scale synthesis.

*a) Electrochemical Nickel-Catalyzed Thiolation of Aryl Bromides **117***

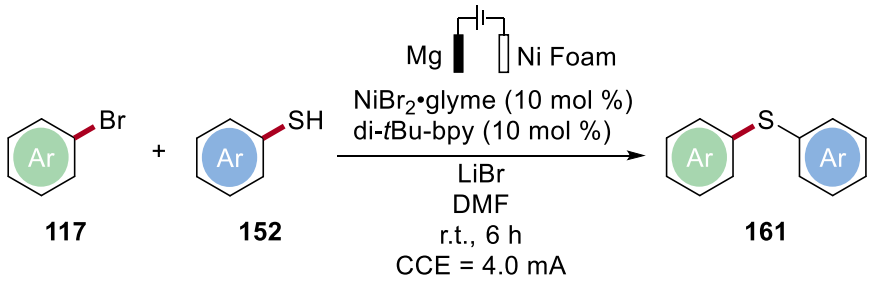

*b) Electrochemical Nickel-Catalyzed Thiolation of Aryl Iodides **159***

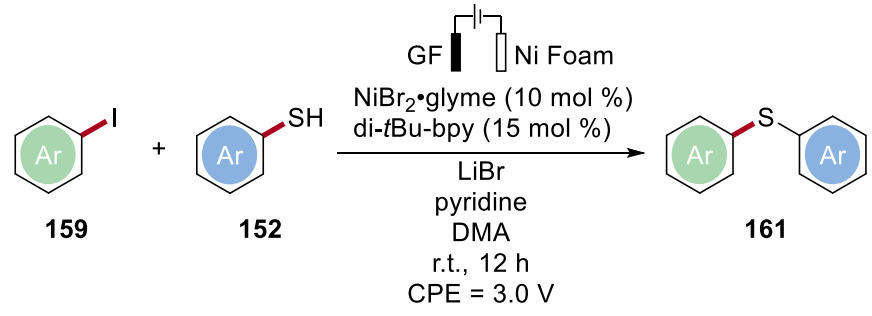

Figure 1.7.2.4. Electrochemical nickel-catalyzed thiolation reactions.

The merger of electrochemistry with 3d transition metal catalysis has brought forth a plethora of opportunities (*vide supra*) and C–S formation with the aid of electrosynthesis was recently explored. Recent studies for electrochemical thiolation feature independent concurrent reports by Mei (**Figure 1.7.2.4a**) as well as Wang and Pan (**Figure 1.7.2.4b**) which both showcased the feasibility of merging sustainable electrochemistry with challenging C–S formation.[220] These electrochemical nickel-catalyzed thiolations of aryl halides with aryl thiols gave rise to diaryl sulfides **161** with moderate to good yield in both reports, yet they represented a major step forward in terms of such innovative and environmentally friendly synthetical protocols. This also showed that the search for more renewable synthesis methods is crucial due to a lack of better alternatives for cross-electrophile couplings.

2. Objectives

In the last few decades, immense progress has been made with transition metal-catalyzed C–H activation[20] as an effective tool for the functionalization of inert C–H bonds in organic molecule. In addition, this exceptional atom-[19c, 19d] and step-economical[19a, 19b] methodology is very potent for the construction of C–C and C–Het bonds. However, most developed C–H activation methods required rather harsh reaction conditions, use of expensive precious metals and generate stoichiometric amount of undesirable chemical waste. Thus, it is important to expand the arsenal of C–H activation reactions in synthetic organic chemistry to realize more efficient and sustainable protocols. The utilization of metalla-electrocatalysis for C–H activation provided a phenomenal step forward in terms of renewability and intellectual discoveries.[102]

In this context, the application of Earth-abundant and inexpensive cobalt salts as catalyst further promotes the green concept without compromising the efficacy, showcasing its viability for oxidative C–H activation reactions.[47] Despite that, many of these transformations requires the indispensable need for stoichiometric amount of toxic metal-based oxidants. These limitations should be addressed with a hypothesis of an innovative strategy encompassing electrochemical cobalt-catalyzed C–H/N–H coupling with unsaturated compounds (**Figure 2.1**). This would allow the manipulation of anodic oxidation to regenerate the active catalyst within the catalytic cycle and furthermore, cathodic reduction to generate molecular hydrogen bypassing the need to use sacrificial oxidants. Thus, a more sustainable synthesis strategy could be realized.

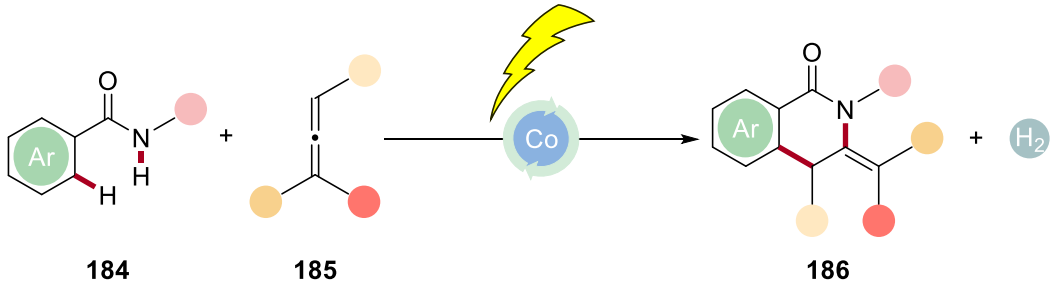

Figure 2.1. Electrochemical cobalt-catalyzed C–H/N–H activation for annulations of allenes **185**.

The alarming proliferation of CO_2 levels in the atmosphere prompted the advancements of CO_2 fixation methodologies.[117, 120] The investments in carbon capture and utilization (CCU) strategies have moved towards using CO_2 as an excellent C1 building block despite its inert nature.[121b, 122] Many transition metal-catalyzed reactions with CO_2 are indeed effective in the valorisation of CO_2 but only few selected ones have been industrialised which allows large-scale consumption of atmospheric CO_2. These includes the synthesis of cyclic and polycarbonates, as well as salicylic acid.[129-131, 152] Hence, there is a strong need to develop efficient and sustainable methodologies for the large-scale fixation of CO_2 into simple valuable compounds.

With utmost relevance, the formation of a stable C–C bond through carboxylation reaction with CO_2 offers value-added carboxylic acid moiety on any substrate which could be further functionalized easily.[127a] Transition metal-catalyzed carboxylation reactions have been performed with organoboron reagents, direct C–H carboxylation of acidic C–H bonds, directing group aided C–H carboxylation and organo(pseudo)halides.[125b] However, harsh reaction conditions were required for the activation of CO_2 and in most cases, the usage of precious metals cannot be bypassed. The renaissance of electrosynthesis allows vast exploration for new sustainable carboxylation protocols.[102a] Therefore, traditional impediment should be countered with a hypothesis of a merger between Earth-abundant 3d metal electrocatalysis and cross-electrophile carboxylation of allylic halides **187** with atmospheric CO_2 (**Figure 2.2**). Fundamentally, the conventional use of super-stoichiometric amount of chemical metal reductant which are frequently pyrophoric in nature can be avoided by the utilization of cathodic reduction.

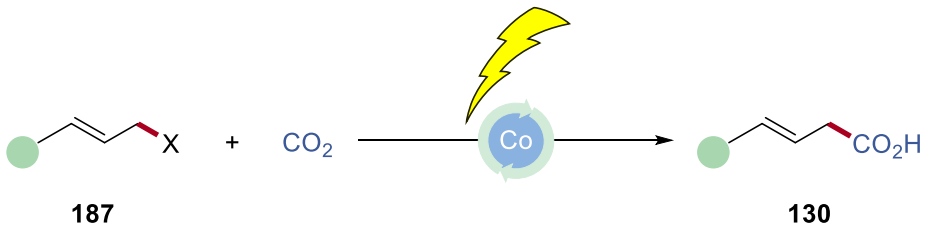

Figure 2.2. Electro-reductive cobalt-catalyzed carboxylation of allylic halides **187**.

Sulfur-containing moieties are frequently found in pharmaceuticals or functional materials.[188] The constant race to discover new drugs with high efficiency and efficacy yet minimal toxicity calls for a high magnitude of innovation with regards to synthetical protocols. In this context, the formation of C–S bonds in the synthesis of diverse compounds from simple molecules is particularly crucial for medicinal chemistry. Hence, great interest exists in simplifying the synthesis of sulfur-containing compounds. Transition metal catalysis have revolutionised C–S formation but in most cases, thiols were used as coupling partners which are highly toxic with foul-smelling odour. As such, they are relatively impractical as large-scale applications. In this circumstances, electrophilic thiosulfonates have been recently included in contemporary methodologies for C–S formation.[212-219] This class of substrates are bench-stable, odourless and easily synthesized under mild reaction conditions ensuring high conversions and functional group tolerance. Even though, there have been reports utilizing thiosulfonates in cross-electrophile coupling for C–S formation, they are relying heavily on super-stoichiometric amounts of chemical metal reductants. Thus, a hypothesis that the C–S formation could be simplified to a more viable method by combining cross-electrophile coupling and the recent success of Earth-abundant 3d metal electrocatalysis should be thoroughly explored (**Figure 2.3**). As aforementioned, electrochemical reduction not only facilitates the cathodic reduction of the catalytic intermediates, but also often provides milder reaction conditions.

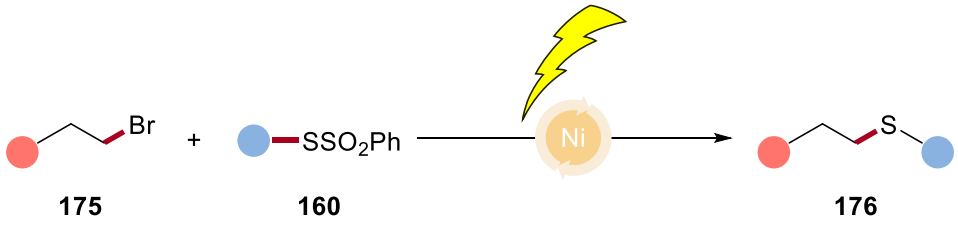

Figure 2.3. Electro-reductive nickel-catalyzed thiolation of alkyl bromides **175**.

3. Results and Discussion

3.1 Cobaltaelectro-Catalyzed C–H/N–H Annulations

Allenes are known to be reactive and versatile unsaturated building blocks for organic syntheses.[67a-e] The use of oxidative C–H activations has shown to be highly effective for annulation reactions with unsaturated compounds within a one-pot fashion.[221] In this regard, allenes offer a unique and exciting reactivity as compared to their alkenyl or alkynyl counterparts[67c] for intermolecular C–H annulation reactions.[52c] Most of the reported C–H annulation reactions with allenes either required precious metal catalyst or expensive and unsustainable silver(I) or copper salts as sacrificial oxidants.[67a, 67b, 69, 222] Nonetheless, great advancements were made for oxidative C–H annulation with allenes but rarely presented with electrochemistry[223] and the inclusion of renewable metalla-electrocatalysis was not conceived until this report.[224] The hypothesis that an electro-oxidative cobalt-catalyzed C–H/N–H annulation protocol could be made feasible based on precedent by Ackermann in electrochemical cobalt-catalyzed C–H oxygenation[225] and subsequent alkyne annulation.[108f]

3.1.1 Optimisation and Substrate Scope of C–H/N–H Annulation Reaction

Optimisation studies on the electro-oxidative allene annulations by mild cobalt-catalyzed C–H activation were done by Dr. T. H. Meyer.[224] The optimisation investigations included the efficacy test of different cobalt salts as catalysts and the choice of solvent. In addition, several different additives, which are mainly carboxylate salts, were tested and control experiments for optimising the catalyst loading, current applied and reaction time. As a result, the use of $Co(OAc)_2•4H_2O$ (20 mol %), NaOPiv (2.0 equiv.) in MeOH at 40 °C for 15 h under a constant current electrolysis of 2.0 mA were identified as optimal. Reticulated vitreous carbon (RVC) and platinum plate were chosen as the best choice for the anode and the cathode, respectively.

With the optimised reaction condition in hand, the robustness of this electro-oxidative allene annulation by cobalt catalysis was investigated with benzamides **8** bearing a 2-pyridyl-*N*-oxide bidentate directing group together with various 1,3-disubstituted internal allenes **185** (**Figure 3.1.1.1**). The electrochemical C–H activation interestingly furnished the corresponding *exo*-methylene isoquinolones **186** with moderate to good yield. 1,3-Disubstituted internal allenes containing esters **185a**-**185d** were tolerated as well as the use of electron-donating *p*-methoxy-containing benzamide proved viable under the mild regime. Consequently, the regioselectivity was especially intriguing as 1-substituted or 1,1-disubstituted allenes gave the *endo*-methylene isoquinolone products.[224]

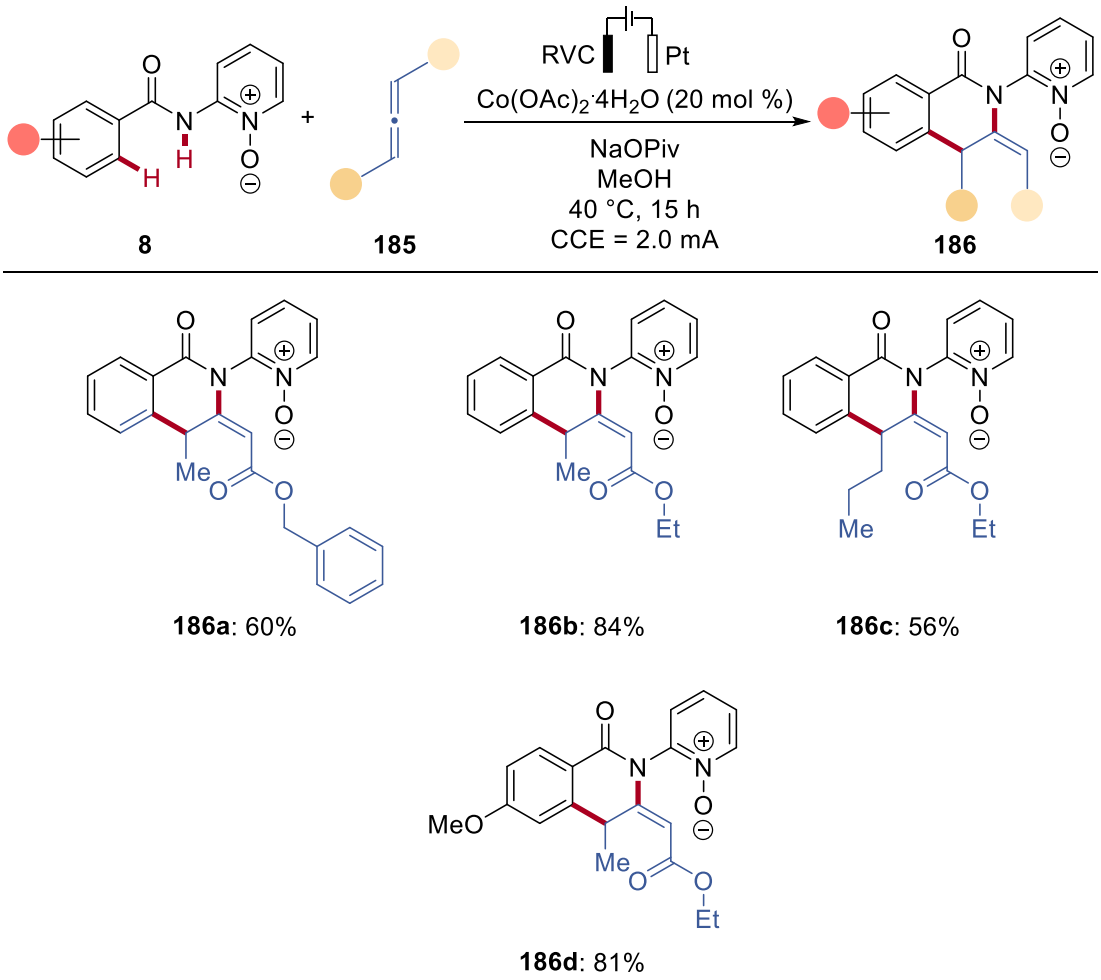

Figure 3.1.1.1. Substrate scope of electro-oxidative allene annulation by cobalt catalysis of benzamides **8** with 1,3-disubstituted internal allenes **185**.

The ^{1}H NMR analysis of the *exo*-methylene products **186** obtained proved to be challenging as they exist apparently as rotamers,[226] since a set of conformers were

formed due to the restricted rotation about the single bond of the 2-pyridyl-*N*-oxide bidentate directing group. Hence, attempts were made to cleave off the oxygen atom of 2-pyridyl-*N*-oxide directing group since it was the main cause of the constraint on the rotation about the single bond. To our delight, the exposure of *exo*-methylene isoquinolones **186** to stoichiometric amount of PCl_3 conducted under inert atmosphere allowed the deoxygenation to occur to obtain both *exo*- **188** and *endo*-methylene deoxygenated products **188'** quantitatively, albeit with partial double bond isomerization (**Figure 3.1.1.2**).

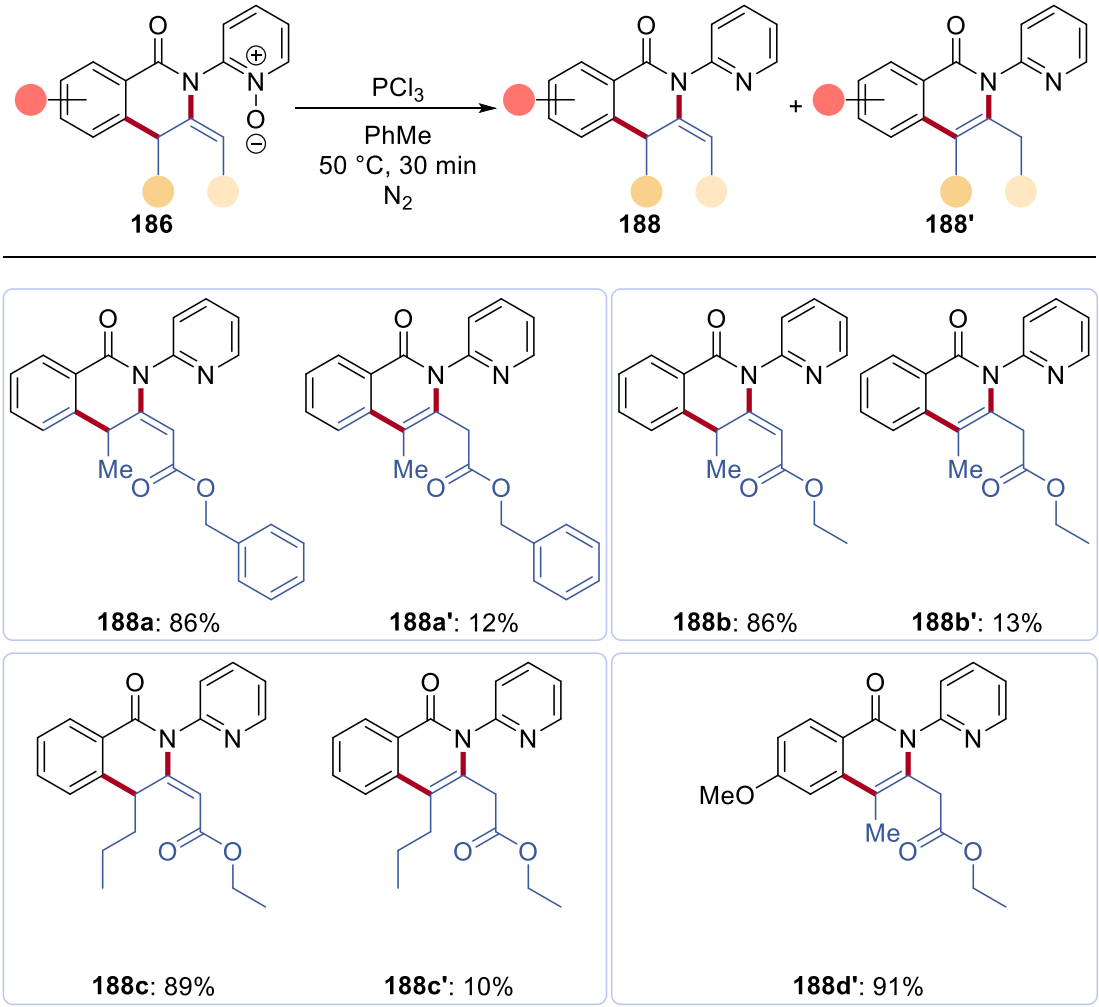

Figure 3.1.1.2. Resolving rotamers through deoxygenation of 2-pyridyl-*N*-oxide.

In the course of the deoxygenation process, the harsh environment causes the isomerisation. Hence, the *endo*-methylene products **188'** were thermodynamically more stable, since they were obtained in a higher yield than the *exo*-form **188**.

3.1.2 Mechanistic Studies

Selected mechanistic investigations were done to elucidate the mode of action for this electro-oxidative cobalt-catalyzed allene annulation reaction. H/D exchange experiments were performed under the standard reaction conditions in isotopically-labelled solvent d_3-MeOH, but no deuterium incorporation was observed in the isolated product **189a** (**Figure 3.1.2.1**).

a) H/D Exchange

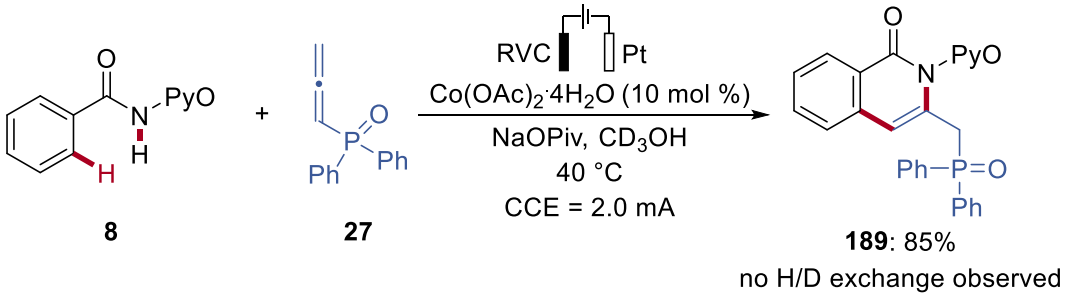

Figure 3.1.2.1. Attempted H/D exchange studies.

3.1.3 Proposed Catalytic Cycle

A minor KIE value of 1.2 was obtained by Dr. T. H. Meyer[224] through the comparison of the initial reaction rates of two independent reactions which suggested that the C–H cleavage step is not the rate-determining step, being analogous to previous studies.[108f, 225] Furthermore, other mechanistic investigations including CV studies were also performed to allow a plausible reaction mechanism to be proposed (**Figure 3.1.3.1**).

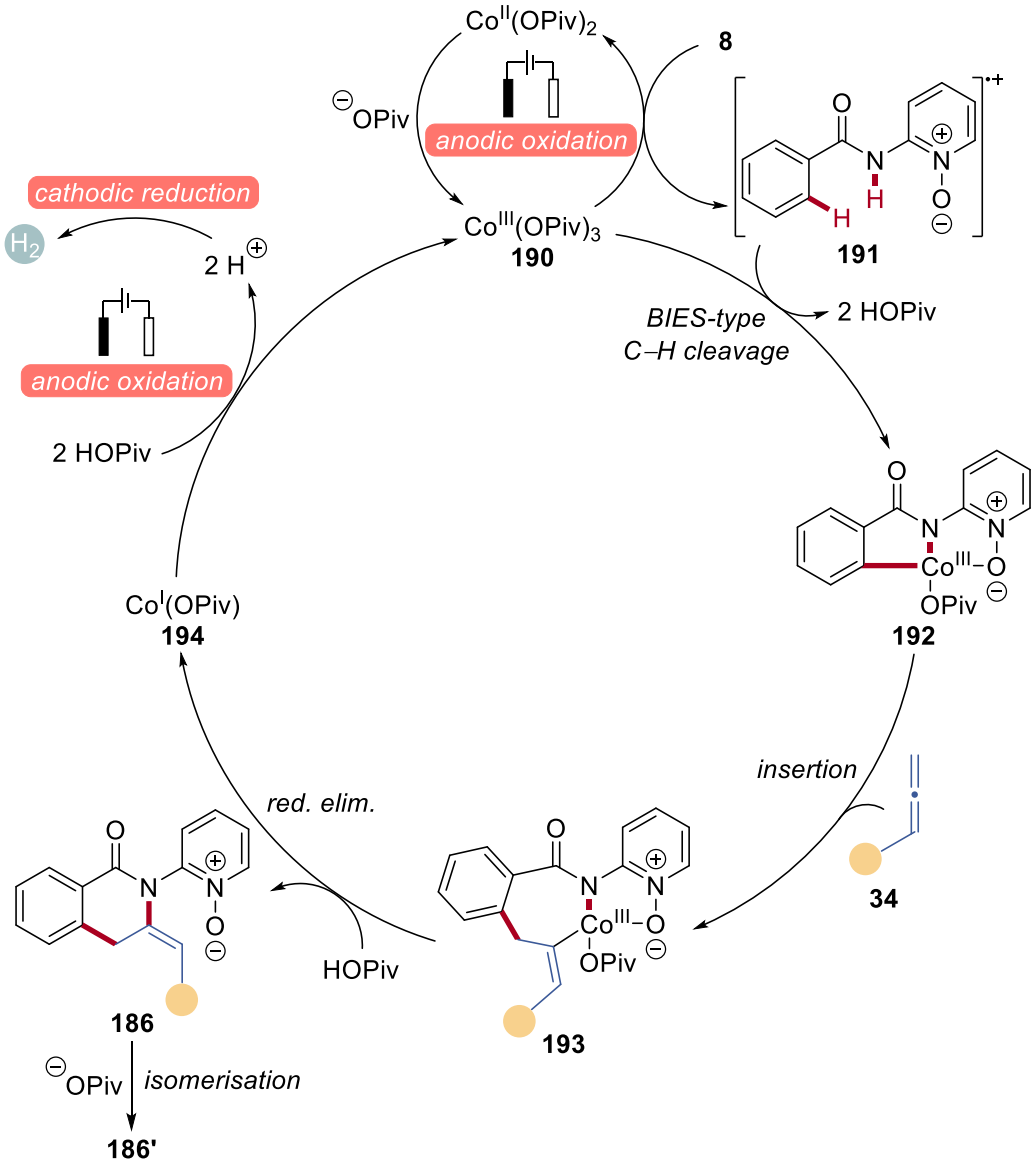

Figure 3.1.3.1. Proposed catalytic cycle for the cobaltaelectro-catalyzed C–H/N–H annulation.

The electrochemical C–H/N–H activation reaction starts with anodic oxidation of the cobalt(II) precatalyst to the active cobalt(III) intermediate **190**. Then, an efficient BIES-

type C–H scission assisted by the carboxylates occurs to give cobaltacycle complex **192**. Subsequent migratory insertion of allene **34** results to deliver a seven-membered cobaltacycle intermediate **193** with the new C–C bond formed. Furthermore, DFT studies by Dr. J. C. A. Oliveira displayed that the insertion of allene **34** distal to the substituent is more preferable by 2.2 kcal mol^{-1} over the insertion pathway proximal to the substituent which allows high regioselectivity to be achieved.[224] The ensuing reductive elimination step provides the *exo*-methylene isoquinolone **186** and the reduced cobalt(I) species **194**. For 1-substituted and 1,1-disubstituted allenes, the *exo*-methylene isoquinolone undergoes an irreversible isomerisation in the presence of base to the *endo*-form **186'** as it is more favoured thermodynamically. Anodic oxidation of the reduced cobalt(I) rejuvenates the active cobalt(III) catalyst **190** with a counter cathodic reduction of the protons to molecular hydrogen gas which closes the catalytic cycle.

3.2 Electro-Reductive Cobalt-Catalyzed Carboxylation with CO_2

Introducing carbon capture and utilization (CCU) protocols in synthetic organic chemistry help to potentially resolve the worldly problem of global warming and climate change.[121b] There are a remarkable number of methodologies and carboxylation is one of the most attractive method as it allows the synthesis of carboxylic acids using CO_2 as an effective and inexpensive C1 synthon.[122e, 123] The value-added products could be further functionalized easily, and, hence, carboxylation is a highly sought-after technique, especially after the successful industrialisation of the synthesis of salicylic acid.[152] Transition metal-catalyzed carboxylation have created facile reductive carboxylation protocols but they were largely dominated by precious metals, such as palladium and rhodium.[227] In addition, the use of super-stoichiometric amounts of metal reductant, which are often pyrophoric, for cross-electrophile coupling reaction impedes the practicality of the transformation. Electrochemical reductive carboxylation reactions were one of the first conceived protocols in the 1980s but the choice of electrodes and the harsh reaction conditions often hinder the scope and feasibility.[154b] Moreover, electrochemical set-ups were tedious and electrosynthesis was not popularly adopted until recent decades. However, the resurgence of this green and sustainable strategy stems from, among many other factors discussed in **Chapter 1.4** (*vide supra*), the development of commercially available electrochemical equipment which are highly user-friendly and easily applicable.[102a] Based on precedents,[186-187] the hypothesis of an electro-reductive cobalt-catalyzed carboxylation of allylic chlorides could be made plausible with atmospheric CO_2, which is devoid of using chemical metal reductant.[228] In addition, it should also feature Earth-abundant cobalt catalysis for the synthesis of styrylacetic acids, which are particularly useful as key synthons of numerous γ-arylbutyrolactones which are structural motifs found in various natural products.[229]

3.2.1 Optimisation Studies

The optimisation investigations were commenced by testing a series of cobalt salts as the pre-catalyst and the search for a suitable ligand for the envisioned electro-reductive cobalt-catalyzed carboxylation system with cinnamyl chloride **144a** as model substrate (**Table 3.2.1.1**). In particular, Co(salen) did not perform well even at higher catalytic loading of 10 mol % (entries 1–2). Simple $Co(OAc)_2$ provided the best results (entry 3), alongside $CoCl_2$ which gave a slightly lower yield (entry 22). A variety of ligands was also tested, which included mono- and bidentate phosphine-based ligands and bidentate nitrogen-based ligands (entries 3–21). However, simple and cost-effective triphenylphosphine gave the best results. In addition, the regioselectivity proved to be a challenge to control and substituted phenathroline ligands gave higher selectivity for the branched product **130a'** (entries 18 and 19). Whereas, phosphine-based ligands did not provide high regioselectivity, although a vast number of secondary phosphine oxides (SPO) remained to be investigated.[230] The synthesized mechanistically relevant cobalt(I) complex **195** (*vide infra*) proved to be effective as the reaction reached completion already after 2 hours of reaction time.

Subsequently, additives and electrolytes were tested (**Table 3.2.1.2**) to probe if the efficacy of the electro-reductive cobalt-catalyzed carboxylation could be increased. Both nBu$_4$NPF$_6$ and nBu$_4$NI (entries 2 and 5) gave comparable yield and no change in the regioselectivity. Notably, the stoichiometrically use of both electrolytes gave yield similar to the use of higher equivalents of Et_4NOTs. Furthermore, the addition of EtOH or CsF (entries 3–4) did not attribute to any positive effect observed by previous reports.[175, 187] It was thought that EtOH may be useful for the activation of CO_2, while CsF was proposed to allow a better dissolution of CO_2 into the solution. The addition of NaI without electrolyte (entry 6) did not give any conversion highlighting the essential need for the electrolyte.

Table 3.2.1.1. Optimisation of catalysts and ligands.[a]

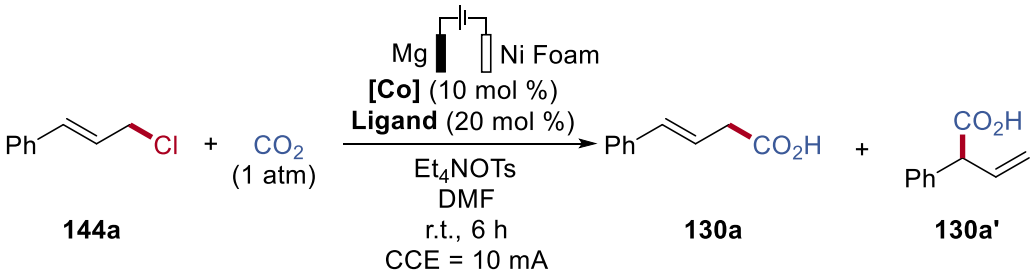

Entry	[Co]	Ligand	Yield (**130a**/**130a'**)[b,c]
1	Co(salen)	---	17% (1:1)[d]
2	Co(salen)	---	25% (1:1)
3	**$Co(OAc)_2$**	**PPh_3**	**57% (1:1)**
4	$Co(OAc)_2$	dppe	25% (1:1)
5	$Co(OAc)_2$	xantphos	49% (1.1:1)
6	$Co(OAc)_2$	DPEphos	57% (1.1:1)
7	$Co(OAc)_2$	bipyridine	12% (1:2)
8	$Co(OAc)_2$	1,10-phenanthroline	8% (1:1.2)
9	$Co(OAc)_2$	*rac*-BINAP	60% (1:2.1)
10	$Co(OAc)_2$	(*S*)-(−)-Cl-MeO-BIPHEP	57% (1:1.1)
11	$Co(OAc)_2$	CyJohnPhos	37% (1.3:1)
12	$Co(OAc)_2$	PCy_3	32% (1:1.1)
13	$Co(acac)_2$	DPEphos	57% (1:1)
14	$Co(OAc)_2$	neocuproine	25% (1:1.4)
15	$Co(OAc)_2$	tri(*t*Bu)terpy	5% (1:1.4)
16	$Co(OAc)_2$	dppf	50% (1:1.2)
17	$Co(OAc)_2$	2,9-di-anisyl-1,10-phen	48% (1:1.2)
18	$Co(OAc)_2$	bathocuproine	5% (1:1.5)
19	$Co(OAc)_2$	4,7-diphenyl-1,10-phen	14% (1:1.9)
20	$Co(acac)_2$	DavePhos	44% (1:1.4)
21	$Co(acac)_2$	dppf	50% (1:1.2)
22	$CoCl_2$	PPh_3	54% (1:1)
23	$CoCl(PPh_3)_3$ **195**	---	58% (1:1)[e]

[a] Reaction conditions: **144a** (0.25 mmol), [Co] (10 mol % unless otherwise stated), ligand (20 mol %), Et_4NOTs (0.38 mmol), DMF (5.0 mL), CCE = 10 mA, 6 h, 25 °C, Mg anode, nickel-foam cathode. [b] Isolated yield (**130a**/**130a'**). [c] Selectivity determined by ^1H NMR. [d] Co(salen) (5.0 mol %). [e] 2 h reaction time.

Table 3.2.1.2. Optimisation of additives.[a]

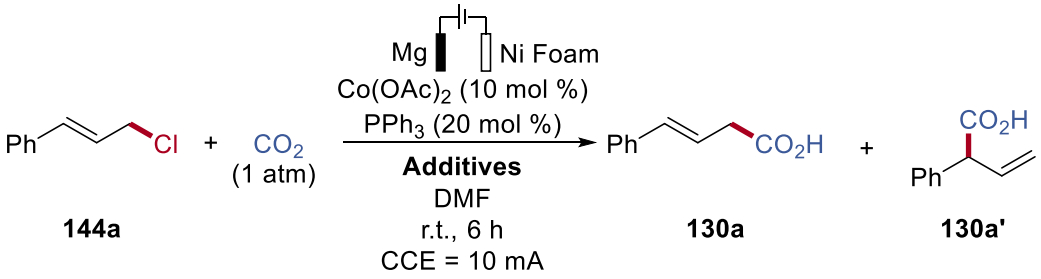

Entry	Additive 1	Additive 2	Yield (**130a**/**130a'**)[b,c]
1	---	Et_4NOTs (1.5 equiv)	57% (1:1)
2	**---**	***n*Bu$_4$NPF$_6$ (1.0 equiv)**	**59% (1:1)**
3	EtOH	Et_4NOTs (1.5 equiv)	42% (1:1)
4	CsF	Et_4NOTs (1.5 equiv)	27% (1.2:1)[d]
5	---	*n*Bu$_4$NI (1.0 equiv)	58% (1:1)
6	NaI	---	traces

[a] Reaction conditions: **144a** (0.25 mmol), $Co(OAc)_2$ (10 mol %), PPh_3 (20 mol %), additives (0.25 mmol unless otherwise stated), DMF (5.0 mL), CCE = 10 mA, 6 h, 25 °C, Mg anode, nickel-foam cathode. [b] Isolated yield (**130a**/**130a'**). [c] Selectivity determined by ^{1}H NMR. [d] 16 h reaction time.

Different concentrations and temperatures were also tested to showcase that the reaction worked optimally at low to ambient temperature (**Table 3.2.1.3**). Higher concentration of cinnamyl chloride **144a** also provided a lower yield (entry 4).

Table 3.2.1.3. Optimisation of temperature and concentration.[a]

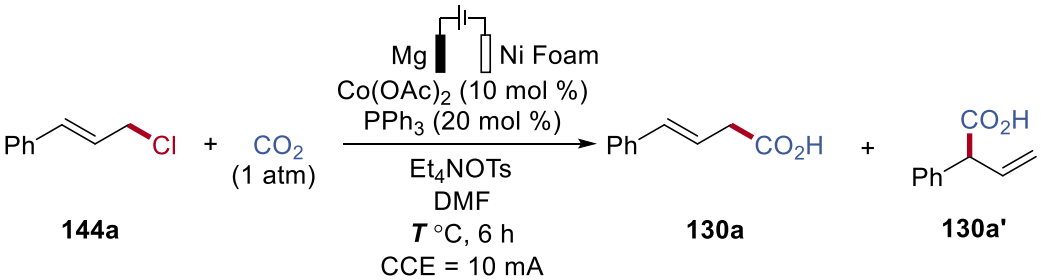

Entry	*T* (°C)	Conc. of **144a**	Yield (**130a**/**130a'**)[b,c]
1	25	0.05 M	57% (1:1)
2	60	0.05 M	42% (1:1)
3	0	0.05 M	59% (1:1)
4	25	0.10 M	44% (1:1)

[a] Reaction conditions: **144a** (as specified), $Co(OAc)_2$ (10 mol %), PPh_3 (20 mol %), Et_4NOTs (0.38 mmol), DMF (5.0 mL), CCE = 10 mA, 6 h, *T* °C (as specified), Mg anode, nickel-foam cathode. [b] Isolated yield (**130a**/**130a'**). [c] Selectivity determined by ^{1}H NMR.

Different solvents were next screened (**Table 3.2.1.4**) as they are highly important for a good dissolution of CO_2 and have high level of conductivity for the electrolysis to take place. It was found that polar aprotic solvents, such as DMF and DMSO (entries 1–3), worked well for the cobaltaelectro-catalyzed carboxylation which is in agreement with preceding investigations.[231] THF was also tested as solvent (entry 4) which gave a lower yield. The combination of the solvent THF and DMPU or DMSO (entries 5–6) did not give any desired product when using [Co(salen)] as the catalyst.

Table 3.2.1.4. Optimisation of solvents.[a]

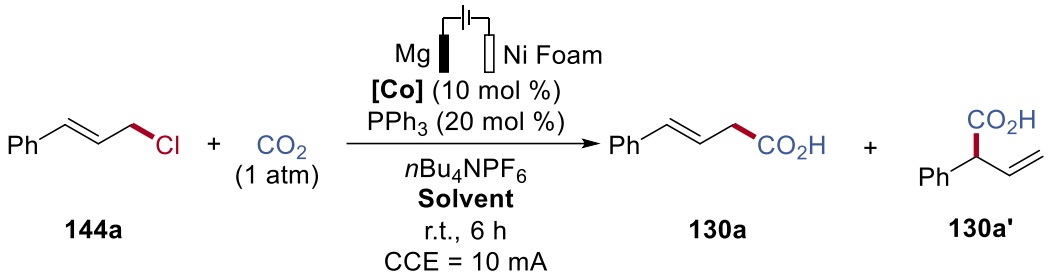

Entry	[Co]	Solvent	Yield (**130a**/**130a'**)[b,c]
1	**$Co(OAc)_2$**	**DMF**	**59% (1:1)**
2	$Co(OAc)_2$	DMSO	42% (1:1)
3	$Co(OAc)_2$	DMA	37% (1:1)
4	$Co(OAc)_2$	THF	31% (1:1)
5	[Co(salen)]	THF/DMSO (1:1)	---
6	[Co(salen)]	THF/DMPU (1:1)	---

[a] Reaction conditions: **144a** (0.25 mmol), $Co(OAc)_2$ (10 mol %), PPh_3 (20 mol %), nBu$_4$NPF$_6$ (0.25 mmol), solvent (5.0 mL), CCE = 10 mA, 6 h, 25 °C, Mg anode, nickel-foam cathode. [b] Isolated yield (**130a**/**130a'**). [c] Selectivity determined by ^{1}H NMR.

Another important factor which was examined during the optimisation studies was the choice of electrodes as they influenced the reaction most fundamentally owing to the potential window required for the transformation to take place (**Table 3.2.1.5**). Several different combinations of anodes and cathodes showed moderate to good response to give the desired product (entries 1–9). In accordance to the electrochemical series, magnesium has one of the lowest reduction potentials and can be easily oxidised among the listed trials of anode materials, which translate to its performance in this electro-reductive cobalt-catalyzed carboxylation. The successful use of an expensive

samarium rod electrode for CO_2 reduction reported by Mellah allowed an *in situ* electrogenerated Kagan-type reductant for the carboxylation reaction of aryl halides prompted the trial with samarium plate anode (entries 6 and 8).[232] However, it did not give the envisioned efficacy. In addition, the change in cathode from nickel-foam to platinum (entry 7) had no apparent difference. Carbon-based material was also attempted (entry 10) as anodes, but to no avail, as there were no sufficient effective reductants present in the system.

Table 3.2.1.5. Optimisation of electrode materials.[a]

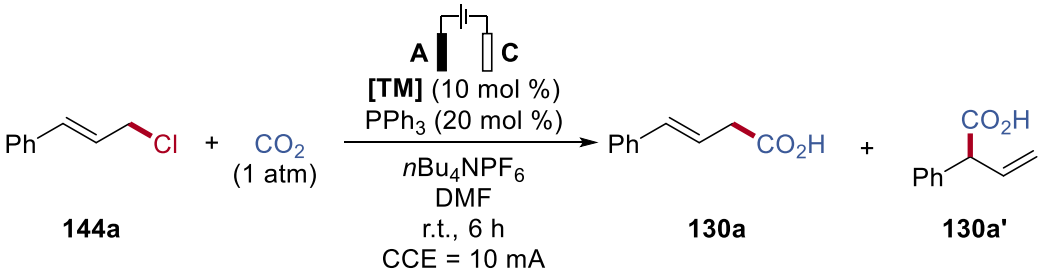

Entry	[TM]	Anode	Cathode	Yield (**130a**/**130a'**)[b,c]
1	**$Co(OAc)_2$**	**Mg**	**Ni-Foam**	**59% (1:1)**
2	$Co(OAc)_2$	Al	Ni-Foam	46% (1:1)
3	$Co(OAc)_2$	Fe	Ni-Foam	37% (1:1)
4	$Co(OAc)_2$	Cu	Ni-Foam	10% (1:1)
5	$Co(OAc)_2$	Zn	Ni-Foam	38% (1:1)
6	$Co(OAc)_2$	Sm	Ni-Foam	25% (1:1)
7	$Co(OAc)_2$	Steel	Pt	42% (1:1)
8	$NiBr_2$·diglyme	Sm Plate	Ni-Foam	37% (1:1)
9	$NiBr_2$·diglyme	Fe	Ni-Foam	45% (1:1)
10	$Co(OAc)_2$	Graphite	Ni-Foam	traces
11	$Co(OAc)_2$	Ni Rod	Ni-Foam	---

[a] Reaction conditions: **144a** (0.25 mmol), [TM] (10 mol %), PPh_3 (20 mol %), *n*Bu_4NPF_6 (0.25 mmol), DMF (5.0 mL), CCE = 10 mA, 6 h, 25 °C, electrodes as specified. [b] Isolated yield (**130a**/**130a'**). [c] Selectivity determined by ^1H NMR.

Control experiments (**Table 3.2.1.6**) were done to verify the essential role of the electricity and of the cobalt pre-catalyst (entries 2–3). Constant current electrolysis was performed at lower current with the same reaction time (entry 4) and the yield decreased. Instead, with longer reaction time of 16 hours, the yield was comparable to the optimised reaction condition (entry 5).

Table 3.2.1.6. Control experiments.[a]

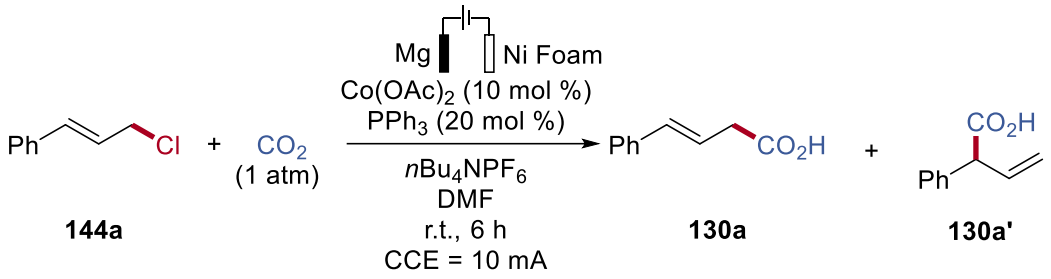

Entry	Variations from the standard conditions	Yield (**130a**/**130a'**)[b,c]
1	---	59% (1:1)
2	Without catalyst	13% (1:1)
3	Without current	---
4	5.0 mA	42% (1:1)
5	5.0 mA for 16 h	52% (1:1)

[a] Reaction conditions: **144a** (0.25 mmol), $Co(OAc)_2$ (10 mol %), PPh_3 (20 mol %), nBu_4NPF_6 (0.25 mmol), DMF (5.0 mL), CCE = 10 mA, 6 h, 25 °C. [b] Isolated yield (**130a**/**130a'**). [c] Selectivity determined by ^1H NMR.

Noteworthy, common chemical metal reductants were tested (**Table 3.2.1.7**) under the mild optimised reaction conditions. Super-stoichiometric amounts of metal reductants were subjected (entries 2–4) and only traces of product **130a** were observed. Elevated reaction temperatures (entries 5–9) failed to produce the desired product and additional trials were made with additives (entries 8–9) known to be beneficial (*vide supra*) for chemically-induced carboxylation reactions, albeit with minor amounts of the product found.

Table 3.2.1.7. Electrochemical *versus* chemical reductants.[a]

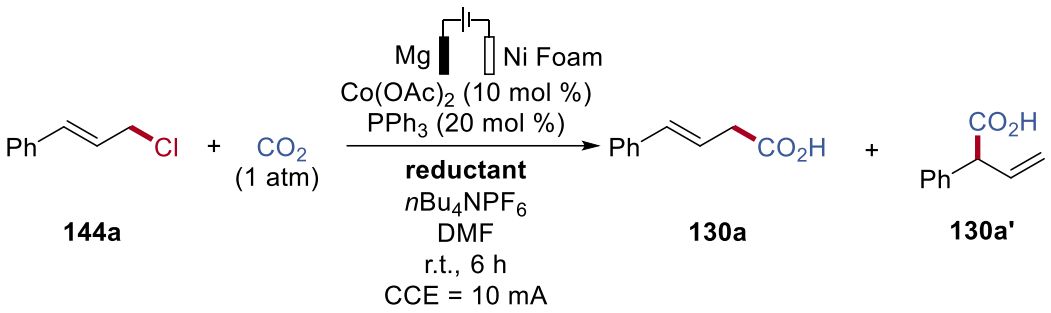

Entry	Variations from the standard conditions	Yield (**130a**/**130a'**)[b,c]
1	---	59% (1:1)
2	Mn[d]	n.d.
3	Zn[d]	n.d.
4	Mg[e]	traces
5	Mg[e] at 60 °C	5% (1:1)
6	Mn[e] at 60 °C	traces
7	Zn[e] at 60 °C	traces
8	Mn[e] and $MgCl_2$[d] at 60 °C	7% (1:1)
9	Zn[e] and Na_2CO_3[d] at 60 °C	traces

[a] Reaction conditions: **144a** (0.25 mmol), $Co(OAc)_2$ (10 mol %), PPh_3 (20 mol %), *n*Bu_4NPF_6 (0.25 mmol), reductant (1.50 or 3.00 equiv.), DMF (5.0 mL), CCE = 10 mA, 6 h, 25 °C, electrodes as specified. [b] Isolated yield (**130a**/**130a'**). [c] Selectivity determined by ^{1}H NMR. [d] 1.50 equivalents used and without electricity. [e] 3.00 equivalents used and without electricity.

3.2.2 Scope of Electro-Reductive Cobalt-Catalyzed Carboxylation

With the optimised reaction conditions in hand, the investigation of the robustness of the cobaltaelectro-reductive carboxylation reaction with atmospheric CO_2 was initiated (**Figure 3.2.2.1**). Alkyl substituted in the *ortho* or *para* position of the cinnamyl chlorides (**144b**–**144d**) were well accepted to furnish the products **130b**–**130d**. Furthermore, substrates containing *para*-substituted phenyl groups such as **130e'** and polycyclic rings such as naphthalene **130f'** gave moderate yield with a preference for the branched product. Electron-donating groups, such as benzodioxole (**130g'**), thioether (**130h'**), and methoxy (**130i**), were well tolerated in this mild reaction. The regioselectivity, however, differed as **144h** provided by a higher margin the branched

product **130h'**, while substrate **144i** reacted with higher preference for the linear product.

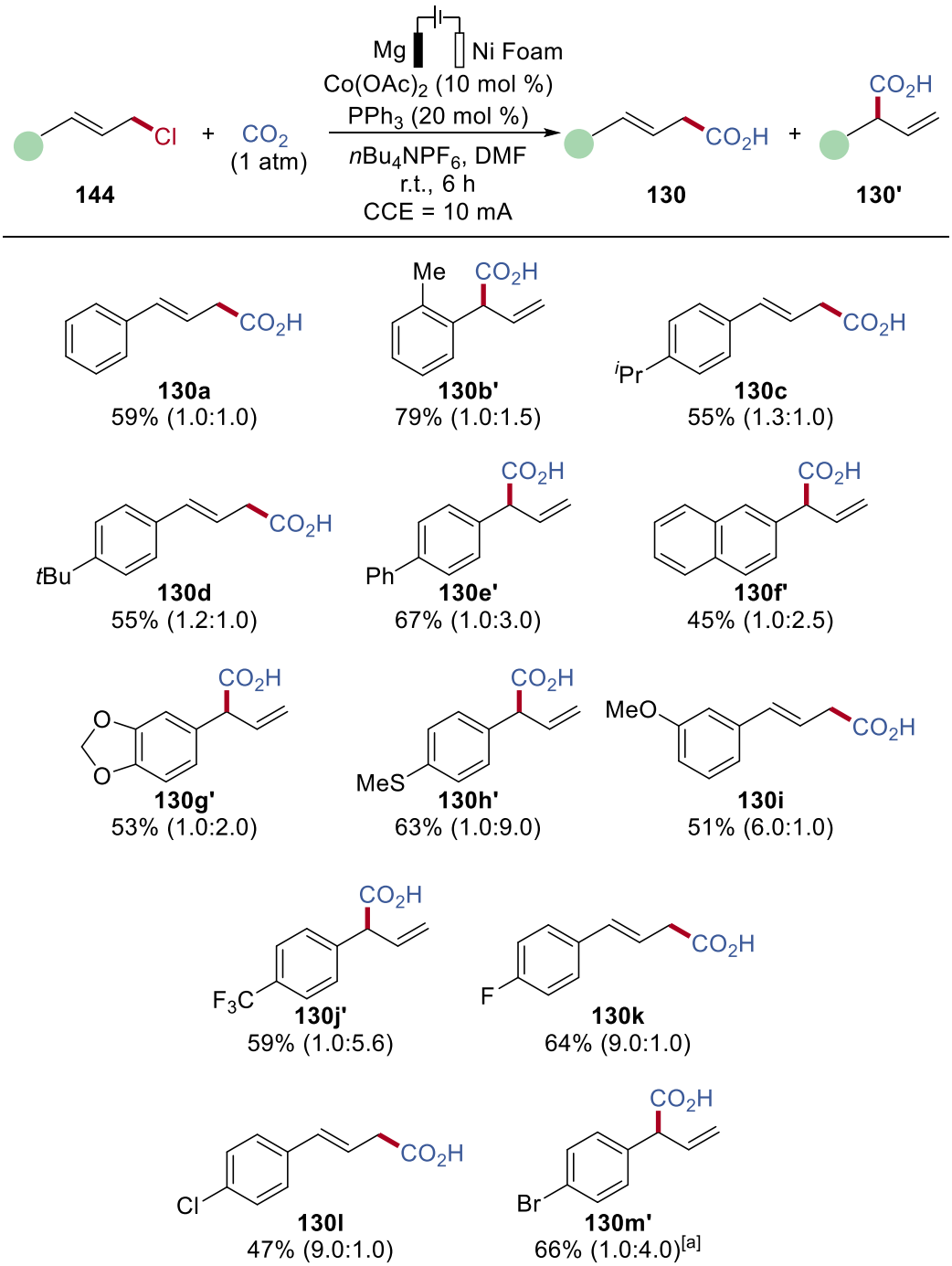

Figure 3.2.2.1. Cobalt-catalyzed electro-reductive carboxylation of cinnamyl chlorides **144**. Regioselectivity **130**/**130'** given in parentheses, only major products are shown. [a] A mixture with 5% dehalogenated product.

Substrates with electron-withdrawing substituents, such as trifluoromethyl (**130j'**) resulted in good yield with improved branched regioselectivity. Halogen-containing

substrates **144k-144m** displayed good yields of the carboxylated product **130k-130m**, with fluoro (**130k**) and chloro (**130l**) giving higher selectivity for the linear product. The product **130m'** gave an indication that halogens are only tolerated to a certain extent as 5–10% of the product was dehalogenated, giving rise to a small amount of **130a** in the product mixture. This was explicitly shown when *para*-iodo-containing substrate was subjected into the optimised reaction condition and the dehalogenated product was isolated in 40% yield.

3.2.3 Scope Limitations

Under otherwise identical standard reaction conditions, the application to alkyl-substituted and heterocycle-containing substrates **130n-130s**, **196-206** proved to be challenging and unsatisfactory results to date (**Figure 3.2.3.1**).

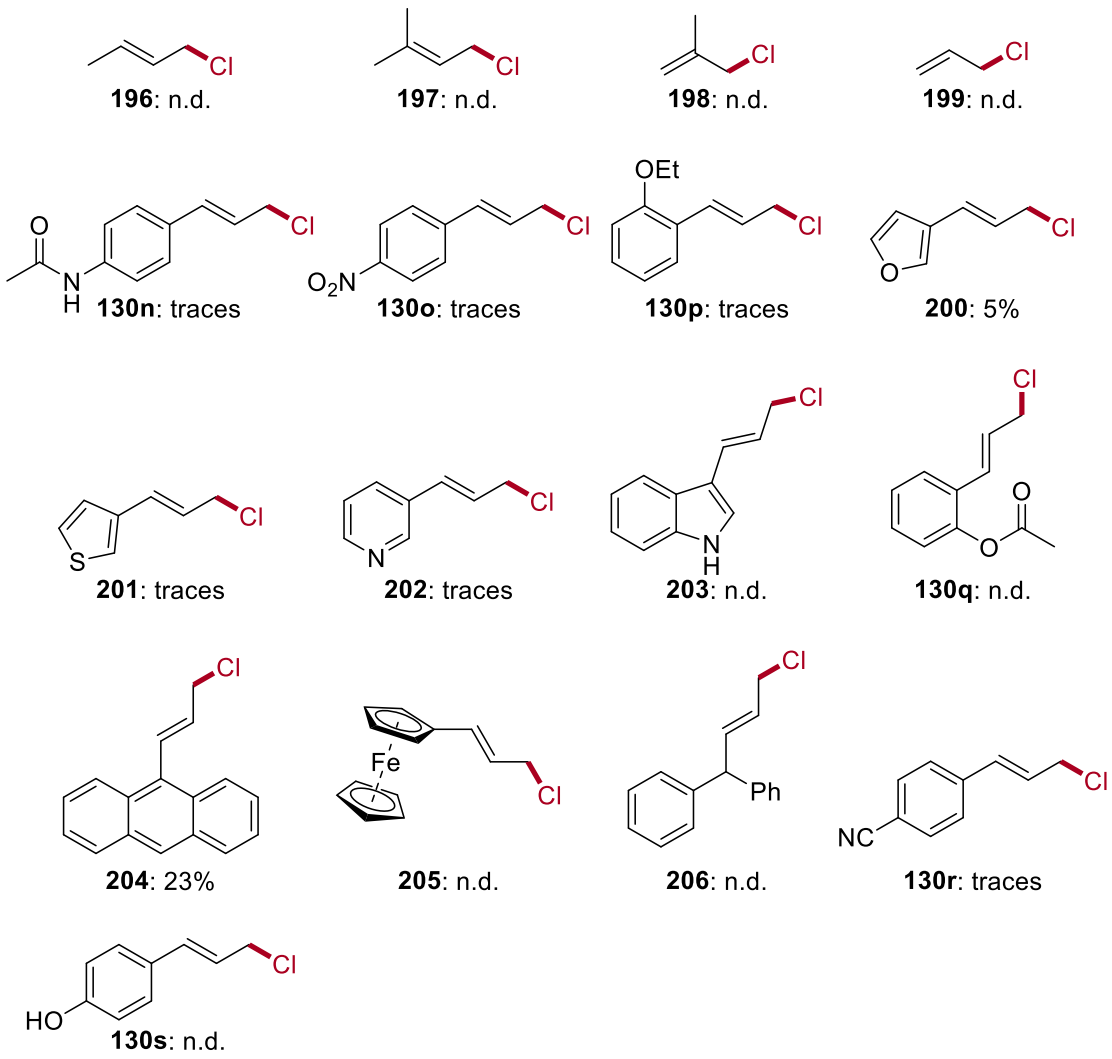

Figure 3.2.3.1. Unsuccessful examples for the cobaltaelectro-reductive carboxylation.

3.2.4 Mechanistic Investigations

Various mechanistic studies were performed in order to elucidate the *modus operandi* of the electro-reductive cobalt-catalyzed carboxylation with CO_2. Thus, DFT calculations were carried out by Dr. J. C. A. Oliveira at the PW6B95 D4/def2 TZVPP+ SMD(DMF)//TPSS-D3(BJ)/def2-SVP level of theory (**Figure 3.2.4.1**).[228] The isomerisation step of η^3-allyl complex to the η^1-allyl complex was shown not to be the rate-determining step due to the minimal energy barrier of 16.1 kcal mol^{-1} for the product **130l** (**Figure 3.2.4.1a**).

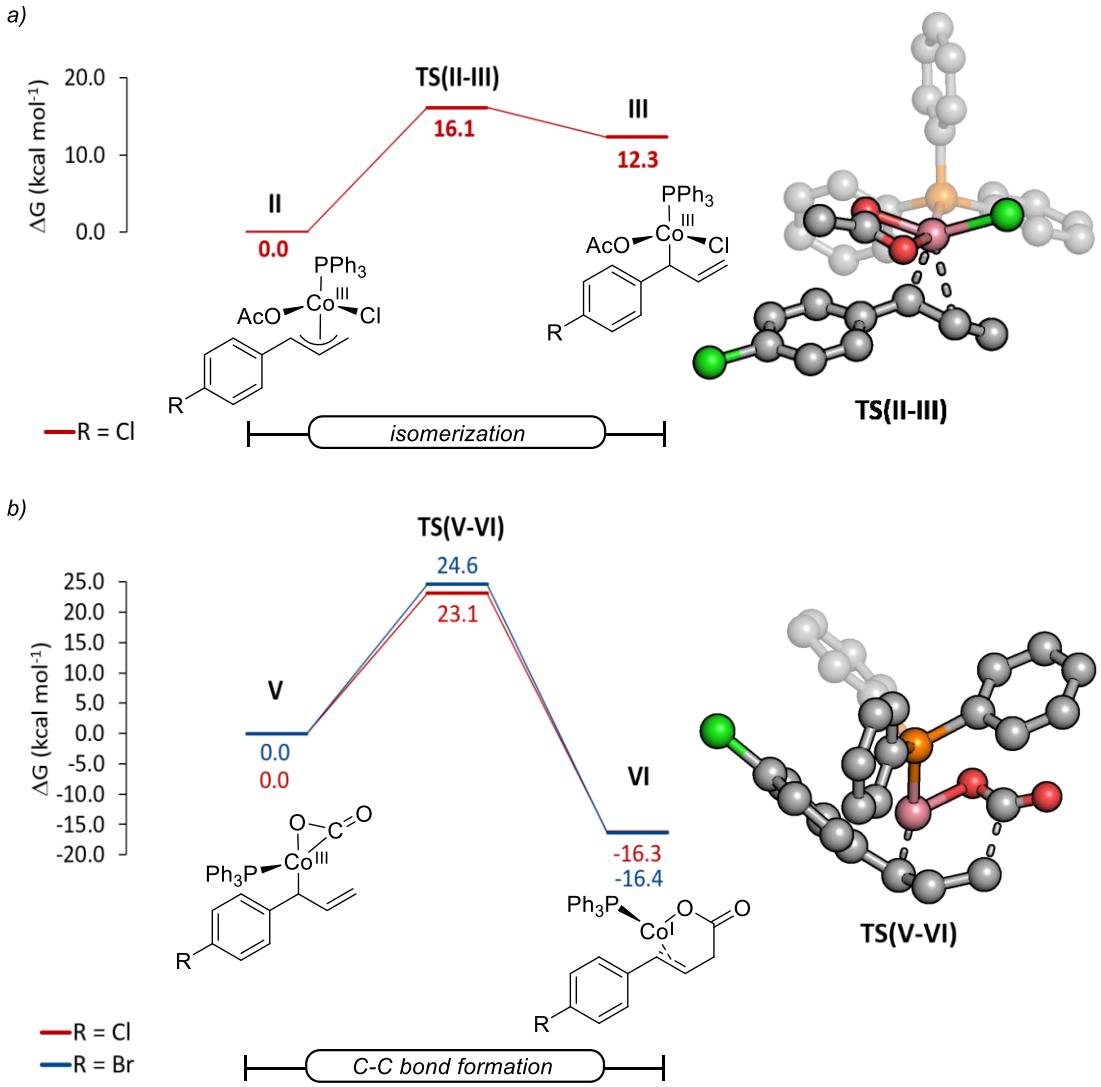

Figure 3.2.4.1. Computed relative Gibbs free energies in kcal mol^{-1} for the a) isomerisation of η^3-allyl complex to η^1-allyl, and b) allylic C–C bond formation at the PW6B95-D4/def2-TZVPP+SMD(DMF)//TPSS-D3(BJ)/def2-SVP level of theory. Hydrogen in the computed transition state structures were omitted for clarity. Performed by Dr. J. C. A. Oliveira.

Given that the reductive electrocatalysis of the cross-electrophiles was performed at substantially high current at 1 atm of CO_2 partial pressure, we directed our focus to the allylic C–C bond formation (**Figure 3.2.4.1b**). The latter is preferred for the chlorinated substrate over the brominated substrate by 1.5 kcal mol^{-1}. Hence, DFT studies have been shown to be in agreement with the experimentally observed regioselectivity of **130l** by Dr. J. C. A. Oliveira.

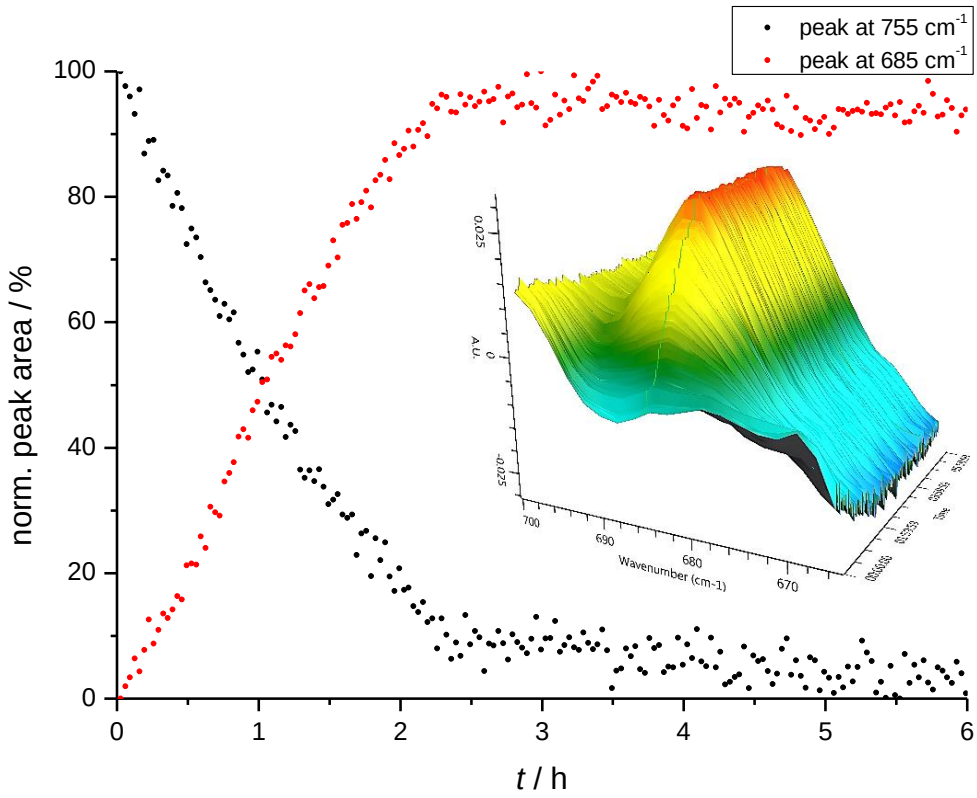

Figure 3.2.4.2. *In-operando* infrared spectroscopy including the 3D surface heat plot at 685 cm^{-1}.

In order to further understand the mechanism of this electro-reductive cobalt-catalyzed carboxylation reaction, the mode of action was investigated. First, the kinetic profile of the standard electrocatalytic reaction condition was elucidated (**Figure 3.2.4.2**) alongside with the use of different simple cobalt salts as pre-catalyst for comparison in terms of reaction rates. An *in-operando* infrared (IR) spectroscopy was adopted in this case to better illustrate the differences. As was previously observed, simple $Co(OAc)_2$ and the halide salts operated in a superior fashion as compared to their counterparts (**Figure 3.2.4.3**). In contrast, a higher catalytic loading of Co(salen) was attempted but it did not improve the yield.[233]

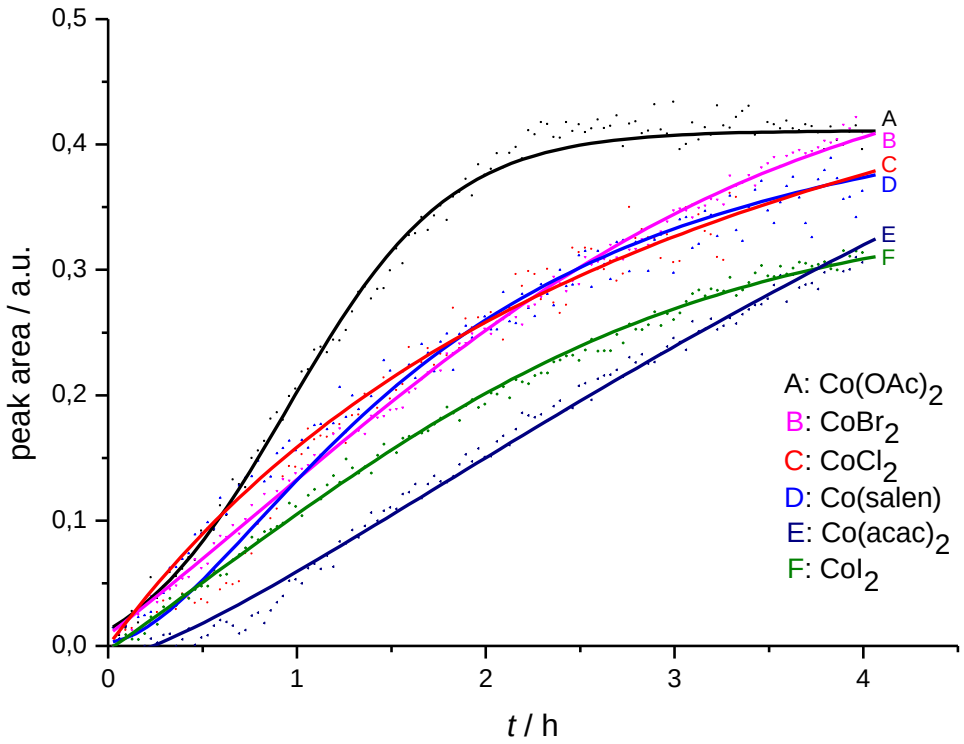

Figure 3.2.4.3. Comparison of the different cobalt pre-catalyst in terms of reaction rates.

Second, the pre-formed cobalt(I) intermediate (*vide infra*) could be of interest as this might suggest whether it has indeed participated in the rate-determining step of this particular reaction system. One such low-valent cobalt(I) intermediate $CoCl(PPh_3)_3$ **195** has been reported in the past for its use in an amination reaction of inactivated aryl iodides[234] and also other cobalt(I) complexes in C–H activation reactions which could help to shed light into the reaction mechanism of this carboxylation protocol.[47c, 235]

Detailed mechanistic investigations performed by means of cyclic voltammetry (CV) revealed that simple cobalt(II) complexes did not interact with the allylic chloride **144a** (**Figure 3.2.4.4**). The reduction potential of the parent cinnamyl chloride was analysed to be irreversible at E_p = − 1.90 V *vs.* SCE. Interestingly, the cobalt(I) complex **195** of interest showed one irreversible reduction at E_p = − 1.82 V *vs.* SCE which could correspond to the reduction of cobalt(I) to cobalt(0) (**Figure 3.2.4.5**).[236]

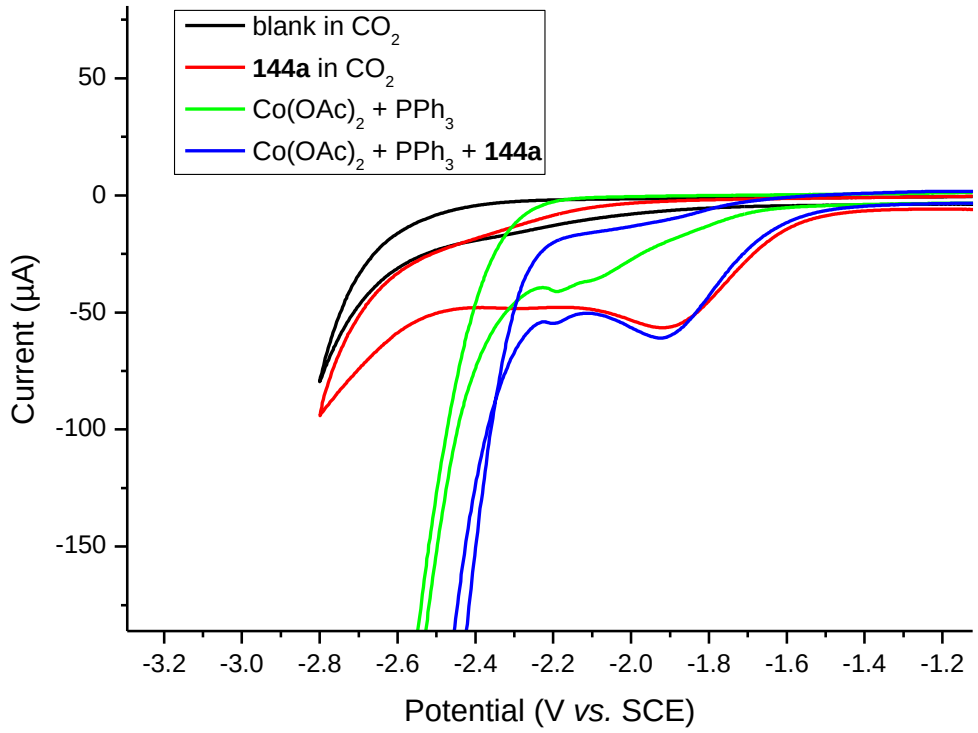

Figure 3.2.4.4. Cyclic voltammograms of individual components under CO_2 and their mixtures. Cyclic voltammograms at 100 mVs^{-1} using DMF and nBu$_4$NPF$_6$ (0.10 M) as electrolyte, and a GC working electrode. Co(OAc)$_2$ (2.0 mM), PPh$_3$ (2.0 mM) and cinnamyl chloride **144a** (2.0 mM). CO_2 gas (1 atm).

However, the addition of cinnamyl chloride **144a** into the system resulted in an oxidative addition of the substrate onto the cobalt(I) complex **195** to give a cobalt(III) intermediate which could showcase a possible cobalt(I)/(III)/(I) catalytic manifold. This inference could be held true as there are two reduction peaks and they are possibly assigned as E_p = − 1.70 V *vs.* SCE for the reduction of cobalt(II) to cobalt(I) and E_p = − 1.95 V *vs.* SCE for the reduction of cobalt(I) to cobalt(0) (**Figure 3.2.4.5**).[237] In this case, the reduction of cobalt(III) to cobalt(II) was not easily observed as it has a much higher reduction potential and they are usually in the positive window.[238] Consequently, these results indicated that the oxidative addition of the substrate onto the active cobalt catalyst is plausibly not involved in the rate-determining step. In addition, stoichiometric reactions were performed with the synthesized cobalt(I) complex **195** without the supply of electricity to dismiss the possibility that an *in situ* formed cobalt(III) intermediate could be in the CO_2 activation step. Hence, cathodic reduction of cobalt(III) intermediate to cobalt(I) is required to facilitate the formation of the carboxylated products **130**.

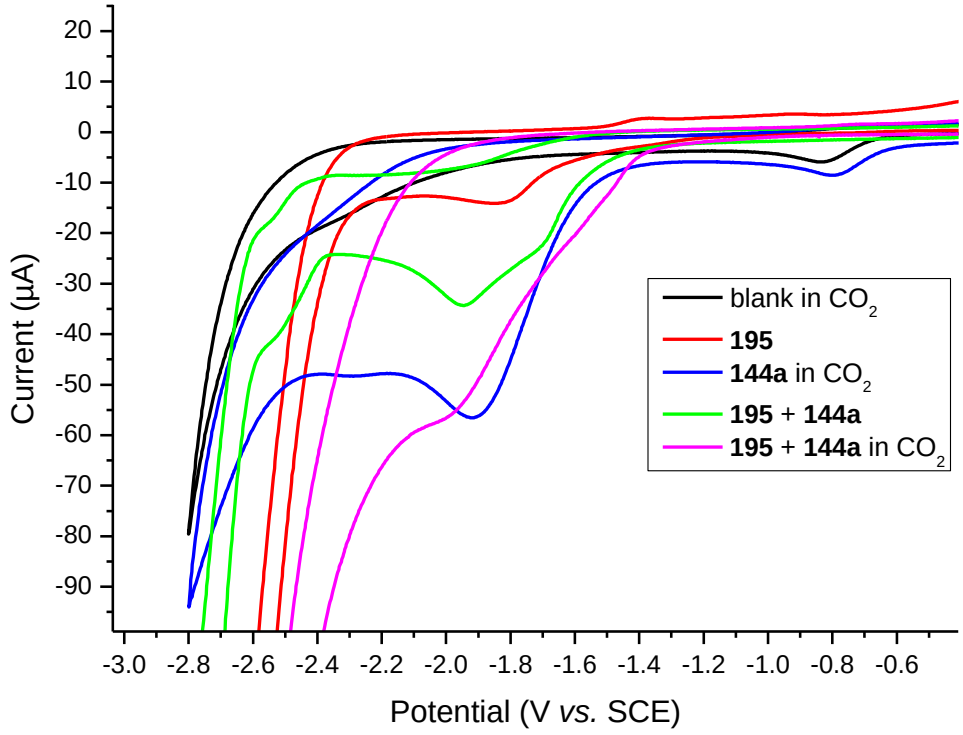

Figure 3.2.4.5. Cyclic voltammograms of Co(I) catalyst and mixtures. Cyclic voltammograms at 100 mVs^{-1} using DMF and $n$$Bu_4NPF_6$ (0.10 M) as electrolyte, and a GC working electrode. $CoCl(PPh_3)_3$ **195** (2.0 mM) and cinnamyl chloride **144a** (2.0 mM). CO_2 gas (1 atm).

3.2.5 Proposed Catalytic Cycle

Based on the mechanistic insights obtained including the DFT studies by Dr. J. C. A. Oliveira, a feasible reaction mechanism is proposed in which the most likely catalytic occurrence is shown here (**Figure 3.2.5.1**). Initially, the coordination of allylic chlorides **144** onto the active cobalt(I) **207** occurs. This subsequently promotes the cleavage of the adjacent allylic C–H bond, resulting in an oxidative addition of substrate **144** to form an η^3-allylcobalt(III) intermediate **208**. At this stage, the cobalt(III) intermediate **208** can undergo rearrangement to either η^1-allylcobalt(III) complexes **209-A** or **209-B** depending on the different ligand effects. For instance, heteroatom-containing ligands, such as O atoms are known to promote the change from η^3- to η^1-allyl intermediates in similar cobalt complexes reported previously.[175] Then, there are two different pathways from intermediate **209**, they can both undergo cathodic reductions to give the corresponding low-valent η^1-allylcobalt(I) species **210**, which could be stabilised by an aryl or alkenyl ligand.[239] This determines the regioselectivity of the final product which is highly dependent on the ligand employed. Here the linear product is generated

through C–C bond formation with CO_2 at the γ-position[140b, 240] to form the carboxylated product **211** and **211'** trapped by the Mg^{2+} ions in the solution.

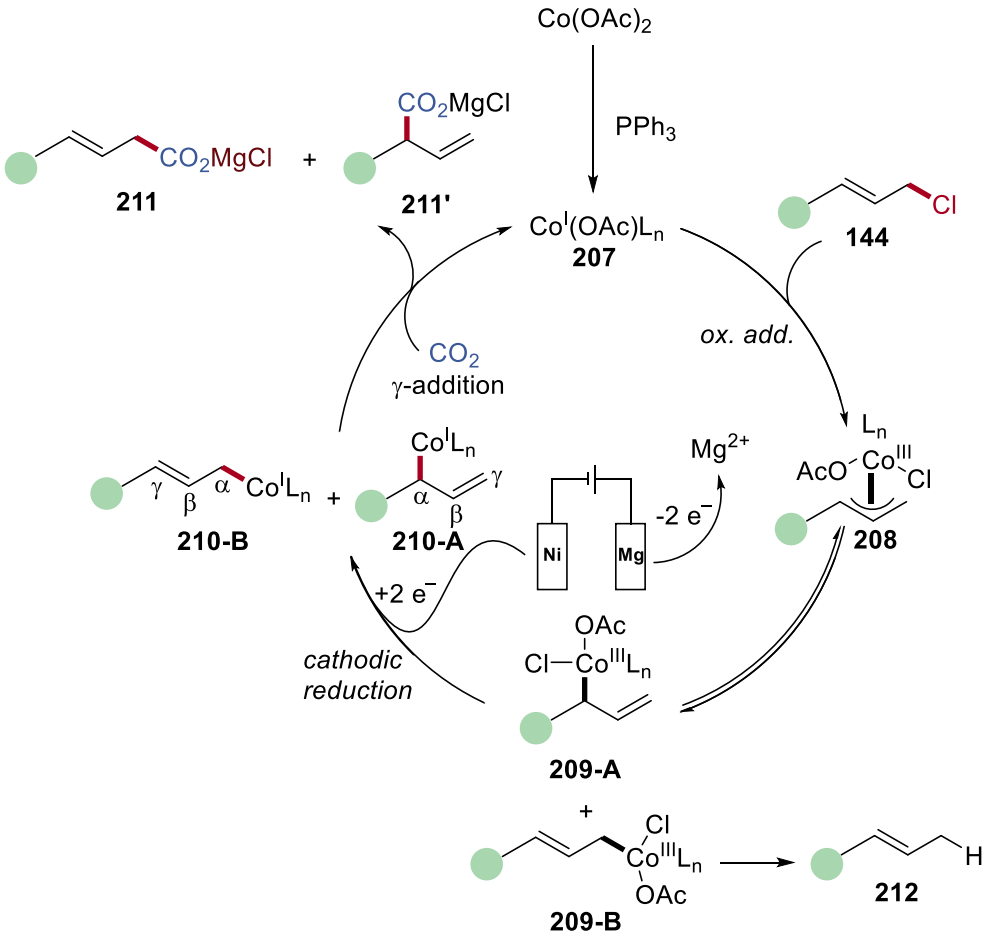

Figure 3.2.5.1. Proposed catalytic cycle based on mechanistic insights.

A second scenario has been proposed as well for this cobaltaelectro-reductive carboxylation with atmospheric CO_2 which will not be shown here. The essential difference depicts that the η^3-allylcobalt(III) intermediate **208** would actually first undergo cathodic reduction to η^3-allylcobalt(I) complex before the reversible change of η^3- to either linear or branched η^1-allylcobalt(I) complex **210** similar to the ones displayed here (**Figure 3.2.5.1**).[228]

3.3 Electro-Reductive Nickel-Catalyzed Thiolation

The formation of C–S bonds have led to extensive advancement and expansion of the medical realm as a huge number of pharmaceutical drugs and natural materials features the importance of sulfur.[241] Hence, the search for simple and mild transformations for C–S formations continues to this date. The use of electrophilic thiosulfonates have revolutionised thiolation protocols as they are bench-stable and odourless as opposed to the toxic and foul-smelling use of thiols which are commonly used as coupling partners. One other huge disadvantage of the use of thiols is that they are unfavorable for large-scale synthesis as per its physical nature. Thus, an effective replacement such as thiosulfonates provide vast opportunities for more practical approaches.[242] A unique method to activate and efficiently utilize thiosulfonates as coupling partners for C–S formation is the application of cross-electrophile coupling reactions with organohalides. As aforementioned (*vide supra*), cross-electrophile couplings are step-economical and there are wide variety of stable electrophiles easily available which translates into possible broad expandable scope. Many recent developments have successfully included the use of thiosulfonates in cross-electrophile coupling reactions, but they often suffer from the utilization of super-stoichiometric amounts of chemical metal reductants.[217-219] Thus, the introduction of the far-reaching strategy of electrocatalysis[102a] could mitigate this impediment efficiently and improve the quality of the synthetic protocol for C–S formation. The supposition that an electrochemically-induced reductive thiolation of alkyl bromides catalytic design by means of nickel catalysis could be implemented which is naturally free from toxic chemical reductant.[243] It should feature electricity as an economical mediator to access alkyl sulfides, which are common structural motifs in numerous drug scaffolds through versatile C–S formation.[244]

3.3.1 Optimisation Studies

The investigations began by probing a suitable optimised reaction condition for the envisioned electro-reductive nickel-catalyzed thiolation of alkyl bromides **175** with thiosulfonates **160** (Table 3.3.1.1).

Table 3.3.1.1. Optimisation of nickel catalysts and ligands.[a]

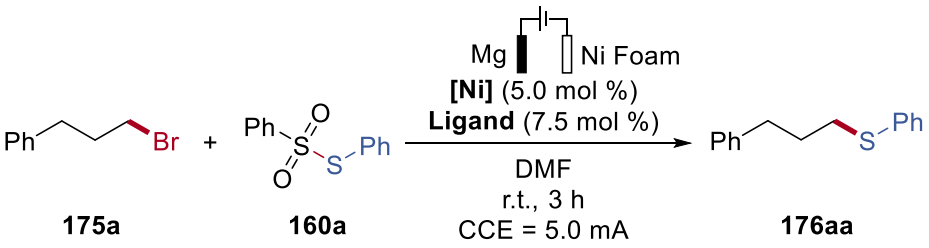

175a **160a** **176aa**

Entry	[Ni]	Ligand	Time (h)	Yield[b]
1	$NiBr_2$•diglyme	neocuproine	6	32%
2	$NiBr_2$•diglyme	neocuproine	6	44%[c]
3	$NiBr_2$•diglyme	bathocuproine	3	82%
4	**$NiBr_2$•diglyme**	**2,2'-bipyridine**	**3**	**86%**
5	$NiBr_2$•diglyme	2,2'-bipyridine	6	---[d,e]
6	$NiBr_2$•diglyme	bathocuproine	6	---[d,e]
7	$NiBr_2$•diglyme	neocuproine	16	11%[f]
8	$NiBr_2$•diglyme	neocuproine	6	43%[g]
9	$NiBr_2$•diglyme	neocuproine	6	---[c,d,e]
10	$NiBr_2$•diglyme	bathocuproine	6	28%[c]
11	$NiBr_2$•diglyme	neocuproine	3	67%[c]
12	$NiCl_2$	2,2'-bipyridine	6	47%[c]
13	$NiBr_2$•diglyme	bathocuproine	3	75%[c]
14	$NiBr_2$•diglyme	neocuproine	3	77%

[a] Reaction conditions: **175a** (0.250 mmol), **160a** (0.275 mmol), [Ni] (5.0 mol %), ligand (7.5 mol %), DMF (5.0 mL), CCE = 5.0 mA, 3 h, 25 °C, Mg anode, nickel-foam cathode. [b] Isolated yield. [c] Et_4NOTs (0.50 equiv.) added as electrolyte. [d] CCE = 10 mA. [e] Diphenyldisulphide formed as side product. [f] CCE = 3.0 mA. [g] nBu_4NPF_6 (0.50 equiv) added as electrolyte.

Several bidentate nitrogen-containing ligands, such as neocuproine, were exposed to the envisioned reaction but failed to give satisfactory results even with longer reaction time (entries 1–2). The relatively inexpensive 2,2'-bipyridine ligand outperformed

marginally bathocuproine within the same reaction time (entries 3–4). The outstanding performance vanished when the reaction time was prolonged to 6 hours and at higher constant current electrolysis of 10 mA (entries 5–6), which resulted in the formation of diphenyldisulfides instead. It became clear that longer reaction times had a detrimental effect on the reaction (*vide infra*), which resulted in the low yield of the product no matter the ligand or nickel catalyst used (entries 5–10 and 12). It was also observed that adding electrolyte, such as Et_4NOTs, decreased the yield (entry 13).

Table 3.3.1.2. Control experiments.[a]

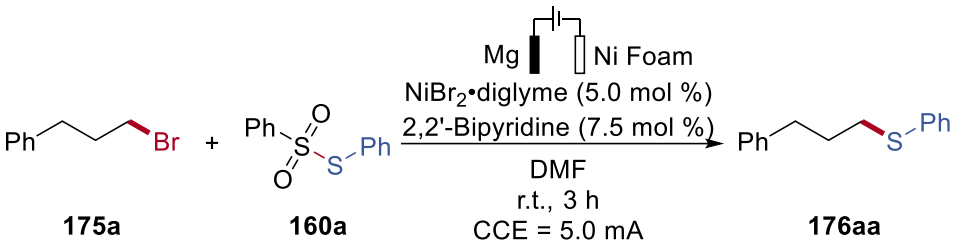

175a **160a** **176aa**

Entry	Variations from the standard conditions	Yield[b]
1	---	86%
2	Without catalyst	37%[c]
3	Without current	---
4	With Et_4NOTs (0.50 equiv) as electrolyte	51%
5	5.0 mA for 6 h	48%
6	With IKA ElectraSyn 2.0®	79%
7	With diphenyldisulfide instead of **160a**	---

[a] Reaction conditions: **175a** (0.250 mmol), **160a** (0.275 mmol), $NiBr_2$•diglyme (5.0 mol %), 2,2'-bipyridine (7.5 mol %), DMF (5.0 mL), CCE = 5.0 mA, 3 h, 25 °C, Mg anode, nickel-foam cathode. [b] Isolated yield. [c] High and unstable potential.

Control experiments were next performed (**Table 3.3.1.2**), which substantiated the importance of electricity and of the nickel catalyst (entries 1–3). Extending the reaction time to 6 hours at the same subjected constant current electrolysis drastically lowered the yield (entry 5). Notably, the electro-thiolation is compatible with the commercially available IKA Electrosyn 2.0® electrochemical system, which exhibited the simplicity of the transformation, furnishing alkyl sulfide product **176aa** with a comparable yield (entry 6). Disulfides, such as diphenyldisulfides, obtained in some cases as side-

product did not provide the formation of the desired product **176aa**, when subjected to the standard reaction condition as the coupling partner (entry 7).

Table 3.3.1.3. Optimisation of electrode materials and solvents.[a]

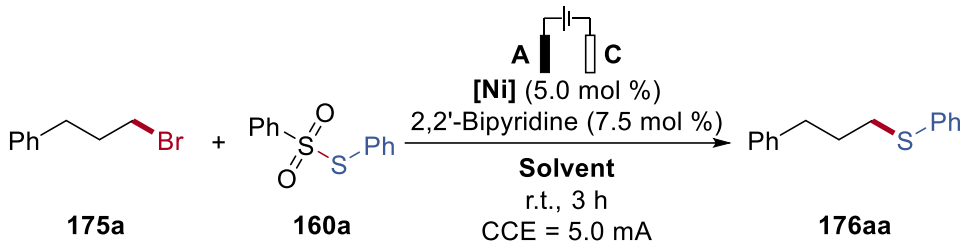

175a **160a** **176aa**

Entry	[Ni]	Anode	Cathode	Solvent	Yield[b]
1	**$NiBr_2$·diglyme**	**Mg**	**Ni Foam**	**DMF**	**86%**
2	$NiBr_2$·diglyme	Fe	Ni Foam	DMF	---[c]
3	$NiBr_2$·diglyme	Zn	Ni Foam	DMF	---[c]
4	$NiBr_2$·diglyme	Cu	Ni Foam	DMF	---[c]
5	$NiBr_2$·diglyme	Mg	Ni Foam	DMA	54%
6	$NiBr_2$·diglyme	Mg	Ni Foam	NMP	68%
7	$NiBr_2$·diglyme	Mg	Ni Foam	DMSO	12%
8	$NiBr_2$·diglyme	Mg	Ni Foam	DME	---
9	$NiBr_2$·diglyme	Mg	Ni Foam	GVL	7%
10	$NiBr_2$·diglyme	Ni Foam	Pt	DMF	---[d]
11	$NiBr_2$·diglyme	Mg	Ni Foam	THF	---
12	$NiBr_2$·diglyme	Mg	Ni Foam	*t*Amyl-OH	---
13	$NiBr_2$·diglyme	Mg	Pt	DMF	70%
14	---	Mg	Pt	DMF	33%[e]
15	---	Al	Pt	DMF	---
16	---	Fe	Pt	DMF	---
17	---	Al	Ni Foam	DMF	---[c]

[a] Reaction conditions: **175a** (0.250 mmol), **160a** (0.275 mmol), [Ni] (5.0 mol %), 2,2'-bipyridine (7.5 mol %), solvent (5.0 mL), CCE = 5.0 mA, 3 h, 25 °C, electrodes as specified. [b] Isolated yield. [c] Diphenyldisulphide formed as side product. [d] Starting material (70 %) recovered. [e] High and unstable potential.

The electrode materials and solvents were subsequently tested as well (**Table 3.3.1.3**). Polar aprotic solvents, such as DMF and DMA, worked decently for the nickela-electro-

reductive thiolation reaction (entries 1, 5–6), whereas solvents like THF, GVL, and *t*Amyl-OH performed sluggishly. Various anodes and cathodes were tested but they did not provide any useful yield other than the use of magnesium anode with nickel foam cathode (entries 1–4, 15–17). A platinum cathode was also attempted, but gave the desired product with a lower yield (entries 10, 13–16).

Table 3.3.1.4. Electrochemical *versus* chemical reductants.[a]

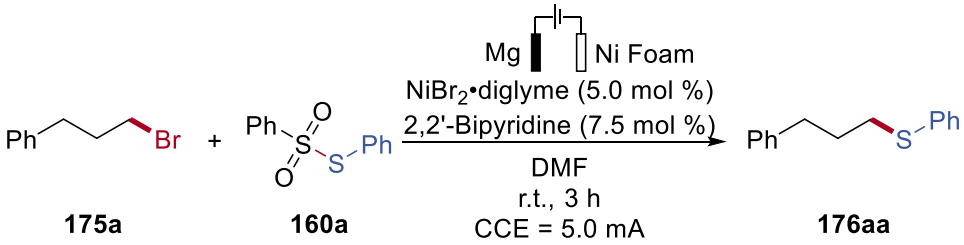

175a **160a** **176aa**

Entry	Variations from the standard conditions	Yield[b]
1	---	86%
2	Without catalyst and with Mn[c]	---
3	Without catalyst and with Mg[c]	---
4	Mg[c]	---
5	Zn[c]	33%
6	Mn[c]	65%

[a] Reaction conditions: **175a** (0.250 mmol), **160a** (0.275 mmol), $NiBr_2$•diglyme (5.0 mol %), 2,2'-bipyridine (7.5 mol %), DMF (5.0 mL), CCE = 5.0 mA, 3 h, 25 °C, Mg anode, nickel-foam cathode. [b] Isolated yield. [c] 1.50 equivalents used and without electricity.

Subsequently, several commonly used chemical metal reductants were tested (**Table 3.3.1.4**) and they gave lower yields in this reaction. The use of chemical reductant without catalyst did not convert any starting material **175a** to the desired product **176aa** (entries 2–3). Moreover, the use of magnesium as chemical reductant gave no detectable product (entry 4), whereas zinc dust and manganese provided useful yields of the alkyl sulfide product **176aa** (entries 5–6).

3.3.2 Scope of Electro-Reductive Nickel-Catalyzed Thiolation

Having the optimised reaction condition in hand, the robustness and substrate scope of the nickela-electro-reductive thiolation reaction were of interest. The robustness was mainly tested with various substituted bench-stable thiosulfonates **160** (Figure 3.3.2.1). Electron-rich groups, such as methyl- **160b** and methoxy- **160c** *para*-substituents, furnished the desired products **176ab**-**176ac** with great efficacy. Halogen-containing substrates (**160d**-**160e**) resulted in excellent yield of the thiolated products (**176ad** and **176ae**) without by-product formation from potential C–X cross-couplings. Furthermore, alkyl thiosulfonates, such as benzyl **160f** and cyclohexyl **160g**, gave the desired products **176af** and **176ag** in high yields.

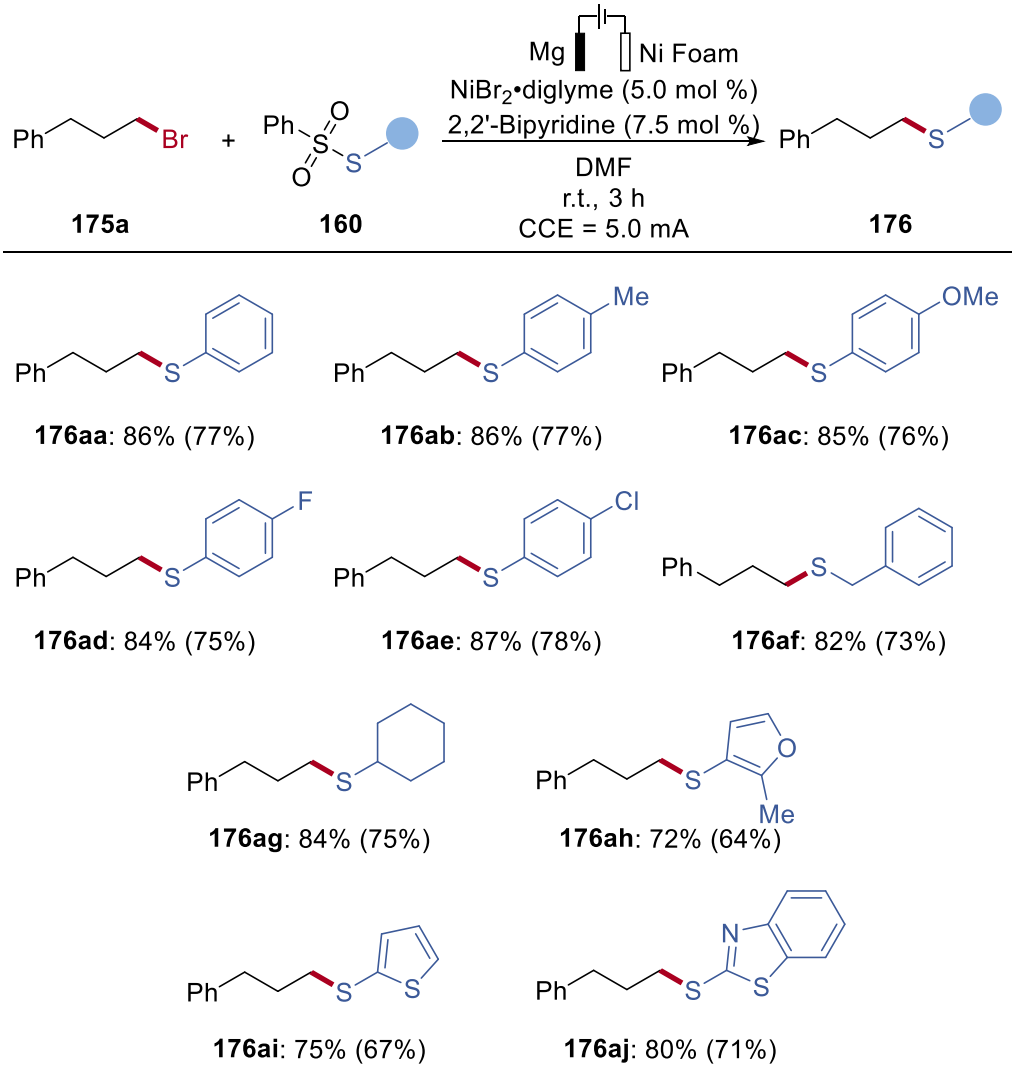

Figure 3.3.2.1. Nickel-catalyzed electro-reductive thiolation of alkyl bromides **175a** with substituted thiosulfonates **160**. Faradaic yield given in parentheses.

Moreover, heterocyclic thiosulfonates (**160h-160j**) were well tolerated and provided the thiolated products with high yields. The noteworthy mild reaction conditions were versatile as various thiosulfonates **160** were efficiently converted to the desired alkyl sulfide products **176**. Thus, we were intrigued to evaluate the performance of the catalytic electro-reductive thiolation on differently substituted bromides (**Figure 3.3.2.2**).

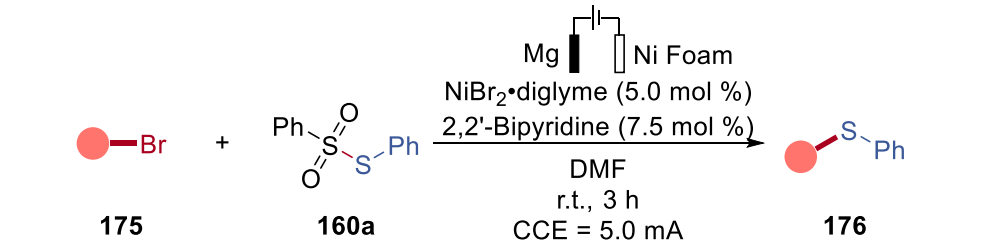

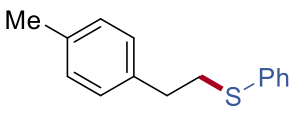

176ba: 88% (79%)

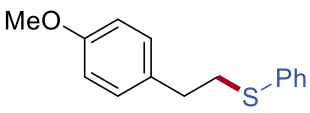

176ca: 86% (77%)

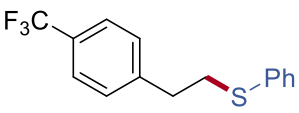

176da: 90% (80%)

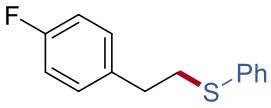

176ea: 90% (80%)

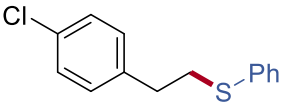

176fa: 97% (87%)

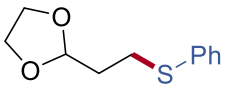

176ga: 82% (73%)

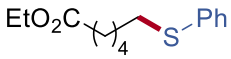

176ha: 80% (71%)

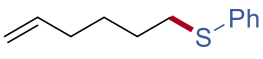

176ia: 88% (79%)

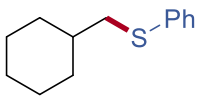

176ja: 84% (75%)

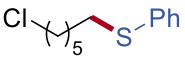

176ka 91% (81%)

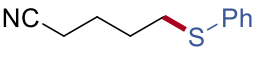

176la: 91% (81%)

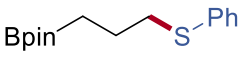

176ma: 51% (46%)

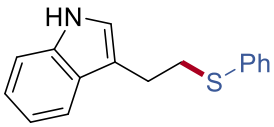

176na 79% (71%)

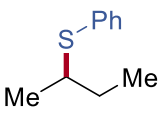

176oa: 36% (32%)

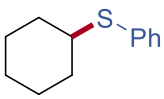

176pa: 38% (34%)

Figure 3.3.2.2. Nickel-catalyzed electro-reductive thiolation of bromides **175**. Faradaic yield given in parentheses.

Much to our delight, *para*-substituted electron-rich groups, such as methyl- **175b** and methoxy- **175c** substituted arenes, both provided the desired alkyl sulfide products **176ba**-**176ca** with high yields. Electron-withdrawing trifluoromethyl arene **175d** also furnished the thiolated product **176da** with high yield, showcasing no obvious preferences in terms of electronic influences. Various halogen-containing bromides (**175e**-**175f**) gave the desired products (**176ea**-**176fa**) in a highly chemoselective fashion. Synthetically useful cyclic 1,3-dioxolane substituted bromide **175g** also underwent facile and efficient thiolation to give exceptional yield of the desired product **176ga**. Moreover, ester-containing substrate **175h** furnished the alkyl sulfide product (**176ha**) with great yield showing good tolerance to the reaction condition. Various interesting functional groups such as terminal alkene (**175i**), sterically crowded 2-cyclohexyl (**175j**), alkyl chloride (**175k**), and cyano (**175l**) were efficiently transformed to the desired product **176**. The otherwise highly labile boronic ester **175m** remained intact in this electro-reductive thiolation regime to deliver the alkyl sulfide product (**176ma**). Furthermore, unprotected indole **175n** also gave the thiolated product as well with high yield. Last but not least, secondary bromides (**175o**-**175p**) were also successfully thiolated, albeit lower yields were obtained.

3.3.3 Mechanistic Insights

In order to understand the actual mode of action for the nickela-electro-catalyzed thiolation reaction with alkyl bromides **175**, mechanistic investigations were sought after in detail.[243] First, radical clock experiments were performed with 6-bromo-1-hexene **175i** to illustrate the formation of primary alkyl radical (**Table 3.3.3.1**).

Table 3.3.3.1. Radical clock experiments.

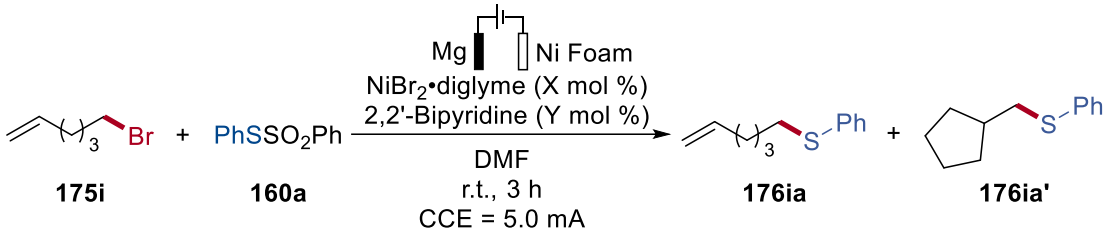

175i **160a** **176ia** **176ia'**

Entry	[Ni] (X mol %)	Bpy (Y mol %)	Yield (%)	**176ia**:**176ia'**
1	2.50	3.75	69	14:1
2	5.00	7.50	96	>20:1

[a] Yield and ratio determined by ^{1}H NMR spectroscopy with 1,3,5-trimethoxybenzene as internal standard.

Second, various reduction potentials of the substrates and catalyst were elucidated by means of cyclic voltammetry (CV) as disulfides were frequently observed as by-product of the reaction system. The cathodic reduction of thiosulfonates was of importance to determine the presence of an off-cycle pathway of this electro-reductive thiolation reaction. Cyclic voltammetry revealed that the reduction of the 2,2'-bipyridine ligated nickel pre-catalyst is more facile than the two-electron-reduction of *S*-phenyl benzenesulfonothioate **160a** to the thiolate anion (**Figure 3.3.3.1**).

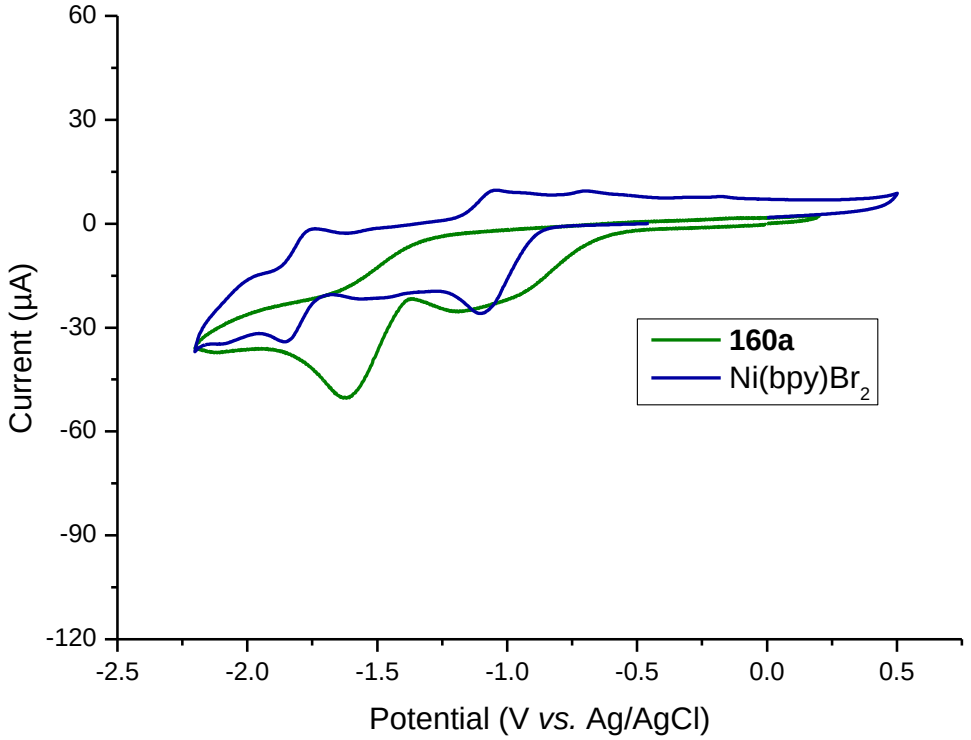

Figure 3.3.3.1. Cyclic voltammograms comparing the ligated Ni complex and thiosulfonate **160a**. Cyclic voltammograms at 100 mVs^{-1} using DMF and *n*Bu$_4$NPF$_6$ (0.10 M) as electrolyte, and a GC working electrode. Ni(bpy)Br$_2$ (2.0 mM) and **160a** (2.0 mM).

The first observed reduction potential of the thiosulfonate **160a** was shown to be irreversible at E_p = − 0.91 V *vs.* Ag/AgCl and this could be possibly assigned to the formation of the thiyl radical. Thiyl radicals are known to recombine to disulfide due to their relative stability.[245] Furthermore, a second reduction potential was shown to be reversible at E_p = − 1.62 V *vs.* Ag/AgCl and this would then be assigned to the thiolate anion after a two-electrons transfer process.[246] The nickel pre-catalyst exhibits an irreversible reduction potential at E_p = − 1.27 V *vs.* Ag/AgCl, which is lowered further to a reversible reduction potential of E_p = − 1.10 V *vs.* Ag/AgCl by the successful ligation of the 2,2'-bipyridine ligand for the reduction of nickel(II) to nickel(I) analogous to previously reported observations.[247] Supplementary observations postulated that the ligated nickel catalyst is found to undergo relatively facile two-electrons reduction synergistically with the reduction of thiosulfonates.

Further mechanistic investigations by means of potentiostatic reactions were conducted to showcase the generation of thiyl radicals and the subsequent disulfide formation through radical recombination (**Figure 3.3.3.2**).

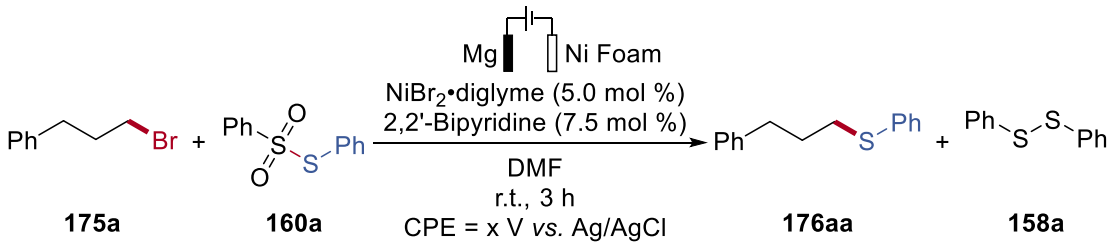

175a **160a** **176aa** **158a**

Reduction Potential	**160a** recovered	Yield of **158a**	Yield of **176aa**
– 0.70 V	77%	18%	traces
– 1.00 V	10%	66%	18%
– 1.80 V	---	44%	53%

Figure 3.3.3.2. Potentiostatic studies.

The potentiostatic reactions were performed under the otherwise standard reaction conditions. As hypothesised, the alkyl sulfide product was not formed during the constant potential electrolysis (CPE) = − 0.70 V *vs.* Ag/AgCl, but the radical rebounded disulfide **158a** was formed instead with 18% yield. It could be due to the early first onset potential of the thiosulfonate **160a** at E_{onset} = − 0.60 V *vs.* Ag/AgCl. In contrast, the thiolated product **176aa** was formed at CPE = − 1.00 V *vs.* Ag/AgCl, albeit with a considerable amount of by-product **158a**, possibly through radical recombination. This particular observation is in good agreement with the CV studies shown indicating plausible formation of thiyl radicals by initial reduction of substrate **160a**. When the potential was higher than the second reduction potential of thiosulfonate substrate **160a** at CPE = − 1.80 V *vs.* Ag/AgCl, the desired alkyl sulfide product **176aa** was furnished with 53% yield, while the by-product **158a** was formed with 44% yield.

3.3.4 Proposed Catalytic Cycle

Based on the mechanistic studies and literature precedent,[209d, 219, 248] a plausible catalytic cycle was proposed (**Figure 3.3.4.1**). Initially, an oxidative addition of **160** occurs onto the active nickel(0) catalyst **213** obtained after ligation and reduction of the nickel pre-catalyst.[103b, 249] This formed nickel(II) intermediate complex **214** then combines with an alkyl radical formed *in situ* to give a nickel(III) complex **215**. Subsequently, it undergoes reductive elimination to furnish the desired alkyl sulfide product **176** through a C–S bond formation. The nickel(I) complex **216** generated will react with another molecule of alkyl bromide rejuvenating the alkyl radical **182** and giving the nickel(II) intermediate **217**. Finally, the intermediate **217** undergoes cathodic reduction to regenerate the active nickel(0) catalyst **213**, thus closing the catalytic cycle.[250]

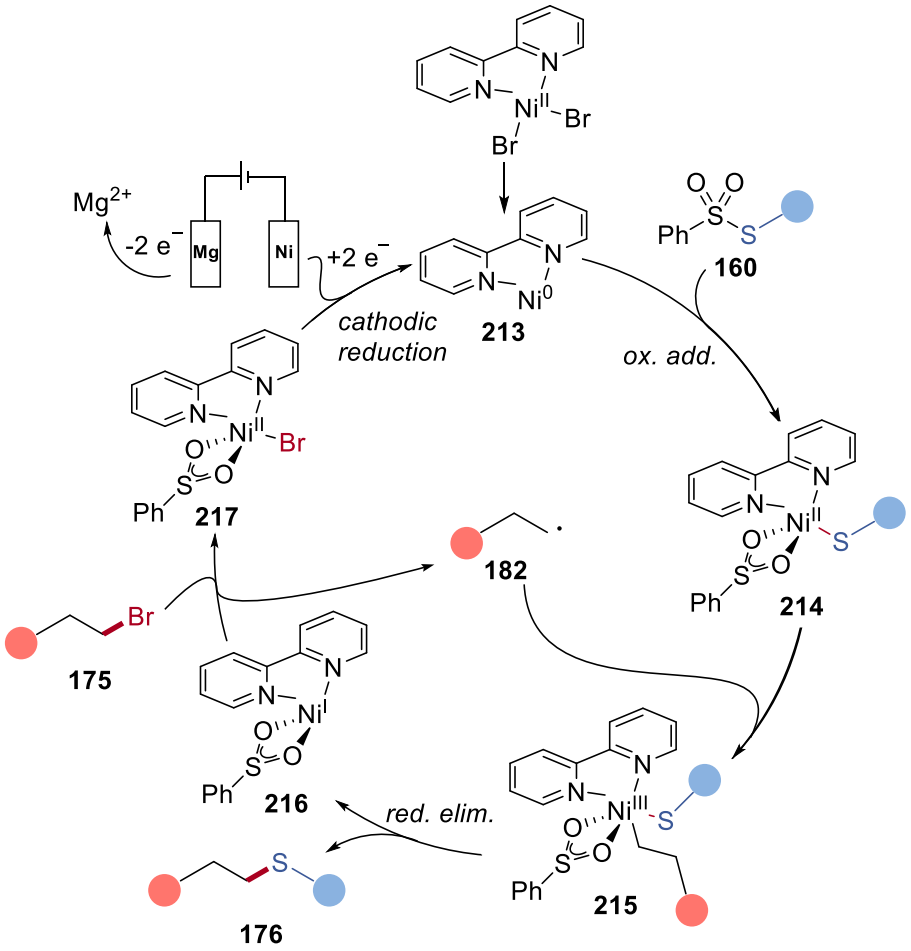

Figure 3.3.4.1. Proposed catalytic cycle.

4. Summary and Outlook

The perpetual demand for advancements in sustainable synthetic organic chemistry is largely caused by quasi-irreversible detrimental effects of climate change, this has indeed created numerous deliberations especially in recent years in the field of *inter alia*, transition metal catalyzed C–H activation, cross-electrophile coupling reactions, CO_2 fixation and the construction of C–S bonds due to its medicinal importance. Electrosynthesis — more than a century-old technique — that have been locked away in the abyss has once again resurfaced itself which was predominantly spurred by key conceptual developments that are substantially environmentally benign and yet prudently attractive transformations.[102a] In particular, the allied cooperation between electrosynthesis and Earth-abundant 3d transition metal catalysis have not only created remarkable atom- and step-economical approaches synergistically but also contain the potential to discover novel mechanistic pathways. Its prime benefit includes as well the unique tunability of the applied potential for sensitive transformation which allows unmatched chemoselectivity and controlled reactivity. Therefore, the combination of green methodologies has granted a viable approach for molecular syntheses with exceptionally mild reaction conditions devoid of unwanted chemical wastes, which have been mainly touched upon in this thesis.

In the first part, an electrochemical cobalt-catalyzed C–H/N–H annulation reaction have been devised which is mild, cost-effective and highly site-, chemo- and regioselective for benzamides **184** bearing 2-pyridyl-*N*-oxide directing group and especially interesting internal allenes **185** allowing the molecular assembly of *exo*-methylene isoquinolones **186** (**Figure 4.1**).[224]

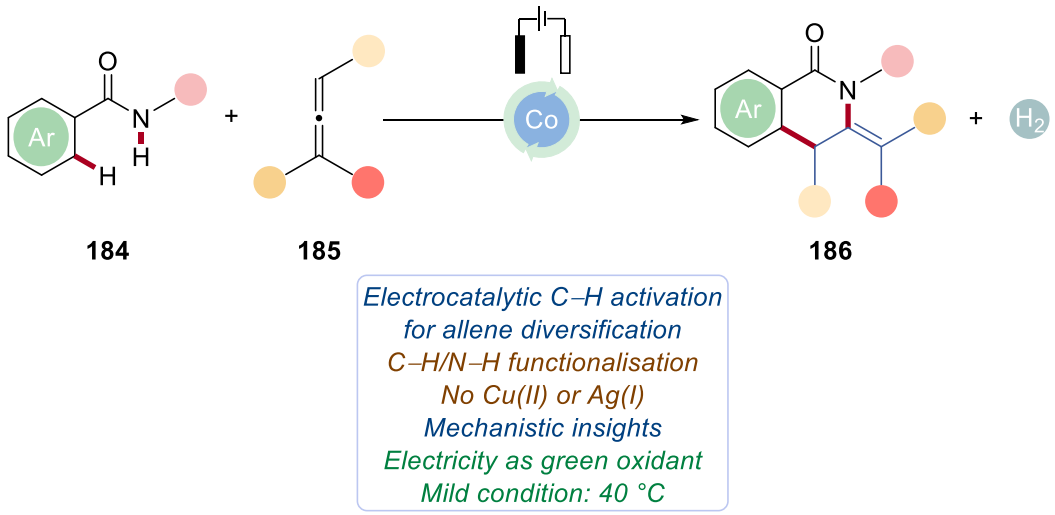

Figure 4.1. Electrocatalytic C–H/N–H activation by mild cobalt catalysis.

Cross-electrophile coupling with atmospheric CO_2 not only addresses the global warming issue but also provide value-added compounds which are highly desirable. In the second part, a contemporary electro-reductive cobalt-catalyzed carboxylation of allylic chlorides **144** with atmospheric CO_2 was constructed to give important styrylacetic acid derivatives **130**[228] which are key synthons to numerous γ-arylbutyrolactones, structural motif found in several natural products (**Figure 4.2**). Preliminary mechanistic insights including kinetic profiling by means of modern React-IR spectroscopy and cyclic voltammetry studies provided evidences for a postulated catalytic cycle which illustrated a cobalt(I)/(III)/(I) catalytic manifold through π-allyl-cobalt complexes.

Thus, electrocarboxylation can provide a myriad of new discoveries. The use of electrochemistry for substrate and CO_2 reduction supplies a greener and more sustainable alternative for cross-electrophile coupling reactions. It is intriguing to unravel effective 3d metal catalysts for the carboxylation reactions that are more environmentally friendly. Hence, we can expect a rising number of electrosynthesis protocols for carboxylation reactions.

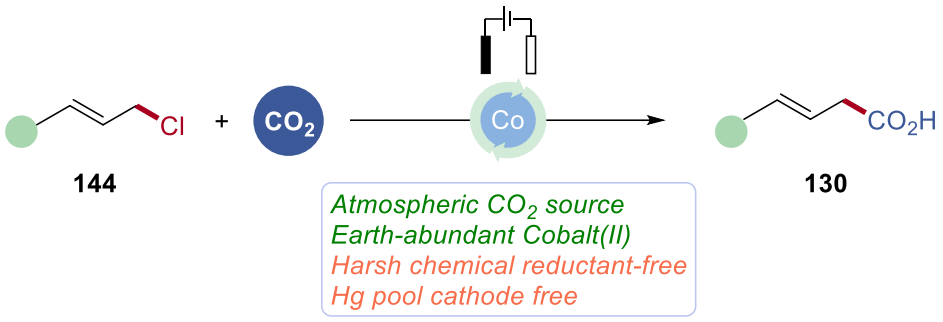

Figure 4.2. Cobalt catalyzed electro-reductive carboxylation with atmospheric CO_2.

In the third part, cross-electrophile coupling was also applied to electrophilic substituted thiosulfonates **160** with alkyl bromides **175** for the exceptionally mild formation of C–S bonds to give alkyl sulfides **176** in excellent yield with great chemoselectivity (**Figure 4.3**).[243] The formation of C–S bonds are extremely appreciated as sulfur-containing structural motifs have tremendous impact in terms of pharmaceutical drugs and functional materials. Hence, exceedingly mild and scalable protocols for C–S formations are valuable. Within this powerful thiolation protocol, harsh chemical reductants are not needed for the reduction of the nickel catalyst and yet a broad and versatile substrate scope with excellent yield was obtained. Detailed mechanistic studies, including cyclic voltammetry and potentiostatic studies, gave evidences for a proposed catalytic cycle.

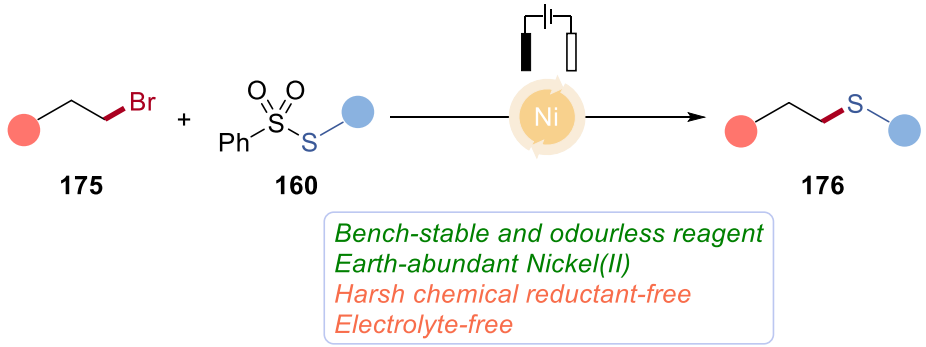

Figure 4.3. Electro-reductive nickel-catalyzed cross-electrophile thiolation.

5. Experiment Section

5.1 General Remarks

Catalysis reactions under an atmosphere of air were conducted in the sealed tubes or Schlenk tubes. Unless otherwise noted, other reactions were performed under N_2 atmosphere using pre-dried glassware and standard Schlenk techniques.
If not otherwise noted, yields refer to isolated compounds, estimated to be >95% pure as determined by ^{1}H NMR.

Vacuum

The following pressures were measured on the used vacuum pump and were not corrected: membrane pump vacuum (MPV): 0.5 mbar, oil pump vacuum (OPV): 0.1 mbar.

Melting Points (M.p.)

Melting points were measured using a *Stuart*® Melting Point Apparatus *SMP3* from BARLOWORLD SCIENTIFIC. The reported values are uncorrected.

Chromatography

Analytical thin layer chromatography (TLC) was performed on 0.25 mm silica gel 60F-plates (MACHEREY-NAGEL) with 254 nm fluorescent indicator from MERCK. Plates were visualized under UV-light. Chromatographic purification of products was accomplished by flash column chromatography on MERCK silica gel, grade 60 (0.040–0.063 mm and 0.063–0.200 mm).

Gas Chromatography (GC)

The conversions of the reactions were monitored by applying coupled gas chromatography/mass spectrometry using G1760C GCDplus with mass detector *HP 5971*, *5890 Series II* with mass detector *HP 5972* from HEWLETT-PACKARD and 7890A *GC-System* with mass detector *5975C (Triplex-Axis-Detector)* from AGILENT TECHNOLOGIES equipped with *HP-5MS* columns (30 m × 0.25 mm × 0.25 m).

Gel Permeation Chromatography (GPC)

GPC purifications were performed on a JAI system (JAI-*LC-9260 II NEXT*) equipped with two sequential columns (*JAIGEL-2HR*, gradient rate: 5.000; *JAIGEL-2.5HR*, gradient rate: 20.000; internal diameter = 20 mm; length = 600 mm; Flush rate = 10.0 mL/min and chloroform (HPLC-quality with 0.6% ethanol as stabilizer) was used as the eluent.

Infrared Spectroscopy

Infrared spectra were recorded with a BRUKER *Alpha-P ATR FT-IR* spectrometer. Liquid samples were measured as a film, solid samples neat. The analysis of the spectra was carried out using the software from BRUKER *OPUS 6*. The absorption was given in wave numbers (cm^{-1}) and the spectra were recorded in the range of 4000–400 cm^{-1}. *In situ*-IR studies were performed on METTLER TOLEDO *ReactIR™ 15* with an *iC IR 4.3* software.

Mass Spectrometry

Electron-ionization (EI) mass spectra were recorded on a Jeol AccuTOF instrument at 70 eV. Electrospray-ionization (ESI) mass spectra were obtained on Bruker micrOTOF and maXis instruments. All systems were equipped with time-of-flight (TOF) analyzers. The ratios of mass to charge (*m*/*z*) were reported and the intensity relative to the base peak (I = 100) is given in parenthesis.

Nuclear Magnetic Resonance Spectroscopy (NMR)

Nuclear magnetic resonance (NMR) spectra were recorded on VARIAN *Inova 500*, *600*, VARIAN *Mercury 300*, *VX 300*, VARIAN *Avance 300*, VARIAN *VNMRS 300* and BRUKER *Avance III 300*, *400* and *HD 500* spectrometers. All chemical shifts were given as *δ*-values in ppm relative to the residual proton peak of the deuterated solvent or its carbon atom, respectively. ^{1}H and ^{13}C NMR spectra were referenced using the residual proton or solvent carbon peak (see table), respectively. ^{13}C and ^{19}F NMR were measured as proton-decoupled spectra.

	^{1}H NMR	^{13}C NMR
$CDCl_3$	7.26	77.16
$[D]_6$-DMSO	2.50	39.52

The observed resonance-multiplicities were described by the following abbreviations: s (singlet), d (doublet), t (triplet), q (quartet), hept (heptet), m (multiplet) or analogous representations. The coupling constants *J* were reported in Hertz (Hz). Analysis of the recorded spectra was carried out with *MestReNova 10* software.

Electrochemistry

Nickel foam (Ni) electrodes (10 mm × 15 mm × 1.4 mm, RCM-Ni5763; obtained from Recemat BV, Germany) and graphite felt (GF) or reticulous vitreous carbon (RVC) electrodes (10 mm × 15 mm × 6 mm, SIGRACELL®GFA 6 EA, obtained from SGL Carbon, Wiesbaden, Germany) were connected using stainless steel adapters. Electrolysis was conducted using an AXIOMET AX-3003P potentiostat in constant current mode, CV studies were performed using a Metrohm Autolab PGSTAT204 workstation and Nova 2.0 software. Divided cells separated by a P4-glassfrit were obtained from Glasgerätebau Ochs Laborfachhandel e. K. (Bovenden, Germany).

Solvents

All solvents for reactions involving moisture-sensitive reagents were dried, distilled and stored under inert atmosphere (N_2) according to the following standard procedures.

Purified by solvent purification system (SPS-800, M. Braun): **CH_2Cl_2**, **toluene**, **tetrahydrofuran**, **dimethylformamide**, **diethylether**. **1,2-dichloroethane**, ***N*-methyl-2-pyrrolidone** (**NMP**), ***N*,*N*-dimethylacetamide** (**DMA**)**, dimethylsulfoxide** (**DMSO**) and ***γ*-valerolactone** (**GVL**) was dried over CaH_2 for 8 h, degassed and distilled under reduced pressure. **1,2-dimethoxyethane** (**DME**) was dried over sodium and freshly distilled under N_2. **1,1,1,3,3,3-hexafluoropropan-2-ol** (**HFIP**) was distilled from 3 Å molecular sieves. **2,2,2-trifluoroethanol** (**TFE**) was stirred over $CaSO_4$ and distilled under reduced pressure. **Water** was degassed by repeated *Freeze-Pump-Thaw* degassing procedure. **1,4-dioxane** and **di-*n*-butyl-ether** (***n*Bu_2O**) were distilled

from sodium benzophenone ketyl.

Reagents

Chemicals obtained from commercial sources with purity above 95% were used without further purification. The following compounds were known and were synthesized according to previously described methods.

Benzamides **8**,[57] allenes **185**,[251] allylic chlorides **144**,[252] $CoCl(PPh_3)_3$ complex **195**[234] and thiosulfonates **160**.[215, 253]

Cooperation Clarification:

In the project of electroreductive carboxylation with atmospheric CO_2, all the DFT calculations were performed by Dr. João C. A. Oliveira.

5.2 General Procedures

General Procedure A: Electrochemical C–H/N–H Annulations of Benzamides with 1,3-substituted Allenes: Access to *exo*-Methylene Isoquinolones 186

The electrocatalysis was carried out in an undivided cell, with a RVC anode (10 mm × 15 mm × 6 mm) and a platinum cathode (10 mm × 15 mm × 0.25 mm). Benzamide **8** (0.250 mmol, 1.00 equiv), allene **185** (0.750 mmol, 3.00 equiv), NaOPiv (62 mg, 0.500 mmol, 2.00 equiv) and $Co(OAc)_2 \cdot 4H_2O$ (12.7 mg, 0.050 mmol, 20 mol %) were placed in a 10 mL cell and dissolved in MeOH (5.0 mL). Electrolysis was performed at 40 °C with a constant current of 2 mA maintained for 15 h (2.34 F/mol). The reaction was stopped by adding H_2O (10 mL). The RVC anode was washed with CH_2Cl_2 (10 mL) in an ultrasonic cleaner. The washing was added to the reaction mixture and the combined phases were extracted with CH_2Cl_2 (3 × 10 mL), and then dried over Na_2SO_4. Evaporation of the solvent and subsequent column chromatography on silica gel using a mixture of CH_2Cl_2/acetone as the eluent yielded the desired products **186**.

General Procedure B for the Deoxygenation of 1,3-Substituted Allenes Annulated Products 186

For resolving the rotamers and analyzing product **186**, deoxygenation of pyridine N-oxide was performed. A 25 mL oven pre-dried schlenk flask was charged with product **186** (0.1 mmol, 1.00 equiv.), PCl_3 (15.9 mg, 0.12 mmol, 1.20 equiv.) and was dissolved in toluene (1.0 mL). The reaction was conducted under N_2 atmosphere for 30 minutes at 50 °C. The reaction was quenched by adding sat. aqueous $NaHCO_3$ (5.0 mL). The organic layer was added additional H_2O (5 mL) and extracted with CH_2Cl_2 (3 x 5.0 mL), then dried over Na_2SO_4. Evaporation of the solvent and subsequent column chromatography yielded the desired product **188** and isomerized product **188'**.

General Procedure C: Electro-Reductive Cobalt-Catalyzed Carboxylation with Atmospheric CO_2

Under an atmosphere of Ar, the oven-dried undivided electrochemical cell with Mg foil anode (3.00 mm x 15.0 mm x 0.02 mm) and Ni foam cathode (10.0 mm x 15.0 mm x 1.00 mm) was charged with allyl chloride **144** (0.250 mmol, 1.00 equiv), $Co(OAc)_2$ (4.43 mg, 0.025 mmol, 10 mol %), PPh_3 (13.1 mg, 0.050 mmol, 20 mol %), $n Bu_4NPF_6$ (96.9 mg, 0.250 mmol, 1.00 equiv) dissolved in DMF (5.0 mL). The reaction vessel was first flushed with CO_2 gas using a pressure of 1 atm for 30 minutes. Electrocatalysis was then performed at 10.0 mA of constant current at ambient temperature for 6 h with constant CO_2 bubbling. The reaction mixture was subsequently treated with HCl (2 M, 5.0 mL) at room temperature. Both electrodes were washed and sonicated thoroughly with EtOAc (3 x 5 mL). The washings were added into the reaction mixture and the combined phases were extracted with EtOAc (3 x 10 mL), the organic phases were then washed with aqueous sat. NH_4Cl solution (3 x 20 mL), dried over $MgSO_4$. Evaporation of the solvents and subsequent column chromatography on silica gel afforded the corresponding products **130**.

General Procedure D: Electro-Reductive Nickel-Catalyzed Thiolation

Under an atmosphere of Ar, the oven-dried undivided electrochemical cell with Mg foil anode (3.00 mm x 15.0 mm x 0.02 mm) and Ni foam cathode (10.0 mm x 15.0 mm x 1.00 mm) was charged with bromide **175** (0.250 mmol, 1.00 equiv), thiosulfonate **160** (0.275 mmol, 1.10 equiv), $NiBr_2$•diglyme (4.41 mg, 0.0125 mmol, 5.0 mol %), 2,2'-bipyridine (2.93 mg, 0.0188 mmol, 7.5 mol %) dissolved in DMF (5.0 mL). Electrocatalysis was then performed at 5.0 mA of constant current at ambient temperature for 3 h. The reaction vessel was first diluted with EtOAc (30 mL). Both electrodes were washed and sonicated thoroughly with EtOAc (3 x 5.0 mL). The washings were added into the reaction mixture and the combined phases were extracted with EtOAc (30 mL), the organic phases were then washed with deionized H_2O (3 x 20 mL), dried over Na_2SO_4. Evaporation of the solvents and subsequent column chromatography on silica gel afforded the corresponding products **176**.

5.3 Experimental Procedures and Analytical Data

5.3.1 Electrochemical C–H/N–H Annulations of Benzamides with 1,3-substituted Allenes

5.3.1.1 Characterization Data

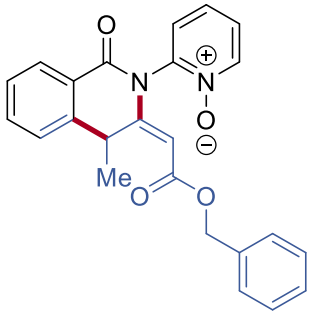

186a

(*E*)-2-[3-[2-(Benzyloxy)-2-oxoethylidene]-4-methyl-1-oxo-3,4-dihydroisoquinolin-2(1*H*)-yl]pyridine 1-oxide (186a)

The general procedure **A** was followed using benzamide **8** (53.5 mg, 0.25 mmol, 1.00 equiv.) and allene **185a** (141 mg, 0.75 mmol). Purification by column chromatography silica gel (CH_2Cl_2/acetone 4:1) yielded **186a** (60.0 mg, 150 µmol, 60%) as a pale yellow oil. **^{1}H NMR** (500 MHz, $CDCl_3$, 2 rotamers): δ = 8.38 – 8.35 (m, 1H), 8.35 – 8.31 (m, 1H), 8.14 (dd, *J* = 7.8, 1.3 Hz, 1H), 8.09 (dd, *J* = 7.8, 1.3 Hz, 1H), 7.59 (qd, *J* = 7.6, 1.4 Hz, 2H), 7.45 – 7.36 (m, 4H), 7.36 – 7.30 (m, 16H), 5.45 (q, 2H), 5.15 – 5.02 (m, 4H), 4.91 (s, 1H), 4.81 (s, 1H), 1.81 (d, *J* = 7.1 Hz, 3H), 1.66 (d, *J* = 7.1 Hz, 3H). **^{13}C NMR** (125 MHz, $CDCl_3$, 2 rotamers): δ = 165.8 (C_q), 165.8 (C_q), 162.0 (C_q), 161.7 (C_q), 159.0 (C_q), 158.2 (C_q), 144.8 (C_q), 142.9 (C_q), 142.8 (C_q), 140.9 (CH), 140.6 (CH), 135.9 (C_q), 135.9 (C_q), 134.2 (CH), 134.2 (CH), 129.0 (CH), 128.6 (CH), 128.6 (CH), 128.6 (CH), 128.5 (CH), 128.4 (CH), 128.3 (CH), 128.3 (CH), 127.5 (CH), 127.3 (CH), 127.2 (CH), 127.1 (CH), 126.7 (CH), 126.3 (CH), 126.1 (CH), 125.9 (CH), 125.3 (CH), 124.7 (C_q), 124.6 (C_q), 99.2 (CH), 99.1 (CH), 66.2 (CH_2), 66.1 (CH_2), 35.5 (CH), 35.0 (CH), 26.7 (CH_3), 26.7 (CH_3). **IR** (ATR): 3058, 2929, 1693, 1617, 1276, 1128, 756, 697 cm^{-1}. **MS** (EI) *m/z* (relative intensity): 400 (4) $[M]^+$, 293 (18), 249 (46), 237 (22), 91 (60), 78 (18). **HR-MS** (ESI) *m/z* calcd for $C_{24}H_{20}N_2O_4$ $[M]^+$: 401.1496, found: 401.1499.

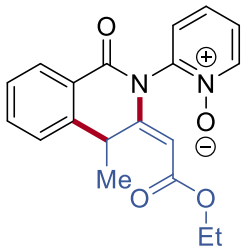

186b

(*E*)-2-[3-(2-Ethoxy-2-oxoethylidene)-4-methyl-1-oxo-3,4-dihydroisoquinolin-2(1*H*)-yl]pyridine 1-oxide (186b)

The general procedure **A** was followed using benzamide **8** (53.5 mg, 0.25 mmol, 1.00 equiv.) and allene **185b** (94.6 mg, 0.75 mmol). Purification by column chromatography silica gel (CH_2Cl_2/acetone 7:3) yielded **186b** (71.0 mg, 210 µmol, 84%) as a pale yellow oil. **^{1}H NMR** (500 MHz, $CDCl_3$, 2 rotamers): δ = 8.33 – 8.28 (m, 1H), 8.27 – 8.17 (m, 1H), 8.11 (dd, *J* = 7.9, 1.4 Hz, 1H), 8.06 (dd, *J* = 7.9, 1.4 Hz, 1H), 7.60 – 7.47 (m, 3H), 7.41 – 7.28 (m, 9H), 5.45 – 5.37 (m, 2H), 4.82 (s, 1H), 4.74 (s, 1H), 4.16 – 4.01 (m, 4H), 1.77 (d, *J* = 7.1 Hz, 3H), 1.62 (d, *J* = 7.1 Hz, 3H). **^{13}C NMR** (125 MHz, $CDCl_3$, 2 rotamers): δ = 166.1 (C_q), 166.0 (C_q), 162.2 (C_q), 161.9 (C_q), 158.4 (C_q), 157.6 (C_q), 142.9 (C_q), 134.2 (CH), 134.2 (CH), 129.0 (CH), 128.6 (CH), 128.5 (CH), 127.4 (CH), 127.3 (CH), 127.2 (CH), 126.6 (CH), 126.6 (CH), 126.0 (CH), 124.7 (C_q), 124.6 (C_q), 99.7 (CH), 99.6 (CH), 60.0 (CH_2), 60.0 (CH_2), 35.2 (CH), 34.7 (CH), 26.5 (CH_3), 26.5 (CH_3), 14.3 (CH_3), 14.3 (CH_3). **IR** (ATR): 2976, 1693, 1619, 1490, 1340, 1146, 884, 758 cm^{-1}. **MS** (EI) *m/z* (relative intensity): 338 (1) $[M]^+$, 265 (25), 249 (35), 237 (100), 142 (30), 78 (35). **HR-MS** (ESI) *m/z* calcd for $C_{19}H_{18}N_2O_4$ $[M]^+$: 339.1339, found: 339.1346.

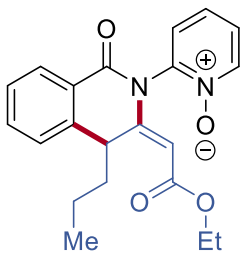

186c

(*E*)-2-[3-(2-Ethoxy-2-oxoethylidene)-1-oxo-4-propyl-3,4-dihydroisoquinolin-2(1*H*)-yl]pyridine 1-oxide (186c)

The general procedure **A** was followed using benzamide **8** (53.5 mg, 0.25 mmol, 1.00 equiv.) and allene **185c** (116 mg, 0.75 mmol). Purification by column chromatography silica gel (CH_2Cl_2/acetone 4:1) yielded **186c** (51.0 mg, 139 µmol, 56%) as a pale yellow oil. **^{1}H NMR** (500 MHz, $CDCl_3$, 2 rotamers): δ = 8.41 – 8.27 (m, 2H), 8.13 (dd, *J* = 7.8, 1.3 Hz, 1H), 8.08 (dd, *J* = 7.8, 1.3 Hz, 1H), 7.56 (qd, *J* = 7.4, 1.4 Hz, 2H), 7.46 – 7.30 (m, 10H), 5.42 – 5.37 (m, 2H), 4.85 (s, 1H), 4.80 (s, 1H), 4.16 – 4.03 (m, 4H), 2.20 – 2.15 (m, 1H), 2.04 – 1.97 (m, 1H) 1.50 – 1.38 (m, 4H), 1.24 – 1.18 (m, 6H), 0.94−0.90 (m, 6H). **^{13}C NMR** (125 MHz, $CDCl_3$, 2 rotamers): δ = 166.1 (C_q), 166.1 (C_q), 162.4 (C_q), 162.1 (C_q), 157.6 (C_q), 156.8 (C_q), 141.3 (C_q), 140.8 (C_q), 133.5 (CH), 133.4 (CH), 129.0 (CH), 128.7 (CH), 128.6 (CH), 127.9 (CH), 127.8 (CH), 127.5 (CH), 127.3 (CH), 126.7 (CH), 126.2 (CH), 126.1 (CH), 125.8 (CH), 125.5 (C_q), 125.5 (C_q), 100.5 (CH), 100.0 (CH), 60.1 (CH_2), 42.5 (CH_2), 42.5 (CH_2), 40.3 (CH), 39.7 (CH), 20.1 (CH_2), 19.8 (CH_2), 14.4 (CH_3), 14.4 (CH_3), 14.2 (CH_3), 14.2 (CH_3). **IR** (ATR): 2960, 2933, 1693, 1618, 1264, 883, 759, 700 cm^{-1}. **MS** (EI) *m/z* (relative intensity): 366 (0.4) $[M]^+$, 293 (25), 277 (30), 265 (100), 234 (30), 78 (35). **HR-MS** (ESI) *m/z* calcd for $C_{21}H_{22}N_2O_4$ $[M]^+$: 367.1652, found: 367.1652.

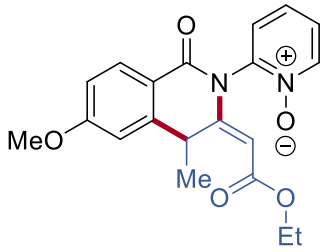

186d

(*E*)-2-[3-(2-Ethoxy-2-oxoethylidene)-6-methoxy-4-methyl-1-oxo-3,4-dihydroisoquinolin-2(1*H*)-yl]pyridine 1-oxide (186d)

The general procedure **A** was followed using benzamide **8** (61.0 mg, 0.25 mmol, 1.00 equiv.) and allene **185d** (94.6 mg, 0.75 mmol). Purification by column chromatography silica gel (CH_2Cl_2/acetone 7:3) yielded **186d** (74.0 mg, 201 µmol, 81%) as a pale yellow oil. **^{1}H NMR** (500 MHz, $CDCl_3$, 2 rotamers): δ = 8.40 – 8.35 (m, 1H), 8.35 – 8.31 (m, 1H), 8.06 (d, *J* = 8.7 Hz, 1H), 8.01 (d, *J* = 8.7 Hz, 1H), 7.49 – 7.42 (m, 1H), 7.39 – 7.32 (m, 5H), 6.89 (dd, *J* = 8.7, 2.5 Hz, 2H), 6.80 (dd, *J* = 4.9, 2.5 Hz, 2H), 5.37 (q, *J* = 7.2

Hz, 2H), 4.80 (s, 1H), 4.71 (s, 1H), 4.17 – 4.02 (m, 4H), 3.87 (s, 3H), 3.86 (s, 3H), 1.78 (d, *J* = 7.1 Hz, 3H), 1.64 (d, *J* = 7.1 Hz, 3H). **^{13}C NMR** (125 MHz, $CDCl_3$, 2 rotamers): *δ* = 166.3 (C_q), 166.2 (C_q), 164.3 (C_q), 164.3 (C_q), 161.8 (C_q), 161.6 (C_q), 158.7 (C_q), 157.9 (C_q), 145.4 (C_q), 144.1 (C_q), 140.9 (CH), 140.7 (CH), 131.4 (CH), 131.0 (CH), 128.8 (CH), 126.9 (CH), 126.3 (CH), 126.2 (CH), 125.9 (CH), 125.4 (CH), 117.5 (C_q), 117.5 (C_q), 114.0 (C_q), 111.4 (CH), 111.3 (CH), 99.2 (CH), 99.2 (CH), 60.0 (CH_2), 60.0 (CH_2), 55.7 (CH_3), 35.7 (CH), 35.1 (CH), 26.6 (CH_3), 26.6 (CH_3), 14.3 (CH_3), 14.3 (CH_3). **IR** (ATR): 2976, 2932, 1689, 1603, 1257, 1027, 883, 770 cm^{-1}. **HR-MS** (ESI) *m/z* calcd for $C_{20}H_{20}N_2O_5$ $[M]^+$: 369.1445, found: 369.1441.

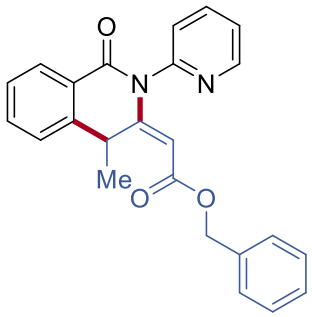

188a

Benzyl (*E*)-2-[4-methyl-1-oxo-2-(pyridin-2-yl)-1,4-dihydroisoquinolin-3(2*H*)-ylidene]acetate (188a)

The general procedure **B** was followed using **186a** (40.0 mg, 0.10 mmol, 1.00 equiv.). Purification by column chromatography silica gel (CH_2Cl_2/acetone 19:1) yielded **188a** (33.0 mg, 86 µmol, 86%) as a pale yellow oil. **^{1}H NMR** (400 MHz, $CDCl_3$): *δ* = 8.70 (ddd, *J* = 4.9, 2.0, 0.9 Hz, 1H), 8.12 (dd, *J* = 7.8, 1.4 Hz, 1H), 7.89 (td, *J* = 7.7, 1.9 Hz, 1H), 7.59 (td, *J* = 7.5, 1.4 Hz, 1H), 7.44 – 7.28 (m, 9H), 5.46 (q, *J* = 7.0 Hz, 1H), 5.09 (q, *J* = 12.3 Hz, 2H), 4.77 (s, 1H), 1.70 (d, *J* = 7.0 Hz, 3H). **^{13}C NMR** (101 MHz, $CDCl_3$): *δ* = 166.2 (C_q), 162.9 (C_q), 160.7 (C_q), 152.0 (C_q), 150.6 (CH), 142.5 (C_q), 139.1 (CH), 136.2 (C_q), 133.9 (CH), 128.8 (CH), 128.7 (CH), 128.4 (CH), 128.3 (CH), 127.4 (CH), 127.1 (CH), 125.5 (C_q), 124.2 (CH), 124.0 (CH), 100.7 (CH), 65.9 (CH_2), 34.9 (CH), 26.7 (CH_3). **IR** (ATR): 2963, 1686, 1605, 1587, 1289, 1131, 747, 697 cm^{-1}. **HR-MS** (ESI) *m/z* calcd for $C_{24}H_{20}N_2O_3$ $[M]^+$: 385.1547, found: 385.1543.

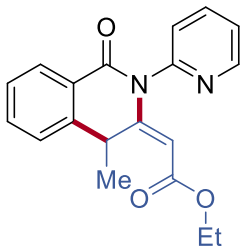

188b

Ethyl (*E*)-2-[4-methyl-1-oxo-2-(pyridin-2-yl)-1,4-dihydroisoquinolin-3(2*H*)-ylidene]acetate (188b)

The general procedure **B** was followed using **186b** (33.8 mg, 0.10 mmol, 1.00 equiv.). Purification by column chromatography silica gel (CH_2Cl_2/acetone 19:1) yielded **188b** (28.7 mg, 86 µmol, 86%) as a pale yellow oil. **^{1}H NMR** (400 MHz, $CDCl_3$): δ = 8.71 (ddd, *J* = 4.9, 2.0, 0.9 Hz, 1H), 8.11 (dd, *J* = 7.9, 1.4 Hz, 1H), 7.90 (td, *J* = 7.7, 1.9 Hz, 1H), 7.57 (td, *J* = 7.5, 1.4 Hz, 1H), 7.43 – 7.29 (m, 4H), 5.43 (q, *J* = 7.0 Hz, 1H), 4.70 (s, 1H), 4.10 (m, 2H), 1.68 (d, *J* = 7.1 Hz, 3H), 1.20 (t, *J* = 7.1 Hz, 3H). **^{13}C NMR** (101 MHz, $CDCl_3$): δ = 166.4 (C_q), 162.9 (C_q), 160.1 (C_q), 152.1 (C_q), 150.6 (CH), 142.6 (C_q), 139.0 (CH), 133.8 (CH), 128.7 (CH), 127.4 (CH), 127.1 (CH), 125.5 (C_q), 124.2 (CH), 124.0 (CH), 101.2 (CH), 59.9 (CH_2), 34.8 (CH), 26.6 (CH_3), 14.4 (CH_3). **IR** (ATR): 2980, 1684, 1605, 1587, 1287, 1132, 1037, 745 cm^{-1}. **HR-MS** (ESI) *m/z* calcd for $C_{19}H_{18}N_2O_3$ $[M]^+$: 323.1390, found: 323.1386.

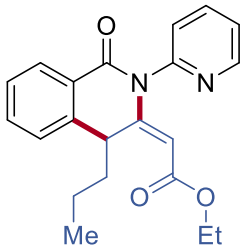

188c

Ethyl (*E*)-2-[1-oxo-4-propyl-2-(pyridin-2-yl)-1,4-dihydroisoquinolin-3(2*H*)-ylidene]acetate (188c)

The general procedure **B** was followed using **186c** (36.6 mg, 0.10 mmol, 1.00 equiv.). Purification by column chromatography silica gel (CH_2Cl_2/acetone 19:1) yielded **188c** (29.3 mg, 91 µmol, 89%) as a pale yellow oil. **^{1}H NMR** (400 MHz, $CDCl_3$): δ = 8.71 (ddd, *J* = 4.9, 2.0, 0.8 Hz, 1H), 8.11 (dd, *J* = 7.8, 1.4 Hz, 1H), 7.90 (td, *J* = 7.7, 2.0 Hz, 1H),

7.56 (td, *J* = 7.5, 1.4 Hz, 1H), 7.45 – 7.37 (m, 2H), 7.32 (ddd, *J* = 7.9, 7.0, 1.1 Hz, 2H), 5.40 (t, *J* = 6.7 Hz, 1H), 4.76 (s, 1H), 4.32 – 3.97 (m, 2H), 2.05 – 1.86 (m, 2H), 1.53 – 1.34 (m, 2H), 1.21 (t, *J* = 7.1 Hz, 3H), 0.92 (t, *J* = 7.3 Hz, 3H). **^{13}C NMR** (101 MHz, $CDCl_3$): *δ* = 166.6 (C_q), 163.3 (C_q), 159.5 (C_q), 152.2 (C_q), 150.6 (CH), 140.9 (C_q), 139.0 (CH), 133.1 (CH), 128.7 (CH), 127.8 (CH), 127.4 (CH), 126.5 (C_q), 124.2 (CH), 123.9 (CH), 101.9 (CH), 60.0 (CH_2), 42.4 (CH_2), 39.7 (CH), 19.6 (CH_2), 14.4 (CH_3), 14.2 (CH_3). **IR** (ATR): 2959, 1685, 1606, 1587, 1296, 1133, 745, 637 cm^{-1}. **HR-MS** (ESI) *m/z* calcd for $C_{21}H_{22}N_2O_3$ $[M]^+$: 351.1703, found: 351.1708.

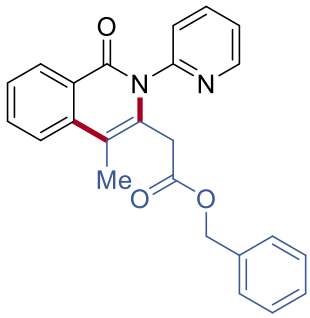

188a'

Benzyl 2-[4-methyl-1-oxo-2-(pyridin-2-yl)-1,2-dihydroisoquinolin-3-yl]acetate (188a')

The general procedure **B** was followed using **186a** (40.0 mg, 0.10 mmol, 1.00 equiv.). Purification by column chromatography silica gel (CH_2Cl_2/acetone 9:1) yielded **188a'** (4.00 mg, 11 µmol, 12%) as a white solid. **M.p.**: 125-126 °C. **^{1}H NMR** (300 MHz, $CDCl_3$): *δ* = 8.54 (ddd, *J* = 4.9, 2.0, 0.9 Hz, 1H), 8.45 (dt, *J* = 7.9, 1.1 Hz, 1H), 7.78 – 7.72 (m, 2H), 7.67 (td, *J* = 7.7, 1.9 Hz, 1H), 7.52 (ddd, *J* = 8.2, 5.1, 3.2 Hz, 1H), 7.36 – 7.21 (m, 7H), 5.02 (s, 2H), 3.56 (s, 2H), 2.34 (s, 3H). **^{13}C NMR** (75 MHz, $CDCl_3$): *δ* = 169.0 (C_q), 162.9 (C_q), 152.6 (C_q), 149.9 (CH), 138.5 (CH), 137.6 (C_q), 135.4 (C_q), 133.0 (CH), 131.2 (C_q), 128.7 (CH), 128.6 (CH), 128.5 (CH), 127.0 (CH), 125.9 (C_q), 125.2 (CH), 123.9 (CH), 123.4 (CH), 112.4 (C_q), 67.1 (CH_2), 36.5 (CH_2), 13.9 (CH_3). **IR** (ATR): 3065, 2168, 1987, 1725, 1656, 1318, 1175, 762 cm^{-1}. **HR-MS** (ESI) *m/z* calcd for $C_{24}H_{20}N_2O_3$ $[M]^+$: 385.1547, found: 385.1544.

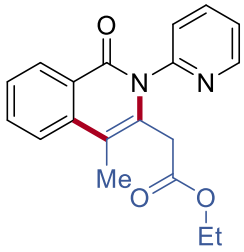

188b'

Ethyl 2-[4-methyl-1-oxo-2-(pyridin-2-yl)-1,2-dihydroisoquinolin-3-yl]acetate (188b')

The general procedure **B** was followed using **186b** (33.8 mg, 0.10 mmol, 1.00 equiv.). Purification by column chromatography silica gel (CH_2Cl_2/acetone 9:1) yielded **188b'** (3.30 mg, 10 µmol, 13%) as a white solid. **M.p.**: 138-140 °C. **^{1}H NMR** (300 MHz, $CDCl_3$): δ = 8.65 (ddd, J = 4.9, 1.9, 0.8 Hz, 1H), 8.46 (dt, J = 7.9, 1.1 Hz, 1H), 7.87 (td, J = 7.7, 1.9 Hz, 1H), 7.83 – 7.66 (m, 2H), 7.51 (ddd, J = 8.1, 5.6, 2.6 Hz, 1H), 7.46 – 7.34 (m, 2H), 4.03 (q, J = 7.1 Hz, 2H), 3.52 (s, 2H), 2.35 (s, 3H), 1.15 (t, J = 7.1 Hz, 3H). **^{13}C NMR** (75 MHz, $CDCl_3$): δ = 169.2 (C_q), 162.9 (C_q), 152.7 (C_q), 149.9 (CH), 138.4 (CH), 137.7 (C_q), 133.0 (CH), 131.4 (C_q), 128.4 (CH), 126.9 (CH), 125.9 (C_q), 125.3 (CH), 123.9 (CH), 123.4 (CH), 112.3 (C_q), 61.3 (CH_2), 36.5 (CH_2), 14.2 (CH_3), 13.8 (CH_3). **IR** (ATR): 2984, 2167, 1987, 1720, 1652, 1283, 967, 694 cm^{-1}. **MS** (EI) *m/z* (relative intensity): 366 (0.4) $[M]^+$, 323 (2), 322 (12), 293 (26), 249 (40), 78 (12). **HR-MS** (EI) *m/z* calcd for $C_{19}H_{18}N_2O_3$ $[M]^+$: 322.1317, found: 322.1306.

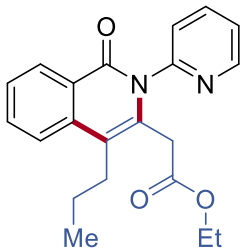

188c'

Ethyl 2-[1-oxo-4-propyl-2-(pyridin-2-yl)-1,2-dihydroisoquinolin-3-yl]acetate (188c')

The general procedure **B** was followed using **186c** (36.6 mg, 0.10 mmol, 1.00 equiv.). Purification by column chromatography silica gel (CH_2Cl_2/acetone 9:1) yielded **188c'** (4.70 mg, 13 µmol, 10%) as a white solid. **M.p.**: 117-119 °C. **^{1}H NMR** (300 MHz, $CDCl_3$):

δ = 8.89 – 8.58 (m, 1H), 8.48 – 8.32 (m, 1H), 7.86 (td, *J* = 7.7, 1.9 Hz, 1H), 7.77 – 7.65 (m, 2H), 7.49 (ddd, *J* = 8.2, 5.6, 2.5 Hz, 1H), 7.44 – 7.35 (m, 2H), 3.99 (q, *J* = 7.1 Hz, 2H), 3.56 (s, 2H), 2.80 – 2.62 (m, 2H), 1.63 (dt, *J* = 15.1, 7.6 Hz, 2H), 1.13 (t, *J* = 7.1 Hz, 3H), 1.06 (t, *J* = 7.3 Hz, 3H). **^{13}C NMR** (75 MHz, $CDCl_3$): δ = 169.4 (C_q), 162.9 (C_q), 152.7 (C_q), 149.8 (CH), 138.3 (CH), 137.0 (C_q), 132.9 (CH), 131.6 (C_q), 128.6 (CH), 126.8 (CH), 126.2 (C_q), 125.6 (CH), 123.9 (CH), 123.4 (CH), 116.9 (C_q), 61.3 (CH_2), 36.0 (CH_2), 30.1 (CH_2), 23.2 (CH_2), 14.5 (CH_3), 14.2 (CH_3). **IR** (ATR): 2958, 2872, 1732, 1656, 1488, 1297, 997, 669 cm^{-1}. **HR-MS** (ESI) *m/z* calcd for $C_{21}H_{22}N_2O_3$ $[M]^+$: 351.1703, found: 351.1701.

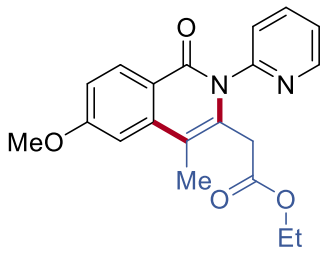

188d'

Ethyl 2-[6-methoxy-4-methyl-1-oxo-2-(pyridin-2-yl)-1,2-dihydroisoquinolin-3-yl]acetate (188d')

The general procedure **B** was followed using **186d** (36.8 mg, 0.10 mmol, 1.00 equiv.). Purification by column chromatography silica gel (CH_2Cl_2/acetone 9:1) yielded **188d'** (32.0 mg, 91 µmol, 91%) as a white solid. **M.p.**: 165-168 °C. **^{1}H NMR** (400 MHz, $CDCl_3$): δ = 8.63 (ddd, *J* = 4.9, 1.9, 0.9 Hz, 1H), 8.37 (d, *J* = 9.5 Hz, 1H), 7.85 (td, *J* = 7.7, 1.9 Hz, 1H), 7.57 – 7.32 (m, 2H), 7.17 – 6.96 (m, 2H), 4.02 (q, *J* = 7.1 Hz, 2H), 3.94 (s, 3H), 3.50 (s, 2H), 2.30 (s, 3H), 1.14 (t, *J* = 7.1 Hz, 3H). **^{13}C NMR** (101 MHz, $CDCl_3$): δ = 168.9 (C_q), 163.2 (C_q), 162.3 (C_q), 152.6 (C_q), 149.6 (CH), 139.6 (C_q), 138.1 (CH), 131.9 (C_q), 130.4 (CH), 125.2 (CH), 123.6 (CH), 119.4 (C_q), 115.0 (CH), 111.6 (C_q), 105.5 (CH), 61.1 (CH_2), 55.4 (CH_3), 36.40 (CH_2), 14.0 (CH_3), 13.8 (CH_3). **IR** (ATR): 2982, 1731, 1651, 1603, 1323, 1209, 1028, 859 cm^{-1}. **HR-MS** (ESI) *m/z* calcd for $C_{20}H_{20}N_2O_4$ $[M]^+$: 353.1496, found: 353.1491.

5.3.1.2 H/D Exchange Experiment

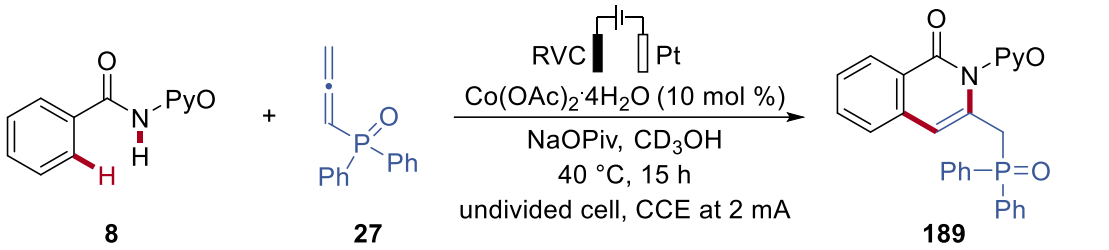

Figure 5.3.1 H/D exchange experiment.

In an undivided cell with a RVC anode (10 mm × 15 mm × 6 mm) and a platinum cathode (10 mm × 15 mm × 0.25 mm), benzamide **8** (107 mg, 0.50 mmol, 1.00 equiv), allene **27** (144 mg, 1.20 equiv), NaOPiv (124 mg, 1.00 mmol, 2.00 equiv) and $Co(OAc)_2{\cdot}4H_2O$ (12.7 mg, 10 mol %) were placed in a 10 mL cell and dissolved in CD_3OH (5 mL). Electrocatalysis was performed at 40 °C with a constant current of 2 mA maintained for 15 h. The reaction was stopped by adding H_2O (10 mL). The RVC anode was washed with CH_2Cl_2 (10 mL) in an ultrasonic cleaner. The washings were added to the reaction mixture and the combined phases were extracted with CH_2Cl_2 (3 × 10 mL), then dried over Na_2SO_4. Evaporation of the solvent and subsequent column chromatography (CH_2Cl_2/MeOH 9:1) gave product **189** (193 mg, 85%) as a white solid. The D-incorporation was estimated by ^{1}H-NMR spectroscopy. No deuterium incorporation was detected.

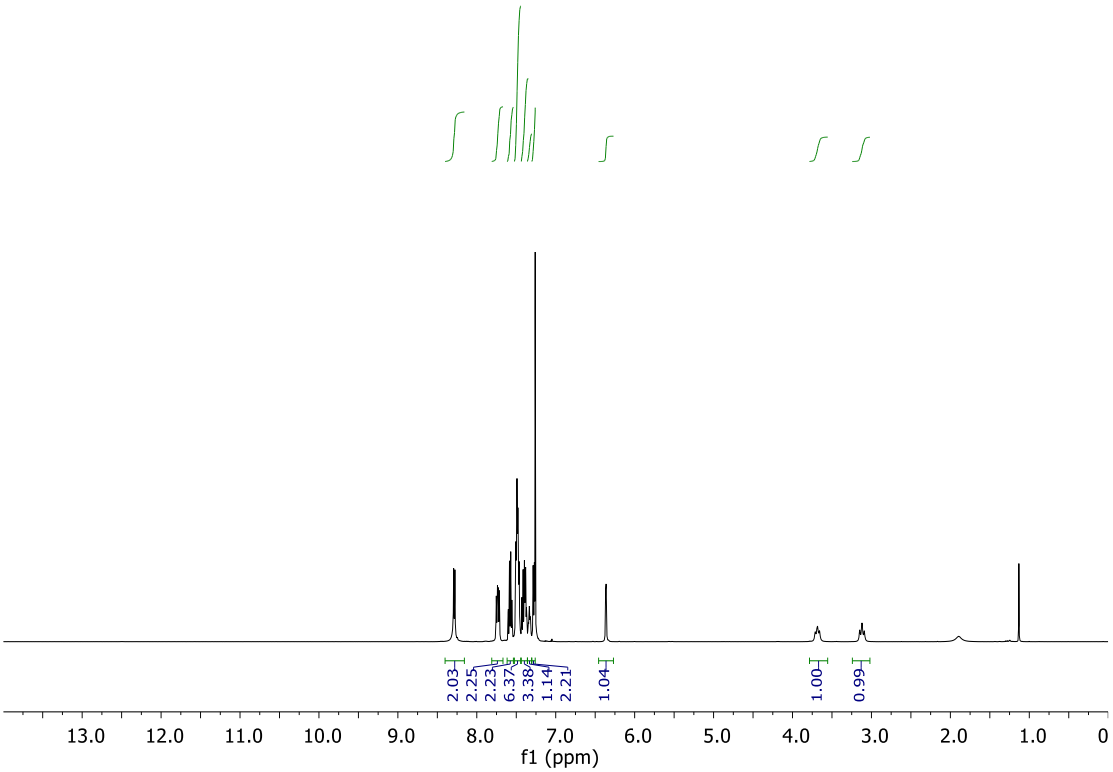

Figure 5.3.2. ^{1}H NMR spectroscopy from the deuteration study.

5.3.2 Electro-Reductive Cobalt-Catalyzed Carboxylation with Atmospheric CO_2

5.3.2.1 Characterization Data

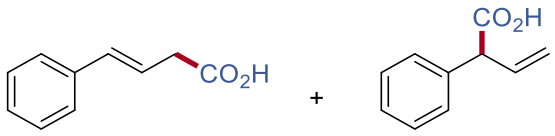

130a **130a'**

(*E*)-4-Phenylbut-3-enoic acid (130a)

The general procedure **C** was followed using cinnamyl chloride **144a** (38.2 mg, 0.25 mmol) and $Co(OAc)_2$ (4.43 mg, 0.025 mmol). Purification by column chromatography on silica gel (*n*-hexane/EtOAc 6:1 with 1% AcOH) yielded **130a** (23.5 mg, 59%, **130a**/**130a'** = 1:1) as a yellow oil. Resonances reported for linear-**130a**: **^{1}H NMR** (300 MHz, $CDCl_3$): δ = 7.47 – 7.19 (m, 5H), 6.54 (d, J = 15.9 Hz, 1H), 6.41 – 6.15 (m, 1H), 3.32 (d, J = 7.0 Hz, 2H). **^{13}C NMR** (75 MHz, $CDCl_3$): δ = 177.9 (C_q),

136.7 (C_q), 134.0 (CH), 128.6 (CH), 127.7 (CH), 126.3 (CH), 120.8 (CH), 38.1 (CH_2). Resonances reported for branch-**130a'**: **^{1}H NMR** (300 MHz, $CDCl_3$): δ = 7.45 – 7.23 (m, 5H), 6.38 – 6.17 (m, 1H), 5.38 – 5.08 (m, 2H), 4.36 (d, *J* = 8.0 Hz, 1H). **^{13}C NMR** (75 MHz, $CDCl_3$): δ = 178.4 (C_q), 137.4 (C_q), 135.0 (CH), 128.8 (CH), 128.1 (CH), 127.6 (CH), 118.1 (CH_2), 55.6 (CH). **IR** (ATR): 2923, 1704, 1495, 1408, 1284, 1211, 1171, 927, 744, 699 cm^{-1}. **MS** (ESI) *m*/*z* (relative intensity): 185 $[M+Na]^+$ (40). **HR-MS** (ESI): *m*/*z* calcd for $C_{10}H_{10}O_2Na^+$ $[M+Na]^+$ 185.0573, found 185.0567. The analytical data are in accordance to those reported in literature.[175]

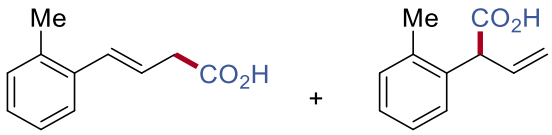

130b **130b'**

(*E*)-4-(*o*-Tolyl)but-3-enoic acid (130b)

The general procedure **C** was followed using allyl chloride **144b** (41.7 mg, 0.25 mmol) and $Co(OAc)_2$ (4.43 mg, 0.025 mmol). Purification by column chromatography on silica gel (*n*-hexane/EtOAc 5:1 with 1% AcOH) yielded **130b** (35.0 mg, 79%, **130b**/**130b'** = 1:1.5) as a yellow oil. Resonances reported for linear-**130b**: **^{1}H NMR** (300 MHz, $CDCl_3$): δ = 7.50 – 7.41 (m, 1H), 7.17 (m, 3H), 6.74 (d, *J* = 15.7, 1H), 6.31 – 6.10 (m, 1H), 3.34 (dd, *J* = 7.1, 1.5 Hz, 2H), 2.35 (s, 3H). **^{13}C NMR** (75 MHz, $CDCl_3$): δ = 178.2 (C_q), 135.8 (C_q), 135.3 (C_q), 131.9 (CH), 130.3 (CH), 127.6 (CH), 126.1 (CH), 125.8 (CH), 122.1 (CH_2), 38.4 (CH_2), 19.8 (CH_3). Resonances reported for branch-**130b'**: **^{1}H NMR** (300 MHz, $CDCl_3$): δ = 7.32 (m, 1H), 7.27 – 7.19 (m, 3H), 6.31 – 6.09 (m, 1H), 5.42 – 4.92 (m, 2H), 4.59 (d, *J* = 7.4 Hz, 1H), 2.38 (s, 3H). **^{13}C NMR** (75 MHz, $CDCl_3$): δ = 178.9 (C_q), 136.2 (C_q), 135.8 (C_q), 134.6 (CH), 130.8 (CH), 128.0 (CH), 126.5 (CH), 127.6 (CH), 117.9 (CH_2), 51.6 (CH), 19.7 (CH_3). **IR** (ATR): 2926, 1704, 1489, 1406, 1286, 1163, 1039, 927, 751, 734 cm^{-1}. **MS** (ESI) *m*/*z* (relative intensity): 199 $[M+Na]^+$ (95), 194 $[M+NH_4]^+$ (50). **HR-MS** (ESI): *m*/*z* calcd for $C_{11}H_{12}O_2Na^+$ $[M+Na]^+$ 199.0730, found 199.0735. The analytical data are in accordance to those reported in literature.[254]

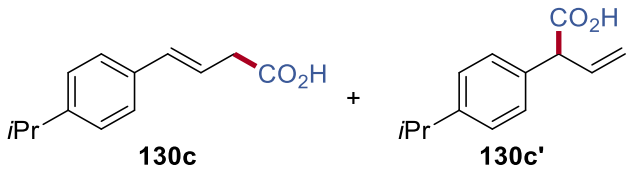

(*E*)-4-(4-Isopropylphenyl)but-3-enoic acid (130c)

The general procedure **C** was followed using allyl chloride **144c** (48.7 mg, 0.25 mmol) and $Co(OAc)_2$ (4.43 mg, 0.025 mmol). Purification by column chromatography on silica gel (*n*-hexane/EtOAc 5:1 with 1% AcOH) yielded **130c** (28.5 mg, 55%, **130c**/**130c'** = 4:3) as a pale yellow oil. Resonances reported for linear-**130c**: **^{1}H NMR** (400 MHz, $CDCl_3$): δ = 7.34 – 7.29 (m, 2H), 7.19 (m, 2H), 6.50 (d, J = 15.8 Hz, 1H), 6.30 – 6.15 (m, 1H), 3.29 (d, J = 7.1 Hz, 2H), 2.97 (p, J = 6.9 Hz, 1H), 1.26 (d, J = 6.9 Hz, 6H). **^{13}C NMR** (100 MHz, $CDCl_3$): δ = 178.2 (C_q), 148.6 (C_q), 134.3 (C_q), 133.8 (CH), 126.9 (CH), 126.6 (CH), 120.0 (CH), 38.2 (CH_2), 33.9 (CH), 24.0 (CH_3). Resonances reported for branch-**130c'**: **^{1}H NMR** (400 MHz, $CDCl_3$): δ = 7.29 – 7.20 (m, 4H), 6.32 – 6.12 (m, 1H), 5.28 – 5.14 (m, 2H), 4.32 (d, J = 8.1 Hz, 1H), 2.97 (p, J = 6.9 Hz, 1H), 1.24 (d, J = 6.9 Hz, 6H). **^{13}C NMR** (100 MHz, $CDCl_3$): δ = 178.9 (C_q), 148.2 (C_q), 135.2 (CH), 134.8 (C_q), 128.0 (CH), 126.3 (CH), 117.9 (CH_2), 55.3 (CH), 33.8 (CH), 24.0 (CH_3). **IR** (ATR): 2959, 1706, 1513, 1415, 1286, 1216, 1054, 967, 925, 550 cm^{-1}. **MS** (ESI) *m*/*z* (relative intensity): 227 $[M+Na]^+$ (100). **HR-MS** (ESI): *m*/*z* calcd for $C_{13}H_{16}O_2Na^+$ $[M+Na]^+$ 227.1043, found 227.1048. The analytical data are in accordance to those reported in literature.[255]

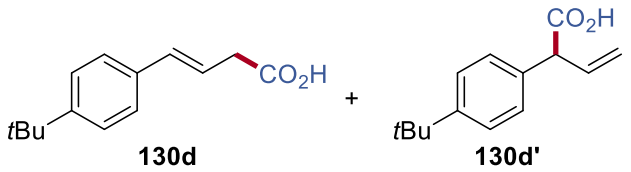

(*E*)-4-[4-(*tert*-Butyl)phenyl]but-3-enoic acid (130d)

The general procedure **C** was followed using allyl chloride **144d** (52.2 mg, 0.25 mmol) and $Co(OAc)_2$ (4.43 mg, 0.025 mmol). Purification by column chromatography on silica gel (*n*-hexane/EtOAc 6:1 with 1% AcOH) yielded **130d** (30.0 mg, 55%, **130d**/**130d'** = 1.2:1) as a yellow oil. Resonances reported for linear-**130d**: **^{1}H NMR** (400 MHz, $CDCl_3$): δ = 7.37 (d, J = 8.4 Hz, 2H), 7.28 – 7.24 (m, 2H), 6.50 (d,

J = 15.8 Hz, 1H), 6.31 – 6.15 (m, 1H), 3.28 (d, *J* = 7.0 Hz, 2H), 1.31 (s, 9H). **^{13}C NMR** (100 MHz, $CDCl_3$): *δ* = 177.8 (C_q), 150.8 (C_q), 133.9 (C_q), 133.7 (CH), 126.0 (CH), 125.5 (CH), 120.0 (CH), 38.1 (CH_2), 34.6 (C_q), 31.3 (CH_3). Resonances reported for branch-**130d'**: **^{1}H NMR** (400 MHz, $CDCl_3$): *δ* = 7.33 (m, 4H), 6.32 – 6.12 (m, 1H), 5.29 – 5.12 (m, 2H), 4.31 (d, *J* = 8.1 Hz, 1H), 1.31 (s, 9H). **^{13}C NMR** (100 MHz, $CDCl_3$) *δ* = 178.5 (C_q), 150.5 (C_q), 135.1 (CH), 134.3 (C_q), 127.7 (CH), 125.8 (CH), 117.9 (CH_2), 55.1 (CH), 34.5 (C_q), 31.3 (CH_3). **IR** (ATR): 2960, 1705, 1409, 1364, 1269, 1108, 924, 826, 704, 558 cm^{-1}. **MS** (ESI) *m*/*z* (relative intensity): 241 $[M+Na]^+$ (60). **HR-MS** (ESI): *m*/*z* calcd for $C_{14}H_{18}O_2Na^+$ $[M+Na]^+$ 241.1199, found 241.1199.

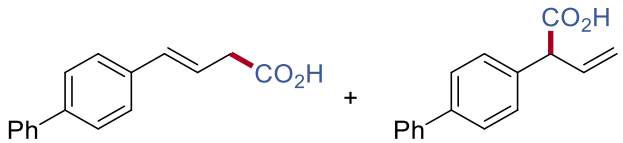

130e **130e'**

(*E*)-4-([1,1'-Biphenyl]-4-yl)but-3-enoic acid (130e)

The general procedure **C** was followed using allyl chloride **144e** (57.2 mg, 0.25 mmol) and $Co(OAc)_2$ (4.43 mg, 0.025 mmol). Purification by column chromatography on silica gel (*n*-hexane/EtOAc 6:1 with 1% AcOH) yielded **130e** (40.0 mg, 67%, **130e**/**130e'** = 1:3) as a pale white solid. **M.p.**: 174 – 177 °C. Resonances reported for linear-**130e**: **^{1}H NMR** (400 MHz, $CDCl_3$): *δ* = 7.62 – 7.54 (m, 4H), 7.47 – 7.39 (m, 4H), 7.38 – 7.32 (m, 1H), 6.55 (d, *J* = 15.8 Hz, 1H), 6.39 – 6.31 (m, 1H), 3.32 (d, *J* = 7.0 Hz, 2H). **^{13}C NMR** (100 MHz, $CDCl_3$): *δ* = 178.0 (C_q), 140.6 (C_q), 140.4 (C_q), 135.7 (C_q), 133.5 (CH), 128.8 (CH), 127.4 (CH), 127.3 (CH), 127.1 (CH), 126.9 (CH), 121.0 (CH), 38.2 (CH_2). Resonances reported for branch-**130e'**: **^{1}H NMR** (400 MHz, $CDCl_3$): *δ* =7.62 – 7.54 (m, 4H), 7.47 – 7.39 (m, 4H), 7.38 – 7.32 (m, 1H), 6.32 – 6.20 (m, 1H), 5.36 – 5.14 (m, 2H), 4.39 (d, *J* = 8.0 Hz, 1H). **^{13}C NMR** (100 MHz, $CDCl_3$): *δ* = 178.3 (C_q), 140.6 (C_q), 140.4 (C_q), 136.4 (C_q), 134.9 (CH), 128.5 (CH), 127.6 (CH), 127.3 (CH), 127.1 (CH), 126.8 (CH), 118.2 (CH_2), 55.3 (CH). **IR** (ATR): 2928, 1696, 1484, 1406, 1215, 933, 829, 758, 739, 694 cm^{-1}. **MS** (ESI) *m*/*z* (relative intensity): 237 $[M-H]^-$ (35), 261 $[M+Na]^+$ (20). **HR-MS** (ESI): *m*/*z* calcd for $C_{16}H_{14}O_2Na^+$ $[M+Na]^+$ 261.0886, found 261.0888. The analytical data are in accordance to those reported in

literature.[175]

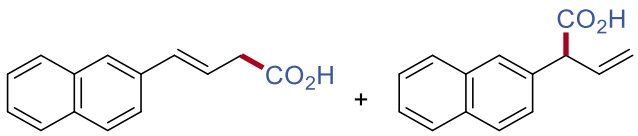

130f **130f'**

(*E*)-4-(Naphthalen-2-yl)but-3-enoic acid (130f)

The general procedure **C** was followed using allyl chloride **144f** (50.7 mg, 0.25 mmol) and $Co(OAc)_2$ (4.43 mg, 0.025 mmol). Purification by column chromatography on silica gel (*n*-hexane/EtOAc 6:1 with 1% AcOH) yielded **130f** (24.0 mg, 45%, **130f**/**130f'** = 1:2.5) as a pale white solid. **M.p.**: 147 – 150 °C. Resonances reported for linear-**130f**: **^{1}H NMR** (400 MHz, $CDCl_3$): δ = 7.85 – 7.80 (m, 4H), 7.72 (dd, *J* = 8.5, 1.6 Hz, 1H), 7.50 – 7.43 (m, 2H), 6.68 (d, *J* = 15.8 Hz, 1H), 6.41 (dt, *J* = 16.0, 7.1 Hz, 1H), 3.36 (d, *J* = 7.0 Hz, 2H). **^{13}C NMR** (100 MHz, $CDCl_3$): δ = 177.6 (C_q), 134.2 (CH), 133.7 (C_q), 133.6 (C_q), 133.1 (C_q), 129.1 (CH), 128.4 (CH), 128.1 (CH), 126.4 (CH), 126.2 (CH), 126.1 (CH), 123.6 (CH), 121.4 (CH), 38.2 (CH_2). Resonances reported for branch-**130f'**: **^{1}H NMR** (400 MHz, $CDCl_3$): δ = 7.79 – 7.76 (m, 2H), 7.59 (dd, *J* = 8.5, 1.7 Hz, 1H), 7.50 – 7.43 (m, 4H), 6.32 (ddd, *J* = 17.5, 10.2, 7.8 Hz, 1H), 5.37 – 5.16 (m, 2H), 4.52 (d, *J* = 7.8 Hz, 1H). **^{13}C NMR** (100 MHz, $CDCl_3$): δ = 178.2 (C_q), 135.0 (CH), 134.9 (C_q), 133.6 (C_q), 132.8 (C_q), 128.0 (CH), 127.8 (CH), 127.2 (CH), 126.4 (CH), 126.3 (CH), 126.1 (CH), 123.6 (CH), 118.5 (CH_2), 55.6 (CH). **IR** (ATR): 2920, 1700, 1407, 1295, 1214, 932, 824, 750, 615, 484 cm^{-1}. **MS** (ESI) *m*/*z* (relative intensity): 235 $[M+Na]^+$ (100). **HR-MS** (ESI): *m*/*z* calcd for $C_{14}H_{12}O_2Na^+$ $[M+Na]^+$ 235.0730, found 235.0725. The analytical data are in accordance to those reported in literature.[175]

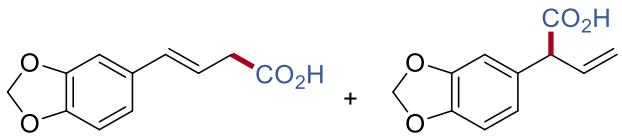

130g **130g'**

(*E*)-4-(Benzo[d][1,3]dioxol-5-yl)but-3-enoic acid (130g)

The general procedure **C** was followed using allyl chloride **144g** (49.2 mg, 0.25 mmol) and $Co(OAc)_2$ (4.43 mg, 0.025 mmol). Purification by column chromatography on silica

gel (*n*-hexane/EtOAc 5:1 with 1% AcOH) yielded **130g** (27.5 mg, 53%, **130g**/**130g'** = 1:2) as a pale yellow oil. Resonances reported for linear-**130g**: **^{1}H NMR** (400 MHz, $CDCl_3$): δ = 6.92 (d, *J* = 1.7 Hz, 1H), 6.80 (d, *J* = 8.0, 1.7 Hz, 1H), 6.74 (d, *J* = 8.0 Hz, 1H), 6.42 (d, *J* = 15.9 Hz, 1H), 6.22 – 6.14 (m, 1H), 5.95 (s, 2H), 3.26 (dd, *J* = 7.1, 1.5 Hz, 2H). **^{13}C NMR** (100 MHz, $CDCl_3$): δ = 176.8 (C_q), 148.2 (C_q), 147.4 (C_q), 133.7 (CH), 131.3 (C_q), 121.1 (CH), 119.1 (CH), 108.4 (CH), 105.8 (CH), 101.2 (CH_2), 37.9 (CH_2). Resonances reported for branch-**130g'**: **^{1}H NMR** (400 MHz, $CDCl_3$): δ = 6.83 (s, 1H), 6.79 – 6.73 (m, 2H), 6.14 – 6.05 (m, 1H), 5.95 (s, 2H), 5.31 – 5.05 (m, 2H), 4.25 (d, *J* = 7.9, 1H). **^{13}C NMR** (100 MHz, $CDCl_3$): δ = 177.3 (C_q), 148.1 (C_q), 147.2 (C_q), 135.1 (CH), 131.2 (C_q), 121.6 (CH), 118.1 (CH_2), 108.7 (CH), 108.6 (CH), 101.3 (CH_2), 55.0 (CH). **IR** (ATR): 2916, 1701, 1487, 1440, 1242, 1034, 927, 808, 723, 540 cm^{-1}. **MS** (ESI) *m*/*z* (relative intensity): 207 $[M+H]^+$ (30). **HR-MS** (ESI): *m*/*z* calcd for $C_{11}H_{11}O_4^+$ $[M+H]^+$ 207.0652, found 207.0650. The analytical data are in accordance to those reported in literature.[175]

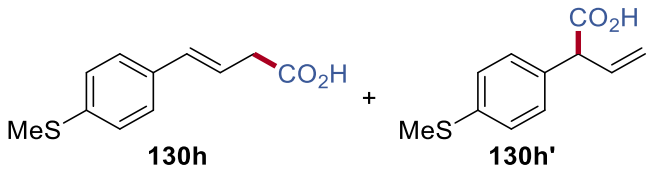

130h **130h'**

(*E*)-4-[4-(Methylthio)phenyl]but-3-enoic acid (130h)

The general procedure **C** was followed using allyl chloride **144h** (49.7 mg, 0.25 mmol) and $Co(OAc)_2$ (4.43 mg, 0.025 mmol). Purification by column chromatography on silica gel (*n*-hexane/EtOAc 5:1 with 1% AcOH) yielded **130h** (33.0 mg, 63%, **130h**/**130h'** = 1:9) as a yellow solid. **M.p.**: 127 – 128 °C. Resonances reported for linear-**130h**: **^{1}H NMR** (400 MHz, $CDCl_3$): δ = 7.27 – 7.25 (m, 1H), 7.25 – 7.23 (m, 3H), 6.46 (d, *J* = 15.8 Hz, 1H), 6.26 – 6.23 (m, 1H), 3.28 (d, *J* = 7.0 Hz, 2H), 2.48 (s, 3H). **^{13}C NMR** (100 MHz, $CDCl_3$): δ = 177.8 (C_q), 138.1 (CH), 133.7 (C_q), 133.5 (C_q), 126.9 (CH), 126.8 (CH), 120.3 (CH), 38.1 (CH_2), 15.4 (CH_3). Resonances reported for branch-**130h'**: **^{1}H NMR** (400 MHz, $CDCl_3$): δ = 7.28 – 7.22 (m, 4H), 6.18 (ddd, *J* = 17.6, 10.1, 7.8 Hz, 1H), 5.30 – 5.08 (m, 2H), 4.29 (d, *J* = 7.8 Hz, 1H), 2.47 (s, 3H). **^{13}C NMR** (100 MHz, $CDCl_3$): δ = 178.3 (C_q), 138.2 (CH), 135.0 (C_q), 134.2 (C_q), 128.7 (CH),

127.1 (CH), 118.3 (CH_2), 55.0 (CH), 16.0 (CH_3). **IR** (ATR): 2917, 1688, 1401, 1212, 1092, 930, 815, 735, 599, 503 cm^{-1}. **MS** (ESI) *m*/*z* (relative intensity): 231 $[M+Na]^+$ (100), 207 $[M-H]^-$ (50). **HR-MS** (ESI): *m*/*z* calcd for $C_{11}H_{12}O_2SNa^+$ $[M+Na]^+$ 231.0450, found 231.0452. The analytical data are in accordance to those reported in literature.[256]

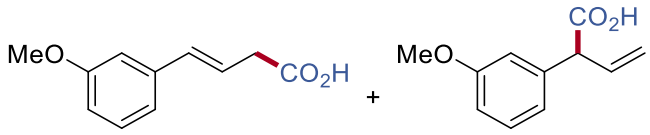

130i **130i'**

(*E*)-4-(3-Methoxyphenyl)but-3-enoic acid (130i)

The general procedure **C** was followed using allyl chloride **144i** (45.7 mg, 0.25 mmol) and $Co(OAc)_2$ (4.43 mg, 0.025 mmol). Purification by column chromatography on silica gel (*n*-hexane/EtOAc 5:1 with 1% AcOH) yielded **130i** (24.5 mg, 51%, **130i**/**130i'** = 6:1) as a yellow oil. Resonances reported for linear-**130i**: **^{1}H NMR** (400 MHz, $CDCl_3$): δ = 7.24 (dd, *J* = 8.2, 7.6 Hz, 1H), 6.97 (d, *J* = 7.6 Hz, 1H), 6.91 (dd, *J* = 2.5, 1.8 Hz, 1H), 6.80 (dd, *J* = 8.2, 2.5 Hz, 1H), 6.49 (d, *J* = 15.8 Hz, 1H), 6.28 (dt, *J* = 15.9, 7.0 Hz, 1H), 3.82 (s, 3H), 3.30 (d, *J* = 7.0 Hz, 2H). **^{13}C NMR** (100 MHz, $CDCl_3$): δ = 177.9 (C_q), 160.0 (C_q), 138.2 (C_q), 134.0 (CH), 129.7 (CH), 121.3 (CH), 119.2 (CH), 113.6 (CH), 111.7 (CH), 55.6 (CH_3), 38.1 (CH_2). Resonances reported for branch-**130i'**: **^{1}H NMR** (400 MHz, $CDCl_3$): δ = 7.30 – 7.24 (m, 1H), 6.94 – 6.88 (m, 2H), 6.86 – 6.81 (m, 1H), 6.24 – 6.16 (m, 1H), 5.30 – 5.15 (m, 2H), 4.31 (d, *J* = 8.0 Hz, 1H), 3.81 (s, 3H). **^{13}C NMR** (100 MHz, $CDCl_3$): δ = 178.4 (C_q), 160.0 (C_q), 139.0 (C_q), 135.0 (CH), 130.0 (CH), 120.5 (CH), 118.3 (CH_2), 114.0 (CH), 113.1 (CH), 55.6 (CH_3), 55.4 (CH). **IR** (ATR): 2938, 1705, 1599, 1489, 1263, 1155, 1042, 968, 777, 692 cm^{-1}. **MS** (ESI) *m*/*z* (relative intensity): 193 $[M+H]^+$ (100), 215 $[M+Na]^+$ (50). **HR-MS** (ESI): *m*/*z* calcd for $C_{11}H_{13}O_3Na^+$ $[M+Na]^+$ 193.0859, found 193.0858. The analytical data are in accordance to those reported in literature.[175]

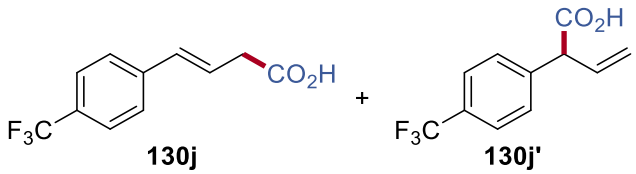

(*E*)-4-[4-(Trifluoromethyl)phenyl]but-3-enoic acid (130j)

The general procedure **C** was followed using allyl chloride **144j** (55.2 mg, 0.25 mmol) and $Co(OAc)_2$ (4.43 mg, 0.025 mmol). Purification by column chromatography on silica gel (*n*-hexane/EtOAc 5:1 with 1% AcOH) yielded **130j** (34.0 mg, 59%, **130j**/**130j'**= 1:5.6) as a yellow oil. Resonances reported for linear-**130j**: **^{1}H NMR** (400 MHz, $CDCl_3$): δ = 7.57 (d, J = 8.2 Hz, 2H), 7.46 (d, J = 8.0 Hz, 2H), 6.55 (d, J = 15.9 Hz, 1H), 6.38 (dt, J = 15.3, 7.0 Hz, 1H), 3.33 (d, J = 7.0 Hz, 2H). **^{13}C NMR** (100 MHz, $CDCl_3$): δ = 177.8 (C_q), 140.2 (C_q), 132.7 (CH), 129.7 (q, $^2J_{C\text{-}F}$ = 32.7 Hz, C_q), 126.6 (CH), 125.7 (q, $^3J_{C\text{-}F}$ = 3.8 Hz, CH), 124.1 (q, $^1J_{C\text{-}F}$ = 272.0 Hz, C_q), 123.7 (CH), 38.1 (CH_2). **^{19}F NMR** (282 MHz, $CDCl_3$): δ = – 62.6 (s). Resonances reported for branch-**130j'**: **^{1}H NMR** (400 MHz, $CDCl_3$): δ = 7.61 (d, J = 7.9 Hz, 2H), 7.45 (d, J = 8.0 Hz, 2H), 6.20 (ddd, J = 17.6, 10.1, 7.9 Hz, 1H), 5.35 – 5.15 (m, 2H), 4.40 (d, J = 7.8 Hz, 1H). **^{13}C NMR** (100 MHz, $CDCl_3$): δ = 177.9 (C_q), 141.3 (C_q), 134.1 (CH), 130.1 (q, $^2J_{C\text{-}F}$ = 32.6 Hz, C_q), 128.8 (CH), 125.9 (q, $^3J_{C\text{-}F}$ = 3.8 Hz, CH), 124.1 (q, $^1J_{C\text{-}F}$ = 272.0 Hz, C_q), 119.0 (CH_2), 55.4 (CH). **^{19}F NMR** (282 MHz, $CDCl_3$): δ = – 62.7 (s). **IR** (ATR): 2918, 1709, 1618, 1412, 1324, 1165, 1124, 1068, 930, 835 cm^{-1}. **MS** (ESI) *m*/*z* (relative intensity): 253 $[M+Na]^+$ (10). **HR-MS** (ESI): *m*/*z* calcd for $C_{11}H_9F_3O_2Na^+$ $[M+Na]^+$ 253.0447, found 253.0444. The analytical data are in accordance to those reported in literature.[175]

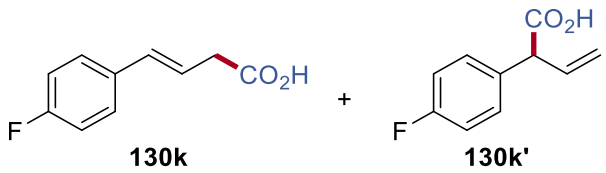

(*E*)-4-(4-Fluorophenyl)but-3-enoic acid (130k)

The general procedure **C** was followed using allyl chloride **144k** (42.7 mg, 0.25 mmol) and $Co(OAc)_2$ (4.43 mg, 0.025 mmol). Purification by column chromatography on silica gel (*n*-hexane/EtOAc 5:1 with 1% AcOH) yielded **130k** (29.0 mg, 64%,

130k/**130k'** = 9:1) as a yellow oil. Resonances reported for linear-**130k**: **^{1}H NMR** (400 MHz, $CDCl_3$): δ = 7.37 – 7.29 (m, 2H), 7.02 – 6.97 (m, 2H), 6.48 (d, J = 15.9 Hz, 1H), 6.19 (dt, J = 15.1, 6.9 Hz, 1H), 3.29 (d, J = 7.0 Hz, 2H). **^{13}C NMR** (100 MHz, $CDCl_3$): δ = 177.6 (C_q), 162.5 (d, $^{1}J_{C\text{-}F}$ = 247.0 Hz, C_q), 133.0 (CH), 132.9 (d, $^{4}J_{C\text{-}F}$ = 3.3 Hz, C_q), 128.0 (d, $^{3}J_{C\text{-}F}$ = 8 Hz, CH), 120.7 (d, $^{4}J_{C\text{-}F}$ = 2.4 Hz, CH), 115.6 (d, $^{2}J_{C\text{-}F}$ = 21.6 Hz, CH), 38.1 (CH_2). **^{19}F NMR** (282 MHz, $CDCl_3$): δ = – 114.3 (s). Resonances reported for branch-**130k'**: **^{1}H NMR** (400 MHz, $CDCl_3$): δ = 7.31 – 7.27 (m, 2H), 7.07 – 7.02 (m, 2H), 6.16 – 6.13 (m, 1H), 5.33 – 5.10 (m, 2H), 4.33 (d, J = 7.7 Hz, 1H). **^{13}C NMR** (100 MHz, $CDCl_3$): δ = 177.9 (C_q), 162.4 (d, $^{1}J_{C\text{-}F}$ = 247.0 Hz, C_q), 134.8 (CH), 133.2 (d, $^{4}J_{C\text{-}F}$ = 3.8 Hz, C_q), 129.9 (d, $^{3}J_{C\text{-}F}$ = 8.1 Hz, CH), 118.4 (CH_2), 115.8 (d, $^{2}J_{C\text{-}F}$ = 21.0 Hz, CH), 54.8 (CH). **^{19}F NMR** (282 MHz, $CDCl_3$): δ = – 114.8 (s). **IR** (ATR): 2923, 1697, 1509, 1400, 1302, 1225, 978, 845, 801, 510 cm^{-1}. **MS** (ESI) m/z (relative intensity): 203 $[M+Na]^+$ (25). **HR-MS** (ESI): m/z calcd for $C_{10}H_9FO_2Na^+$ $[M+Na]^+$ 203.0479, found 203.0472. The analytical data are in accordance to those reported in literature.[256]

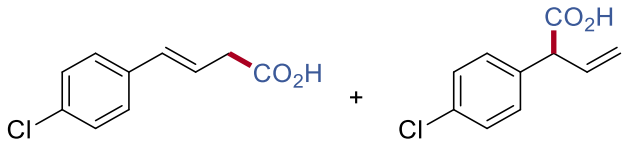

130l **130l'**

(*E*)-4-(4-Chlorophenyl)but-3-enoic acid (130l)

The general procedure **C** was followed using allyl chloride **144l** (0.25 mmol, 46.8 mg) and $Co(OAc)_2$ (0.025 mmol, 4.43 mg). Purification by column chromatography on silica gel (*n*-hexane/EtOAc 5:1 with 1% AcOH) yielded **130l** (29.0 mg, 47%, **130l**/**130l'** = 9:1) as a pale white solid. **M.p.**: 105 – 106 °C. Resonance reported for linear-**130l**: **^{1}H NMR** (400 MHz, $CDCl_3$): δ = 7.36 – 7.23 (m, 4H), 6.47 (d, J = 15.8 Hz, 1H), 6.26 (dt, J = 15.8, 7.1 Hz, 1H), 3.30 (d, J = 7.1 Hz, 2H). **^{13}C NMR** (100 MHz, $CDCl_3$): δ = 177.6 (C_q), 135.2 (C_q), 133.5 (C_q), 133.0 (CH), 128.9 (CH), 127.7 (CH), 121.7 (CH), 38.1 (CH_2). Resonance reported for branch-**130l'**: **^{1}H NMR** (400 MHz, $CDCl_3$): δ = 7.34 – 7.25 (m, 4H), 6.21 – 6.09 (m, 1H), 5.30 – 5.16 (m, 2H), 4.32 (d, J = 7.9 Hz, 1H). **^{13}C NMR** (100 MHz, $CDCl_3$): δ = 177.7 (C_q), 135.9 (C_q), 134.6 (C_q), 133.8 (CH), 129.7 (CH),

129.1 (CH), 118.7 (CH_2), 55.4 (CH). **IR** (ATR): 2922, 1715, 1491, 1400, 1300, 1212, 974, 790, 686, 504 cm^{-1}. **MS** (ESI) *m*/*z* (relative intensity): 195 [^{35}M-H]$^-$ (10). **HR-MS** (ESI): *m*/*z* calcd for $C_{10}H_8ClO_2^-$ [^{35}M-H]$^-$ 195.0218, found 195.0216. The analytical data are in accordance to those reported in literature.[256]

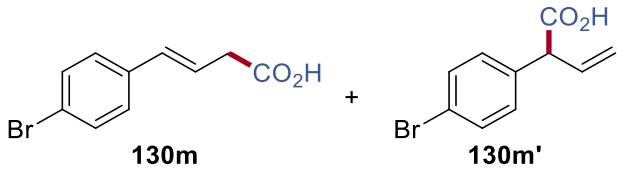

130m **130m'**

(*E*)-4-(4-Bromophenyl)but-3-enoic acid (130m)

The general procedure **C** was followed using allyl chloride **144m** (0.25 mmol, 57.9 mg) and $Co(OAc)_2$ (0.025 mmol, 4.43 mg). Purification by column chromatography on silica gel (*n*-hexane/EtOAc 5:1 with 1% AcOH) yielded **130m** (40.0 mg, 66%, **130m**/**130m'** = 1:4 with approx. 5% dehalogenated linear-**130a** and 10% dehalogenated branch-**130a'**) as a yellow solid. **M.p.**: 104 – 107 °C. Resonance reported for linear-**130m**: **^{1}H NMR** (400 MHz, $CDCl_3$): δ = 7.43 (d, *J* = 8.4 Hz, 2H), 7.25 (d, *J* = 8.4 Hz, 2H), 6.45 (d, *J* = 15.9 Hz, 1H), 6.26 (dt, *J* = 15.9, 7.4 Hz, 1H), 3.28 (d, *J* = 6.7 Hz, 2H). **^{13}C NMR** (100 MHz, $CDCl_3$): δ = 177.8 (C_q), 135.7 (C_q), 133.0 (CH), 131.8 (CH), 128.0 (CH), 121.8 (CH), 121.7 (C_q), 38.1 (CH_2). Resonance reported for branch-**130m'**: **^{1}H NMR** (400 MHz, $CDCl_3$): δ = 7.47 (d, *J* = 8.2 Hz, 2H), 7.20 (d, *J* = 8.3 Hz, 2H), 6.16 (ddd, *J* = 17.5, 10.2, 7.8 Hz, 1H), 5.30 – 5.14 (m, 2H), 4.29 (d, *J* = 7.8 Hz, 1H). **^{13}C NMR** (100 MHz, $CDCl_3$): δ = 178.2 (C_q), 136.3 (C_q), 134.5 (CH), 132.0 (CH), 130.0 (CH), 121.9 (C_q), 118.6 (CH_2), 55.0 (CH). **IR** (ATR): 2921, 1704, 1487, 1398, 1211, 1071, 973, 789, 668, 501 cm^{-1}. **MS** (ESI) *m*/*z* (relative intensity): 239 [^{79}M-H]$^-$ (20). **HR-MS** (ESI): *m*/*z* calcd for $C_{10}H_8BrO_2^-$ [^{79}M-H]$^-$ 238.9713, found 238.9708. The analytical data are in accordance to those reported in literature.[254]

5.3.2.2 Kinetic Profile

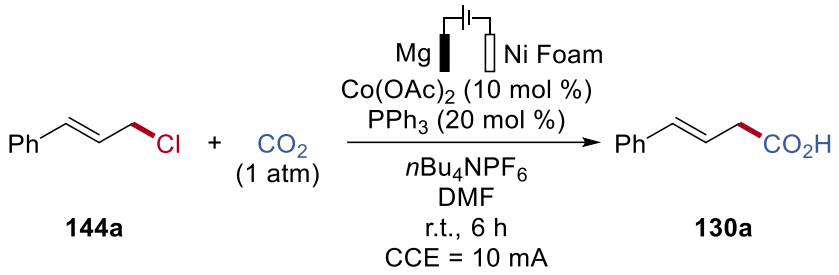

Figure 5.3.3. General reaction scheme for kinetic profiling.

Under an atmosphere of N_2, cinnamyl chloride **144a** (76.4 mg, 0.50 mmol), $Co(OAc)_2$ (8.85 mg, 0.05 mmol, 10.0 mol %), PPh_3 (26.2 mg, 0.10 mmol, 20.0 mol %), nBu$_4$NPF$_6$ (193.8 mg, 0.5 mmol, 1.00 equiv) were dissolved in DMF (10.0 mL) and stirred at 25 ℃. The reaction vessel was bubbled for 30 minutes under CO_2 gas. The CO_2 gas (1 atm) was constantly supplied throughout the course of the reaction. For 6 h, an *in situ* IR spectrum was acquired every 2 mins. The full kinetic profile was determined from the decrease of the peak at 755 cm^{-1}, which corresponds to the C–Cl stretching frequency of substrate **144a**. The absolute peak area was measured from 696 to 675 cm^{-1} with a two-point baseline at 696 and 675 cm^{-1} (see **Figure 5.3.4** and **Figure 5.3.5**).

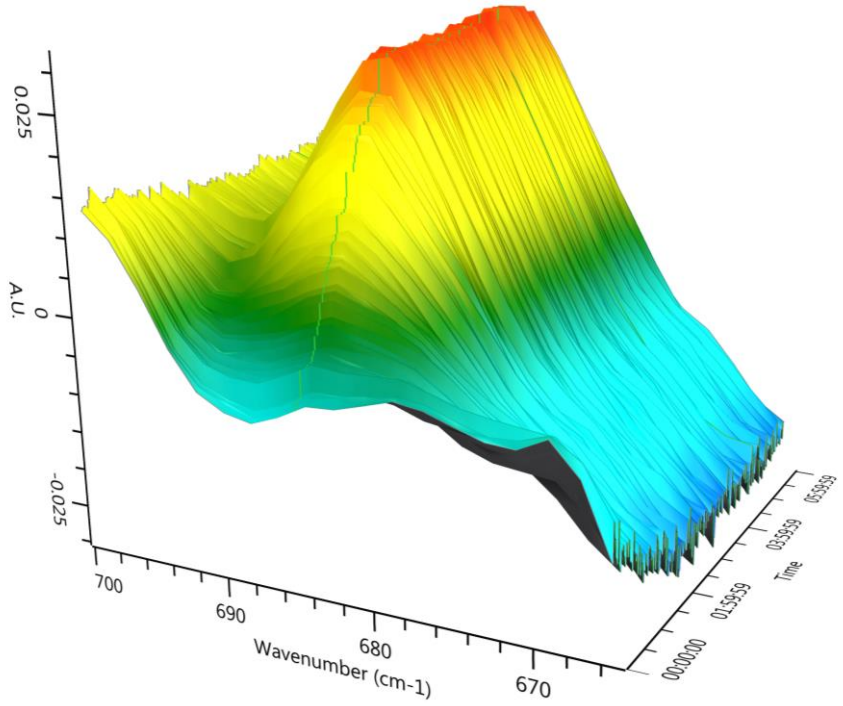

Figure 5.3.4. 3D surface plot for the C=C vibration of carboxylated product **130a**.

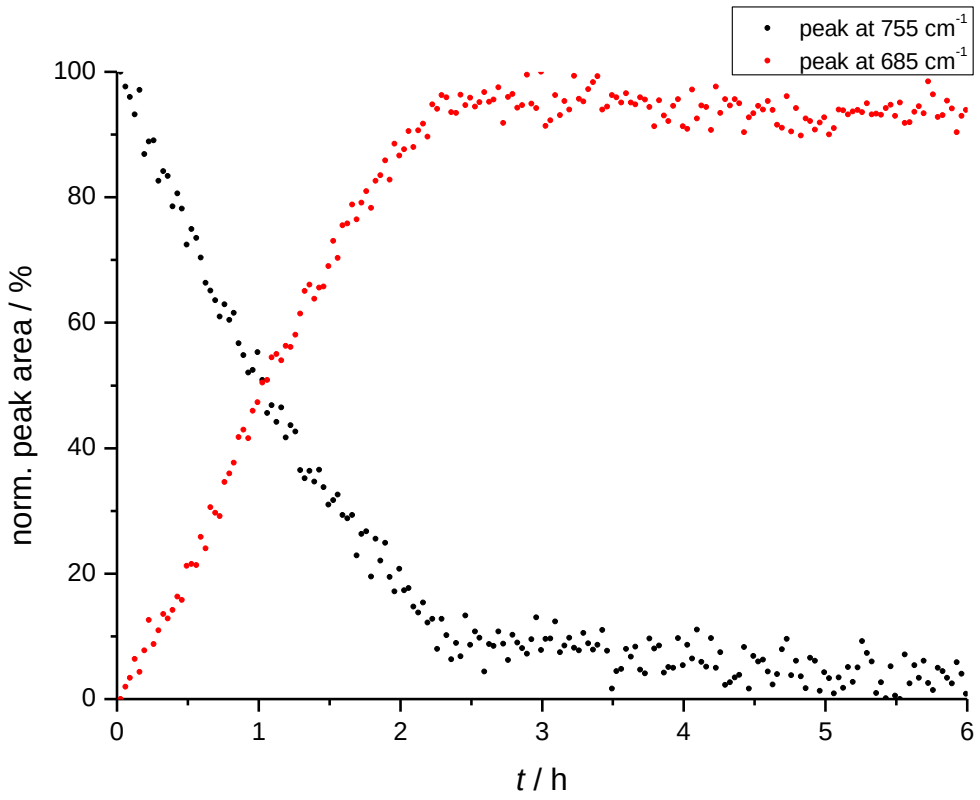

Figure 5.3.5. Plot of the normalised peak area (%) vs time of the consumption of starting material **144a** and the production of **130a**.

5.3.2.3 Rates of Cobalt Salts as Pre-catalyst

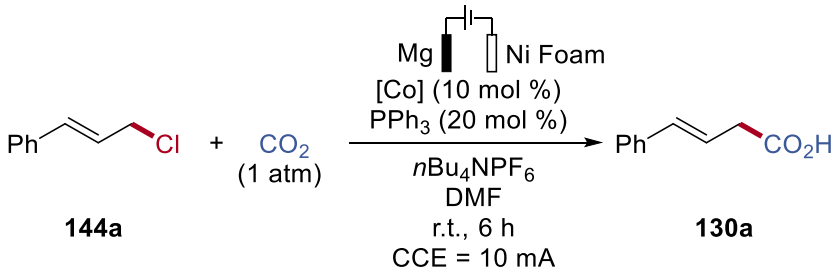

Figure 5.3.6. Investigation on the rates of different cobalt salts.

Under an atmosphere of N_2, cinnamyl chloride **144a** (76.4 mg, 0.50 mmol), [Co] (10.0 mol %), PPh_3 (26.2 mg, 0.10 mmol, 20.0 mol %), nBu$_4$NPF$_6$ (193.8 mg, 0.5 mmol, 1.00 equiv) were dissolved in DMF (10.0 mL) and stirred at 25 ℃. The reaction vessel was bubbled for 30 minutes under CO_2 gas before initiation. CO_2 gas (1 atm) was constantly supplied throughout the course of the reaction. For 6 h, an *in situ* IR spectrum was acquired every 2 mins. The absolute peak area was measured from 696 to 675 cm^{-1} with a two-point baseline at 696 and 675 cm^{-1}.

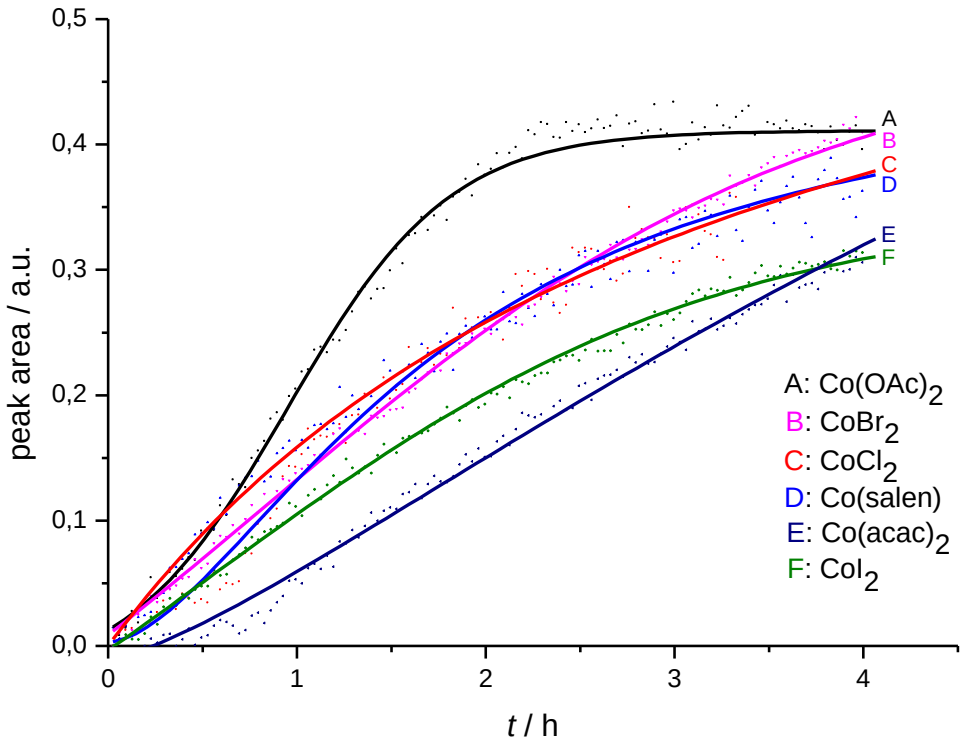

Figure 5.3.7. Plot of the peak area (a.u.) vs time on the comparison of the profile of different simple cobalt salts.

5.3.2.4 Cyclic Voltammetry

The cyclic voltammetry measurements were performed with a Metrohm Autolab PGSTAT204 workstation and the following analysis was performed with a Nova 2.1 application. For all experiments, a saturated calomel electrode (SCE) was used as the reference electrode and a glassy-carbon (GC) electrode (3 mm-diameter, disc electrode) was used as the working electrode. The measurements were recorded at a scan rate of 100 mVs^{-1}. The operating temperature was at 298 K. All solutions were degassed via freeze-pump-thaw method prior to use and N_2 gas was bubbled through the solutions for at least 5 mins before the experiment was performed. These experiments were performed under inert conditions with cinnamyl chloride **144a** as the model substrate (constant flow of dry N_2 gas).

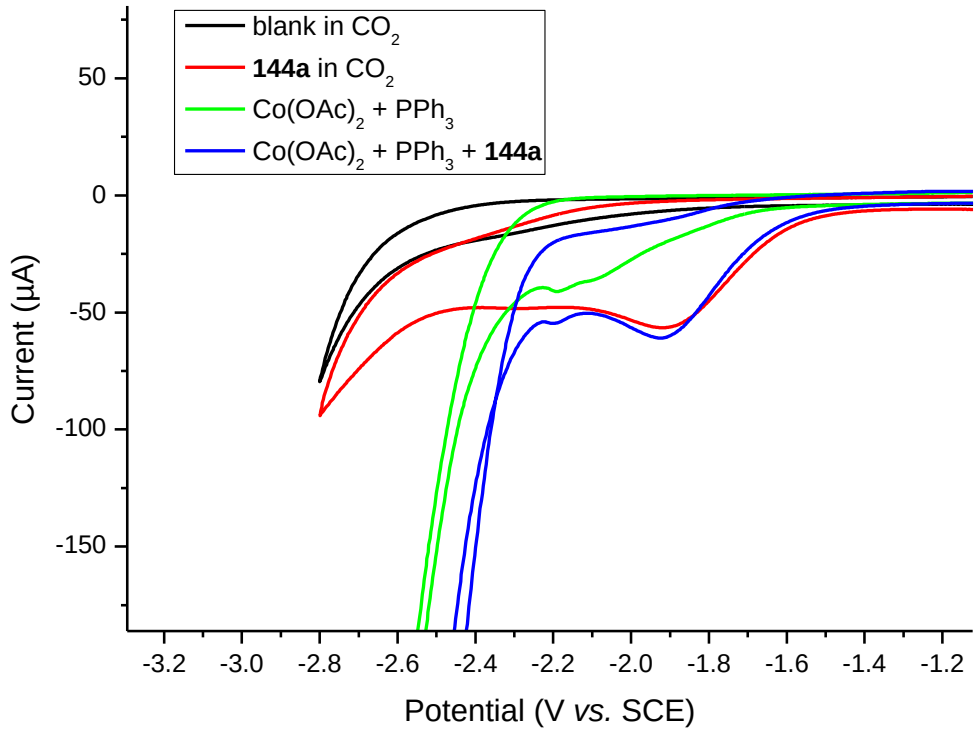

Figure 5.3.8. Cyclic voltammograms of individual components under CO_2 and their mixtures. Cyclic voltammograms at 100 mVs^{-1} using DMF and nBu$_4$NPF$_6$ (0.10 M) as electrolyte, and a GC working electrode. Co(OAc)$_2$ (2.0 mM), PPh$_3$ (2.0 mM) and cinnamyl chloride **144a** (2.0 mM). CO_2 gas (1 atm).

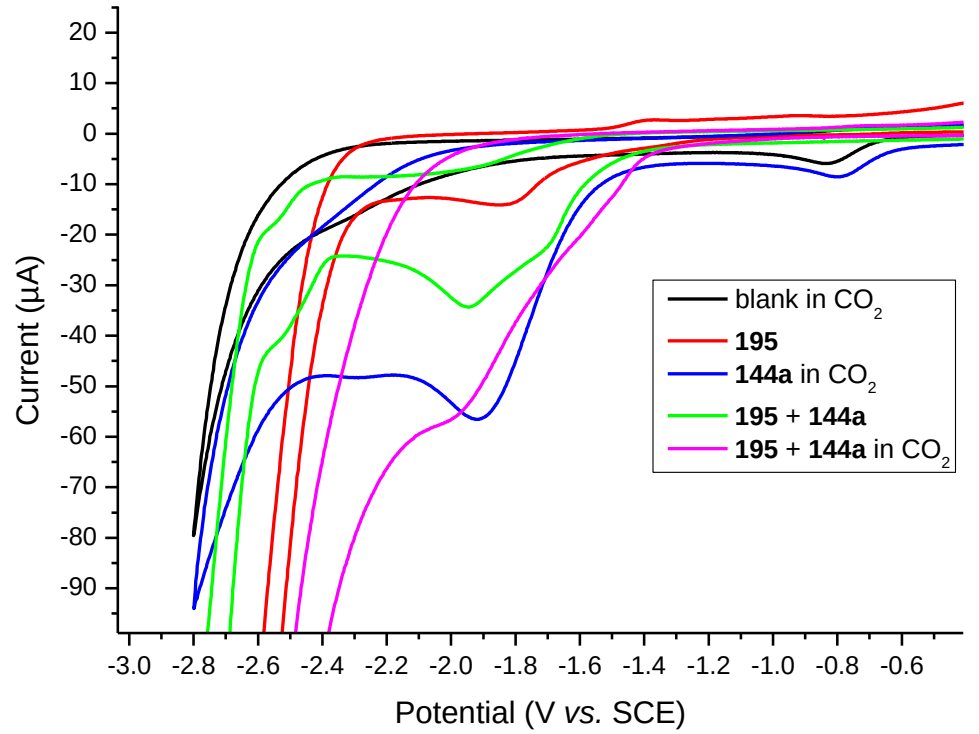

Figure 5.3.9. Cyclic voltammograms of Co(I) catalyst and mixtures. Cyclic voltammograms at 100 mVs^{-1} using DMF and nBu$_4$NPF$_6$ (0.10 M) as electrolyte, and a GC working electrode. CoCl(PPh$_3$)$_3$ **195** (2.0 mM) and cinnamyl chloride **144a** (2.0 mM). CO_2 gas (1 atm).

5.3.3 Electro-Reductive Nickel-Catalyzed Thiolation

5.3.3.1 Characterization Data

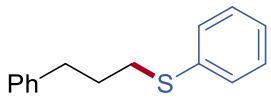

176aa

Phenyl(3-phenylpropyl)sulfane (176aa)

The general procedure **D** was followed using 1-bromo-3-phenylpropane **175a** (38.0 µL, 0.250 mmol) and *S*-phenyl benzenesulfonothioate **160a** (68.8 mg, 0.275 mmol, 1.1 equiv). Purification by column chromatography on silica gel (*n*-hexane/EtOAc 19:1) yielded **176aa** (49.1 mg, 86%) as a pale yellow oil. Resonances reported for **176aa**: **^{1}H NMR** (300 MHz, $CDCl_3$): δ = 7.30 – 7.18 (m, 6H), 7.18 – 7.09 (m, 4H), 2.88 (t, *J* = 7.3 Hz, 2H), 2.72 (t, *J* = 7.5 Hz, 2H), 1.93 (p, *J* = 7.4 Hz, 2H). **^{13}C NMR** (75 MHz, $CDCl_3$): δ = 141.4 (C_q), 136.7 (C_q), 129.3 (CH), 129.0 (CH), 128.6 (CH), 128.5 (CH), 126.1 (CH), 126.0 (CH), 34.8 (CH_2), 33.0 (CH_2), 30.8 (CH_2). **IR** (ATR): 3025, 2932, 1584, 1480, 1438, 1025, 736, 690, 567, 475 cm^{-1}. **MS** (EI) *m*/*z* (relative intensity): 228 $[M]^+$ (55), 110 (40), 65 (40). **HR-MS** (EI+): *m*/*z* calcd for $C_{15}H_{16}S^+$ $[M]^+$ 228.0973, found 228.0967. The analytical data are in accordance to those reported in literature.[219]

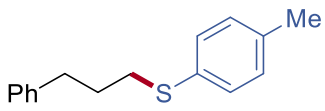

176ab

(3-Phenylpropyl)(*p*-tolyl)sulfane (176ab)

The general procedure **D** was followed using 1-bromo-3-phenylpropane **175a** (38.0 µL, 0.250 mmol) and *S*-(*p*-tolyl) benzenesulfonothioate **160b** (72.7 mg, 0.275 mmol, 1.1 equiv). Purification by column chromatography on silica gel (*n*-hexane/EtOAc 19:1) yielded **176ab** (52.1 mg, 86%) as a pale yellow oil. Resonances reported for **176ab**: **^{1}H NMR** (300 MHz, $CDCl_3$): δ = 7.39 – 7.29 (m, 4H), 7.29 – 7.11 (m, 5H), 2.96 (t, *J* = 7.3 Hz, 2H), 2.82 (t, *J* = 7.5 Hz, 2H), 2.40 (s, 3H), 2.02 (p, *J* = 7.4 Hz, 2H). **^{13}C NMR**

(75 MHz, $CDCl_3$): δ = 141.5 (C_q), 136.1 (C_q), 132.8 (C_q), 130.1 (CH), 129.8 (CH), 128.6 (CH), 128.5 (CH), 126.1 (CH), 34.8 (CH_2), 33.8 (CH_2), 30.8 (CH_2), 21.1 (CH_3). **IR** (ATR): 3025, 2920, 2855, 1492, 1453, 1092, 801, 743, 697, 488 cm^{-1}. **MS** (ESI) *m*/*z* (relative intensity): 243 $[M+H]^+$ (50), 141 (15). **HR-MS** (ESI): *m*/*z* calcd for $C_{16}H_{19}S^+$ $[M+H]^+$ 243.1202, found 243.1194. The analytical data are in accordance to those reported in literature.[257]

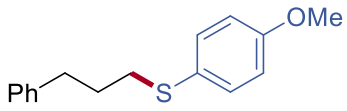

176ac

(4-Methoxyphenyl)(3-phenylpropyl)sulfane (176ac)

The general procedure **D** was followed using 1-bromo-3-phenylpropane **175a** (38.0 µL, 0.250 mmol) and *S*-(4-methoxyphenyl) benzenesulfonothioate **160c** (77.1 mg, 0.275 mmol, 1.1 equiv). Purification by column chromatography on silica gel (*n*-hexane/EtOAc 19:1) yielded **176ac** (54.9 mg, 85%) as a colourless oil. Resonances reported for **176ac**: **^{1}H NMR** (300 MHz, $CDCl_3$): δ = 7.35 – 7.21 (m, 4H), 7.21 – 7.11 (m, 3H), 6.85 – 6.78 (m, 2H), 3.76 (s, 3H), 2.81 (t, *J* = 7.4 Hz, 2H), 2.71 (t, *J* = 7.5 Hz, 2H), 1.89 (p, *J* = 7.4 Hz, 2H). **^{13}C NMR** (75 MHz, $CDCl_3$): δ = 158.9 (C_q), 141.5 (C_q), 133.2 (CH), 128.6 (CH), 128.5 (CH), 126.6 (C_q), 126.0 (CH), 114.6 (CH), 55.4 (CH_3), 35.2 (CH_2), 34.7 (CH_2), 30.9 (CH_2). **IR** (ATR): 2932, 1592, 1492, 1283, 1242, 1173, 1030, 825, 699, 522 cm^{-1}. **MS** (EI) *m*/*z* (relative intensity): 258 $[M]^+$ (60), 125 (15). **HR-MS** (EI+): *m*/*z* calcd for $C_{16}H_{18}OS^+$ $[M]^+$ 258.1073, found 258.1074. The analytical data are in accordance to those reported in literature.[257]

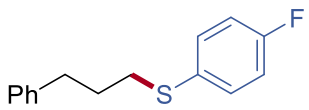

176ad

(4-Fluorophenyl)(3-phenylpropyl)sulfane (176ad)

The general procedure **D** was followed using 1-bromo-3-phenylpropane **175a** (38.0 µL, 0.250 mmol) and *S*-(4-fluorophenyl) benzenesulfonothioate **160d** (73.8 mg, 0.275 mmol, 1.1 equiv). Purification by column chromatography on silica gel (*n*-

hexane/EtOAc 19:1) yielded **176ad** (51.7 mg, 84%) as a colourless oil. Resonances reported for **176ad**: **^{1}H NMR** (300 MHz, $CDCl_3$): δ = 7.38 (ddd, J = 7.6, 5.7, 1.9 Hz, 4H), 7.32 – 7.22 (m, 3H), 7.10 – 7.01 (m, 2H), 2.95 (t, J = 7.4 Hz, 2H), 2.83 (t, J = 7.5 Hz, 2H), 2.01 (p, J = 7.4 Hz, 2H). **^{13}C NMR** (75 MHz, $CDCl_3$): δ = 161.7 (d, $^{1}J_{C\text{-}F}$ = 246.0 Hz, C_q), 141.3 (C_q), 132.3 (CH), 132.2 (CH), 131.4 (d, $^{4}J_{C\text{-}F}$ = 3.3 Hz, C_q), 128.5 (d, $^{4}J_{C\text{-}F}$ = 4.1 Hz, CH), 126.1 (CH), 116.0 (d, $^{2}J_{C\text{-}F}$ = 21.8 Hz, CH), 34.6 (CH_2), 34.3 (CH_2), 30.7 (CH_2). **^{19}F NMR** (282 MHz, $CDCl_3$): δ = – 115.7 (s). **IR** (ATR): 3026, 2931, 1589, 1489, 1226, 1156, 1091, 822, 700, 503 cm^{-1}. **MS** (EI) m/z (relative intensity): 246 $[M]^+$ (50), 128 (25). **HR-MS** (EI+): m/z calcd for $C_{15}H_{15}FS^+$ $[M]^+$ 246.0873, found 246.0874.

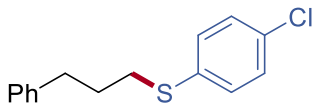

176ae

(4-Chlorophenyl)(3-phenylpropyl)sulfane (176ae)

The general procedure **D** was followed using 1-bromo-3-phenylpropane **175a** (38.0 µL, 0.250 mmol) and *S*-(4-chlorophenyl) benzenesulfonothioate **160e** (78.3 mg, 0.275 mmol, 1.1 equiv). Purification by column chromatography on silica gel (*n*-hexane/EtOAc 19:1) yielded **176ae** (57.2 mg, 87%) as a pale yellow oil. Resonances reported for **176ae**: **^{1}H NMR** (300 MHz, $CDCl_3$): δ = 7.39 – 7.31 (m, 2H), 7.31 – 7.18 (m, 7H), 2.95 (t, J = 7.3 Hz, 2H), 2.81 (t, J = 7.5 Hz, 2H), 2.01 (p, J = 7.4 Hz, 2H). **^{13}C NMR** (75 MHz, $CDCl_3$): δ = 141.2 (C_q), 135.2 (C_q), 131.9 (C_q), 130.5 (CH), 129.1 (CH), 128.6 (CH), 128.6 (CH), 126.2 (CH), 34.7 (CH_2), 33.2 (CH_2), 30.6 (CH_2). **IR** (ATR): 2929, 1475, 1388, 1094, 1010, 809, 744, 697, 536, 485 cm^{-1}. **MS** (ESI) m/z (relative intensity): 263 $[^{35}M+H]^+$ (40). **HR-MS** (ESI): m/z calcd for $C_{15}H_{16}{}^{35}ClS^+$ $[^{35}M+H]^+$ 263.0656, found 263.0653. The analytical data are in accordance to those reported in literature.[258]

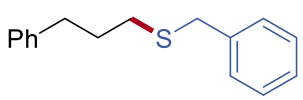

176af

Benzyl(3-phenylpropyl)sulfane (176af)

The general procedure **D** was followed using 1-bromo-3-phenylpropane **175a** (38.0 µL, 0.250 mmol) and *S*-benzyl benzenesulfonothioate **160f** (72.7 mg, 0.275 mmol, 1.1 equiv). Purification by column chromatography on silica gel (*n*-hexane/EtOAc 19:1) yielded **176af** (49.7 mg, 82%) as a pale yellow oil. Resonances reported for **176af**: **^{1}H NMR** (300 MHz, $CDCl_3$): δ = 7.39 – 7.25 (m, 8H), 7.25 – 7.14 (m, 2H), 3.75 (s, 3H), 2.73 (t, *J* = 7.6 Hz, 2H), 2.48 (t, *J* = 7.3 Hz, 2H), 1.93 (p, *J* = 7.4 Hz, 2H). **^{13}C NMR** (75 MHz, $CDCl_3$): δ = 141.7 (C_q), 138.7 (C_q), 129.5 (CH), 128.9 (CH), 128.6 (CH), 128.5 (CH), 127.0 (CH), 126.0 (CH), 36.3 (CH_2), 34.9 (CH_2), 30.9 (CH_2), 30.8 (CH_2). **IR** (ATR): 3026, 2919, 1494, 1453, 1072, 1029, 743, 696, 594, 471 cm^{-1}. **MS** (ESI) *m*/*z* (relative intensity): 265 $[M+Na]^+$ (40), 259 (30). **HR-MS** (ESI): *m*/*z* calcd for $C_{16}H_{18}SNa^+$ $[M+Na]^+$ 265.1021, found 265.1017. The analytical data are in accordance to those reported in literature.[257]

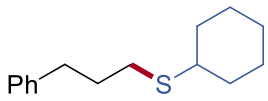

176ag

Cyclohexyl(3-phenylpropyl)sulfane (176ag)

The general procedure **D** was followed using 1-bromo-3-phenylpropane **175a** (38.0 µL, 0.250 mmol) and *S*-cyclohexyl benzenesulfonothioate **160g** (70.5 mg, 0.275 mmol, 1.1 equiv). Purification by column chromatography on silica gel (*n*-hexane/EtOAc 19:1) yielded **176ag** (49.2 mg, 84%) as a yellow oil. Resonances reported for **176ag**: **^{1}H NMR** (300 MHz, $CDCl_3$): δ = 7.38 – 7.29 (m, 2H), 7.29 – 7.20 (m, 3H), 2.78 (t, *J* = 7.6 Hz, 2H), 2.73 – 2.65 (m, 1H), 2.60 (t, *J* = 7.4 Hz, 2H), 2.05 – 1.90 (m, 4H), 1.88 – 1.76 (m, 2H), 1.71 – 1.58 (m, 1H), 1.42 – 1.27 (m, 5H). **^{13}C NMR** (75 MHz, $CDCl_3$): δ = 141.8 (C_q), 128.6 (CH), 128.5 (CH), 126.0 (CH), 43.7 (CH), 35.1 (CH_2), 33.9 (CH_2), 31.8 (CH_2), 29.7 (CH_2), 26.3 (CH_2), 26.0 (CH_2). **IR** (ATR): 2925, 2851, 1496, 1448, 1262, 998, 744, 698, 492, 408 cm^{-1}. **MS** (ESI) *m*/*z* (relative intensity):

235 $[M+H]^+$ (40). **HR-MS** (ESI): *m*/*z* calcd for $C_{15}H_{23}S^+$ $[M+H]^+$ 235.1515, found 235.1510.

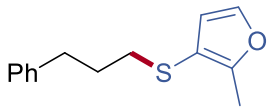

176ah

2-Methyl-3-[(3-phenylpropyl)thio]furan (176ah)

The general procedure **D** was followed using 1-bromo-3-phenylpropane **175a** (38.0 µL, 0.250 mmol) and *S*-(2-methylfuran-3-yl) benzenesulfonothioate **160h** (69.9 mg, 0.275 mmol, 1.1 equiv). Purification by column chromatography on silica gel (*n*-hexane/EtOAc 19:1) yielded **176ah** (41.8 mg, 72%) as a yellow oil. Resonances reported for **176ah**: **^{1}H NMR** (300 MHz, $CDCl_3$): δ = 7.34 – 7.27 (m, 3H), 7.25 – 7.15 (m, 3H), 6.35 (d, *J* = 1.9 Hz, 1H), 2.74 (t, *J* = 7.6 Hz, 2H), 2.65 (t, *J* = 7.2 Hz, 2H), 2.37 (s, 3H), 1.88 (p, *J* = 7.3 Hz, 2H). **^{13}C NMR** (75 MHz, $CDCl_3$): δ = 154.8 (C_q), 141.6 (C_q), 140.6 (CH), 128.6 (CH), 128.5 (CH), 126.0 (CH), 115.1 (CH), 110.4 (C_q), 35.3 (CH_2), 34.6 (CH_2), 31.2 (CH_2), 12.0 (CH_3). **IR** (ATR): 3025, 2919, 2854, 1754, 1496, 1453, 1222, 1088, 742, 700 cm^{-1}. **MS** (EI) *m*/*z* (relative intensity): 232 $[M]^+$ (95). **HR-MS** (EI+): *m*/*z* calcd for $C_{14}H_{16}OS^+$ $[M]^+$ 232.0922, found 232.0923.

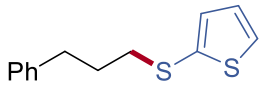

176ai

2-[(3-Phenylpropyl)thio]thiophene (176ai)

The general procedure **D** was followed using 1-bromo-3-phenylpropane **175a** (38.0 µL, 0.250 mmol) and *S*-(thiophen-2-yl) benzenesulfonothioate **160i** (70.5 mg, 0.275 mmol, 1.1 equiv). Purification by column chromatography on silica gel (*n*-hexane/EtOAc 19:1) yielded **176ai** (43.9 mg, 75%) as a colourless oil. Resonances reported for **176ai**: **^{1}H NMR** (300 MHz, $CDCl_3$): δ = 7.38 – 7.30 (m, 3H), 7.27 – 7.19 (m, 3H), 7.17 (dd, *J* = 3.4, 1.5 Hz, 1H), 7.02 (ddd, *J* = 5.1, 3.5, 1.3 Hz, 1H), 2.85 (t, *J* = 7.2 Hz, 2H), 2.79 (t, *J* = 7.6 Hz, 2H), 1.99 (p, *J* = 7.4 Hz, 2H). **^{13}C NMR** (75 MHz, $CDCl_3$): δ = 141.4 (C_q), 134.6 (C_q), 133.6 (CH), 129.2 (CH), 128.6 (CH), 128.5 (CH), 127.6 (CH), 126.0 (CH), 38.3 (CH_2), 34.4 (CH_2), 30.9 (CH_2). **IR** (ATR): 3025, 2926, 2853, 1495, 1453, 1216,

988, 845, 743, 699 cm^{-1}. **MS** (EI) *m*/*z* (relative intensity): 234 $[M]^+$ (85), 115 (60). **HR-MS** (EI+): *m*/*z* calcd for $C_{13}H_{14}S_2^+$ $[M]^+$ 234.0531, found 234.0529.

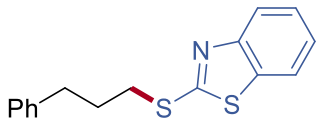

176aj

2-[(3-Phenylpropyl)thio]benzo[*d*]thiazole (176aj)

The general procedure **D** was followed using 1-bromo-3-phenylpropane **175a** (38.0 µL, 0.250 mmol) and *S*-(benzo[*d*]thiazol-2-yl) benzenesulfonothioate **160j** (84.5 mg, 0.275 mmol, 1.1 equiv) for 6 h. Purification by column chromatography on silica gel (*n*-hexane/EtOAc 9:1) yielded **176aj** (57.1 mg, 80%) as a yellow oil. Resonances reported for **176aj**: **^{1}H NMR** (400 MHz, $CDCl_3$): δ = 7.88 (d, *J* = 8.2 Hz, 1H), 7.73 (d, *J* = 8.1 Hz, 1H), 7.45 – 7.37 (m, 1H), 7.34 – 7.25 (m, 3H), 7.24 – 7.16 (m, 3H), 3.35 (t, *J* = 7.2 Hz, 2H), 2.81 (t, *J* = 7.5 Hz, 2H), 2.17 (p, *J* = 7.4 Hz, 2H). **^{13}C NMR** (100 MHz, $CDCl_3$): δ = 167.0 (C_q), 153.4 (C_q), 140.9 (C_q), 135.3 (C_q), 128.6 (CH), 128.5 (CH), 126.2 (CH), 126.1 (CH), 124.2 (CH), 121.6 (CH), 121.0 (CH), 34.7 (CH_2), 32.9 (CH_2), 30.8 (CH_2). **IR** (ATR): 3025, 2933, 1495, 1455, 1425, 1075, 992, 752, 725, 697 cm^{-1}. **MS** (ESI) *m*/*z* (relative intensity): 286 $[M+H]^+$ (100). **HR-MS** (ESI): *m*/*z* calcd for $C_{16}H_{16}NS_2^+$ $[M+H]^+$ 286.0719, found 286.0722.

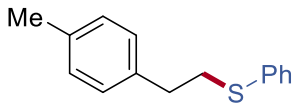

176ba

(4-Methylphenethyl)(phenyl)sulfane (176ba)

The general procedure **D** was followed using 1-(2-bromoethyl)-4-methylbenzene **175b** (49.8 mg, 0.250 mmol) and *S*-phenyl benzenesulfonothioate **160a** (68.8 mg, 0.275 mmol, 1.1 equiv). Purification by column chromatography on silica gel (*n*-hexane/EtOAc 19:1) yielded **176ba** (49.7 mg, 88%) as a yellow oil. Resonances reported for **176ba**: **^{1}H NMR** (300 MHz, $CDCl_3$): δ = 7.53 – 7.47 (m, 2H), 7.46 – 7.38 (m, 2H), 7.35 – 7.28 (m, 1H), 7.27 – 7.18 (m, 4H), 3.29 (dd, *J* = 9.3, 6.2 Hz, 2H), 3.03 (dd, *J* = 9.4, 6.4 Hz, 2H), 2.46 (s, 3H). **^{13}C NMR** (75 MHz, $CDCl_3$): δ = 137.2 (C_q), 136.6

(C_q), 136.0 (C_q), 129.3 (CH), 129.2 (CH), 129.0 (CH), 128.4 (CH), 125.9 (CH), 35.2 (CH_2), 35.2 (CH_2), 21.1 (CH_3). **IR** (ATR): 3017, 2920, 1584, 1514, 1480, 1438, 1024, 807, 737, 690 cm^{-1}. **MS** (EI) *m*/*z* (relative intensity): 228 $[M]^+$ (50), 105 (30). **HR-MS** (EI+): *m*/*z* calcd for $C_{15}H_{16}S^+$ $[M]^+$ 228.0967, found 228.0968. The analytical data are in accordance to those reported in literature.[258]

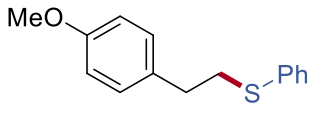

176ca

(4-Methoxyphenethyl)(phenyl)sulfane (176ca)

The general procedure **D** was followed using 1-(2-bromoethyl)-4-methoxybenzene **175c** (53.8 mg, 0.250 mmol) and *S*-phenyl benzenesulfonothioate **160a** (68.8 mg, 0.275 mmol, 1.1 equiv). Purification by column chromatography on silica gel (*n*-hexane/EtOAc 19:1) yielded **176ca** (52.5 mg, 86%) as a pale yellow oil. Resonances reported for **176ca**: **^{1}H NMR** (300 MHz, $CDCl_3$): δ = 7.44 – 7.28 (m, 4H), 7.27 – 7.20 (m, 1H), 7.20 – 7.13 (m, 2H), 6.93 – 6.86 (m, 2H), 3.84 (s, 3H), 3.27 – 3.07 (dd, *J* = 9.1, 6.3 Hz, 2H), 2.93 (dd, *J* = 9.2, 6.4 Hz, 2H). **^{13}C NMR** (75 MHz, $CDCl_3$): δ = 158.3 (C_q), 136.6 (C_q), 132.4 (C_q), 129.6 (CH), 129.3 (CH), 129.0 (CH), 126.0 (CH), 114.0 (CH), 55.4 (CH_3), 35.5 (CH_2), 34.8 (CH_2). **IR** (ATR): 2930, 2833, 1611, 1583, 1510, 1438, 1300, 1244, 737, 690 cm^{-1}. **MS** (ESI) *m*/*z* (relative intensity): 267 $[M+Na]^+$ (50), 256 (10). **HR-MS** (ESI): *m*/*z* calcd for $C_{15}H_{16}OSNa^+$ $[M+Na]^+$ 267.0814, found 267.0819. The analytical data are in accordance to those reported in literature.[259]

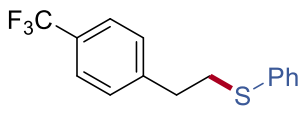

176da

Phenyl[4-(trifluoromethyl)phenethyl]sulfane (176da)

The general procedure **D** was followed using 1-(2-bromoethyl)-4-(trifluoromethyl)benzene **175d** (63.3 mg, 0.250 mmol) and *S*-phenyl benzenesulfonothioate **160a** (68.8 mg, 0.275 mmol, 1.1 equiv). Purification by column

chromatography on silica gel (*n*-hexane/EtOAc 19:1) yielded **176da** (62.8 mg, 90%) as a pale yellow oil. Resonances reported for **176da**: **^{1}H NMR** (300 MHz, $CDCl_3$): δ = 7.51 (d, J = 8.0 Hz, 2H), 7.36 – 7.21 (m, 6H), 7.20 – 7.12 (m, 1H), 3.20 – 3.05 (m, 2H), 2.93 (dd, J = 8.8, 6.5 Hz, 2H). **^{13}C NMR** (75 MHz, $CDCl_3$): δ = 144.2 (d, $^{5}J_{C\text{-}F}$ = 1.6 Hz, C_q), 136.0 (C_q), 129.6 (CH), 129.1 (CH), 129.0 (CH), 128.6 (C_q), 126.3 (CH), 125.5 (q, $^{4}J_{C\text{-}F}$ = 3.8 Hz, CH), 124.4 (d, $^{1}J_{C\text{-}F}$ = 271.8 Hz, C_q), 35.4 (CH_2), 34.9 (CH_2). **^{19}F NMR** (282 MHz, $CDCl_3$): δ = – 62.3 (s). **IR** (ATR): 2925, 1618, 1583, 1324, 1163, 1121, 1067, 822, 738, 690 cm^{-1}. **MS** (EI) *m*/*z* (relative intensity): 282 $[M]^+$ (40), 110 (10). **HR-MS** (EI+): *m*/*z* calcd for $C_{15}H_{13}F_3S^+$ $[M]^+$ 282.0685, found 282.0683.

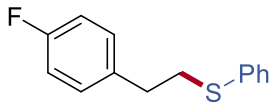

176ea

(4-Fluorophenethyl)(phenyl)sulfane (176ea)

The general procedure **D** was followed using 1-(2-bromoethyl)-4-fluorobenzene **175e** (50.8 mg, 0.250 mmol) and *S*-phenyl benzenesulfonothioate **160a** (68.8 mg, 0.275 mmol, 1.1 equiv). Purification by column chromatography on silica gel (*n*-hexane/EtOAc 19:1) yielded **176ea** (52.3 mg, 90%) as a pale yellow oil. Resonances reported for **176ea**: **^{1}H NMR** (300 MHz, $CDCl_3$): δ = 7.44 – 7.29 (m, 4H), 7.29 – 7.13 (m, 3H), 7.07 – 6.96 (m, 2H), 3.28 – 3.11 (m, 2H), 2.94 (dd, J = 9.1, 6.3 Hz, 2H). **^{13}C NMR** (75 MHz, $CDCl_3$): δ = 161.6 (d, $^{1}J_{C\text{-}F}$ = 244.3 Hz, C_q), 136.2 (C_q), 135.9 (d, $^{4}J_{C\text{-}F}$ = 3.2 Hz, C_q), 130.0 (d, $^{3}J_{C\text{-}F}$ = 7.8 Hz, CH), 129.4 (CH), 129.0 (CH), 126.1 (CH), 115.3 (d, $^{2}J_{C\text{-}F}$ = 21.1 Hz, CH), 35.3 (d, $^{5}J_{C\text{-}F}$ = 1.4 Hz, CH_2), 34.8 (CH_2). **^{19}F NMR** (282 MHz, $CDCl_3$): δ = – 116.5 (s). **IR** (ATR): 2924, 1600, 1508, 1480, 1221, 823, 738, 690, 531, 492 cm^{-1}. **MS** (EI) *m*/*z* (relative intensity): 232 $[M]^+$ (50), 110 (20). **HR-MS** (EI+): *m*/*z* calcd for $C_{14}H_{13}FS^+$ $[M]^+$ 232.0717, found 232.0717.

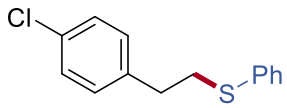

176fa

(4-chlorophenethyl)(phenyl)sulfane (176fa)

The general procedure **D** was followed using 1-(2-bromoethyl)-4-chlorobenzene **175f** (54.9 mg, 0.250 mmol) and *S*-phenyl benzenesulfonothioate **160a** (68.8 mg, 0.275 mmol, 1.1 equiv). Purification by column chromatography on silica gel (*n*-hexane/EtOAc 19:1) yielded **176fa** (60.3 mg, 97%) as a pale yellow oil. Resonances reported for **176fa**: **^{1}H NMR** (300 MHz, $CDCl_3$): δ = 7.44 – 7.29 (m, 6H), 7.29 – 7.22 (m, 1H), 7.20 – 7.14 (m, 2H), 3.24 – 3.12 (m, 2H), 2.94 (dd, *J* = 8.8, 6.6 Hz, 2H). **^{13}C NMR** (75 MHz, $CDCl_3$): δ = 138.6 (C_q), 136.2 (C_q), 132.3 (C_q), 130.0 (CH), 129.5 (CH), 129.1 (CH), 128.7 (CH), 126.2 (CH), 35.1 (CH_2), 35.0 (CH_2). **IR** (ATR): 2922, 1583, 1491, 1480, 1406, 1092, 1015, 805, 737, 690 cm^{-1}. **MS** (EI) *m*/*z* (relative intensity): 248 $[M]^+$ (40), 139 (15). **HR-MS** (EI+): *m*/*z* calcd for $C_{14}H_{13}{}^{35}ClS^+$ $[^{35}M]^+$ 248.0421, found 248.0422. The analytical data are in accordance to those reported in literature.[258]

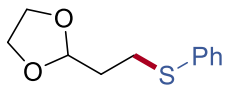

176ga

2-[2-(Phenylthio)ethyl]-1,3-dioxolane (176ga)

The general procedure **D** was followed using 2-(2-bromoethyl)-1,3-dioxolane **175g** (45.3 mg, 0.250 mmol) and *S*-phenyl benzenesulfonothioate **160a** (68.8 mg, 0.275 mmol, 1.1 equiv). Purification by column chromatography on silica gel (*n*-hexane/EtOAc 19:1) yielded **176ga** (43.1 mg, 82%) as a colourless oil. Resonances reported for **176ga**: **^{1}H NMR** (400 MHz, $CDCl_3$): δ = 7.37 (dt, *J* = 8.3, 1.9 Hz, 2H), 7.30 (dd, *J* = 8.3, 6.8 Hz, 2H), 7.22 – 7.15 (m, 1H), 5.01 (t, *J* = 4.5 Hz, 1H), 4.02 – 3.92 (m, 2H), 3.92 – 3.83 (m, 2H), 3.10 – 2.99 (t, *J* = 7.3 Hz, 2H), 2.08 – 1.98 (m, 2H). **^{13}C NMR** (100 MHz, $CDCl_3$): δ = 136.3 (C_q), 129.1 (CH), 128.9 (CH), 125.9 (CH), 103.1 (CH), 65.0 (CH_2), 33.6 (CH_2), 27.8 (CH_2). **IR** (ATR): 2952, 2880, 1583, 1480, 1438, 1131, 1024, 876, 739, 691 cm^{-1}. **MS** (ESI) *m*/*z* (relative intensity): 233 $[M+Na]^+$ (60). **HR-MS**

(ESI): *m*/*z* calcd for $C_{11}H_{14}O_2SNa^+$ $[M+Na]^+$ 233.0607, found 233.0609.

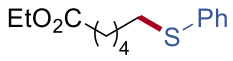

176ha

Ethyl 6-(phenylthio)hexanoate (176ha)

The general procedure **D** was followed using ethyl 6-bromohexanoate **175h** (55.8 mg, 0.250 mmol) and *S*-phenyl benzenesulfonothioate **160a** (68.8 mg, 0.275 mmol, 1.1 equiv). Purification by column chromatography on silica gel (*n*-hexane/EtOAc 19:1) yielded **176ha** (50.5 mg, 80%) as a colourless oil. Resonances reported for **176ha**: **^{1}H NMR** (400 MHz, $CDCl_3$): δ = 7.36 – 7.24 (m, 4H), 7.17 (td, *J* = 7.0, 6.6, 1.4 Hz, 1H), 4.13 (q, *J* = 7.1 Hz, 2H), 2.92(t, *J* = 7.2 Hz, 2H), 2.30 (t, *J* = 7.4 Hz, 2H), 1.66 (h, *J* = 7.8 Hz, 4H), 1.52 – 1.42 (m, 2H), 1.26 (t, *J* = 7.1 Hz, 3H). **^{13}C NMR** (100 MHz, $CDCl_3$): δ = 173.5 (C_q), 136.8 (C_q), 129.0 (CH), 128.8 (CH), 125.8 (CH), 60.2 (CH_2), 34.2 (CH_2), 33.4 (CH_2), 28.8 (CH_2), 28.3 (CH_2), 24.5 (CH_2), 14.3 (CH_3). **IR** (ATR): 2933, 2860, 1730, 1480, 1255, 1178, 1092, 1025, 737, 690 cm^{-1}. **MS** (ESI) *m*/*z* (relative intensity): 275 $[M+Na]^+$ (100), 253 $[M+H]^+$ (5). **HR-MS** (ESI): *m*/*z* calcd for $C_{14}H_{20}O_2SNa^+$ $[M+Na]^+$ 275.1076, found 275.1076. The analytical data are in accordance to those reported in literature.[260]

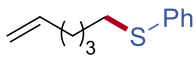

176ia

Hex-5-en-1-yl(phenyl)sulfane (176ia)

The general procedure **D** was followed using 6-bromohex-1-ene **175i** (40.8 mg, 0.250 mmol) and *S*-phenyl benzenesulfonothioate **160a** (68.8 mg, 0.275 mmol, 1.1 equiv). Purification by column chromatography on silica gel (*n*-hexane/EtOAc 19:1) yielded **176ia** (42.3 mg, 88%) as a colourless oil. Resonances reported for **176ia**: **^{1}H NMR** (400 MHz, $CDCl_3$): δ = 7.36 – 7.21 (m, 4H), 7.19 – 7.10 (m, 1H), 5.78 (ddt, *J* = 16.9, 10.1, 6.6 Hz, 1H), 5.07 – 4.89 (m, 2H), 2.98 – 2.86 (t, *J* = 7.2 Hz, 2H), 2.10 – 2.01 (m, 2H), 1.70 – 1.62 (m, 2H), 1.57 – 1.47 (m, 2H). **^{13}C NMR** (100 MHz, $CDCl_3$): δ = 138.5 (CH), 137.0 (C_q), 129.0 (CH), 128.9 (CH), 125.8 (CH), 114.9 (CH_2), 33.6 (CH_2), 33.4 (CH_2), 28.7 (CH_2), 28.1 (CH_2). **IR** (ATR): 3075, 2925, 1640, 1584,

1480, 1438, 1025, 911, 737, 690 cm^{-1}. **MS** (EI) *m*/*z* (relative intensity): 192 $[M]^+$ (40), 135 (15). **HR-MS** (EI+): *m*/*z* calcd for $C_{12}H_{16}S^+$ $[M]^+$ 192.0967, found 192.0969. The analytical data are in accordance to those reported in literature.[261]

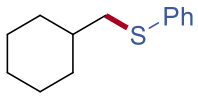

176ja

(Cyclohexylmethyl)(phenyl)sulfane (176ja)

The general procedure **D** was followed using (bromomethyl)cyclohexane **175j** (44.3 mg, 0.250 mmol) and *S*-phenyl benzenesulfonothioate **160a** (68.8 mg, 0.275 mmol, 1.1 equiv). Purification by column chromatography on silica gel (*n*-hexane/EtOAc 19:1) yielded **176ja** (43.3 mg, 84%) as a yellow oil. Resonances reported for **176ja**: **^{1}H NMR** (300 MHz, $CDCl_3$): δ = 7.40 – 7.24 (m, 4H), 7.21 – 7.13 (m, 1H), 2.85 (d, *J* = 6.9 Hz, 2H), 1.93 (dd, *J* = 12.9, 3.4 Hz, 2H), 1.81 – 1.63 (m, 3H), 1.62 – 1.50 (m, 1H), 1.35 – 1.14 (m, 3H), 1.12 – 0.94 (m, 2H). **^{13}C NMR** (75 MHz, $CDCl_3$): δ = 128.9 (CH), 128.7 (CH), 125.6 (CH), 119.2 (C_q), 41.1 (CH_2), 37.7 (CH_2), 33.0 (CH_2), 26.5 (CH_2), 26.2 (CH_2). **IR** (ATR): 2921, 2850, 1583, 1467, 1257, 1155, 1028, 735, 688, 636 cm^{-1}. **MS** (EI) *m*/*z* (relative intensity): 206 $[M]^+$ (50), 123 (20). **HR-MS** (EI+): *m*/*z* calcd for $C_{13}H_{18}S^+$ $[M]^+$ 206.1129, found 206.1131. The analytical data are in accordance to those reported in literature.[262]

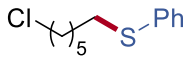

176ka

(6-Chlorohexyl)(phenyl)sulfane (176ka)

The general procedure **D** was followed using 1-bromo-6-chlorohexane **175k** (49.9 mg, 0.250 mmol) and *S*-phenyl benzenesulfonothioate **160a** (68.8 mg, 0.275 mmol, 1.1 equiv). Purification by column chromatography on silica gel (*n*-hexane/EtOAc 19:1) yielded **176ka** (52.0 mg, 91%) as a colourless solid. **M.p.**: 22 – 23 °C. Resonances reported for **176ka**: **^{1}H NMR** (400 MHz, $CDCl_3$): δ = 7.37 – 7.24 (m, 4H), 7.21 – 7.14 (m, 1H), 3.52 (t, *J* = 6.7 Hz, 2H), 2.93 (t, *J* = 6.9 Hz, 2H), 1.81 – 1.72 (m, 2H), 1.72 – 1.62 (m, 2H), 1.50 – 1.42 (m, 4H). **^{13}C NMR** (100 MHz, $CDCl_3$): δ = 136.9 (C_q),

129.1 (CH), 129.0 (CH), 125.9 (CH), 45.1 (CH_2), 33.6 (CH_2), 32.6 (CH_2), 29.1 (CH_2), 28.2 (CH_2), 26.6 (CH_2). **IR** (ATR): 2924, 2853, 1583, 1478, 1438, 1090, 731, 689, 650, 480 cm^{-1}. **MS** (EI) *m*/*z* (relative intensity): 228 $[M]^+$ (50), 123 (40). **HR-MS** (EI+): *m*/*z* calcd for $C_{12}H_{17}{}^{35}ClS^+$ $[^{35}M]^+$ 228.0734, found 228.0735. The analytical data are in accordance to those reported in literature.[263]

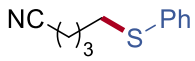

176la

5-(Phenylthio)valeronitrile (176la)

The general procedure **D** was followed using 5-bromovaleronitrile **175l** (40.5 mg, 0.250 mmol) and *S*-phenyl benzenesulfonothioate **160a** (68.8 mg, 0.275 mmol, 1.1 equiv). Purification by column chromatography on silica gel (*n*-hexane/EtOAc 9:1) yielded **176la** (43.5 mg, 91%) as a yellow oil. Resonances reported for **176la**: **^{1}H NMR** (300 MHz, $CDCl_3$): δ = 7.36 – 7.25 (m, 4H), 7.23 – 7.15 (m, 1H), 2.97 – 2.90 (m, 2H), 2.36 – 2.28 (m, 2H), 1.81 – 1.74 (m, 4H). **^{13}C NMR** (75 MHz, $CDCl_3$): δ = 135.8 (C_q), 129.4 (CH), 129.0 (CH), 126.2 (CH), 119.3 (C_q), 32.8 (CH_2), 27.9 (CH_2), 24.2 (CH_2), 16.7 (CH_2). **IR** (ATR): 2931, 2245, 1582, 1480, 1438, 1089, 1025, 739, 691, 478 cm^{-1}. **MS** (ESI) *m*/*z* (relative intensity): 192 $[M+H]^+$ (60), 214 $[M+Na]^+$ (40). **HR-MS** (ESI): *m*/*z* calcd for $C_{11}H_{14}NS^+$ $[M+H]^+$ 192.0841, found 192.0842. The analytical data are in accordance to those reported in literature.[264]

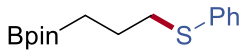

176ma

4,4,5,5-Tetramethyl-2-[3-(phenylthio)propyl]-1,3,2-dioxaborolane (176ma)

The general procedure **D** was followed using 3-bromopropylboronic acid pinacol ester **175m** (62.2 mg, 0.250 mmol) and *S*-phenyl benzenesulfonothioate **160a** (68.8 mg, 0.275 mmol, 1.1 equiv). Purification by column chromatography on silica gel (*n*-hexane/EtOAc 9:1) yielded **176ma** (35.5 mg, 51%) as a yellow oil. Resonances reported for **176ma**: **^{1}H NMR** (300 MHz, $CDCl_3$): δ = 7.39 – 7.23 (m, 4H), 7.20 – 7.12 (m, 1H), 3.01 – 2.90 (m, 2H), 1.86 – 1.75 (m, 2H), 1.27 (s, 12H), 0.95 (t, *J* = 7.7 Hz, 2H). **^{13}C NMR** (75 MHz, $CDCl_3$): δ = 137.2 (C_q), 128.8 (CH), 128.7 (CH), 125.5 (CH),

83.2 (C_q), 35.6 (CH_2), 24.9 (CH_3), 24.1 (CH_2), 10.7 (br C-B, CH_2). **^{11}B NMR** (96 MHz, $CDCl_3$): δ = 33.7 (s). **IR** (ATR): 2977, 2928, 1584, 1371, 1316, 1143, 969, 847, 737, 691 cm^{-1}. **MS** (ESI) *m*/*z* (relative intensity): 301 $[M+Na]^+$ (100), 279 $[M+H]^+$ (10). **HR-MS** (ESI): *m*/*z* calcd for $C_{15}H_{23}BO_2SNa^+$ $[M+Na]^+$ 301.1407, found 301.1411.

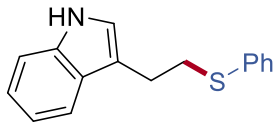

176na

3-[2-(Phenylthio)ethyl]-1*H*-indole (176na)

The general procedure **D** was followed using 3-(2-bromoethyl)-1*H*-indole **175n** (56.0 mg, 0.250 mmol) and *S*-phenyl benzenesulfonothioate **160a** (68.8 mg, 0.275 mmol, 1.1 equiv). Purification by column chromatography on silica gel (*n*-hexane/EtOAc 9:1) yielded **176na** (50.0 mg, 79%) as a pale white solid. **M.p.**: 115 – 116 °C. Resonances reported for **176na**: **^{1}H NMR** (400 MHz, CD_2Cl_2): δ = 8.03 (s, 1H), 7.62 (d, *J* = 7.8 Hz, 1H), 7.45 (dd, *J* = 8.2, 1.4 Hz, 2H), 7.41 – 7.33 (m, 3H), 7.25 (ddd, *J* = 8.2, 7.1, 1.4 Hz, 2H), 7.17 (ddd, *J* = 7.8, 7.1, 1.4 Hz, 1H), 7.09 – 7.01 (m, 1H), 3.33 (dd, *J* = 8.4, 6.9 Hz, 2H), 3.16 (t, *J* = 7.6 Hz, 2H). **^{13}C NMR** (100 MHz, CD_2Cl_2): δ = 137.4 (C_q), 136.8 (C_q), 129.5 (CH), 129.4 (CH), 127.7 (C_q), 126.3 (CH), 122.5 (CH), 122.5 (CH), 119.8 (CH), 119.1 (CH), 115.0 (C_q), 111.7 (CH), 34.6 (CH_2), 25.8 (CH_2). **IR** (ATR): 3389, 2923, 1579, 1477, 1456, 1220, 1087, 1008, 731, 689 cm^{-1}. **MS** (ESI) *m*/*z* (relative intensity): 276 $[M+Na]^+$ (40), 254 $[M+H]^+$ (30). **HR-MS** (ESI): *m*/*z* calcd for $C_{16}H_{15}NSNa^+$ $[M+Na]^+$ 276.0817, found 276.0816.

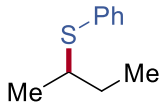

176oa

***rac*-*sec*-Butyl(phenyl)sulfane (176oa)**

The general procedure **D** was followed using 2-bromobutane **175o** (34.3 mg, 0.250 mmol) and *S*-phenyl benzenesulfonothioate **160a** (68.8 mg, 0.275 mmol, 1.1 equiv). Purification by column chromatography on silica gel (*n*-hexane) yielded **176oa** (15.0 mg, 36%) as a colourless oil. Resonances reported for **176oa**: **^{1}H NMR** (400 MHz, $CDCl_3$): δ = 7.43 – 7.37 (m, 2H), 7.32 – 7.25 (m, 2H), 7.25 – 7.19 (m, 1H),

3.22 – 3.11 (m, 1H), 1.73 – 1.60 (m, 1H), 1.60 – 1.49 (m, 1H), 1.28 (d, *J* = 6.7 Hz, 3H), 1.04 (t, *J* = 7.6 Hz, 3H). **^{13}C NMR** (100 MHz, $CDCl_3$): *δ* = 135.7 (C_q), 132.0 (CH), 128.9 (CH), 126.7 (CH), 45.0 (CH), 29.6 (CH_2), 20.7 (CH_3), 11.6 (CH_3). **IR** (ATR): 2962, 2874, 1584, 1479, 1438, 1377, 1025, 747, 738, 691 cm^{-1}. **MS** (EI) *m*/*z* (relative intensity): 166 $[M]^+$ (50), 137 (10). **HR-MS** (EI+): *m*/*z* calcd for $C_{10}H_{14}S^+$ $[M]^+$ 166.0811, found 166.0810. The analytical data are in accordance to those reported in literature.[265]

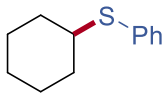

176pa

Cyclohexyl(phenyl)sulfane (176pa)

The general procedure **D** was followed using cyclohexyl bromide **175p** (40.8 mg, 0.250 mmol) and *S*-phenyl benzenesulfonothioate **160a** (68.8 mg, 0.275 mmol, 1.1 equiv). Purification by column chromatography on silica gel (*n*-hexane) yielded **176pa** (19.0 mg, 38%) as a colourless oil. Resonances reported for **176pa**: **^{1}H NMR** (400 MHz, $CDCl_3$): *δ* = 7.39 (dd, *J* = 7.8, 2.3 Hz, 2H), 7.28 (td, *J* = 7.7, 2.2 Hz, 2H), 7.24 – 7.17 (m, 1H), 3.15 – 3.06 (m, 1H), 2.09 – 1.91 (m, 2H), 1.83 – 1.72 (m, 2H), 1.67 – 1.53 (m, 1H), 1.48 – 1.16 (m, 5H). **^{13}C NMR** (100 MHz, $CDCl_3$): *δ* = 135.3 (C_q), 132.0 (CH), 128.9 (CH), 126.7 (CH), 46.7 (CH), 33.5 (CH_2), 26.2 (CH_2), 25.9 (CH_2). **IR** (ATR): 2928, 2852, 1584, 1479, 1449, 1438, 997, 751, 735, 691 cm^{-1}. **MS** (EI) *m*/*z* (relative intensity): 192 $[M]^+$ (60), 84 (10), 66 (5). **HR-MS** (EI+): *m*/*z* calcd for $C_{12}H_{16}S^+$ $[M]^+$ 192.0967, found 192.0968. The analytical data are in accordance to those reported in literature.[265]

5.3.3.2 Constant Potential Experiments

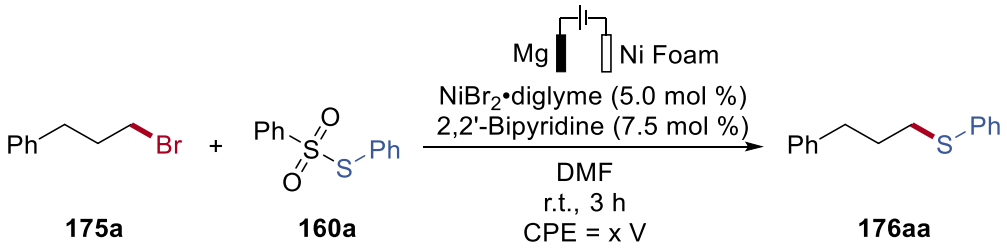

Figure 5.3.10. Constant potential electrolysis based on CV studies.

Under an atmosphere of Ar, an oven-dried undivided electrochemical cell with graphite rod (5.00 mm x 15.0 mm) and Pt plate (10.0 mm x 15.0 mm x 0.125 mm) was charged with 1-bromo-3-phenylpropane **175a** (38.0 µL, 0.250 mmol), *S*-phenyl benzenesulfonothioate **160a** (68.8 mg, 0.275 mmol, 1.1 equiv), $NiBr_2$•diglyme (4.40 mg, 0.0125 mmol, 5.0 mol %), 2,2'-bipyridine (2.90 mg, 0.0188 mmol, 7.5 mol %) dissolved in DMF (5.0 mL). Electrolysis was done with Metrohm Dropsens Multi Potentialstat/Galvanostat *µ*STAT 4000 at constant potential (reference to Ag wire) of different potentials at ambient temperature for 6 h (see **Table 5.3.1**). The reactions were performed independently.

Table 5.3.1. Comparisons of the constant potential studies.

Entry	Reduction Peak Potential of **160a** (CV)	CPE (x V) *vs.* $Ag^+/AgCl$	Note	**160a** recovered	Isolated Yield
1	1^{st}: − 0.91 V	− 1.00 V	66% PhSSPh	10%	18%
2	2^{nd}: − 1.62 V	− 1.80 V	44% PhSSPh	---	53%
3	---	− 0.70 V	18% PhSSPh	77%	traces

5.3.3.3 Further Investigations on the Formation of Disulfide 158a

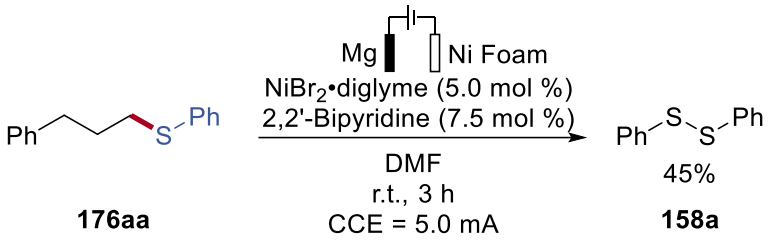

Figure 5.3.11. Further electrolysis of product **176aa** to disulfide **158a**.

Under an atmosphere of Ar, the oven-dried undivided electrochemical cell with graphite rod (5.00 mm x 15.0 mm) and Pt plate (10.0 mm x 15.0 mm x 0.125 mm) was charged with 1- Phenyl(3-phenylpropyl)sulfane **176aa** (57.1 mg, 0.250 mmol), $NiBr_2$•diglyme (4.40 mg, 0.0125 mmol, 5.0 mol %), 2,2'-bipyridine (2.90 mg, 0.0188 mmol, 7.5 mol %) dissolved in DMF (5.0 mL). Electrocatalysis was then performed at 5.0 mA of constant current at ambient temperature for 3 h. Purification by column chromatography on silica gel (*n*-hexane) yielded only disulfide **158aa** (13.0 mg, 45%) as a white powder.

5.3.3.4 Radical Clock Experiments

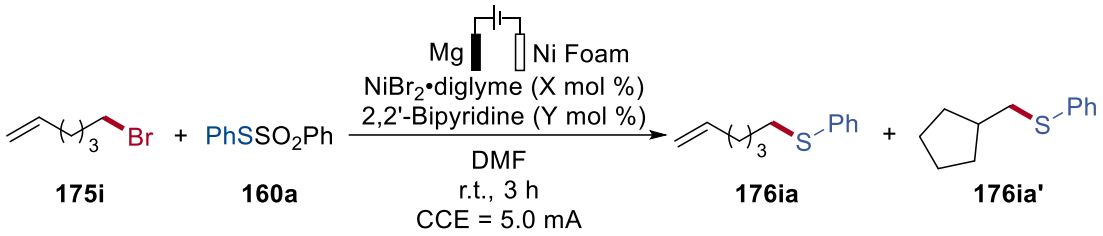

Figure 5.3.12. Radical clock studies.

Under an atmosphere of Ar, an oven-dried undivided electrochemical cell with Mg foil anode (3.00 mm x 15.0 mm x 0.02 mm) and Ni foam cathode (10.0 mm x 15.0 mm x 1.00 mm) was charged with 6-bromo-1-hexene **175i** (40.8 mg, 0.250 mmol, 1.00 equiv), *S*-phenyl benzenesulfonothioate **160a** (0.275 mmol, 1.1 equiv), $NiBr_2$•diglyme (2.5 or 5.0 mol %), 2,2'-bipyridine (3.75 or 7.50 mol %) dissolved in DMF (5.0 mL). Electrocatalysis was then performed at 5.0 mA of constant current at ambient temperature for 3 h. The reaction vessel was first diluted with EtOAc (30 mL). Both electrodes were washed and sonicated thoroughly with EtOAc (3 x 5.0 mL). The washings were added into the reaction mixture and the combined phases were

extracted with EtOAc (30 mL), the organic phases were then washed with deionized H_2O (3 x 20 mL), dried over Na_2SO_4. Evaporation of the solvents and the ratio of **176ia** and **176ia'** were determined by ^1H NMR spectroscopy with 1,3,5-trimethoxybenzene as internal standard.

Table 5.3.2. Results of the radical clock investigations.

Entry	[Ni] (X mol%)	2,2'-Bipyridine	Yield (%)	**176ia**:**176ia'**
1	2.5	3.75	69	14:1
2	5.0	7.50	96	>20:1

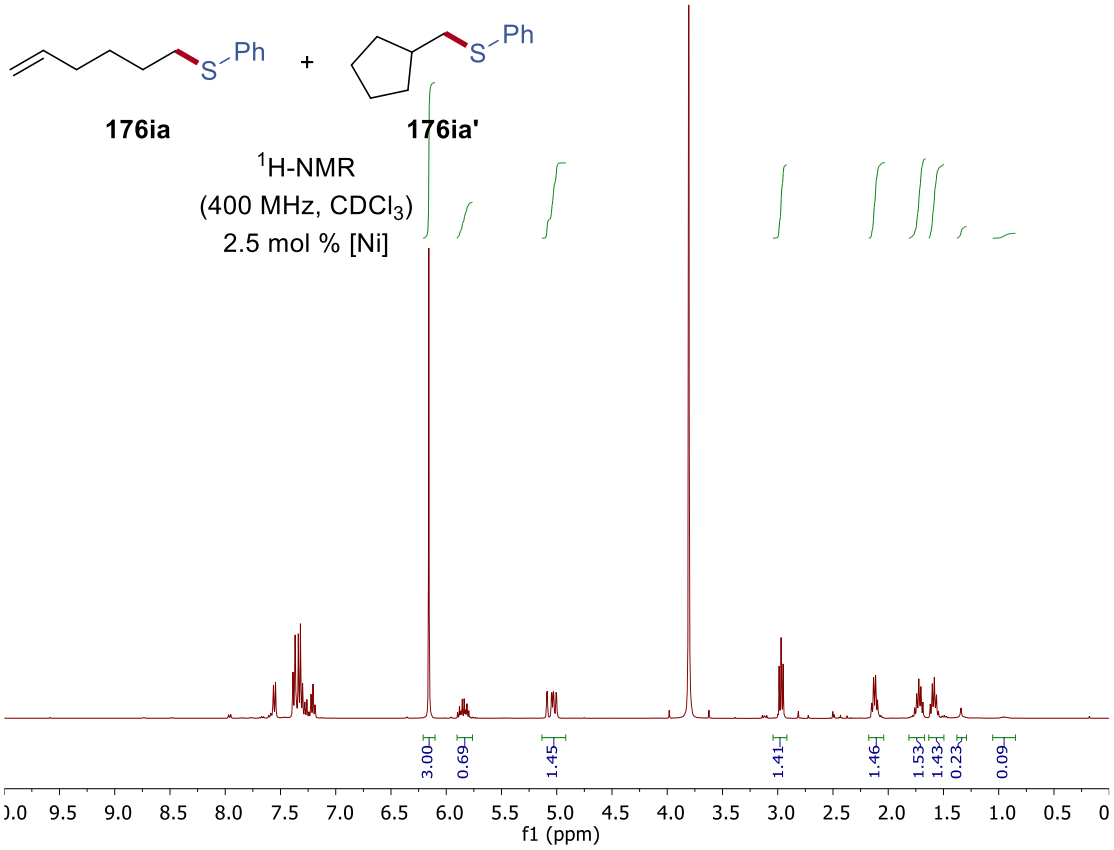

Figure 5.3.13. ^1H NMR spectroscopy of radical clock experiment with 2.5 mol % of [Ni].

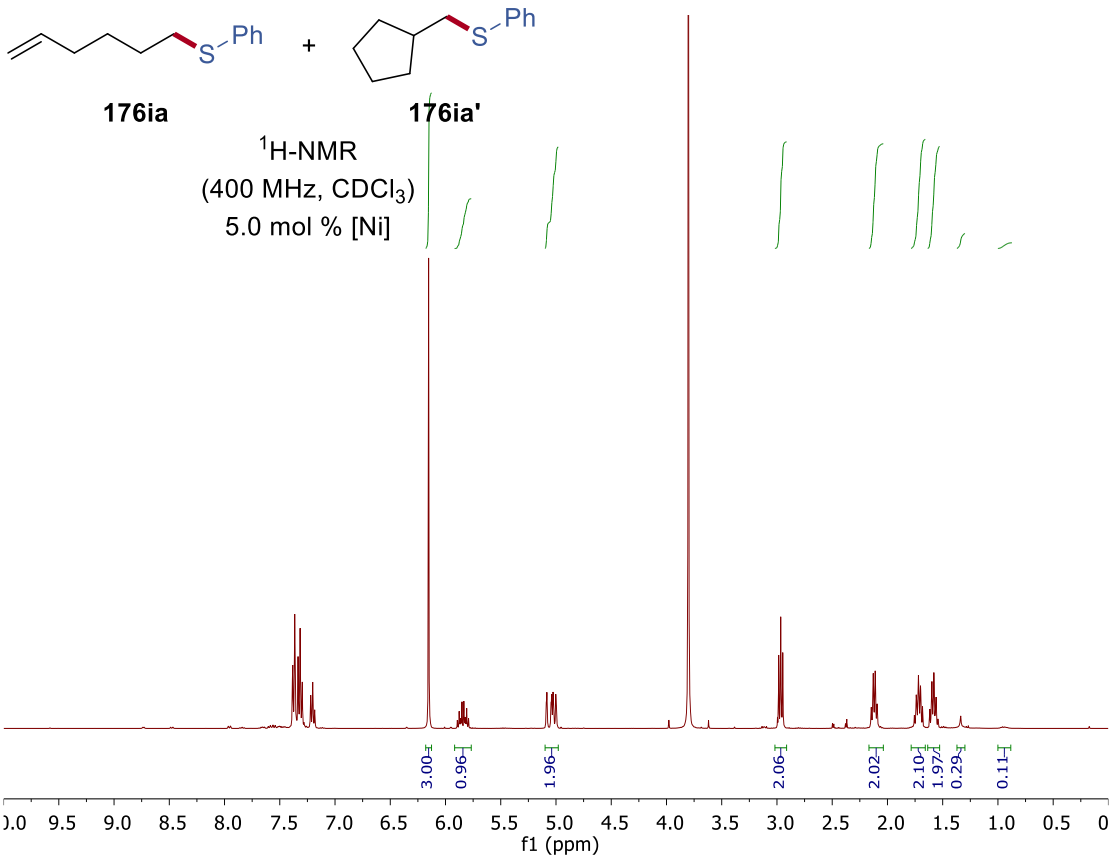

Figure 5.3.14. ^{1}H NMR spectroscopy of radical clock experiment at 5.0 mol % of [Ni].

5.3.3.5 Cyclic Voltammetry

The cyclic voltammetry measurements were performed with a Metrohm Autolab PGSTAT204 workstation and the following analysis was performed with a Nova 2.1 application. For all experiments, a saturated calomel electrode (SCE) was used as the reference electrode and a glassy-carbon (GC) electrode (3 mm-diameter, disc electrode) was used as the working electrode. The measurements were recorded at a scan rate of 100 mVs^{-1}. The operating temperature was at 298 K. All solutions were degassed via freeze-pump-thaw method prior to use and N_2 gas was bubbled through the solutions for at least 5 mins before the experiment was performed. These experiments were performed under inert conditions with 1-bromo-3-phenylpropane **175a** and *S*-phenyl benzenesulfonothioate **160a** as the model substrate (constant flow of dry N_2 gas).

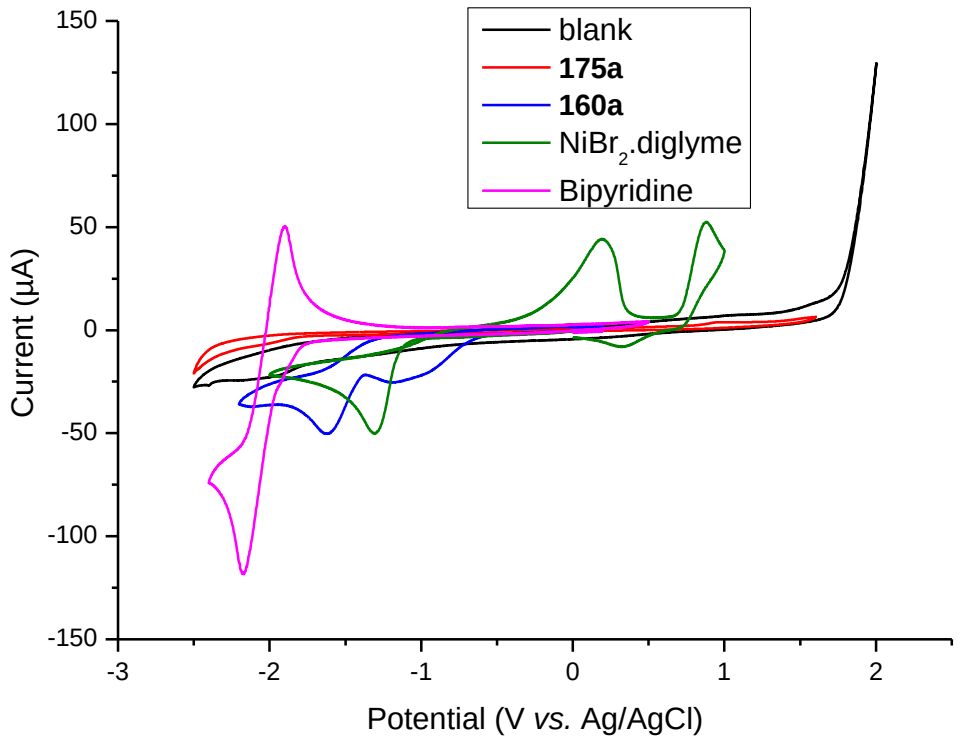

Figure 5.3.15. Cyclic voltammograms of individual components. Cyclic voltammograms at 100 mVs^{-1} using DMF and nBu$_4$NPF$_6$ (0.10 M) as electrolyte, and a GC working electrode. $NiBr_2$•diglyme (2.0 mM), 2,2'-bipyridine (2.0 mM), bromide **175a** (2.0 mM) and thiosulfonate **160a** (2.0 mM).

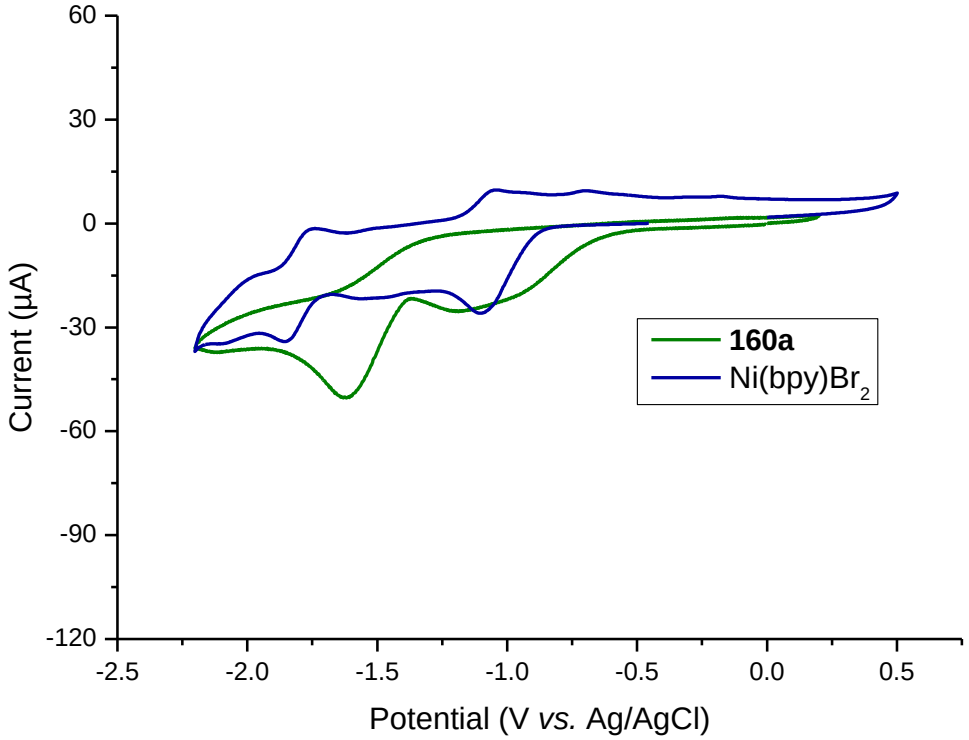

Figure 5.3.16. Cyclic voltammograms comparing the ligated nickel complex and thiosulfonate **160a**. Cyclic voltammograms at 100 mVs^{-1} using DMF and nBu$_4$NPF$_6$ (0.10 M) as electrolyte, and a GC working electrode. $Ni(bpy)Br_2$ (2.0 mM) and **160a** (2.0 mM).

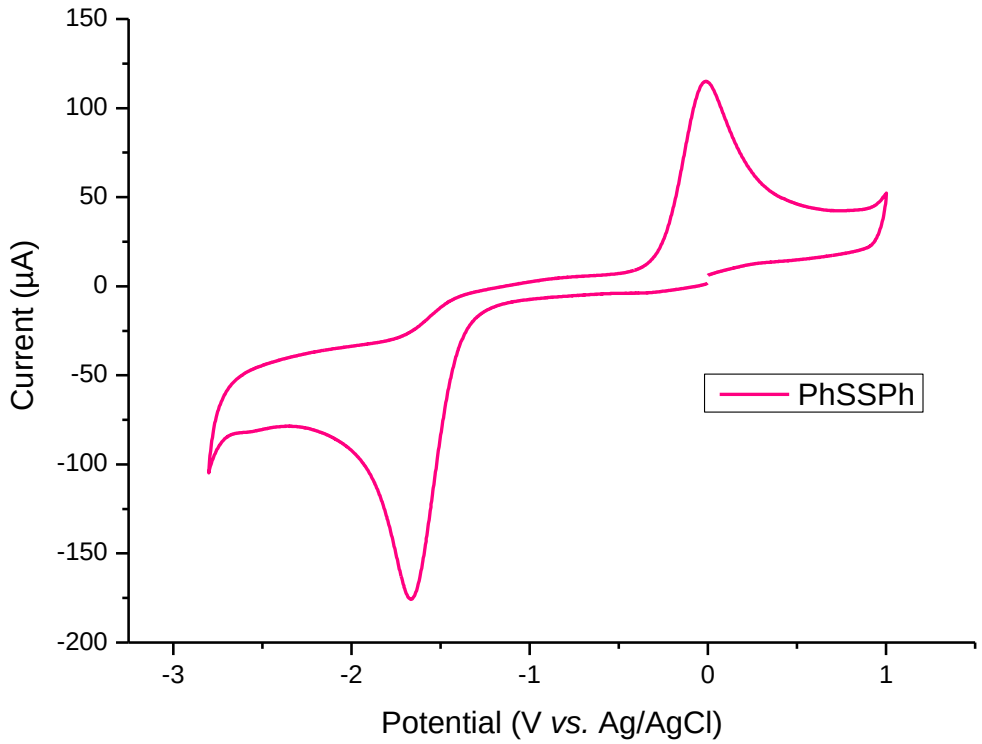

Figure 5.3.17. Cyclic voltammogram of disulfide **158a** at 100 mVs^{-1} using DMF and nBu$_4$NPF$_6$ (0.10 M) as electrolyte, and a GC working electrode. Diphenyl disulphide **158a** (2.0 mM).

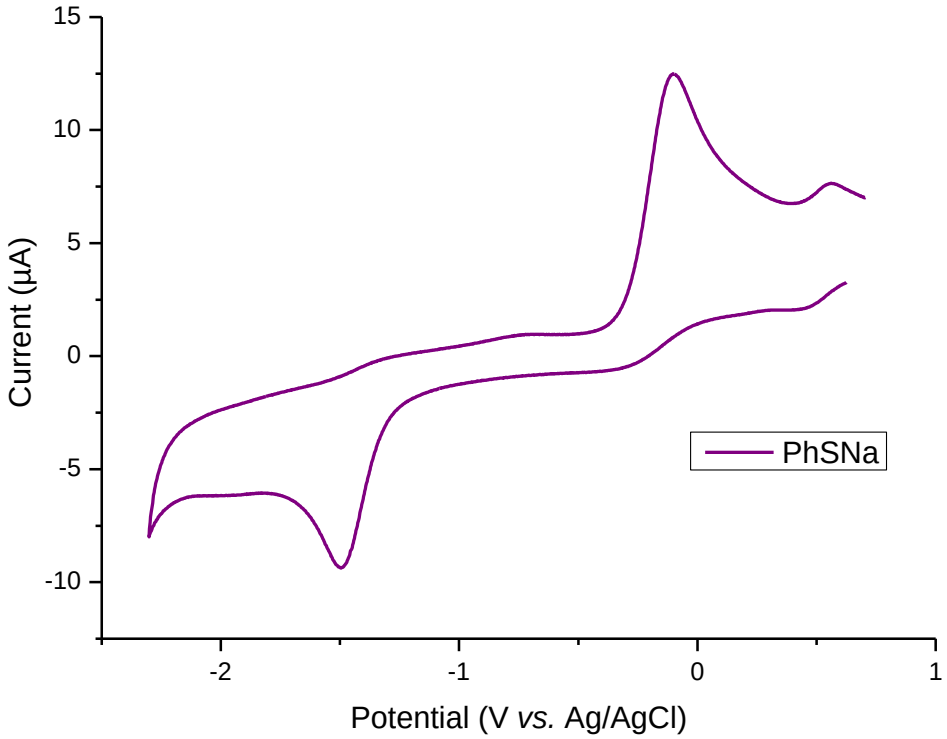

Figure 5.3.18. Cyclic voltammogram of phenyl thiolate salt at 100 mVs^{-1} using DMF and nBu$_4$NPF$_6$ (0.10 M) as electrolyte, and a GC working electrode. PhSNa (2.0 mM).

6. References

[1] a) P. T. Anastas, J. C. Warner, *Green Chemistry : Theory and Practice*, Oxford University Press, Oxford [England]; New York, **1998**; b) P. T. Anastas, J. J. Breen, *J. Clean. Prod.* **1997**, *5*, 97-102.

[2] a) A. G. Atanasov, S. B. Zotchev, V. M. Dirsch, T. the International Natural Product Sciences, C. T. Supuran, *Nat. Rev. Drug Discov.* **2021**, *20*, 200-216; b) D. Taylor, in *Pharmaceuticals in the Environment*, The Royal Society of Chemistry, **2016**, pp. 1-33; c) P. Thirumurugan, D. Matosiuk, K. Jozwiak, *Chem. Rev.* **2013**, *113*, 4905-4979; d) J. G. Lombardino, J. A. Lowe, *Nat. Rev. Drug Discov.* **2004**, *3*, 853-862.

[3] a) G. T. Whiteker, *Org. Process Res. Dev.* **2019**, *23*, 2109-2121; b) K. Racke, P. Spanoghe, N. D. Geyter, B. Saha, *Chem. Int.* **2019**, *41*, 53-55; c) T. J. C. O'Riordan, *Curr. Opin. Green Sustain. Chem.* **2018**, *13*, 158-163; d) J. B. Unsworth, N. A. Shakil, J. Kumar, *Chem. Int.* **2016**, *38*, 34-36; e) C. Lamberth, *J. Sulfur Chem.* **2004**, *25*, 39-62.

[4] F. Diederich, A. De Meijere, *Metal-catalyzed cross-coupling reactions*, Wiley-VCH, Weinheim, **2004**.

[5] The Nobel Prize in Chemistry 2010, https://www.nobelprize.org/prizes/chemistry/2010/summary/, **Accessed on June 11th, 2021**.

[6] a) R. F. Heck, *Synlett* **2006**, *2006*, 2855-2860; b) R. F. Heck, *Acc. Chem. Res* **1979**, *12*, 146-151; c) R. F. Heck, J. P. Nolley, *J. Org. Chem.* **1972**, *37*, 2320-2322; d) T. Mizoroki, K. Mori, A. Ozaki, *Bull. Chem. Soc. Jap.* **1971**, *44*, 581-581.

[7] a) K. Tamao, K. Sumitani, M. Kumada, *J. Am. Chem. Soc.* **1972**, *94*, 4374-4376; b) R. J. P. Corriu, J. P. Masse, *J. Chem. Soc., Chem. Commun.* **1972**, 144a-144a.

[8] a) K. Sonogashira, *J. Organomet. Chem.* **2002**, *653*, 46-49; b) K. Sonogashira, Y. Tohda, N. Hagihara, *Tetrahedron Lett.* **1975**, *16*, 4467-4470.

[9] a) E. Negishi, *Acc. Chem. Res.* **1982**, *15*, 340-348; b) E. Negishi, A. O. King, N. Okukado, *J. Org. Chem.* **1977**, *42*, 1821-1823; c) S. Baba, E. Negishi, *J. Am. Chem. Soc.* **1976**, *98*, 6729-6731.

[10] a) J. K. Stille, *Angew. Chem. Int. Ed.* **1986**, *25*, 508-524; b) D. Milstein, J. K. Stille, *J. Am. Chem. Soc.* **1978**, *100*, 3636-3638; c) M. Kosugi, Y. Shimizu, T. Migita, *Chem. Lett.* **1977**, *6*, 1423-1424.

[11] a) N. Miyaura, A. Suzuki, *Chem. Rev.* **1995**, *95*, 2457-2483; b) N. Miyaura, K. Yamada, A. Suzuki, *Tetrahedron Lett.* **1979**, *20*, 3437-3440.

[12] a) M. Fujita, T. Hiyama, *J. Org. Chem.* **1988**, *53*, 5415-5421; b) T. Hiyama, M. Obayashi, I. Mori, H. Nozaki, *J. Org. Chem.* **1983**, *48*, 912-914.

[13] a) M. J. Buskes, M.-J. Blanco, *Molecules* **2020**, *25*, 3493; b) *Applied Cross-Coupling Reactions*, Springer, Berlin, Heidelberg, **2013**.

[14] a) H. Lin, D. Sun, *Org. Prep. Proced. Int.* **2013**, *45*, 341-394; b) A. Casitas, X. Ribas, in *Copper‐Mediated Cross‐Coupling Reactions*, **2013**, pp. 253-279;

c) F. Monnier, M. Taillefer, *Angew. Chem. Int. Ed.* **2009**, *48*, 6954-6971; d) G. Evano, N. Blanchard, M. Toumi, *Chem. Rev.* **2008**, *108*, 3054-3131; e) W. R. H. Hurtley, *J. Chem. Soc.* **1929**, 1870-1873; f) I. Goldberg, *Ber. d. Dt. Chem. Ges.* **1906**, *39*, 1691-1692; g) F. Ullmann, P. Sponagel, *Ber. d. Dt. Chem. Ges.* **1905**, *38*, 2211-2212.

[15] a) J. F. Hartwig, *Nature* **2008**, *455*, 314-322; b) A. R. Muci, S. L. Buchwald, in *Cross-Coupling Reactions: A Practical Guide* (Ed.: N. Miyaura), Springer, Berlin, Heidelberg, **2002**, pp. 131-209; c) J. F. Hartwig, *Angew. Chem. Int. Ed.* **1998**, *37*, 2046-2067.

[16] a) J. X. Qiao, P. Y. S. Lam, *Synthesis* **2011**, *2011*, 829-856; b) J. X. Qiao, P. Y. S. Lam, in *Boronic Acids*, **2011**, pp. 315-361; c) P. Y. S. Lam, G. Vincent, D. Bonne, C. G. Clark, *Tetrahedron Lett.* **2003**, *44*, 4927-4931; d) D. M. T. Chan, K. L. Monaco, R. Li, D. Bonne, C. G. Clark, P. Y. S. Lam, *Tetrahedron Lett.* **2003**, *44*, 3863-3865; e) P. Y. S. Lam, C. G. Clark, S. Saubern, J. Adams, M. P. Winters, D. M. T. Chan, A. Combs, *Tetrahedron Lett.* **1998**, *39*, 2941-2944.

[17] F. Ullmann, J. Bielecki, *Ber. d. Dt. Chem. Ges.* **1901**, *34*, 2174-2185.

[18] L. Ackermann, in *Modern Arylation Methods* (Ed.: L. Ackermann), Wiley-VCH, Weinheim, **2009**.

[19] a) P. A. Wender, B. L. Miller, *Nature* **2009**, *460*, 197-201; b) P. A. Wender, M. P. Croatt, B. Witulski, *Tetrahedron* **2006**, *62*, 7505-7511; c) B. M. Trost, *Angew. Chem. Int. Ed.* **1995**, *34*, 259-281; d) B. M. Trost, *Science* **1991**, *254*, 1471-1477.

[20] a) F. Colobert, J. Wencel-Delord, *C–H Activation for Asymmetric Synthesis*, Wiley-VCH, Weinheim, **2019**; b) L. Ackermann, T. B. Gunnoe, L. G. Habgood, *Catalytic hydroarylation of carbon-carbon multiple bonds*, Wiley-VCH, Weinheim, **2018**; c) P. H. Dixneuf, H. Doucel, *C–H Bond Activation and Catalytic Functionalization I*, Springer International Publishing, Switzerland, **2016**; d) P. H. Dixneuf, H. Doucel, *C–H Bond Activation and Catalytic Functionalization II*, Springer International Publishing, Switzerland, **2016**; e) J. J. Li, *C-H bond activation in organic synthesis*, CRC Press, Boca Raton, **2015**; f) X. Ribas, Royal Society of Chemistry, Thomas Graham House, Cambridge, **2013**; g) J.-Q. Yu, Z. Shi, *C–H Activation*, Springer-Verlag Berlin, Heidelberg, **2010**.

[21] a) R. C. Samanta, T. H. Meyer, I. Siewert, L. Ackermann, *Chem. Sci.* **2020**, *11*, 8657-8670; b) P. Gandeepan, L. H. Finger, T. H. Meyer, L. Ackermann, *Chem. Soc. Rev.* **2020**, *49*, 4254-4272; c) L. Ackermann, S.-L. You, M. Oestreich, S. Meng, D. MacFarlene, Y. Yin, *Trends Chem.* **2020**, *2*, 275-277; d) T. H. Meyer, L. H. Finger, P. Gandeepan, L. Ackermann, *Trends Chem.* **2019**, *1*, 63-76.

[22] a) J. Wencel-Delord, T. Dröge, F. Liu, F. Glorius, *Chem. Soc. Rev.* **2011**, *40*, 4740-4761; b) H. Lu, X. P. Zhang, *Chem. Soc. Rev.* **2011**, *40*, 1899-1909; c) L. Ackermann, *Chem. Rev.* **2011**, *111*, 1315-1345; d) D. Balcells, E. Clot, O. Eisenstein, *Chem. Rev.* **2010**, *110*, 749-823; e) H. M. L. Davies, J. R. Manning, *Nature* **2008**, *451*, 417-424; f) L. Ackermann, in *Directed Metallation* (Ed.: N. Chatani), Springer Berlin Heidelberg, Berlin, Heidelberg, **2007**, pp. 35-60.

[23] a) S. A. Girard, T. Knauber, C.-J. Li, *Angew. Chem. Int. Ed.* **2014**, *53*, 74-100; b) C. S. Yeung, V. M. Dong, *Chem. Rev.* **2011**, *111*, 1215-1292; c) C. J. Scheuermann, *Chem. Asian J.* **2010**, *5*, 436-451; d) C.-J. Li, Z. Li, *Pure Appl. Chem.* **2006**, *78*, 935-945.

[24] a) S. Rej, Y. Ano, N. Chatani, *Chem. Rev.* **2020**, *120*, 1788-1887; b) H. Yi, G. Zhang, H. Wang, Z. Huang, J. Wang, A. K. Singh, A. Lei, *Chem. Rev.* **2017**, *117*, 9016-9085.

[25] J. R. Webb, S. A. Burgess, T. R. Cundari, T. B. Gunnoe, *Dalton Trans.* **2013**, *42*, 16646-16665.

[26] J. Kua, X. Xu, R. A. Periana, W. A. Goddard, *Organometallics* **2002**, *21*, 511-525.

[27] Z. Lin, *Coord. Chem. Rev.* **2007**, *251*, 2280-2291.

[28] a) T. R. Cundari, T. R. Klinckman, P. T. Wolczanski, *J. Am. Chem. Soc.* **2002**, *124*, 1481-1487; b) J. L. Bennett, P. T. Wolczanski, *J. Am. Chem. Soc.* **1997**, *119*, 10696-10719.

[29] a) J. C. Gaunt, B. L. Shaw, *J. Organomet. Chem.* **1975**, *102*, 511-516; b) J. M. Duff, B. E. Mann, B. L. Shaw, B. Turtle, *J. Chem. Soc., Dalton Trans.* **1974**, 139-145; c) J. M. Duff, B. L. Shaw, *J. Chem. Soc., Dalton Trans.* **1972**, 2219-2225.

[30] a) L. Wang, L. Ackermann, *Org. Lett.* **2013**, *15*, 176-179; b) W. Ma, K. Graczyk, L. Ackermann, *Org. Lett.* **2012**, *14*, 6318-6321; c) B. Li, H. Feng, N. Wang, J. Ma, H. Song, S. Xu, B. Wang, *Chem. Eur. J.* **2012**, *18*, 12873-12879; d) L. Ackermann, L. Wang, A. V. Lygin, *Chem. Sci.* **2012**, *3*, 177-180; e) L. Ackermann, A. V. Lygin, *Org. Lett.* **2012**, *14*, 764-767; f) L. Ackermann, A. V. Lygin, N. Hofmann, *Angew. Chem. Int. Ed.* **2011**, *50*, 6379-6382; g) L. Ackermann, A. V. Lygin, N. Hofmann, *Org. Lett.* **2011**, *13*, 3278-3281; h) L. Ackermann, R. Vicente, A. Althammer, *Org. Lett.* **2008**, *10*, 2299-2302.

[31] S. I. Gorelsky, D. Lapointe, K. Fagnou, *J. Am. Chem. Soc.* **2008**, *130*, 10848-10849.

[32] a) Y. Boutadla, D. L. Davies, S. A. Macgregor, A. I. Poblador-Bahamonde, *Dalton Trans.* **2009**, 5887-5893; b) D. L. Davies, S. M. A. Donald, S. A. Macgregor, *J. Am. Chem. Soc.* **2005**, *127*, 13754-13755.

[33] a) D. Zell, M. Bursch, V. Müller, S. Grimme, L. Ackermann, *Angew. Chem. Int. Ed.* **2017**, *56*, 10378-10382; b) W. Ma, R. Mei, G. Tenti, L. Ackermann, *Chem. Eur. J.* **2014**, *20*, 15248-15251.

[34] R. G. Bergman, *Nature* **2007**, *446*, 391-393.

[35] a) J. Wang, G. Dong, *Chem. Rev.* **2019**, *119*, 7478-7528; b) B. Niu, K. Yang, B. Lawrence, H. Ge, *ChemSusChem* **2019**, *12*, 2955-2969; c) C. Sambiagio, D. Schönbauer, R. Blieck, T. Dao-Huy, G. Pototschnig, P. Schaaf, T. Wiesinger, M. F. Zia, J. Wencel-Delord, T. Besset, B. U. W. Maes, M. Schnürch, *Chem. Soc. Rev.* **2018**, *47*, 6603-6743; d) M. Ghosh, S. De Sarkar, *Asian J. Org. Chem.* **2018**, *7*, 1236-1255; e) P. Gandeepan, L. Ackermann, *Chem* **2018**, *4*, 199-222; f) X.-S. Xue, P. Ji, B. Zhou, J.-P. Cheng, *Chem. Rev.* **2017**, *117*, 8622-8648; g) J. A. Leitch, C. G. Frost, *Chem. Soc. Rev.* **2017**, *46*, 7145-7153; h) M. Font, J.

M. Quibell, G. J. P. Perry, I. Larrosa, *Chem. Commun.* **2017**, *53*, 5584-5597; i) Z. Chen, B. Wang, J. Zhang, W. Yu, Z. Liu, Y. Zhang, *Org. Chem. Front.* **2015**, *2*, 1107-1295.

[36] K. Shen, Y. Fu, J.-N. Li, L. Liu, Q.-X. Guo, *Tetrahedron* **2007**, *63*, 1568-1576.

[37] a) J. Li, S. De Sarkar, L. Ackermann, in *C-H Bond Activation and Catalytic Functionalization I* (Eds.: P. H. Dixneuf, H. Doucet), Springer International Publishing, Cham, **2016**, pp. 217-257; b) G. Cera, L. Ackermann, *Top. Curr. Chem.* **2016**, *374*, 57; c) L. Ackermann, J. Li, *Nat. Chem.* **2015**, *7*, 686-687; d) L. Ackermann, R. Vicente, in *C-H Activation* (Eds.: J.-Q. Yu, Z. Shi), Springer, Berlin, Heidelberg, **2010**, pp. 211-229; e) L. Ackermann, R. Vicente, A. R. Kapdi, *Angew. Chem. Int. Ed.* **2009**, *48*, 9792-9826.

[38] N. Y. P. Kumar, A. Bechtoldt, K. Raghuvanshi, L. Ackermann, *Angew. Chem. Int. Ed.* **2016**, *55*, 6929-6932.

[39] a) C. L. Tucker, E. van Steen, *Catal. Today* **2020**, *342*, 115-123; b) Z. Li, M. Si, L. Xin, R. Liu, R. Liu, J. Lü, *Chin. J. Chem. Eng.* **2018**, *26*, 747-752; c) F. Hebrard, P. Kalck, *Chem. Rev.* **2009**, *109*, 4272-4282; d) A. Y. Khodakov, W. Chu, P. Fongarland, *Chem. Rev.* **2007**, *107*, 1692-1744.

[40] M. S. Kharasch, E. K. Fields, *J. Am. Chem. Soc.* **1941**, *63*, 2316-2320.

[41] M. Giedyk, K. Goliszewska, D. Gryko, *Chem. Soc. Rev.* **2015**, *44*, 3391-3404.

[42] a) P. Gandeepan, C.-H. Cheng, *Acc. Chem. Res.* **2015**, *48*, 1194-1206; b) B. Heller, M. Hapke, *Chem. Soc. Rev.* **2007**, *36*, 1085-1094.

[43] a) T. Shibata, *Adv. Synth. Catal.* **2006**, *348*, 2328-2336; b) I. U. Khand, G. R. Knox, P. L. Pauson, W. E. Watts, *J. Chem. Soc., Perkin Trans. 1* **1973**, 975-977.

[44] a) B. J. Teobald, *Tetrahedron* **2002**, *58*, 4133-4170; b) K. M. Nicholas, *Acc. Chem. Res.* **1987**, *20*, 207-214.

[45] a) J. R. Ludwig, E. M. Simmons, S. R. Wisniewski, P. J. Chirik, *Org. Lett.* **2021**, *23*, 625-630; b) R. J. M. Gebbink, M.-E. Moret, **2019**; c) H. A. Duong, Z.-H. Yeow, Y.-L. Tiong, N. H. B. Mohamad Kamal, W. Wu, *J. Org. Chem.* **2019**, *84*, 12686-12691; d) S. Asghar, S. B. Tailor, D. Elorriaga, R. B. Bedford, *Angew. Chem. Int. Ed.* **2017**, *56*, 16367-16370; e) G. Cahiez, A. Moyeux, *Chem. Rev.* **2010**, *110*, 1435-1462; f) C. Gosmini, J.-M. Bégouin, A. Moncomble, *Chem. Commun.* **2008**, 3221-3233.

[46] a) T. Dalton, T. Faber, F. Glorius, *ACS Cent. Sci.* **2021**, *7*, 245-261; b) O. Baudoin, *Angew. Chem. Int. Ed.* **2020**, *59*, 17798-17809; c) Ł. Woźniak, N. Cramer, *Trends Chem.* **2019**, *1*, 471-484; d) J. Loup, U. Dhawa, F. Pesciaioli, J. Wencel-Delord, L. Ackermann, *Angew. Chem. Int. Ed.* **2019**, *58*, 12803-12818; e) W. Wang, M. M. Lorion, J. Shah, A. R. Kapdi, L. Ackermann, *Angew. Chem. Int. Ed.* **2018**, *57*, 14700-14717; f) Y. Park, Y. Kim, S. Chang, *Chem. Rev.* **2017**, *117*, 9247-9301; g) M. M. Lorion, K. Maindan, A. R. Kapdi, L. Ackermann, *Chem. Soc. Rev.* **2017**, *46*, 7399-7420; h) J. He, M. Wasa, K. S. L. Chan, Q. Shao, J.-Q. Yu, *Chem. Rev.* **2017**, *117*, 8754-8786.

[47] a) R. Mei, U. Dhawa, R. C. Samanta, W. Ma, J. Wencel-Delord, L. Ackermann, *ChemSusChem* **2020**, *13*, 3306-3356; b) P. Gandeepan, T. Müller, D. Zell, G.

Cera, S. Warratz, L. Ackermann, *Chem. Rev.* **2019**, *119*, 2192-2452; c) M. Moselage, J. Li, L. Ackermann, *ACS Catal.* **2016**, *6*, 498-525; d) L. Ackermann, *J. Org. Chem.* **2014**, *79*, 8948-8954.

[48] a) N. Yoshikai, in *Cobalt Catalysis in Organic Synthesis*, **2020**, pp. 89-161; b) N. Yoshikai, *Bull. Chem .Soc. Jap.* **2014**, *87*, 843-857; c) K. Gao, N. Yoshikai, *Acc. Chem. Res.* **2014**, *47*, 1208-1219.

[49] a) T. Yoshino, S. Matsunaga, *Synlett* **2019**, *30*, 1384-1400; b) T. Yoshino, S. Matsunaga, in *Advances in Organometallic Chemistry, Vol. 68* (Ed.: P. J. Pérez), Academic Press, **2017**, pp. 197-247; c) T. Yoshino, S. Matsunaga, *Adv. Synth. Catal.* **2017**, *359*, 1245-1262.

[50] O. Planas, P. G. Chirila, C. J. Whiteoak, X. Ribas, in *Advances in Organometallic Chemistry, Vol. 69* (Ed.: P. J. Pérez), Academic Press, **2018**, pp. 209-282.

[51] Y. Kommagalla, N. Chatani, *Coord. Chem. Rev.* **2017**, *350*, 117-135.

[52] a) L. Lukasevics, L. Grigorjeva, *Org. Biomol. Chem.* **2020**, *18*, 7460-7466; b) A. Baccalini, S. Vergura, P. Dolui, G. Zanoni, D. Maiti, *Org. Biomol. Chem.* **2019**, *17*, 10119-10141; c) S. Prakash, R. Kuppusamy, C.-H. Cheng, *ChemCatChem* **2018**, *10*, 683-705; d) S. Wang, S.-Y. Chen, X.-Q. Yu, *Chem. Commun.* **2017**, *53*, 3165-3180; e) P. G. Chirila, C. J. Whiteoak, *Dalton Trans.* **2017**, *46*, 9721-9739; f) D. Wei, X. Zhu, J.-L. Niu, M.-P. Song, *ChemCatChem* **2016**, *8*, 1242-1263.

[53] L. Grigorjeva, O. Daugulis, *Angew. Chem. Int. Ed.* **2014**, *53*, 10209-10212.

[54] L. Grigorjeva, O. Daugulis, *Org. Lett.* **2014**, *16*, 4684-4687.

[55] X.-L. Han, P.-P. Lin, Q. Li, *Chin. Chem. Lett.* **2019**, *30*, 1495-1502.

[56] R. Gujjarappa, N. Vodnala, C. C. Malakar, *Adv. Synth. Catal.* **2020**, *362*, 4896-4990.

[57] R. Mei, H. Wang, S. Warratz, S. A. Macgregor, L. Ackermann, *Chem. Eur. J.* **2016**, *22*, 6759-6763.

[58] K. Cheng, N. J. Rahier, B. M. Eisenhauer, R. Gao, S. J. Thomas, S. M. Hecht, *J. Am. Chem. Soc.* **2005**, *127*, 838-839.

[59] X.-Q. Hao, C. Du, X. Zhu, P.-X. Li, J.-H. Zhang, J.-L. Niu, M.-P. Song, *Org. Lett.* **2016**, *18*, 3610-3613.

[60] Á. M. Martínez, N. Rodríguez, R. Gómez-Arrayás, J. C. Carretero, *Chem. Eur. J.* **2017**, *23*, 11669-11676.

[61] C. Kuai, L. Wang, B. Li, Z. Yang, X. Cui, *Org. Lett.* **2017**, *19*, 2102-2105.

[62] S. Zhai, S. Qiu, X. Chen, J. Wu, H. Zhao, C. Tao, Y. Li, B. Cheng, H. Wang, H. Zhai, *Chem. Commun.* **2018**, *54*, 98-101.

[63] H. Zhao, X. Shao, T. Wang, S. Zhai, S. Qiu, C. Tao, H. Wang, H. Zhai, *Chem. Commun.* **2018**, *54*, 4927-4930.

[64] T. T. Nguyen, L. Grigorjeva, O. Daugulis, *Angew. Chem. Int. Ed.* **2018**, *57*, 1688-1691.

[65] S. Kathiravan, I. A. Nicholls, *Org. Lett.* **2017**, *19*, 4758-4761.

[66] J. Zhang, H. Chen, C. Lin, Z. Liu, C. Wang, Y. Zhang, *J. Am. Chem. Soc.* **2015**, *137*, 12990-12996.

[67] a) B. Yang, Y. Qiu, J.-E. Bäckvall, *Acc. Chem. Res.* **2018**, *51*, 1520-1531; b) J. Ye, S. Ma, *Acc. Chem. Res.* **2014**, *47*, 989-1000; c) S. Yu, S. Ma, *Angew. Chem. Int. Ed.* **2012**, *51*, 3074-3112; d) C. Aubert, L. Fensterbank, P. Garcia, M. Malacria, A. Simonneau, *Chem. Rev.* **2011**, *111*, 1954-1993; e) S. Ma, *Chem. Rev.* **2005**, *105*, 2829-2872; f) A. Hoffmann-Röder, N. Krause, *Angew. Chem. Int. Ed.* **2004**, *43*, 1196-1216; g) A. S. K. Hashmi, *Angew. Chem. Int. Ed.* **2000**, *39*, 3590-3593.

[68] N. Thrimurtulu, A. Dey, D. Maiti, C. M. R. Volla, *Angew. Chem. Int. Ed.* **2016**, *55*, 12361-12365.

[69] a) X.-F. Xia, Y.-Q. Wang, L.-L. Zhang, X.-R. Song, X.-Y. Liu, Y.-M. Liang, *Chem. Eur. J.* **2014**, *20*, 5087-5091; b) A. Rodríguez, J. Albert, X. Ariza, J. Garcia, J. Granell, J. Farràs, A. La Mela, E. Nicolás, *J. Org. Chem.* **2014**, *79*, 9578-9585; c) H. Wang, F. Glorius, *Angew. Chem. Int. Ed.* **2012**, *51*, 7318-7322.

[70] R. Boobalan, R. Kuppusamy, R. Santhoshkumar, P. Gandeepan, C.-H. Cheng, *ChemCatChem* **2017**, *9*, 273-277.

[71] T. Li, C. Zhang, Y. Tan, W. Pan, Y. Rao, *Org. Chem. Front.* **2017**, *4*, 204-209.

[72] X. Yao, L. Jin, Y. Rao, *Asian J. Org. Chem.* **2017**, *6*, 825-830.

[73] S. Zhai, S. Qiu, X. Chen, C. Tao, Y. Li, B. Cheng, H. Wang, H. Zhai, *ACS Catal.* **2018**, *8*, 6645-6649.

[74] a) N. Thrimurtulu, R. Nallagonda, C. M. R. Volla, *Chem. Commun.* **2017**, *53*, 1872-1875; b) T. Lan, L. Wang, Y. Rao, *Org. Lett.* **2017**, *19*, 972-975.

[75] a) S. Syed Shoaib Ahmad, R. Gildardo, A. Muhammad, *Mini-Rev. Med. Chem.* **2013**, *13*, 70-86; b) G. J. Wells, M. Tao, K. A. Josef, R. Bihovsky, *J. Med. Chem.* **2001**, *44*, 3488-3503.

[76] a) L. Guillemard, J. Wencel-Delord, *Beilstein J. Org. Chem.* **2020**, *16*, 1754-1804; b) L. Marzo, S. K. Pagire, O. Reiser, B. König, *Angew. Chem. Int. Ed.* **2018**, *57*, 10034-10072; c) K. L. Skubi, T. R. Blum, T. P. Yoon, *Chem. Rev.* **2016**, *116*, 10035-10074; d) M. D. Kärkäs, J. A. Porco, C. R. J. Stephenson, *Chem. Rev.* **2016**, *116*, 9683-9747; e) R. Brimioulle, D. Lenhart, M. M. Maturi, T. Bach, *Angew. Chem. Int. Ed.* **2015**, *54*, 3872-3890; f) C. K. Prier, D. A. Rankic, D. W. C. MacMillan, *Chem. Rev.* **2013**, *113*, 5322-5363.

[77] a) I. Huskić, C. B. Lennox, T. Friščić, *Green Chem.* **2020**, *22*, 5881-5901; b) P. F. M. de Oliveira, R. M. Torresi, F. Emmerling, P. H. C. Camargo, *J. Mat. Chem. A* **2020**, *8*, 16114-16141; c) C. Bolm, J. G. Hernández, *Angew. Chem. Int. Ed.* **2019**, *58*, 3285-3299.

[78] a) S. Santoro, F. Ferlin, L. Ackermann, L. Vaccaro, *Chem. Soc. Rev.* **2019**, *48*, 2767-2782; b) D. Pletcher, R. A. Green, R. C. D. Brown, *Chem. Rev.* **2018**, *118*, 4573-4591; c) M. B. Plutschack, B. Pieber, K. Gilmore, P. H. Seeberger, *Chem. Rev.* **2017**, *117*, 11796-11893; d) A. A. Folgueiras-Amador, T. Wirth, *J. Flow Chem.* **2017**, *7*, 94-95; e) H. P. L. Gemoets, Y. Su, M. Shang, V. Hessel, R. Luque, T. Noël, *Chem. Soc. Rev.* **2016**, *45*, 83-117; f) J. C. Pastre, D. L. Browne, S. V. Ley, *Chem. Soc. Rev.* **2013**, *42*, 8849-8869; g) T. Noël, S. L. Buchwald, *Chem. Soc. Rev.* **2011**, *40*, 5010-5029; h) S. Saaby, K. R. Knudsen, M. Ladlow, S. V. Ley, *Chem. Commun.* **2005**, 2909-2911.

[79] a) O. A. von Lilienfeld, K.-R. Müller, A. Tkatchenko, *Nat. Rev. Chem.* **2020**, *4*, 347-358; b) A. Zhavoronkov, *Mol. Pharma.* **2018**, *15*, 4311-4313.

[80] a) D. Pollok, S. R. Waldvogel, *Chem. Sci.* **2020**, *11*, 12386-12400; b) T. H. Meyer, I. Choi, C. Tian, L. Ackermann, *Chem* **2020**, *6*, 2484-2496; c) Y. Kawamata, P. S. Baran, *Joule* **2020**, *4*, 701-704.

[81] A. Volta, *Philos. Trans. R. Soc. London* **1800**, *90*, 403-431.

[82] M. Faraday, *Ann. Phys.* **1834**, *109*, 481-520.

[83] a) M. C. Leech, K. Lam, *Acc. Chem. Res.* **2020**, *53*, 121-134; b) H.-J. Schäfer, Springer, Berlin, Heidelberg, **1990**, pp. 91-151; c) L. Becking, H. J. Schäfer, *Tetrahedron Lett.* **1988**, *29*, 2797-2800; d) H. Kolbe, *Liebigs Ann. Chem.* **1849**, *69*, 257-294; e) H. Kolbe, *J. Prakt. Chem.* **1847**, *41*, 137-139; f) H. Kolbe, *Liebigs Ann. Chem.* **1845**, *54*, 145-188.

[84] a) J. J. Lingane, C. G. Swain, M. Fields, *J. Am. Chem. Soc.* **1943**, *65*, 1348-1353; b) A. Hickling, *Trans. Faraday Soc.* **1942**, *38*, 27-33.

[85] a) *Chem. Rec.* **2012**, *12*, 17-25; b) *Chem. Rec.* **2012**, *12*, 26-26; c) *Anal. Chem.* **2000**, *72*, 346 A-352 A; d) J. Heinze, *Angew. Chem. Int. Ed. Engl.* **1984**, *23*, 831-847; e) J. E. B. Randles, *Trans. Faraday Soc.* **1948**, *44*, 327-338.

[86] J. H. Simons, *J. Electrochem. Soc.* **1949**, *95*, 47-67.

[87] a) M. M. Baizer, *Tetrahedron* **1984**, *40*, 935-969; b) M. M. Baizer, *J. Electrochem. Soc.* **1964**, *111*, 215.

[88] a) M. C. Leech, A. D. Garcia, A. Petti, A. P. Dobbs, K. Lam, *React. Chem. Eng.* **2020**, *5*, 977-990; b) D. S. P. Cardoso, B. Šljukić, D. M. F. Santos, C. A. C. Sequeira, *Org. Process Res. Dev.* **2017**, *21*, 1213-1226.

[89] J.-i. Yoshida, T. Murata, S. Isoe, *Tetrahedron Lett.* **1986**, *27*, 3373-3376.

[90] a) C. Costentin, J.-M. Savéant, *Proc. Natl. Acad. Sci.* **2019**, *116*, 11147-11152; b) R. Francke, R. D. Little, *Chem. Soc. Rev.* **2014**, *43*, 2492-2521; c) Y. Oh, X. Hu, *Chem. Soc. Rev.* **2013**, *42*, 2253-2261; d) C. Amatore, C. Cammoun, A. Jutand, *Adv. Synth. Catal.* **2007**, *349*, 292-296; e) E. Steckhan, Springer, Berlin, Heidelberg, **1987**, pp. 1-69; f) M. Le Blanc, *Z. Elektrochem. Angew. Phys. Chem.* **1900**, *7*, 287-290.

[91] a) C. Lefrou, P. Fabry, J.-C. Poignet, C. Amatore, *Electrochemistry: The basics, with examples*, Springer, Heidelberg, **2012**; b) C. Amatore, C. Cammoun, A. Jutand, *Eur. J. Org. Chem.* **2008**, *2008*, 4567-4570; c) A. J. L. Pombeiro, C. Amatore, *Trends in molecular electrochemistry*, Marcel Dekker, New York, **2004**.

[92] a) A. Jutand, *Chem. Rev.* **2008**, *108*, 2300-2347; b) C. Amatore, E. Carre, A. Jutand, A. M'Barki, G. Meyer, Springer Japan, Tokyo, **1998**, pp. 379-382.

[93] a) H. J. Schäfer, *C. R. Chim.* **2011**, *14*, 745-765; b) H. J. Schäfer, *Angew. Chem. Int. Ed. Engl.* **1981**, *20*, 911-934.

[94] a) R. D. Little, M. K. Schwaebe, in *Electrochemistry VI Electroorganic Synthesis: Bond Formation at Anode and Cathode* (Ed.: E. Steckhan), Springer, Berlin, Heidelberg, **1997**, pp. 1-48; b) C. Gregory Sowell, R. L. Wolin, R. Daniel Little, *Tetrahedron Lett.* **1990**, *31*, 485-488; c) R. D. Little, D. P. Fox, L. Van Hijfte, R. Dannecker, G. Sowell, R. L. Wolin, L. Moens, M. M. Baizer, *J. Org. Chem.* **1988**,

53, 2287-2294.

[95] a) J.-i. Yoshida, K. Kataoka, R. Horcajada, A. Nagaki, *Chem. Rev.* **2008**, *108*, 2265-2299; b) J.-i. Yoshida, S. Suga, S. Suzuki, N. Kinomura, A. Yamamoto, K. Fujiwara, *J. Am. Chem. Soc.* **1999**, *121*, 9546-9549.

[96] a) P. E. Iversen, H. Lund, *Tetrahedron Lett.* **1969**, *10*, 3523-3524; b) H. Lund, P. Lunde, *Acta Chem. Scand.* **1967**, *21*, 1067-1080.

[97] a) T. Gieshoff, A. Kehl, D. Schollmeyer, K. D. Moeller, S. R. Waldvogel, *J. Am. Chem. Soc.* **2017**, *139*, 12317-12324; b) H.-C. Xu, J. M. Campbell, K. D. Moeller, *J. Org. Chem.* **2014**, *79*, 379-391; c) K. D. Moeller, *Tetrahedron* **2000**, *56*, 9527-9554; d) *The list of names is not intended to be comprehensive and any omissions are unintended.*

[98] a) C. Tian, T. H. Meyer, M. Stangier, U. Dhawa, K. Rauch, L. H. Finger, L. Ackermann, *Nat. Protoc.* **2020**, *15*, 1760-1774; b) M. Yan, Y. Kawamata, P. S. Baran, *Angew. Chem. Int. Ed.* **2018**, *57*, 4149-4155.

[99] a) R. D. Little, *J. Org. Chem.* **2020**, *85*, 13375-13390; b) C. Kingston, M. D. Palkowitz, Y. Takahira, J. C. Vantourout, B. K. Peters, Y. Kawamata, P. S. Baran, *Acc. Chem. Res.* **2020**, *53*, 72-83; c) S. R. Waldvogel, S. Lips, M. Selt, B. Riehl, C. J. Kampf, *Chem. Rev.* **2018**, *118*, 6706-6765; d) M. Yan, Y. Kawamata, P. S. Baran, *Chem. Rev.* **2017**, *117*, 13230-13319; e) J. B. Sperry, D. L. Wright, *Chem. Soc. Rev.* **2006**, *35*, 605-621.

[100] a) C. Jia, T. Kitamura, Y. Fujiwara, *Acc. Chem. Res.* **2001**, *34*, 633-639; b) Y. Fujiwara, I. Moritani, S. Danno, R. Asano, S. Teranishi, *J. Am. Chem. Soc.* **1969**, *91*, 7166-7169; c) I. Moritanl, Y. Fujiwara, *Tetrahedron Lett.* **1967**, *8*, 1119-1122.

[101] a) J. E. Erchinger, M. van Gemmeren, *Asian J. Org. Chem.* **2021**, *10*, 50-60; b) H. Wu, Q. An, C. He, X. Fan, W. Guo, M. Zuo, C. Xu, R. Guo, W. Chu, Z. Sun, *Adv. Synth. Catal.* **2020**, *362*, 2459-2465; c) U. Dhawa, C. Tian, T. Wdowik, J. C. A. Oliveira, J. Hao, L. Ackermann, *Angew. Chem. Int. Ed.* **2020**, *59*, 13451-13457; d) Q.-L. Yang, X.-Y. Wang, T.-L. Wang, X. Yang, D. Liu, X. Tong, X.-Y. Wu, T.-S. Mei, *Org. Lett.* **2019**, *21*, 2645-2649; e) A. Shrestha, M. Lee, A. L. Dunn, M. S. Sanford, *Org. Lett.* **2018**, *20*, 204-207; f) K. Sano, N. Kimura, T. Kochi, F. Kakiuchi, *Asian J. Org. Chem.* **2018**, *7*, 1311-1314; g) Q.-L. Yang, Y.-Q. Li, C. Ma, P. Fang, X.-J. Zhang, T.-S. Mei, *J. Am. Chem. Soc.* **2017**, *139*, 3293-3298; h) Y.-Q. Li, Q.-L. Yang, P. Fang, T.-S. Mei, D. Zhang, *Org. Lett.* **2017**, *19*, 2905-2908; i) M. Konishi, K. Tsuchida, K. Sano, T. Kochi, F. Kakiuchi, *J. Org. Chem.* **2017**, *82*, 8716-8724; j) F. Saito, H. Aiso, T. Kochi, F. Kakiuchi, *Organometallics* **2014**, *33*, 6704-6707; k) H. Aiso, T. Kochi, H. Mutsutani, T. Tanabe, S. Nishiyama, F. Kakiuchi, *J. Org. Chem.* **2012**, *77*, 7718-7724; l) F. Kakiuchi, T. Kochi, H. Mutsutani, N. Kobayashi, S. Urano, M. Sato, S. Nishiyama, T. Tanabe, *J. Am. Chem. Soc.* **2009**, *131*, 11310-11311; m) D. Kalyani, A. R. Dick, W. Q. Anani, M. S. Sanford, *Org. Lett.* **2006**, *8*, 2523-2526.

[102] a) C. Zhu, N. W. J. Ang, T. H. Meyer, Y. Qiu, L. Ackermann, *ACS Cent. Sci.* **2021**, *7*, 415-431; b) A. Dey, T. B. Gunnoe, V. R. Stamenkovic, *ACS Catal.* **2020**, *10*, 13156-13158; c) R. Francke, R. D. Little, *ChemElectroChem* **2019**, *6*, 4373-4382.

[103] a) Y. Qiu, C. Zhu, M. Stangier, J. Struwe, L. Ackermann, *CCS Chem.* **2021**, *3*, 1529-1552; b) S.-K. Zhang, R. C. Samanta, A. Del Vecchio, L. Ackermann, *Chem. Eur. J.* **2020**, *26*, 10936-10947; c) L. Ackermann, *Acc. Chem. Res.* **2020**, *53*, 84-104; d) Y. Qiu, J. Struwe, L. Ackermann, *Synlett* **2019**, *30*, 1164-1173; e) N. Sauermann, T. H. Meyer, Y. Qiu, L. Ackermann, *ACS Catal.* **2018**, *8*, 7086-7103; f) N. Sauermann, T. H. Meyer, L. Ackermann, *Chem. Eur. J.* **2018**, *24*, 16209-16217.

[104] a) P. Wang, X. Gao, P. Huang, A. Lei, *ChemCatChem* **2020**, *12*, 27-40; b) Y. Yuan, A. Lei, *Acc. Chem. Res.* **2019**, *52*, 3309-3324; c) H. Wang, X. Gao, Z. Lv, T. Abdelilah, A. Lei, *Chem. Rev.* **2019**, *119*, 6769-6787; d) S. Tang, L. Zeng, A. Lei, *J. Am. Chem. Soc.* **2018**, *140*, 13128-13135.

[105] a) Z.-J. Wu, F. Su, W. Lin, J. Song, T.-B. Wen, H.-J. Zhang, H.-C. Xu, *Angew. Chem. Int. Ed.* **2019**, *58*, 16770-16774; b) F. Xu, Y.-J. Li, C. Huang, H.-C. Xu, *ACS Catal.* **2018**, *8*, 3820-3824.

[106] a) K.-J. Jiao, Y.-K. Xing, Q.-L. Yang, H. Qiu, T.-S. Mei, *Acc. Chem. Res.* **2020**, *53*, 300-310; b) Q.-L. Yang, P. Fang, T.-S. Mei, *Chin. J. Chem.* **2018**, *36*, 338-352; c) C. Ma, P. Fang, T.-S. Mei, *ACS Catal.* **2018**, *8*, 7179-7189; d) K.-J. Jiao, C.-Q. Zhao, P. Fang, T.-S. Mei, *Tetrahedron Lett.* **2017**, *58*, 797-802.

[107] a) Y. H. Budnikova, *Chem. Rec.* **2021**, *21*, DOI: 10.1002/tcr.202100009; b) X. Ye, C. Wang, S. Zhang, J. Wei, C. Shan, L. Wojtas, Y. Xie, X. Shi, *ACS Catal.* **2020**, *10*, 11693-11699; c) Z.-Q. Wang, C. Hou, Y.-F. Zhong, Y.-X. Lu, Z.-Y. Mo, Y.-M. Pan, H.-T. Tang, *Org. Lett.* **2019**, *21*, 9841-9845; d) M.-J. Luo, T.-T. Zhang, F.-J. Cai, J.-H. Li, D.-L. He, *Chem. Commun.* **2019**, *55*, 7251-7254; e) M.-J. Luo, M. Hu, R.-J. Song, D.-L. He, J.-H. Li, *Chem. Commun.* **2019**, *55*, 1124-1127; f) S. Kathiravan, S. Suriyanarayanan, I. A. Nicholls, *Org. Lett.* **2019**, *21*, 1968-1972.

[108] a) R. Mei, X. Fang, L. He, J. Sun, L. Zou, W. Ma, L. Ackermann, *Chem. Commun.* **2020**, *56*, 1393-1396; b) U. Dhawa, C. Tian, W. Li, L. Ackermann, *ACS Catal.* **2020**, *10*, 6457-6462; c) S. C. Sau, R. Mei, J. Struwe, L. Ackermann, *ChemSusChem* **2019**, *12*, 3023-3027; d) R. Mei, W. Ma, Y. Zhang, X. Guo, L. Ackermann, *Org. Lett.* **2019**, *21*, 6534-6538; e) L. Zeng, H. Li, S. Tang, X. Gao, Y. Deng, G. Zhang, C.-W. Pao, J.-L. Chen, J.-F. Lee, A. Lei, *ACS Catal.* **2018**, *8*, 5448-5453; f) C. Tian, L. Massignan, T. H. Meyer, L. Ackermann, *Angew. Chem. Int. Ed.* **2018**, *57*, 2383-2387; g) S. Tang, D. Wang, Y. Liu, L. Zeng, A. Lei, *Nat. Commun.* **2018**, *9*, 798; h) R. Mei, N. Sauermann, J. C. A. Oliveira, L. Ackermann, *J. Am. Chem. Soc.* **2018**, *140*, 7913-7921.

[109] a) C. Tian, U. Dhawa, J. Struwe, L. Ackermann, *Chin. J. Chem.* **2019**, *37*, 552-556; b) N. Sauermann, R. Mei, L. Ackermann, *Angew. Chem. Int. Ed.* **2018**, *57*, 5090-5094; c) X. Gao, P. Wang, L. Zeng, S. Tang, A. Lei, *J. Am. Chem. Soc.* **2018**, *140*, 4195-4199.

[110] a) T. Moragas, A. Correa, R. Martin, *Chem. Eur. J.* **2014**, *20*, 8242-8258; b) C. E. I. Knappke, S. Grupe, D. Gärtner, M. Corpet, C. Gosmini, A. Jacobi von Wangelin, *Chem. Eur. J.* **2014**, *20*, 6828-6842; c) D. A. Everson, D. J. Weix, *J. Org. Chem.* **2014**, *79*, 4793-4798.

[111] *Handbook of Functionalized Organometallics: Applications in Synthesis*, Wiley-VCH, Weinheim, **2005**.

[112] D. F. Shriver, M. A. Drezdzon, *The manipulation of air-sensitive compounds*, Wiley, New York, **1986**.

[113] A. Wurtz, *Liebigs Ann. Chem.* **1855**, *96*, 364-375.

[114] a) H. Gilman, G. F. Wright, *J. Am. Chem. Soc.* **1933**, *55*, 2893-2896; b) W. E. Bachmann, H. T. Clarke, *J. Am. Chem. Soc.* **1927**, *49*, 2089-2098; c) B. Tollens, R. Fittig, *Liebigs Ann. Chem.* **1864**, *131*, 303-323.

[115] a) A. Klein, Y. H. Budnikova, O. G. Sinyashin, *J. Organomet. Chem.* **2007**, *692*, 3156-3166; b) M. Durandetti, J.-Y. Nédélec, J. Périchon, *J. Org. Chem.* **1996**, *61*, 1748-1755; c) C. Amatore, A. Jutand, *Organometallics* **1988**, *7*, 2203-2214; d) G. Schiavon, G. Bontempelli, B. Corain, *J. Chem. Soc., Dalton Trans.* **1981**, 1074-1081.

[116] a) M. Amatore, C. Gosmini, *Angew. Chem. Int. Ed.* **2008**, *47*, 2089-2092; b) P. Gomes, H. Fillon, C. Gosmini, E. Labbé, J. Périchon, *Tetrahedron* **2002**, *58*, 8417-8424.

[117] E. M. Aresta, *Carbon Dioxide as Chemical Feedstock*, John Wiley & Sons, **2010**.

[118] Z. Liu, *Appl. Energy* **2016**, *166*, 239-244.

[119] a) S. Buratti, S. Benedetti, in *Electronic Noses and Tongues in Food Science* (Ed.: M. L. Rodríguez Méndez), Academic Press, San Diego, **2016**, pp. 291-299; b) M. Ciani, F. Comitini, I. Mannazzu, in *Encyclopedia of Ecology* (Eds.: S. E. Jørgensen, B. D. Fath), Academic Press, Oxford, **2008**, pp. 1548-1557; c) H. S. Kheshgi, R. C. Prince, *Energy* **2005**, *30*, 1865-1871.

[120] T. A. Jacobson, J. S. Kler, M. T. Hernke, R. K. Braun, K. C. Meyer, W. E. Funk, *Nat. Sustain.* **2019**, *2*, 691-701.

[121] a) P. K. Sahoo, Y. Zhang, S. Das, *ACS Catal.* **2021**, *11*, 3414-3442; b) H.-C. Fu, F. You, H.-R. Li, L.-N. He, *Front. Chem.* **2019**, *7*, 525; c) W. Schilling, S. Das, *Tetrahedron Lett.* **2018**, *59*, 3821-3828; d) S. Das, F. D. Bobbink, A. Gopakumar, P. J. Dyson, *CHIMIA* **2015**, *69*, 765-768.

[122] a) L. Zhang, Z. Hou, *Chem. Sci.* **2013**, *4*, 3395-3403; b) Y. Tsuji, T. Fujihara, *Chem. Commun.* **2012**, *48*, 9956-9964; c) M. Cokoja, C. Bruckmeier, B. Rieger, W. A. Herrmann, F. E. Kühn, *Angew. Chem. Int. Ed.* **2011**, *50*, 8510-8537; d) L. Ackermann, *Angew. Chem. Int. Ed.* **2011**, *50*, 3842-3844; e) T. Sakakura, J.-C. Choi, H. Yasuda, *Chem. Rev.* **2007**, *107*, 2365-2387.

[123] a) C. Maeda, Y. Miyazaki, T. Ema, *Catal. Sci. Technol.* **2014**, *4*, 1482-1497; b) M. Mikkelsen, M. Jørgensen, F. C. Krebs, *Energy Environ. Sci.* **2010**, *3*, 43-81.

[124] a) D. Riemer, W. Schilling, A. Goetz, Y. Zhang, S. Gehrke, I. Tkach, O. Hollóczki, S. Das, *ACS Catal.* **2018**, *8*, 11679-11687; b) D. Riemer, B. Mandaviya, W. Schilling, A. C. Götz, T. Kühl, M. Finger, S. Das, *ACS Catal.* **2018**, *8*, 3030-3034; c) P. Hirapara, D. Riemer, N. Hazra, J. Gajera, M. Finger, S. Das, *Green Chem.* **2017**, *19*, 5356-5360.

[125] a) S.-S. Yan, Q. Fu, L.-L. Liao, G.-Q. Sun, J.-H. Ye, L. Gong, Y.-Z. Bo-Xue, D.-G. Yu, *Coord. Chem. Rev.* **2018**, *374*, 439-463; b) Q. Liu, L. Wu, R. Jackstell, M. Beller, *Nat. Commun.* **2015**, *6*, 5933; c) J. Wu, X. Yang, Z. He, X. Mao, T. A.

Hatton, T. F. Jamison, *Angew. Chem. Int. Ed.* **2014**, *53*, 8416-8420; d) S. Li, B. Miao, W. Yuan, S. Ma, *Org. Lett.* **2013**, *15*, 977-979; e) H. Ochiai, M. Jang, K. Hirano, H. Yorimitsu, K. Oshima, *Org. Lett.* **2008**, *10*, 2681-2683.

[126] a) N. Hazari, N. Iwasawa, K. H. Hopmann, *Organometallics* **2020**, *39*, 1457-1460; b) *Advances in Organometallic Chemistry, Vol. 71*, Elsevier Academic Press, **2019**; c) W.-Y. Wong, *Organometallics and related molecules for energy conversion*, Springer-Verlag, Berlin, Heidelberg, **2015**.

[127] a) K. Huang, C.-L. Sun, Z.-J. Shi, *Chem. Soc. Rev.* **2011**, *40*, 2435-2452; b) A. Behr, *Angew. Chem. Int. Ed.* **1988**, *27*, 661-678.

[128] a) D. H. Gibson, *Chem. Rev.* **1996**, *96*, 2063-2096; b) D. A. Palmer, R. Van Eldik, *Chem. Rev.* **1983**, *83*, 651-731.

[129] G. W. Coates, D. R. Moore, *Angew. Chem. Int. Ed.* **2004**, *43*, 6618-6639.

[130] a) T. K. Pal, D. De, P. K. Bharadwaj, *Coord. Chem. Rev.* **2020**, *408*, 213173; b) R. Azzouz, V. Contreras Moreno, C. Herasme-Grullon, V. Levacher, L. Estel, A. Ledoux, S. Derrouiche, F. Marsais, L. Bischoff, *Synlett* **2020**, *31*, 183-188; c) T. Sakakura, K. Kohno, *Chem. Commun.* **2009**, 1312-1330.

[131] J. H. Clements, *Ind. Eng. Chem. Res.* **2003**, *42*, 663-674.

[132] a) T.-d. Hu, Y.-h. Ding, *Organometallics* **2020**, *39*, 505-515; b) U. R. Seo, Y. K. Chung, *Green Chem.* **2017**, *19*, 803-808; c) R. L. Paddock, D. Adhikari, R. L. Lord, M.-H. Baik, S. T. Nguyen, *Chem. Commun.* **2014**, *50*, 15187-15190; d) T. Y. Ma, S. Z. Qiao, *ACS Catal.* **2014**, *4*, 3847-3855; e) Z.-Z. Yang, L.-N. He, J. Gao, A.-H. Liu, B. Yu, *Energy Environ. Sci.* **2012**, *5*, 6602-6639; f) J. Seayad, A. M. Seayad, J. K. P. Ng, C. L. L. Chai, *ChemCatChem* **2012**, *4*, 774-777; g) Z.-Z. Yang, Y.-N. Li, Y.-Y. Wei, L.-N. He, *Green Chem.* **2011**, *13*, 2351-2353; h) F. Fontana, C. C. Chen, V. K. Aggarwal, *Org. Lett.* **2011**, *13*, 3454-3457; i) Z.-Z. Yang, L.-N. He, S.-Y. Peng, A.-H. Liu, *Green Chem.* **2010**, *12*, 1850-1854; j) C. Qi, J. Ye, W. Zeng, H. Jiang, *Adv. Synth. Catal.* **2010**, *352*, 1925-1933; k) H.-F. Jiang, J.-W. Ye, C.-R. Qi, L.-B. Huang, *Tetrahedron Lett.* **2010**, *51*, 928-932; l) Y. Du, Y. Wu, A.-H. Liu, L.-N. He, *J. Org. Chem.* **2008**, *73*, 4709-4712; m) A. Sudo, Y. Morioka, F. Sanda, T. Endo, *Tetrahedron Lett.* **2004**, *45*, 1363-1365; n) A. W. Miller, S. T. Nguyen, *Org. Lett.* **2004**, *6*, 2301-2304; o) A. Sudo, Y. Morioka, E. Koizumi, F. Sanda, T. Endo, *Tetrahedron Lett.* **2003**, *44*, 7889-7891; p) P. Tascedda, E. Duñach, *Chem. Commun.* **2000**, 449-450.

[133] a) M. Hulla, F. D. Bobbink, S. Das, P. J. Dyson, *ChemCatChem* **2016**, *8*, 3338-3342; b) S. Das, F. D. Bobbink, S. Bulut, M. Soudani, P. J. Dyson, *Chem. Commun.* **2016**, *52*, 2497-2500; c) S. Das, F. D. Bobbink, G. Laurenczy, P. J. Dyson, *Angew. Chem. Int. Ed.* **2014**, *53*, 12876-12879.

[134] a) Q. Zou, G. Long, T. Zhao, X. Hu, *Green Chem.* **2020**, *22*, 1134-1138; b) M. Hulla, G. Laurenczy, P. J. Dyson, *ACS Catal.* **2018**, *8*, 10619-10630; c) F. D. Bobbink, S. Das, P. J. Dyson, *Nat. Protoc.* **2017**, *12*, 417-428; d) C. Fang, C. Lu, M. Liu, Y. Zhu, Y. Fu, B.-L. Lin, *ACS Catal.* **2016**, *6*, 7876-7881; e) A. Tlili, E. Blondiaux, X. Frogneux, T. Cantat, *Green Chem.* **2015**, *17*, 157-168.

[135] C.-H. Lim, A. M. Holder, J. T. Hynes, C. B. Musgrave, *Inorg. Chem.* **2013**, *52*, 10062-10066.

[136] a) W. Schilling, S. Das, *ChemSusChem* **2020**, *13*, 6246-6258; b) D. Riemer, P. Hirapara, S. Das, *ChemSusChem* **2016**, *9*, 1916-1920; c) A. Tlili, X. Frogneux, E. Blondiaux, T. Cantat, *Angew. Chem. Int. Ed.* **2014**, *53*, 2543-2545; d) C. Das Neves Gomes, O. Jacquet, C. Villiers, P. Thuéry, M. Ephritikhine, T. Cantat, *Angew. Chem. Int. Ed.* **2012**, *51*, 187-190.

[137] Y. Zhang, T. Zhang, S. Das, *Green Chem.* **2020**, *22*, 1800-1820.

[138] a) P. Ju, J. Chen, A. Chen, L. Chen, Y. Yu, *ACS Sustain. Chem. Eng.* **2017**, *5*, 2516-2528; b) X.-L. Du, G. Tang, H.-L. Bao, Z. Jiang, X.-H. Zhong, D. S. Su, J.-Q. Wang, *ChemSusChem* **2015**, *8*, 3489-3496; c) X. Cui, Y. Zhang, Y. Deng, F. Shi, *Chem. Commun.* **2014**, *50*, 13521-13524; d) Y. Li, I. Sorribes, T. Yan, K. Junge, M. Beller, *Angew. Chem. Int. Ed.* **2013**, *52*, 12156-12160.

[139] M. Aresta, C. F. Nobile, V. G. Albano, E. Forni, M. Manassero, *J. Chem. Soc., Chem. Commun.* **1975**, 636-637.

[140] a) J. A. Garduño, A. Arévalo, J. J. García, *Dalton Trans.* **2015**, *44*, 13419-13438; b) J. Wu, J. C. Green, N. Hazari, D. P. Hruszkewycz, C. D. Incarvito, T. J. Schmeier, *Organometallics* **2010**, *29*, 6369-6376; c) C. S. Yeung, V. M. Dong, *J. Am. Chem. Soc.* **2008**, *130*, 7826-7827; d) M. Takimoto, Y. Nakamura, K. Kimura, M. Mori, *J. Am. Chem. Soc.* **2004**, *126*, 5956-5957; e) M. Takimoto, M. Mori, *J. Am. Chem. Soc.* **2002**, *124*, 10008-10009; f) J. Louie, J. E. Gibby, M. V. Farnworth, T. N. Tekavec, *J. Am. Chem. Soc.* **2002**, *124*, 15188-15189; g) M. Takimoto, M. Mori, *J. Am. Chem. Soc.* **2001**, *123*, 2895-2896; h) H. Hoberg, Y. Peres, C. Krüger, Y.-H. Tsay, *Angew. Chem. Int. Ed. Engl.* **1987**, *26*, 771-773; i) G. Burkhart, H. Hoberg, *Angew. Chem. Int. Ed. Engl.* **1982**, *21*, 76-76.

[141] A. Behr, K.-D. Juszak, *J. Organomet. Chem.* **1983**, *255*, 263-268.

[142] a) F. G. Delolo, J. Yang, H. Neumann, E. N. dos Santos, E. V. Gusevskaya, M. Beller, *ACS Sustain. Chem. Eng.* **2021**, *9*, 5148-5154; b) S. Wang, J. Zhang, F. Peng, Z. Tang, Y. Sun, *Ind. Eng. Chem. Res.* **2020**, *59*, 88-98; c) J. Amsler, B. B. Sarma, G. Agostini, G. Prieto, P. N. Plessow, F. Studt, *J. Am. Chem. Soc.* **2020**, *142*, 5087-5096; d) J.-B. Peng, F.-P. Wu, X.-F. Wu, *Chem. Rev.* **2019**, *119*, 2090-2127; e) R. G. Grim, A. T. To, C. A. Farberow, J. E. Hensley, D. A. Ruddy, J. A. Schaidle, *ACS Catal.* **2019**, *9*, 4145-4172; f) J. Liu, Z. Wei, H. Jiao, R. Jackstell, M. Beller, *ACS Cent. Sci.* **2018**, *4*, 30-38; g) R. Franke, D. Selent, A. Börner, *Chem. Rev.* **2012**, *112*, 5675-5732.

[143] G. R. Eastham, M. Waugh, P. Pringle, T. P. W. Turner, in *WO2011083305*, **2011**.

[144] K.-i. Tominaga, Y. Sasaki, *Catal. Commun.* **2000**, *1*, 1-3.

[145] a) L. Feng, X. Li, B. Liu, E. Vessally, *J. CO2 Util.* **2020**, *40*, 101220; b) Y.-X. Luan, M. Ye, *Tetrahedron Lett.* **2018**, *59*, 853-861; c) X. Ren, Z. Zheng, L. Zhang, Z. Wang, C. Xia, K. Ding, *Angew. Chem. Int. Ed.* **2017**, *56*, 310-313; d) Q. Liu, L. Wu, I. Fleischer, D. Selent, R. Franke, R. Jackstell, M. Beller, *Chem. Eur. J.* **2014**, *20*, 6888-6894; e) T. G. Ostapowicz, M. Schmitz, M. Krystof, J. Klankermayer, W. Leitner, *Angew. Chem. Int. Ed.* **2013**, *52*, 12119-12123; f) Y. Zhang, S. N. Riduan, *Angew. Chem. Int. Ed.* **2011**, *50*, 6210-6212; g) S.-i. Fujita, S. Okamura, Y. Akiyama, M. Arai, *Int. J. Mol. Sci.* **2007**, *8*, 749-759.

[146] a) H. Shen, T. Peppel, J. Strunk, Z. Sun, *Sol. RRL* **2020**, *4*, 1900546; b) Ž.

Kovačič, B. Likozar, M. Huš, *ACS Catal.* **2020**, *10*, 14984-15007; c) T. Kong, Y. Jiang, Y. Xiong, *Chem. Soc. Rev.* **2020**, *49*, 6579-6591; d) J. Albero, Y. Peng, H. García, *ACS Catal.* **2020**, *10*, 5734-5749; e) J. L. White, M. F. Baruch, J. E. Pander, Y. Hu, I. C. Fortmeyer, J. E. Park, T. Zhang, K. Liao, J. Gu, Y. Yan, T. W. Shaw, E. Abelev, A. B. Bocarsly, *Chem. Rev.* **2015**, *115*, 12888-12935; f) C. S. Jeffrey, in *Developments and Innovation in Carbon Dioxide (CO2) Capture and Storage Technology, Vol. 2* (Ed.: M. M. Maroto-Valer), Woodhead Publishing, **2010**, pp. 463-501.

[147] R. Cauwenbergh, S. Das, *Green Chem.* **2021**, *23*, 2553-2574.

[148] R. Reithmeier, C. Bruckmeier, B. Rieger, *Catalysts* **2012**, *2*, 544-571.

[149] a) J. Hawecker, J.-M. Lehn, R. Ziessel, *J. Chem. Soc., Chem. Commun.* **1983**, 536-538; b) J.-M. Lehn, R. Ziessel, *Proc. Natl. Acad. Sci.* **1982**, *79*, 701-704.

[150] a) H. Takeda, K. Koike, H. Inoue, O. Ishitani, *J. Am. Chem. Soc.* **2008**, *130*, 2023-2031; b) Z.-Y. Bian, K. Sumi, M. Furue, S. Sato, K. Koike, O. Ishitani, *Inorg. Chem.* **2008**, *47*, 10801-10803; c) B. Gholamkhass, H. Mametsuka, K. Koike, T. Tanabe, M. Furue, O. Ishitani, *Inorg. Chem.* **2005**, *44*, 2326-2336; d) Y. Hayashi, S. Kita, B. S. Brunschwig, E. Fujita, *J. Am. Chem. Soc.* **2003**, *125*, 11976-11987; e) J. Hawecker, J.-M. Lehn, R. Ziessel, *Helv. Chim. Acta* **1986**, *69*, 1990-2012.

[151] S. Sato, T. Morikawa, T. Kajino, O. Ishitani, *Angew. Chem. Int. Ed.* **2013**, *52*, 988-992.

[152] a) I. Bonneau-Gubelmann, M. Michel, B. Besson, S. Ratton, J.-R. Desmurs, in *The Roots of Organic Development, Vol. 8* (Eds.: J.-R. Desmurs, S. Ratton), Elsevier, **1996**, pp. 116-128; b) A. S. Lindsey, H. Jeskey, *Chem. Rev.* **1957**, *57*, 583-620; c) R. Schmitt, *J. Prakt. Chem.* **1885**, *31*, 397-411; d) H. Kolbe, *Liebigs Ann. Chem.* **1860**, *113*, 125-127.

[153] J. Choi, G. C. Fu, *Science* **2017**, *356*, eaaf7230.

[154] a) A. Tortajada, F. Juliá-Hernández, M. Börjesson, T. Moragas, R. Martin, *Angew. Chem. Int. Ed.* **2018**, *57*, 15948-15982; b) Y.-G. Chen, X.-T. Xu, K. Zhang, Y.-Q. Li, L.-P. Zhang, P. Fang, T.-S. Mei, *Synthesis* **2018**, *50*, 35-48; c) D. M. Dalton, T. Rovis, *Nat. Chem.* **2010**, *2*, 710-711; d) A. Correa, R. Martín, *Angew. Chem. Int. Ed.* **2009**, *48*, 6201-6204.

[155] K. Ukai, M. Aoki, J. Takaya, N. Iwasawa, *J. Am. Chem. Soc.* **2006**, *128*, 8706-8707.

[156] a) D. J. Darensbourg, G. Groetsch, P. Wiegreffe, A. L. Rheingold, *Inorg. Chem.* **1987**, *26*, 3827-3830; b) P. Albano, M. Aresta, M. Manassero, *Inorg. Chem.* **1980**, *19*, 1069-1072; c) I. S. Kolomnikov, A. O. Gusev, T. S. Belopotapova, M. K. Grigoryan, T. V. Lysyak, Y. T. Struchkov, M. E. Vol'pin, *J. Organomet. Chem.* **1974**, *69*, C10-C12.

[157] a) M. F. Obst, A. Gevorgyan, A. Bayer, K. H. Hopmann, *Organometallics* **2020**, *39*, 1545-1552; b) H. Ohmiya, M. Tanabe, M. Sawamura, *Org. Lett.* **2011**, *13*, 1086-1088; c) T. Ohishi, L. Zhang, M. Nishiura, Z. Hou, *Angew. Chem. Int. Ed.* **2011**, *50*, 8114-8117; d) J. Takaya, S. Tadami, K. Ukai, N. Iwasawa, *Org. Lett.* **2008**, *10*, 2697-2700; e) T. Ohishi, M. Nishiura, Z. Hou, *Angew. Chem. Int. Ed.*

2008, *47*, 5792-5795.

[158] X. Zhang, W.-Z. Zhang, L.-L. Shi, C.-X. Guo, L.-L. Zhang, X.-B. Lu, *Chem. Commun.* **2012**, *48*, 6292-6294.

[159] a) X. Zhang, W.-Z. Zhang, X. Ren, L.-L. Zhang, X.-B. Lu, *Org. Lett.* **2011**, *13*, 2402-2405; b) Y. Dingyi, Z. Yugen, *Green Chem.* **2011**, *13*, 1275-1279; c) D. Yu, Y. Zhang, *Proc. Natl. Acad. Sci.* **2010**, *107*, 20184-20189; d) L. J. Gooßen, N. Rodríguez, F. Manjolinho, P. P. Lange, *Adv. Synth. Catal.* **2010**, *352*, 2913-2917.

[160] a) T. M. Porter, M. W. Kanan, *Chem. Sci.* **2020**, *11*, 11936-11944; b) J. Luo, I. Larrosa, *ChemSusChem* **2017**, *10*, 3317-3332; c) S. Fenner, L. Ackermann, *Green Chem.* **2016**, *18*, 3804-3807; d) L. Zhang, J. Cheng, T. Ohishi, Z. Hou, *Angew. Chem. Int. Ed.* **2010**, *49*, 8670-8673; e) O. Vechorkin, N. Hirt, X. Hu, *Org. Lett.* **2010**, *12*, 3567-3569; f) I. I. F. Boogaerts, S. P. Nolan, *J. Am. Chem. Soc.* **2010**, *132*, 8858-8859; g) I. I. F. Boogaerts, G. C. Fortman, M. R. L. Furst, C. S. J. Cazin, S. P. Nolan, *Angew. Chem. Int. Ed.* **2010**, *49*, 8674-8677.

[161] a) T. Saitou, Y. Jin, K. Isobe, T. Suga, J. Takaya, N. Iwasawa, *Chem. Asian J.* **2020**, *15*, 1941-1944; b) K. Sasano, J. Takaya, N. Iwasawa, *J. Am. Chem. Soc.* **2013**, *135*, 10954-10957; c) H. Mizuno, J. Takaya, N. Iwasawa, *J. Am. Chem. Soc.* **2011**, *133*, 1251-1253.

[162] M. Börjesson, T. Moragas, D. Gallego, R. Martin, *ACS Catal.* **2016**, *6*, 6739-6749.

[163] A. Correa, R. Martín, *J. Am. Chem. Soc.* **2009**, *131*, 15974-15975.

[164] T. Fujihara, K. Nogi, T. Xu, J. Terao, Y. Tsuji, *J. Am. Chem. Soc.* **2012**, *134*, 9106-9109.

[165] T. León, A. Correa, R. Martin, *J. Am. Chem. Soc.* **2013**, *135*, 1221-1224.

[166] a) G. Wu, J.-R. Wu, Y. Huang, Y.-W. Yang, *Chem. Asian J.* **2021**, *16*, 1864-1877; b) L. Mohammadkhani, M. M. Heravi, *Chem. Rec.* **2021**, *21*, 29-68.

[167] T. Mita, Y. Higuchi, Y. Sato, *Chem. Eur. J.* **2015**, *21*, 16391-16394.

[168] M. van Gemmeren, M. Börjesson, A. Tortajada, S.-Z. Sun, K. Okura, R. Martin, *Angew. Chem. Int. Ed.* **2017**, *56*, 6558-6562.

[169] Y.-G. Chen, B. Shuai, C. Ma, X.-J. Zhang, P. Fang, T.-S. Mei, *Org. Lett.* **2017**, *19*, 2969-2972.

[170] K. Osakada, R. Sato, T. Yamamoto, *Organometallics* **1994**, *13*, 4645-4647.

[171] a) F. Juliá-Hernández, T. Moragas, J. Cornella, R. Martin, *Nature* **2017**, *545*, 84-88; b) T. Moragas, R. Martin, *Synthesis* **2016**, *48*, 2816-2822; c) T. Moragas, M. Gaydou, R. Martin, *Angew. Chem. Int. Ed.* **2016**, *55*, 5053-5057; d) M. Börjesson, T. Moragas, R. Martin, *J. Am. Chem. Soc.* **2016**, *138*, 7504-7507; e) X. Wang, Y. Liu, R. Martin, *J. Am. Chem. Soc.* **2015**, *137*, 6476-6479; f) T. Moragas, J. Cornella, R. Martin, *J. Am. Chem. Soc.* **2014**, *136*, 17702-17705; g) Y. Liu, J. Cornella, R. Martin, *J. Am. Chem. Soc.* **2014**, *136*, 11212-11215; h) A. Correa, T. León, R. Martin, *J. Am. Chem. Soc.* **2014**, *136*, 1062-1069.

[172] a) T. Fujihara, Y. Tsuji, *Front. Chem.* **2019**, *7*; b) K. Nogi, T. Fujihara, J. Terao, Y. Tsuji, *J. Org. Chem.* **2015**, *80*, 11618-11623; c) K. Nogi, T. Fujihara, J. Terao, Y. Tsuji, *Chem. Commun.* **2014**, *50*, 13052-13055.

[173] H. Tran-Vu, O. Daugulis, *ACS Catal.* **2013**, *3*, 2417-2420.
[174] S. Zhang, W.-Q. Chen, A. Yu, L.-N. He, *ChemCatChem* **2015**, *7*, 3972-3977.
[175] K. Michigami, T. Mita, Y. Sato, *J. Am. Chem. Soc.* **2017**, *139*, 6094-6097.
[176] E. Lamy, L. Nadjo, J. M. Saveant, *J. Electroanal. Chem. Interf. Electrochem.* **1977**, *78*, 403-407.
[177] a) W. H. Koppenol, J. D. Rush, *J. Phys. Chem.* **1987**, *91*, 4429-4430; b) J. Lilie, G. Beck, A. Henglein, *Ber. Bunsenges. Phys. Chem.* **1971**, *75*, 458-465.
[178] C. Amatore, A. Jutand, F. Khalil, M. F. Nielsen, *J. Am. Chem. Soc.* **1992**, *114*, 7076-7085.
[179] J. F. Fauvarque, C. Chevrot, A. Jutand, M. François, J. Perichon, *J. Organomet. Chem.* **1984**, *264*, 273-281.
[180] C. Amatore, A. Jutand, *J. Am. Chem. Soc.* **1991**, *113*, 2819-2825.
[181] S. Torii, H. Tanaka, T. Hamatani, K. Morisaki, A. Jutand, F. Peluger, J.-F. Fauvarque, *Chem. Lett.* **1986**, *15*, 169-172.
[182] a) O. Sock, M. Troupel, J. Perichon, *Tetrahedron Lett.* **1985**, *26*, 1509-1512; b) F. Barba, A. Guirado, A. Zapata, *Electrochim. Acta* **1982**, *27*, 1335-1337.
[183] A. Jutand, S. Négri, *Synlett* **1997**, *1997*, 719-721.
[184] Y. Sasaki, Y. Inoue, H. Hashimoto, *J. Chem. Soc., Chem. Commun.* **1976**, 605-606.
[185] C. Floriani, G. Fachinetti, *J. Chem. Soc., Chem. Commun.* **1974**, 615-616.
[186] J.-C. Folest, J.-M. Duprilot, J. Perichon, Y. Robin, J. Devynck, *Tetrahedron Lett.* **1985**, *26*, 2633-2636.
[187] K.-J. Jiao, Z.-M. Li, X.-T. Xu, L.-P. Zhang, Y.-Q. Li, K. Zhang, T.-S. Mei, *Org. Chem. Front.* **2018**, *5*, 2244-2248.
[188] a) M. D. McReynolds, J. M. Dougherty, P. R. Hanson, *Chem. Rev.* **2004**, *104*, 2239-2258; b) N. V. Zyk, E. K. Beloglazkina, M. A. Belova, N. y. S. Dubinina, *Russ. Chem. Rev.* **2003**, *72*, 769-786; c) A. Y. Sizov, A. N. Kovregin, A. F. Ermolov, *Russ. Chem. Rev.* **2003**, *72*, 357-374; d) F. Bernardi, I. G. Csizmadia, A. Mangini, *Organic sulfur chemistry : theoretical and experimental advances*, Elsevier Science Publishers, Amsterdam; New York, **1985**.
[189] a) N. Kardos, A. L. Demain, *Appl. Microbiol. Biotechnol.* **2011**, *92*, 677-687; b) A. Fleming, *Br. J. Exp. Pathol.* **1979**, *60*, 3-13; c) L. P. Garrod, *Br. Med. J.* **1960**, *2*, 1695-1696; d) L. P. Garrod, *Br. Med. J.* **1960**, *1*, 527-529; e) F. A. Robinson, *Analyst* **1947**, *72*, 274-276; f) A. Fleming, *Lancet* **1943**, *242*, 434-438.
[190] S. C. Piscitelli, T. F. Goss, J. H. Wilton, D. T. D'Andrea, H. Goldstein, J. J. Schentag, *Antimicrob. Agents Chemother.* **1991**, *35*, 1765-1771.
[191] a) S. L. Anderson, J. P. Vande Griend, *Am. J. Health-Syst. Pharm.* **2014**, *71*, 394-402; b) G. I. Spielmans, M. I. Berman, E. Linardatos, N. Z. Rosenlicht, A. Perry, A. C. Tsai, *PLoS Med.* **2013**, *10*, e1001403; c) P. M. Becker, *Curr. Treat. Options Neurol.* **2006**, *8*, 367-375; d) V. Dev, J. Raniwalla, *Drug Saf.* **2000**, *23*, 295-307.
[192] M. E. Thase, W. Macfadden, R. H. Weisler, W. Chang, B. Paulsson, A. Khan, J. R. Calabrese, f. t. B. I. S. Group, *J. Clin. Psychopharmacol.* **2006**, *26*, 600-609.

[193] a) H. Yamazaki, O. Takahashi, R. Kirikoshi, A. Yagi, T. Ogasawara, Y. Bunya, H. Rotinsulu, R. Uchida, M. Namikoshi, *J. Antibiot.* **2020**, *73*, 559-567; b) N. Boyer, K. C. Morrison, J. Kim, P. J. Hergenrother, M. Movassaghi, *Chem. Sci.* **2013**, *4*, 1646-1657; c) J.-M. Wang, G.-Z. Ding, L. Fang, J.-G. Dai, S.-S. Yu, Y.-H. Wang, X.-G. Chen, S.-G. Ma, J. Qu, S. Xu, D. Du, *J. Nat. Prod.* **2010**, *73*, 1240-1249; d) H. Guo, B. Sun, H. Gao, X. Chen, S. Liu, X. Yao, X. Liu, Y. Che, *J. Nat. Prod.* **2009**, *72*, 2115-2119.

[194] a) S. W. Kaldor, V. J. Kalish, J. F. Davies, B. V. Shetty, J. E. Fritz, K. Appelt, J. A. Burgess, K. M. Campanale, N. Y. Chirgadze, D. K. Clawson, B. A. Dressman, S. D. Hatch, D. A. Khalil, M. B. Kosa, P. P. Lubbehusen, M. A. Muesing, A. K. Patick, S. H. Reich, K. S. Su, J. H. Tatlock, *J. Med. Chem.* **1997**, *40*, 3979-3985; b) G. I. Birnbaum, S. R. Hall, *J. Am. Chem. Soc.* **1976**, *98*, 1926-1931.

[195] H. Gilman, N. J. Beaber, *J. Am. Chem. Soc.* **1925**, *47*, 1449-1451.

[196] a) W. Ma, N. Kaplaneris, X. Fang, L. Gu, R. Mei, L. Ackermann, *Org. Chem. Front.* **2020**, *7*, 1022-1060; b) C. Shen, P. Zhang, Q. Sun, S. Bai, T. S. A. Hor, X. Liu, *Chem. Soc. Rev.* **2015**, *44*, 291-314; c) I. P. Beletskaya, V. P. Ananikov, *Chem. Rev.* **2011**, *111*, 1596-1636.

[197] a) S. D. Timpa, C. J. Pell, O. V. Ozerov, *J. Am. Chem. Soc.* **2014**, *136*, 14772-14779; b) C.-S. Lai, H.-L. Kao, Y.-J. Wang, C.-F. Lee, *Tetrahedron Lett.* **2012**, *53*, 4365-4367; c) M. Arisawa, T. Suzuki, T. Ishikawa, M. Yamaguchi, *J. Am. Chem. Soc.* **2008**, *130*, 12214-12215.

[198] K. Masanori, S. Tomiya, M. Toshihiko, *Chem. Lett.* **1978**, *7*, 13-14.

[199] M. Toshihiko, S. Tomiya, A. Yoriyoshi, S. Jun-ichi, K. Yasuki, K. Masanori, *Bull. Chem. Soc. Jap.* **1980**, *53*, 1385-1389.

[200] a) J. F. Hartwig, *Acc. Chem. Res.* **2008**, *41*, 1534-1544; b) M. A. Fernández-Rodríguez, Q. Shen, J. F. Hartwig, *J. Am. Chem. Soc.* **2006**, *128*, 2180-2181.

[201] M. Sayah, M. G. Organ, *Chem. Eur. J.* **2011**, *17*, 11719-11722.

[202] Z. Lian, B. N. Bhawal, P. Yu, B. Morandi, *Science* **2017**, *356*, 1059-1063.

[203] a) M. Jean, J. Renault, P. van de Weghe, N. Asao, *Tetrahedron Lett.* **2010**, *51*, 378-381; b) N. Morita, N. Krause, *Angew. Chem. Int. Ed.* **2006**, *45*, 1897-1899.

[204] R. Das, D. Chakraborty, *Tetrahedron Lett.* **2012**, *53*, 7023-7027.

[205] a) J.-R. Wu, C.-H. Lin, C.-F. Lee, *Chem. Commun.* **2009**, 4450-4452; b) A. Correa, M. Carril, C. Bolm, *Angew. Chem. Int. Ed.* **2008**, *47*, 2880-2883.

[206] a) C. G. Bates, P. Saejueng, M. Q. Doherty, D. Venkataraman, *Org. Lett.* **2004**, *6*, 5005-5008; b) F. Y. Kwong, S. L. Buchwald, *Org. Lett.* **2002**, *4*, 3517-3520.

[207] a) M.-T. Lan, W.-Y. Wu, S.-H. Huang, K.-L. Luo, F.-Y. Tsai, *RSC Adv.* **2011**, *1*, 1751-1755; b) Y.-C. Wong, T. T. Jayanth, C.-H. Cheng, *Org. Lett.* **2006**, *8*, 5613-5616.

[208] a) T.-J. Liu, C.-L. Yi, C.-C. Chan, C.-F. Lee, *Chem. Asian J.* **2013**, *8*, 1029-1034; b) B. Madhav, S. N. Murthy, K. Ramesh, Y. V. D. Nageswar, *Chem. Lett.* **2010**, *39*, 1149-1151.

[209] a) B. A. Vara, X. Li, S. Berritt, C. R. Walters, E. J. Petersson, G. A. Molander, *Chem. Sci.* **2018**, *9*, 336-344; b) K. D. Jones, D. J. Power, D. Bierer, K. M. Gericke, S. G. Stewart, *Org. Lett.* **2018**, *20*, 208-211; c) N. Ichiishi, C. A. Malapit,

Ł. Woźniak, M. S. Sanford, *Org. Lett.* **2018**, *20*, 44-47; d) M. S. Oderinde, M. Frenette, D. W. Robbins, B. Aquila, J. W. Johannes, *J. Am. Chem. Soc.* **2016**, *138*, 1760-1763; e) M. Jouffroy, C. B. Kelly, G. A. Molander, *Org. Lett.* **2016**, *18*, 876-879; f) X.-B. Xu, J. Liu, J.-J. Zhang, Y.-W. Wang, Y. Peng, *Org. Lett.* **2013**, *15*, 550-553; g) P. Guan, C. Cao, Y. Liu, Y. Li, P. He, Q. Chen, G. Liu, Y. Shi, *Tetrahedron Lett.* **2012**, *53*, 5987-5992; h) O. Baldovino-Pantaleón, S. Hernández-Ortega, R. Reyes-Martínez, D. Morales-Morales, *Acta Crystallogr. Sect E* **2012**, *68*, m134-m134; i) N. Taniguchi, *J. Org. Chem.* **2004**, *69*, 6904-6906.

[210] a) N. Park, K. Park, M. Jang, S. Lee, *J. Org. Chem.* **2011**, *76*, 4371-4378; b) F. Ke, Y. Qu, Z. Jiang, Z. Li, D. Wu, X. Zhou, *Org. Lett.* **2011**, *13*, 454-457.

[211] a) Z. Qiao, H. Liu, X. Xiao, Y. Fu, J. Wei, Y. Li, X. Jiang, *Org. Lett.* **2013**, *15*, 2594-2597; b) Y. Jiang, Y. Qin, S. Xie, X. Zhang, J. Dong, D. Ma, *Org. Lett.* **2009**, *11*, 5250-5253.

[212] a) F. F. Fleming, S. Gudipati, V. A. Vu, R. J. Mycka, P. Knochel, *Org. Lett.* **2007**, *9*, 4507-4509; b) A. H. Stoll, A. Krasovskiy, P. Knochel, *Angew. Chem. Int. Ed.* **2006**, *45*, 606-609.

[213] G. Palumbo, C. Ferreri, C. D'Ambrosio, R. Caputo, *Phosphorus Sulfur* **1984**, *19*, 235-238.

[214] P. Mampuys, Y. Zhu, T. Vlaar, E. Ruijter, R. V. A. Orru, B. U. W. Maes, *Angew. Chem. Int. Ed.* **2014**, *53*, 12849-12854.

[215] W. Wang, X. Peng, F. Wei, C.-H. Tung, Z. Xu, *Angew. Chem. Int. Ed.* **2016**, *55*, 649-653.

[216] P. Xu, Y.-M. Zhu, X.-J. Li, F. Wang, S.-Y. Wang, S.-J. Ji, *Adv. Synth. Catal.* **2019**, *361*, 4909-4913.

[217] J. Li, W. Rao, S.-Y. Wang, S.-J. Ji, *J. Org. Chem.* **2019**, *84*, 11542-11552.

[218] J. Li, S.-Y. Wang, S.-J. Ji, *J. Org. Chem.* **2019**, *84*, 16147-16156.

[219] Y. Fang, T. Rogge, L. Ackermann, S.-Y. Wang, S.-J. Ji, *Nat. Commun.* **2018**, *9*, 2240.

[220] a) Y. Wang, L. Deng, X. Wang, Z. Wu, Y. Wang, Y. Pan, *ACS Catal.* **2019**, *9*, 1630-1634; b) D. Liu, H.-X. Ma, P. Fang, T.-S. Mei, *Angew. Chem. Int. Ed.* **2019**, *58*, 5033-5037.

[221] a) J. C. K. Chu, T. Rovis, *Angew. Chem. Int. Ed.* **2018**, *57*, 62-101; b) W. Ma, P. Gandeepan, J. Li, L. Ackermann, *Org. Chem. Front.* **2017**, *4*, 1435-1467; c) J. F. Hartwig, M. A. Larsen, *ACS Cent. Sci.* **2016**, *2*, 281-292; d) T. Cernak, K. D. Dykstra, S. Tyagarajan, P. Vachal, S. W. Krska, *Chem. Soc. Rev.* **2016**, *45*, 546-576; e) A. F. M. Noisier, M. A. Brimble, *Chem. Rev.* **2014**, *114*, 8775-8806; f) J. Yamaguchi, A. D. Yamaguchi, K. Itami, *Angew. Chem. Int. Ed.* **2012**, *51*, 8960-9009; g) M. C. White, *Science* **2012**, *335*, 807-809; h) T. Brückl, R. D. Baxter, Y. Ishihara, P. S. Baran, *Acc. Chem. Res.* **2012**, *45*, 826-839.

[222] a) D.-S. Kong, Y.-F. Wang, Y.-S. Zhao, Q.-H. Li, Y.-X. Chen, P. Tian, G.-Q. Lin, *Org. Lett.* **2018**, *20*, 1154-1157; b) Z.-J. Jia, C. Merten, R. Gontla, C. G. Daniliuc, A. P. Antonchick, H. Waldmann, *Angew. Chem. Int. Ed.* **2017**, *56*, 2429-2434; c) S. Nakanowatari, L. Ackermann, *Chem. Eur. J.* **2015**, *21*, 16246-16251; d)

B. Ye, N. Cramer, *J. Am. Chem. Soc.* **2013**, *135*, 636-639; e) H. Wang, B. Beiring, D.-G. Yu, K. D. Collins, F. Glorius, *Angew. Chem. Int. Ed.* **2013**, *52*, 12430-12434; f) N. Guimond, K. Fagnou, *J. Am. Chem. Soc.* **2009**, *131*, 12050-12051.

[223] a) S. Torii, H. Okumoto, M. A. Rashid, M. Mohri, *Synlett* **1992**, 721-722; b) G. Pattenden, G. M. Robertson, *Tetrahedron* **1985**, *41*, 4001-4011; c) G. Schlegel, H. J. Schäfer, *Chem. Ber.* **1983**, *116*, 960-969.

[224] T. H. Meyer, J. C. A. Oliveira, S. C. Sau, N. W. J. Ang, L. Ackermann, *ACS Catal.* **2018**, *8*, 9140-9147.

[225] N. Sauermann, T. H. Meyer, C. Tian, L. Ackermann, *J. Am. Chem. Soc.* **2017**, *139*, 18452-18455.

[226] a) S. Liu, *J. Phys. Chem. A* **2013**, *117*, 962-965; b) D. X. Hu, P. Grice, S. V. Ley, *J. Org. Chem.* **2012**, *77*, 5198-5202; c) D. H. R. Barton, *Science* **1970**, *169*, 539-544.

[227] a) J. Song, Q. Liu, H. Liu, X. Jiang, *Eur. J. Org. Chem.* **2018**, *2018*, 696-713; b) T. Fujihara, Y. Tsuji, *Beilstein J. Org. Chem.* **2018**, *14*, 2435-2460.

[228] N. W. J. Ang, J. C. A. Oliveira, L. Ackermann, *Angew. Chem. Int. Ed.* **2020**, *59*, 12842-12847.

[229] a) Y. Zhang, X. Wang, M. Sunkara, Q. Ye, L. V. Ponomereva, Q.-B. She, A. J. Morris, J. S. Thorson, *Org. Lett.* **2013**, *15*, 5566-5569; b) K.-i. Takao, R. Nanamiya, Y. Fukushima, A. Namba, K. Yoshida, K.-i. Tadano, *Org. Lett.* **2013**, *15*, 5582-5585; c) P. Radha Krishna, S. Prabhakar, C. Sravanthi, *Tetrahedron Lett.* **2013**, *54*, 669-671; d) S. G. Davies, P. M. Roberts, P. T. Stephenson, H. R. Storr, J. E. Thomson, *Tetrahedron* **2009**, *65*, 8283-8296; e) P. Wipf, S. R. Spencer, *J. Am. Chem. Soc.* **2005**, *127*, 225-235.

[230] a) J. Loup, D. Zell, J. C. A. Oliveira, H. Keil, D. Stalke, L. Ackermann, *Angew. Chem. Int. Ed.* **2017**, *56*, 14197-14201; b) D. Ghorai, V. Müller, H. Keil, D. Stalke, G. Zanoni, B. A. Tkachenko, P. R. Schreiner, L. Ackermann, *Adv. Synth. Catal.* **2017**, *359*, 3137-3141; c) L. Ackermann, S. Barfüsser, C. Kornhaass, A. R. Kapdi, *Org. Lett.* **2011**, *13*, 3082-3085.

[231] a) F. Tan, G. Yin, *Chin. J. Chem.* **2018**, *36*, 545-554; b) M. D. Otero, B. Batanero, F. Barba, *Tetrahedron Lett.* **2006**, *47*, 2171-2173; c) D. Ballivet-Tkatchenko, J.-C. Folest, J. Tanji, *Appl. Organomet. Chem.* **2000**, *14*, 847-849.

[232] S. Bazzi, G. Le Duc, E. Schulz, C. Gosmini, M. Mellah, *Org. Biomol. Chem.* **2019**, *17*, 8546-8550.

[233] G. Musie, M. Wei, B. Subramaniam, D. H. Busch, *Coord. Chem. Rev.* **2001**, 789-820.

[234] M. R. Brennan, D. Kim, A. R. Fout, *Chem. Sci.* **2014**, *5*, 4831-4839.

[235] a) B. J. Fallon, E. Derat, M. Amatore, C. Aubert, F. Chemla, F. Ferreira, A. Perez-Luna, M. Petit, *J. Am. Chem. Soc.* **2015**, *137*, 2448-2451; b) W. Song, L. Ackermann, *Angew. Chem. Int. Ed.* **2012**, *51*, 8251-8254; c) Z. Ding, N. Yoshikai, *Angew. Chem. Int. Ed.* **2012**, *51*, 4698-4701; d) L. Ilies, Q. Chen, X. Zeng, E. Nakamura, *J. Am. Chem. Soc.* **2011**, *133*, 5221-5223.

[236] T. Shimoda, T. Morishima, K. Kodama, T. Hirose, D. E. Polyansky, G. F.

Manbeck, J. T. Muckerman, E. Fujita, *Inorg. Chem.* **2018**, *57*, 5486-5498.

[237] a) C. Sandford, L. R. Fries, T. E. Ball, S. D. Minteer, M. S. Sigman, *J. Am. Chem. Soc.* **2019**, *141*, 18877-18889; b) D. P. Hickey, C. Sandford, Z. Rhodes, T. Gensch, L. R. Fries, M. S. Sigman, S. D. Minteer, *J. Am. Chem. Soc.* **2019**, *141*, 1382-1392.

[238] a) A. Pui, I. Berdan, I. Morgenstern-Badarau, A. Gref, M. Perrée-Fauvet, *Inorg. Chim. Acta* **2001**, *320*, 167-171; b) H. Ogino, K. Ogino, *Inorg. Chem.* **1983**, *22*, 2208-2211.

[239] a) C. Zucchi, G. Pályi, V. Galamb, E. Sámpár-Szerencsés, L. Markó, P. Li, H. Alper, *Organometallics* **1996**, *15*, 3222-3231; b) V. Galamb, G. Pályi, *J. Chem. Soc., Chem. Commun.* **1982**, 487-488.

[240] a) H. A. Duong, P. B. Huleatt, Q.-W. Tan, E. L. Shuying, *Org. Lett.* **2013**, *15*, 4034-4037; b) M. T. Johnson, R. Johansson, M. V. Kondrashov, G. Steyl, M. S. G. Ahlquist, A. Roodt, O. F. Wendt, *Organometallics* **2010**, *29*, 3521-3529; c) J. Takaya, N. Iwasawa, *J. Am. Chem. Soc.* **2008**, *130*, 15254-15255; d) N. Solin, J. Kjellgren, K. J. Szabó, *J. Am. Chem. Soc.* **2004**, *126*, 7026-7033.

[241] H. Liu, X. Jiang, *Chem. Asian J.* **2013**, *8*, 2546-2563.

[242] a) P. Mampuys, C. R. McElroy, J. H. Clark, R. V. A. Orru, B. U. W. Maes, *Adv. Synth. Catal.* **2020**, *362*, 3-64; b) N. S. Zefirov, N. V. Zyk, E. K. Beloglazkina, A. G. Kutateladze, *Sulfur Rep.* **1993**, *14*, 223-240.

[243] N. W. J. Ang, L. Ackermann, *Chem. Eur. J.* **2021**, *27*, 4883-4887.

[244] a) A. S. Surur, L. Schulig, A. Link, *Arch. Pharm. Chem. Life. Sci.* **2019**, *352*, 1800248; b) M. Feng, B. Tang, S. H. Liang, X. Jiang, *Curr. Top. Med. Chem.* **2016**, *16*, 1200-1216; c) A. V. Bogolubsky, Y. S. Moroz, P. K. Mykhailiuk, E. N. Ostapchuk, A. V. Rudnichenko, Y. V. Dmytriv, A. N. Bondar, O. A. Zaporozhets, S. E. Pipko, R. A. Doroschuk, L. N. Babichenko, A. I. Konovets, A. Tolmachev, *ACS Comb. Sci.* **2015**, *17*, 348-354; d) H. L. Holland, *Nat. Prod. Rep.* **2001**, *18*, 171-181.

[245] a) C. Schöneich, *Molecules* **2019**, *24*, 4357; b) F. Dénès, M. Pichowicz, G. Povie, P. Renaud, *Chem. Rev.* **2014**, *114*, 2587-2693; c) R. P. Steer, B. L. Kalra, A. R. Knight, *J. Phys. Chem.* **1967**, *71*, 783-784.

[246] a) G. Roos, F. De Proft, P. Geerlings, *Chem. Eur. J.* **2013**, *19*, 5050-5060; b) D. A. Armstrong, Q. Sun, R. H. Schuler, *J. Phys. Chem.* **1996**, *100*, 9892-9899; c) P. S. Surdhar, D. A. Armstrong, *J. Phys. Chem.* **1987**, *91*, 6532-6537; d) P. Surdhar, D. A. Armstrong, *J. Phys. Chem.* **1986**, *90*, 5915-5917.

[247] a) Y. Kawamata, J. C. Vantourout, D. P. Hickey, P. Bai, L. Chen, Q. Hou, W. Qiao, K. Barman, M. A. Edwards, A. F. Garrido-Castro, J. N. deGruyter, H. Nakamura, K. Knouse, C. Qin, K. J. Clay, D. Bao, C. Li, J. T. Starr, C. Garcia-Irizarry, N. Sach, H. S. White, M. Neurock, S. D. Minteer, P. S. Baran, *J. Am. Chem. Soc.* **2019**, *141*, 6392-6402; b) M. Durandetti, J. Maddaluno, in *Encyclopedia of Reagents for Organic Synthesis*, Wiley-VCH, Weinheim, **2014**, pp. 1-3; c) I. Zilbermann, E. Maimon, H. Cohen, D. Meyerstein, *Chem. Rev.* **2005**, *105*, 2609-2626; d) A. G. Lappin, A. McAuley, *Adv. Inorg. Chem.* **1988**, *32*, 241-295.

[248] a) G. T. Venkanna, H. D. Arman, Z. J. Tonzetich, *ACS Catal.* **2014**, *4*, 2941-2950; b) S. Biswas, D. J. Weix, *J. Am. Chem. Soc.* **2013**, *135*, 16192-16197.

[249] D. Vasudevan, *Russ. J. Electrochem.* **2005**, *41*, 310-314.

[250] a) V. B. Mostardeiro, M. C. Dilelio, T. S. Kaufman, C. C. Silveira, *RSC Adv.* **2020**, *10*, 482-491; b) E. Dmitrieva, X. Yu, H. Hartmann, *Electrochem. Commun.* **2020**, *114*, 106706; c) B. Janhsen, C. G. Daniliuc, A. Studer, *Chem. Sci.* **2017**, *8*, 3547-3553.

[251] a) C. Hurtado-Rodrigo, S. Hoehne, M. P. Muñoz, *Chem. Commun.* **2014**, *50*, 1494-1496; b) L. Rout, A. M. Harned, *Chem. Eur. J.* **2009**, *15*, 12926-12928; c) H. Guo, R. Qian, Y. Guo, S. Ma, *J. Org. Chem.* **2008**, *73*, 7934-7938.

[252] a) W.-F. Wang, J.-B. Peng, X. Qi, J. Ying, X.-F. Wu, *Chem. Eur. J.* **2019**, *25*, 3521-3524; b) F. Pape, L. T. Brechmann, J. F. Teichert, *Chem. Eur. J.* **2019**, *25*, 985-988; c) L. A. Brozek, M. J. Ardolino, J. P. Morken, *J. Am. Chem. Soc.* **2011**, *133*, 16778-16781; d) D. J. Vyas, M. Oestreich, *Chem. Commun.* **2010**, *46*, 568-570; e) M. J. Fuchter, J.-N. Levy, *Org. Lett.* **2008**, *10*, 4919-4922; f) Y. Takahashi, T. Inagaki, H. Mori, S. Sakai, Y. Ishii, *J. Soc. Chem. Industry Jap.* **1970**, *73*, 760-764.

[253] a) T. Niu, J. Liu, X. Wu, C. Zhu, *Chin. J. Chem.* **2020**, *38*, 803-806; b) Q. Chen, Y. Huang, X. Wang, J. Wu, G. Yu, *Org. Biomol. Chem.* **2018**, *16*, 1713-1719; c) W. Kong, H. An, Q. Song, *Chem. Commun.* **2017**, *53*, 8968-8971; d) G. Liang, M. Liu, J. Chen, J. Ding, W. Gao, H. Wu, *Chin. J. Chem.* **2012**, *30*, 1611-1616; e) T. Hideo, T. Masatoshi, U. Seiryu, S. Takashi, S. Michio, T. Sigeru, *Bull. Chem. Soc. Jap.* **1991**, *64*, 1416-1418.

[254] C. Alamillo-Ferrer, M. Karabourniotis-Sotti, A. R. Kennedy, M. Campbell, N. C. O. Tomkinson, *Org. Lett.* **2016**, *18*, 3102-3105.

[255] X. Liu, R. An, X. Zhang, J. Luo, X. Zhao, *Angew. Chem. Int. Ed.* **2016**, *55*, 5846-5850.

[256] M.-C. Fu, R. Shang, W.-M. Cheng, Y. Fu, *Chem. Eur. J.* **2017**, *23*, 8818-8822.

[257] T. Miyazaki, S. Kasai, Y. Ogiwara, N. Sakai, *Eur. J. Org. Chem.* **2016**, 1043-1049.

[258] R. Kumar, Saima, A. Shard, N. H. Andhare, Richa, A. K. Sinha, *Angew. Chem. Int. Ed.* **2015**, *54*, 828-832.

[259] R. Maity, B. Das, I. Das, *Adv. Synth. Catal.* **2019**, *361*, 2347-2353.

[260] M. Amézquita-Valencia, H. Alper, *J. Org. Chem.* **2016**, *81*, 3860-3867.

[261] Y. Nishimoto, A. Okita, M. Yasuda, A. Baba, *Org. Lett.* **2012**, *14*, 1846-1849.

[262] K. Colas, R. Martín-Montero, A. Mendoza, *Angew. Chem. Int. Ed.* **2017**, *56*, 16042-16046.

[263] T. Tamai, K. Fujiwara, S. Higashimae, A. Nomoto, A. Ogawa, *Org. Lett.* **2016**, *18*, 2114-2117.

[264] H. Jian, Q. Wang, W.-H. Wang, Z.-J. Li, C.-Z. Gu, B. Dai, L. He, *Tetrahedron* **2018**, *74*, 2876-2883.

[265] C.-W. Chen, Y.-L. Chen, D. M. Reddy, K. Du, C.-E. Li, B.-H. Shih, Y.-J. Xue, C.-F. Lee, *Chem. Eur. J.* **2017**, *23*, 10087-10091.

7. NMR Spectra

7.1 Electrochemical C–H Annulations of Benzamides with Internal Allenes

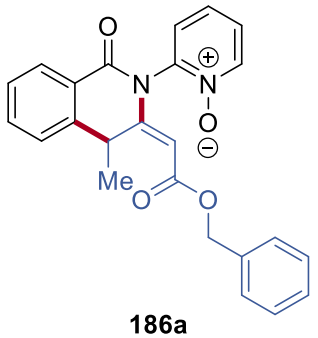

186a

^{1}H-NMR

(500 MHz, $CDCl_3$)

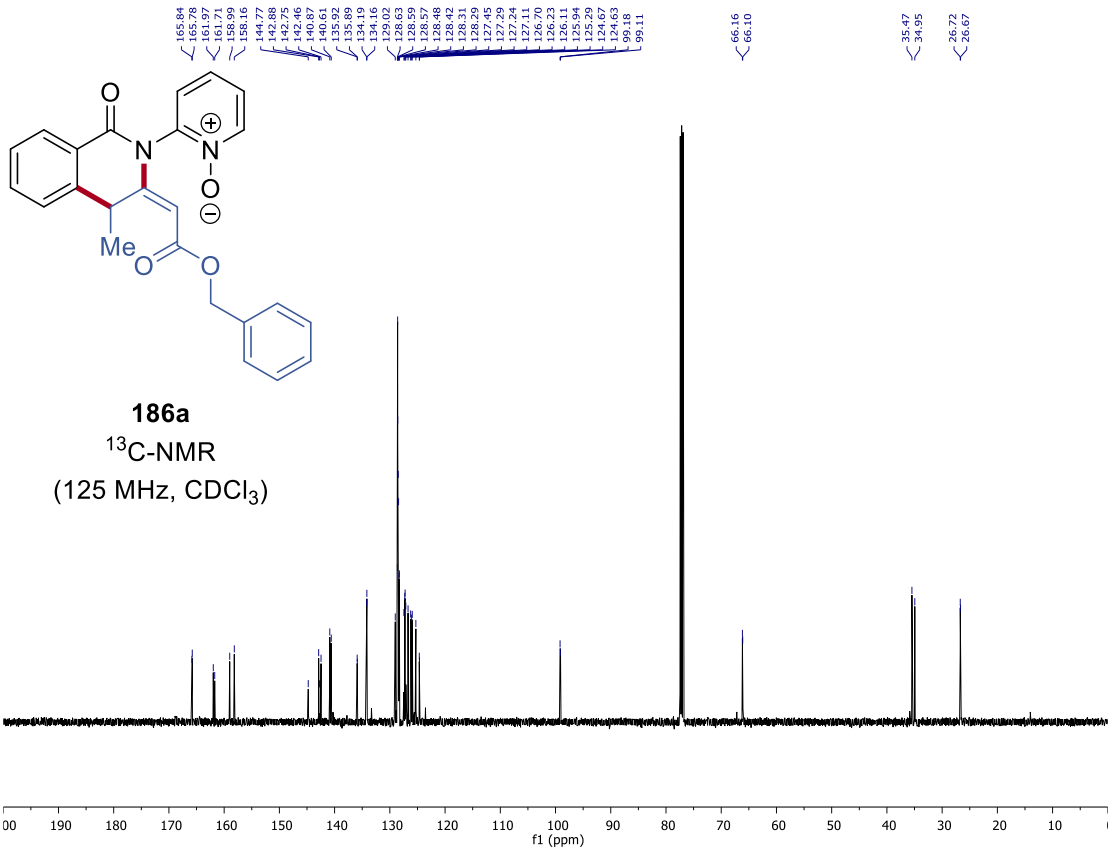

186a

^{13}C-NMR

(125 MHz, $CDCl_3$)

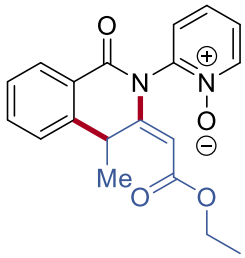

186b

^{1}H-NMR

(500 MHz, $CDCl_3$)

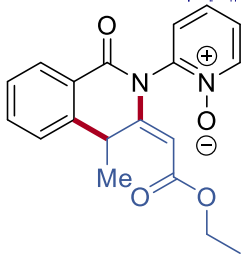

186b

^{13}C-NMR

(125 MHz, $CDCl_3$)

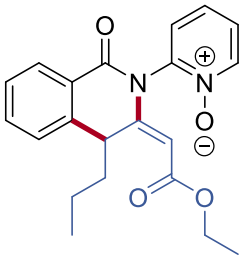

186c

^{1}H-NMR

(500 MHz, $CDCl_3$)

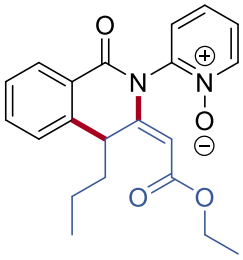

186c

^{13}C-NMR

(125 MHz, $CDCl_3$)

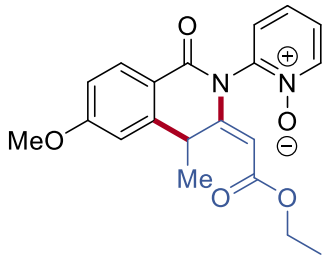

186d

^{1}H-NMR

(500 MHz, $CDCl_3$)

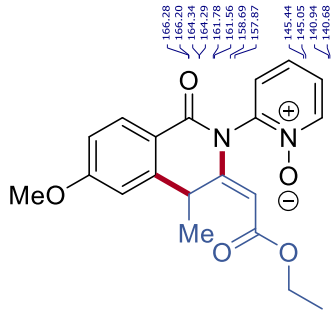

186d

^{13}C-NMR

(125 MHz, $CDCl_3$)

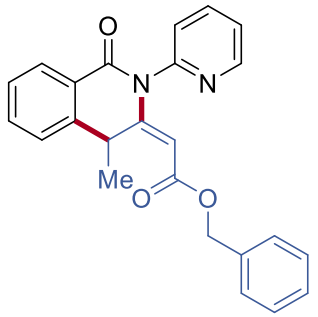

188a

^{1}H-NMR

(400 MHz, $CDCl_3$)

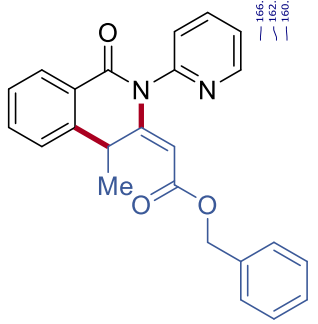

188a

^{13}C-NMR

(101 MHz, $CDCl_3$)

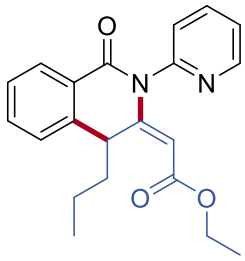

188b

^{1}H-NMR

(400 MHz, $CDCl_3$)

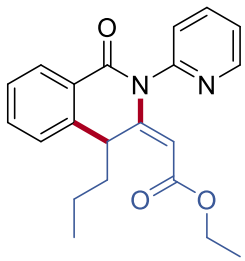

188b

^{13}C-NMR

(101 MHz, $CDCl_3$)

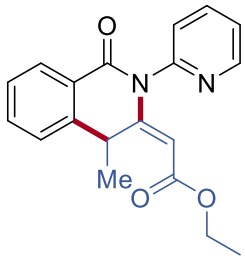

188c

^{1}H-NMR

(400 MHz, $CDCl_3$)

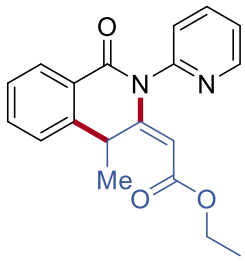

188c

^{13}C-NMR

(101 MHz, $CDCl_3$)

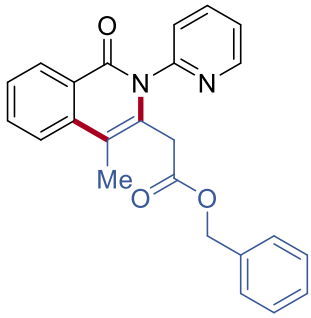

188a'

^{1}H-NMR

(300 MHz, $CDCl_3$)

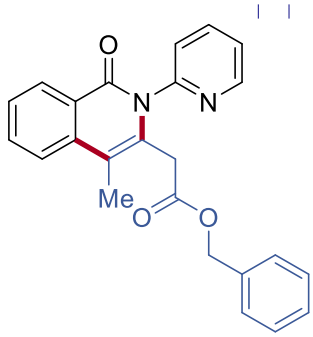

188a'

^{13}C-NMR

(75 MHz, $CDCl_3$)

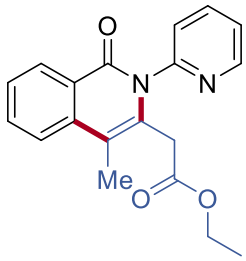

188b'

^{1}H-NMR

(300 MHz, $CDCl_3$)

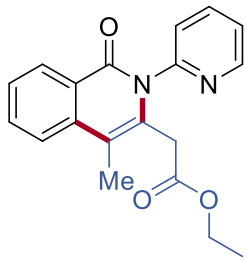

188b'

^{13}C-NMR

(75 MHz, $CDCl_3$)

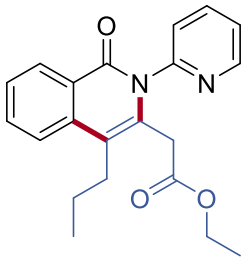

188c'

^{1}H-NMR

(300 MHz, $CDCl_3$)

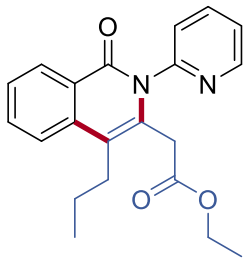

188c'

^{13}C-NMR

(75 MHz, $CDCl_3$)

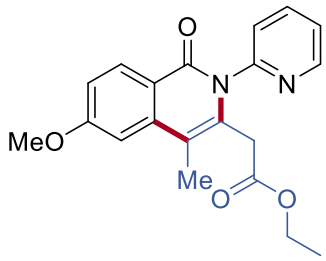

188d'

^{1}H-NMR

(400 MHz, $CDCl_3$)

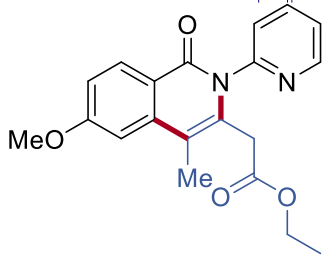

188d'

^{13}C-NMR

(101 MHz, $CDCl_3$)

7.2 Electro-Reductive Cobalt-Catalyzed Carboxylation with CO_2

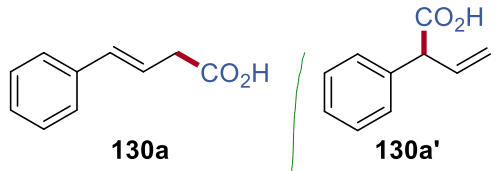

130a **130a'**

(linear/branch = 1:1)

^{1}H-NMR

(300 MHz, $CDCl_3$)

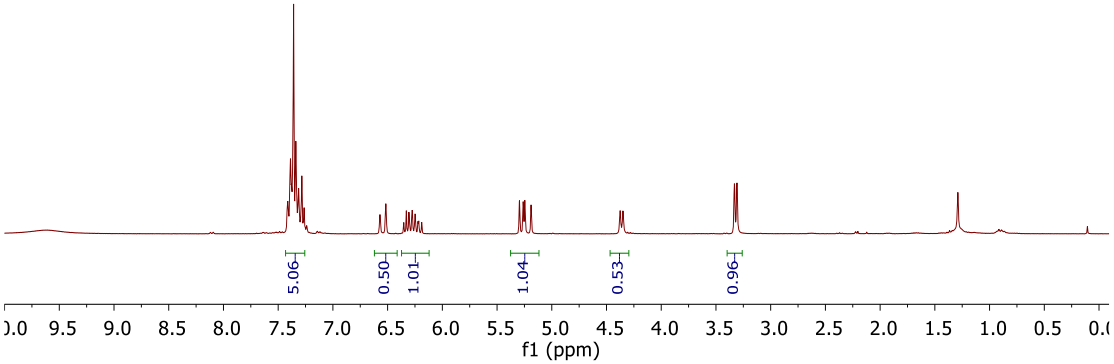

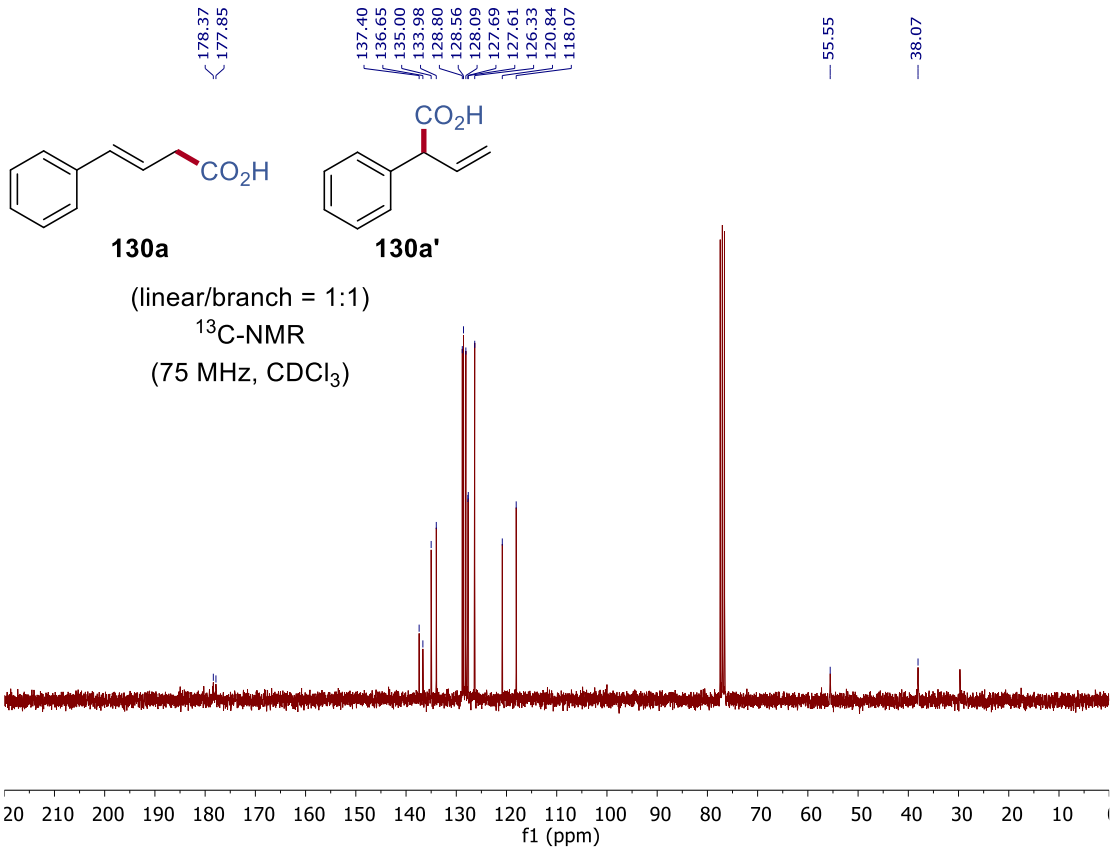

130a **130a'**

(linear/branch = 1:1)

^{13}C-NMR

(75 MHz, $CDCl_3$)

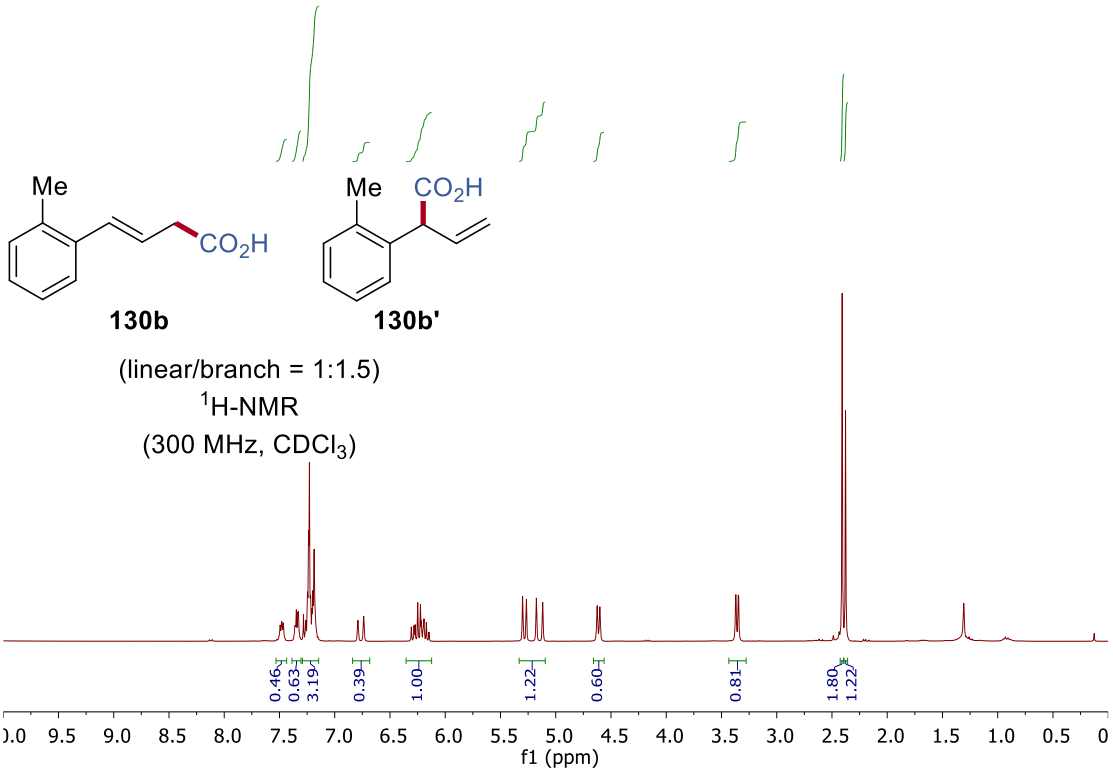
Me
CO2H
Me
CO2H
130b
130b'
(linear/branch = 1:1.5)
1H-NMR
(300 MHz, CDCl3)
0.46
0.63
3.19
0.39
1.00
1.22
0.60
0.81
1.80
1.22
f1 (ppm)

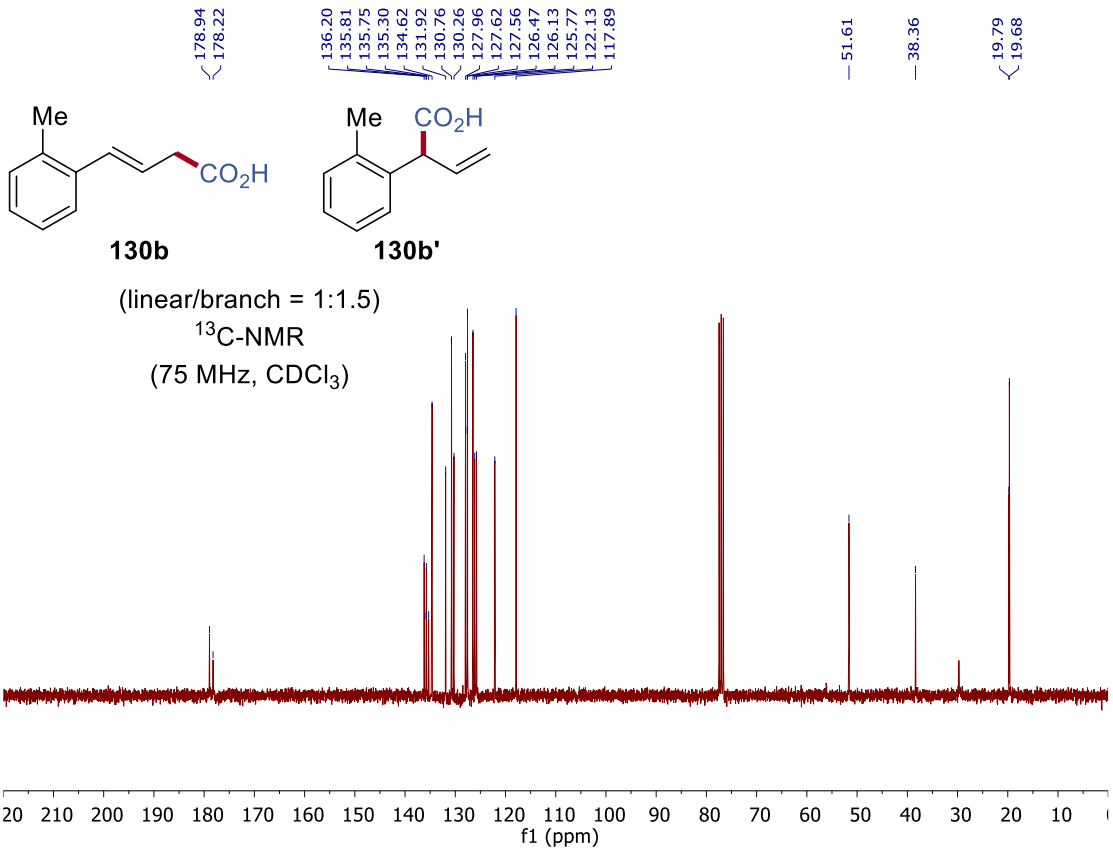
178.94
178.22
136.20
135.81
135.75
135.30
134.62
131.92
130.76
130.26
127.96
127.62
127.56
126.47
126.13
125.77
122.13
117.89
51.61
38.36
19.79
19.68
Me
CO2H
Me
CO2H
130b
130b'
(linear/branch = 1:1.5)
13C-NMR
(75 MHz, CDCl3)
f1 (ppm)

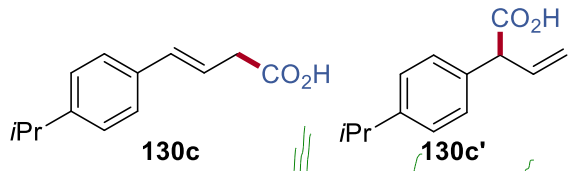

130c **130c'**

(linear/branch = 4:3)

^{1}H-NMR

(400 MHz, $CDCl_3$)

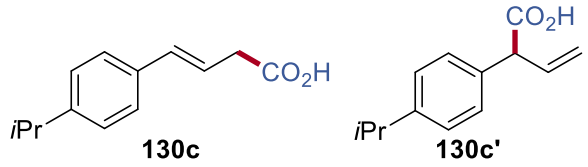

130c **130c'**

(linear/branch = 4:3)

^{13}C-NMR

(100 MHz, $CDCl_3$)

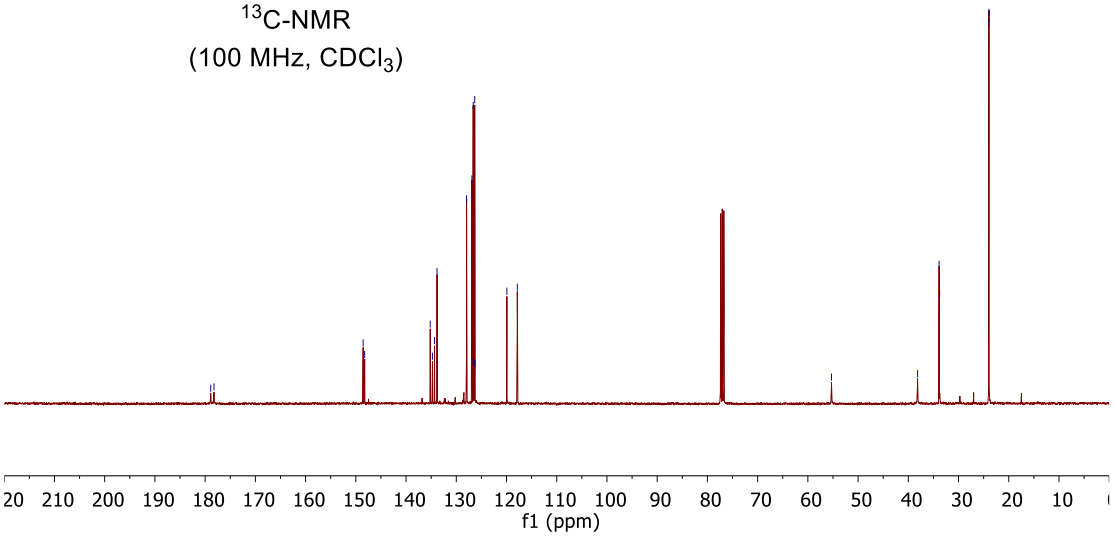

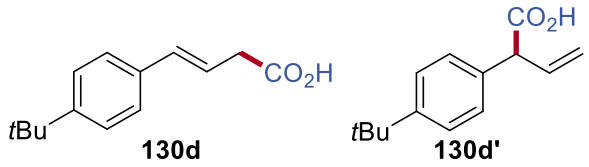

130d **130d'**

(linear/branch = 1.2:1)

^{1}H-NMR

(400 MHz, $CDCl_3$)

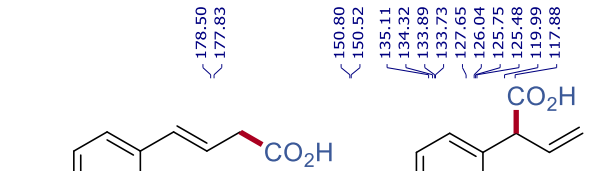

130d **130d'**

(linear/branch = 1.2:1)

^{13}C-NMR

(100 MHz, $CDCl_3$)

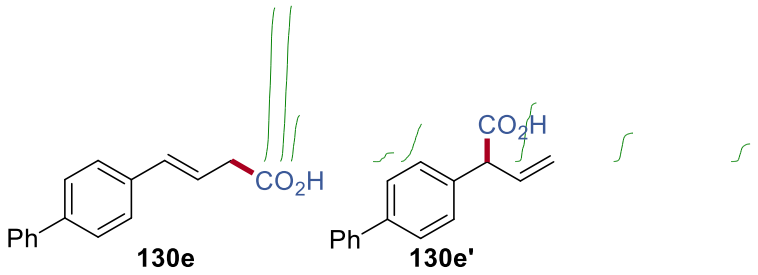

130e **130e'**

(linear/branch = 1:3)

^{1}H-NMR

(400 MHz, $CDCl_3$)

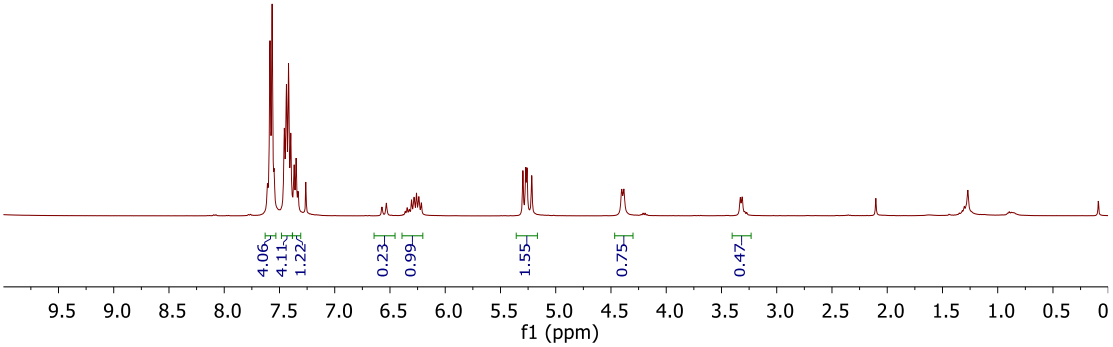

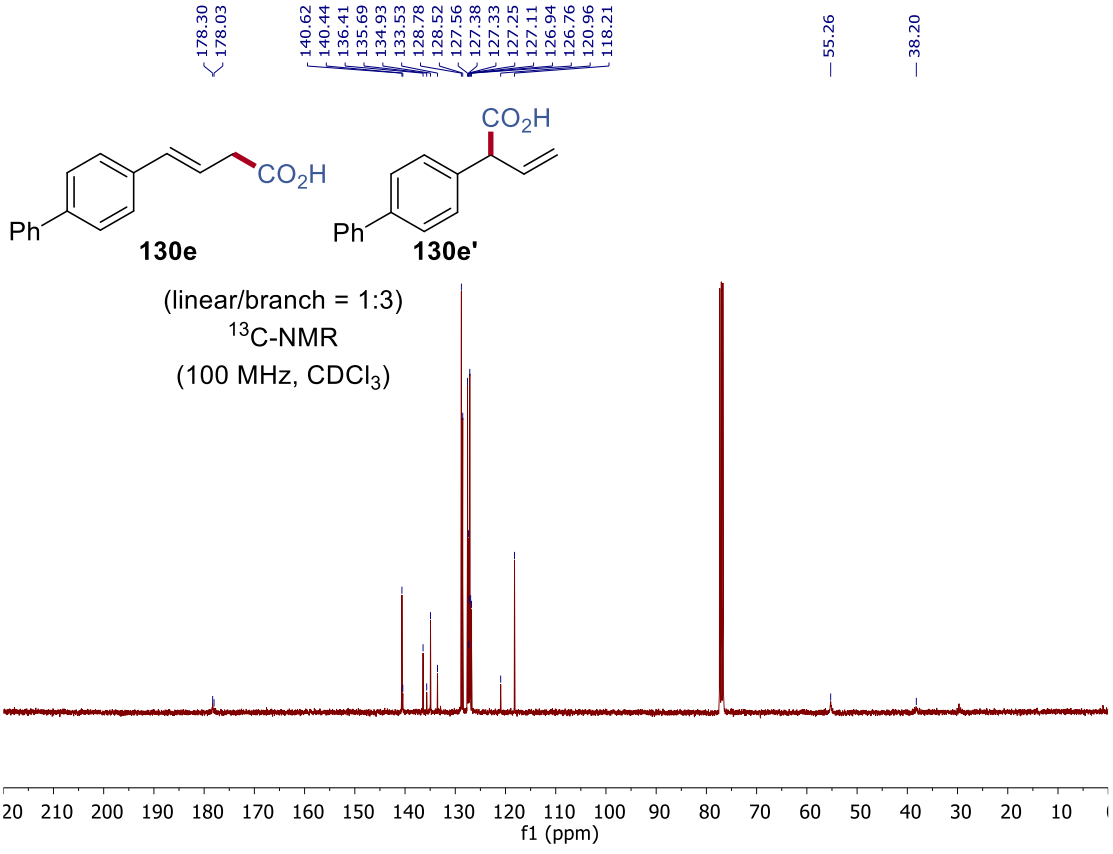

130e **130e'**

(linear/branch = 1:3)

^{13}C-NMR

(100 MHz, $CDCl_3$)

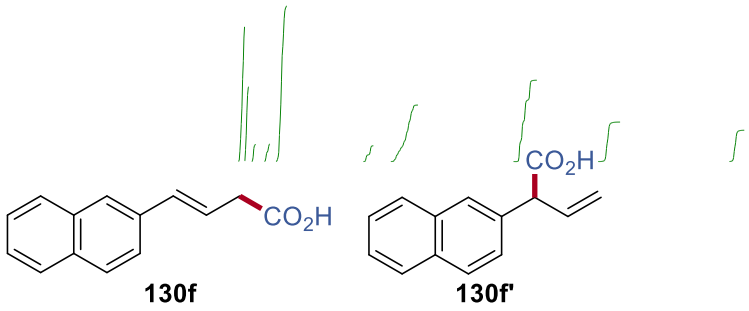

130f **130f'**

(linear/branch = 1:2.5)

^{1}H-NMR

(400 MHz, $CDCl_3$)

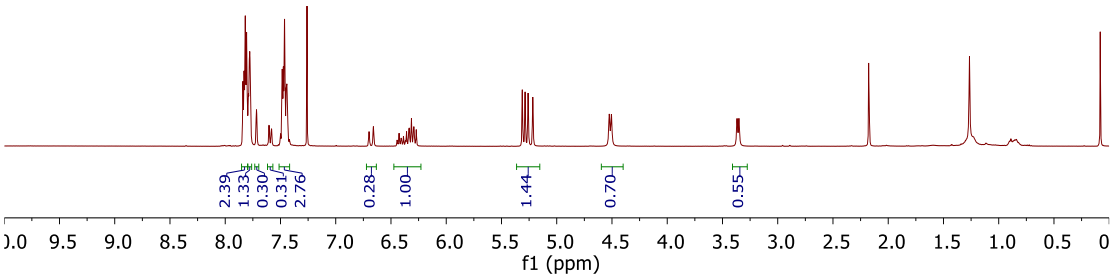

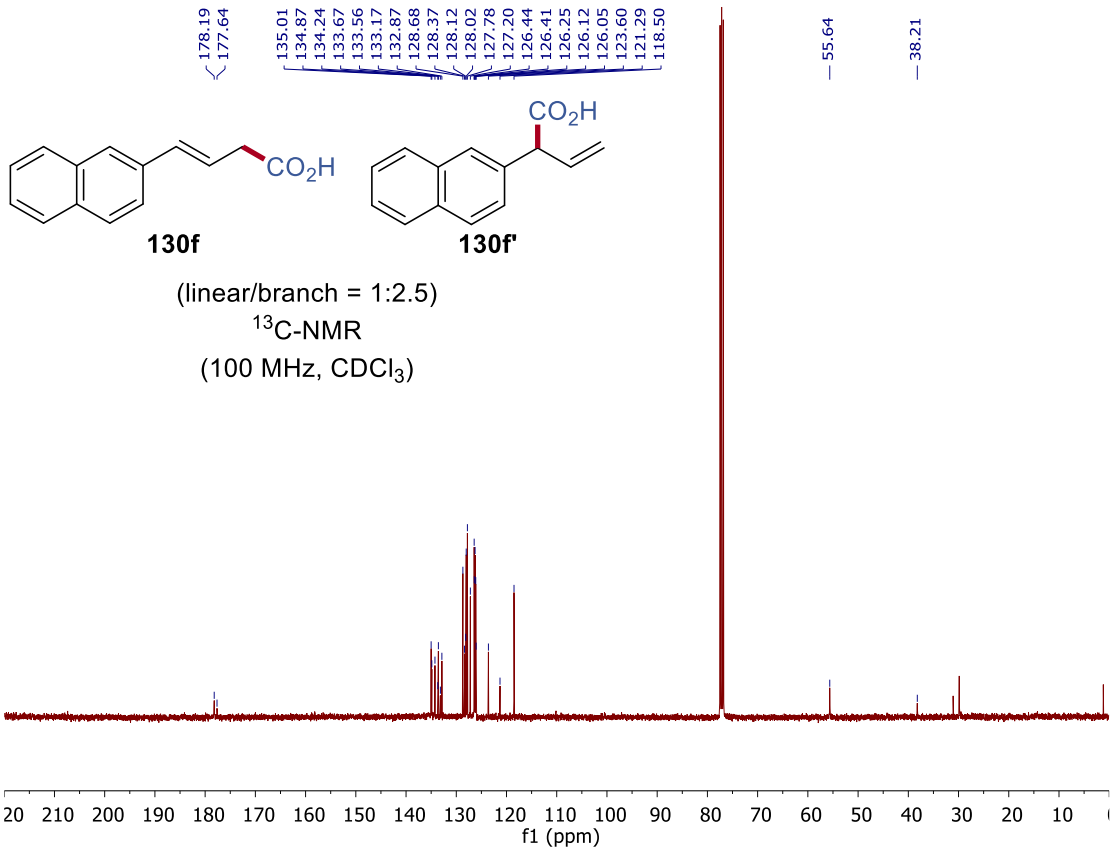

130f **130f'**

(linear/branch = 1:2.5)

^{13}C-NMR

(100 MHz, $CDCl_3$)

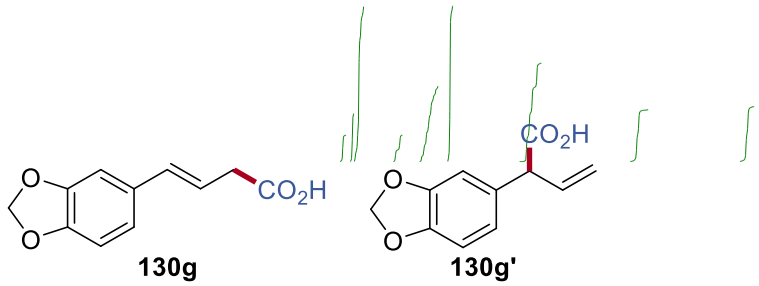

130g **130g'**

(linear/branch = 1:2)

^{1}H-NMR

(400 MHz, $CDCl_3$)

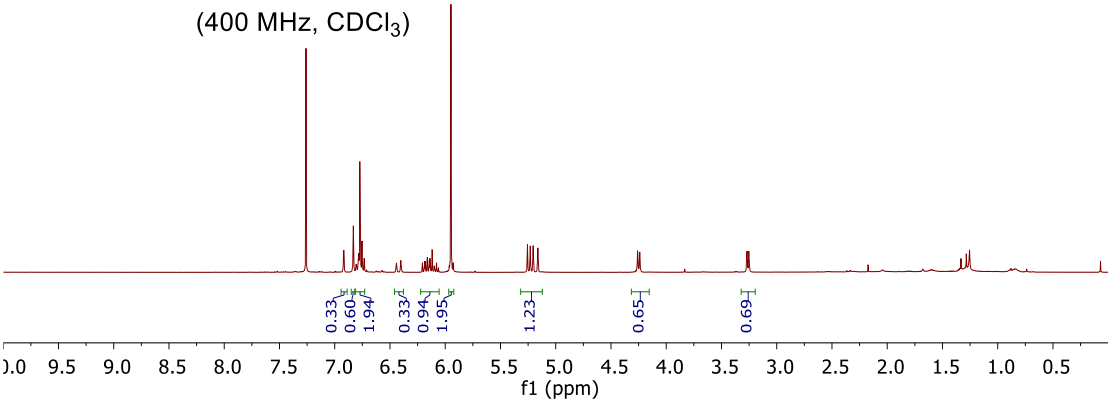

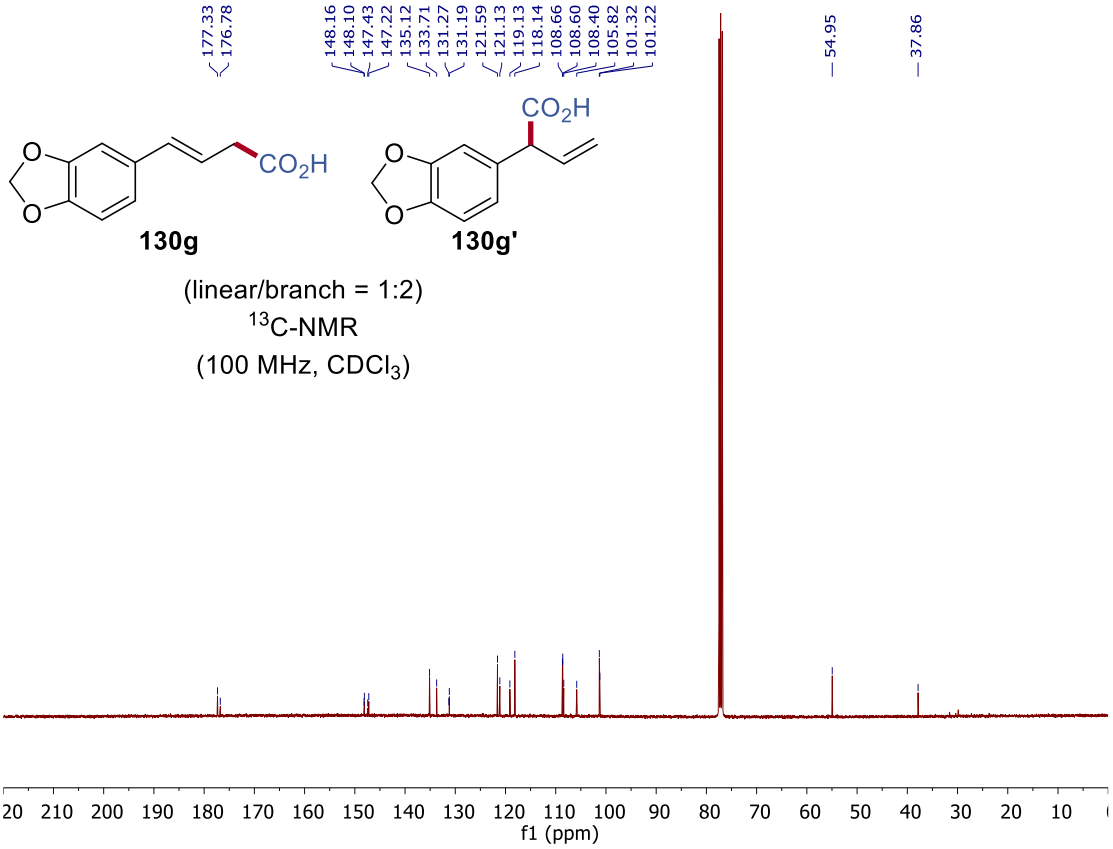

130g **130g'**

(linear/branch = 1:2)

^{13}C-NMR

(100 MHz, $CDCl_3$)

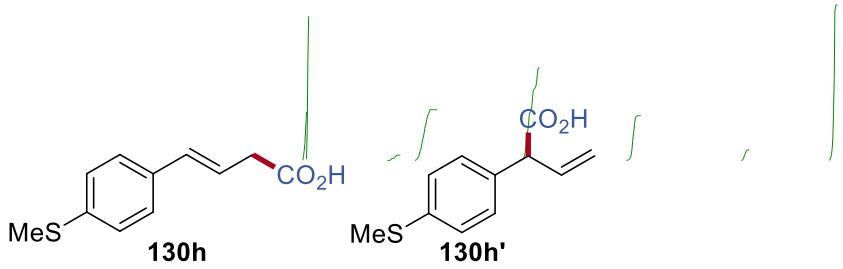

(linear/branch = 1:9)

^{1}H-NMR

(400 MHz, $CDCl_3$)

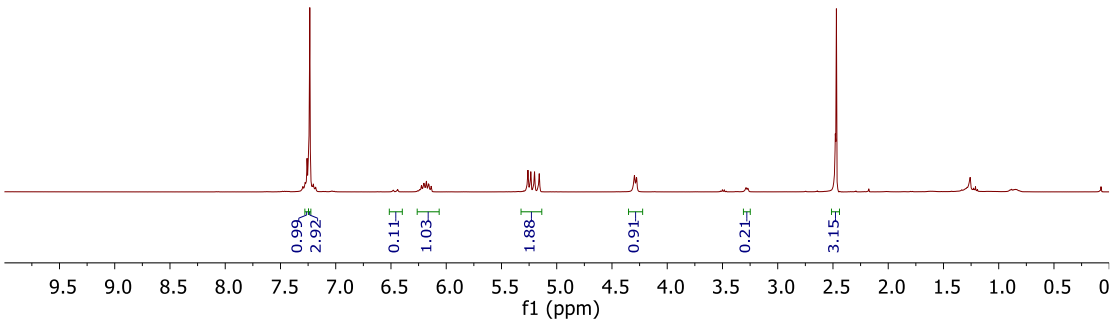

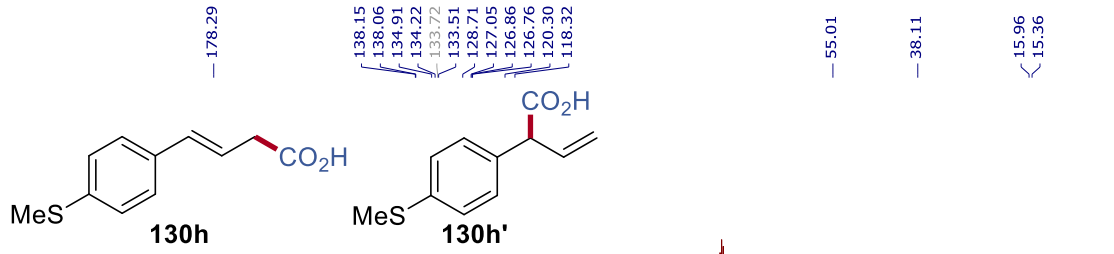

(linear/branch = 1:9)

^{13}C-NMR

(100 MHz, $CDCl_3$)

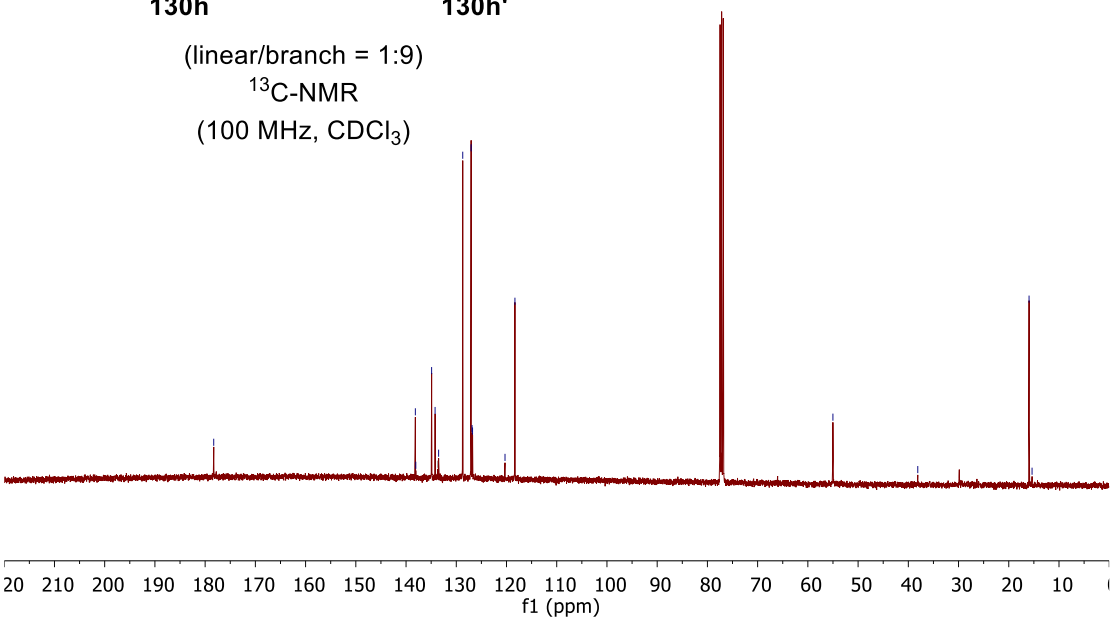

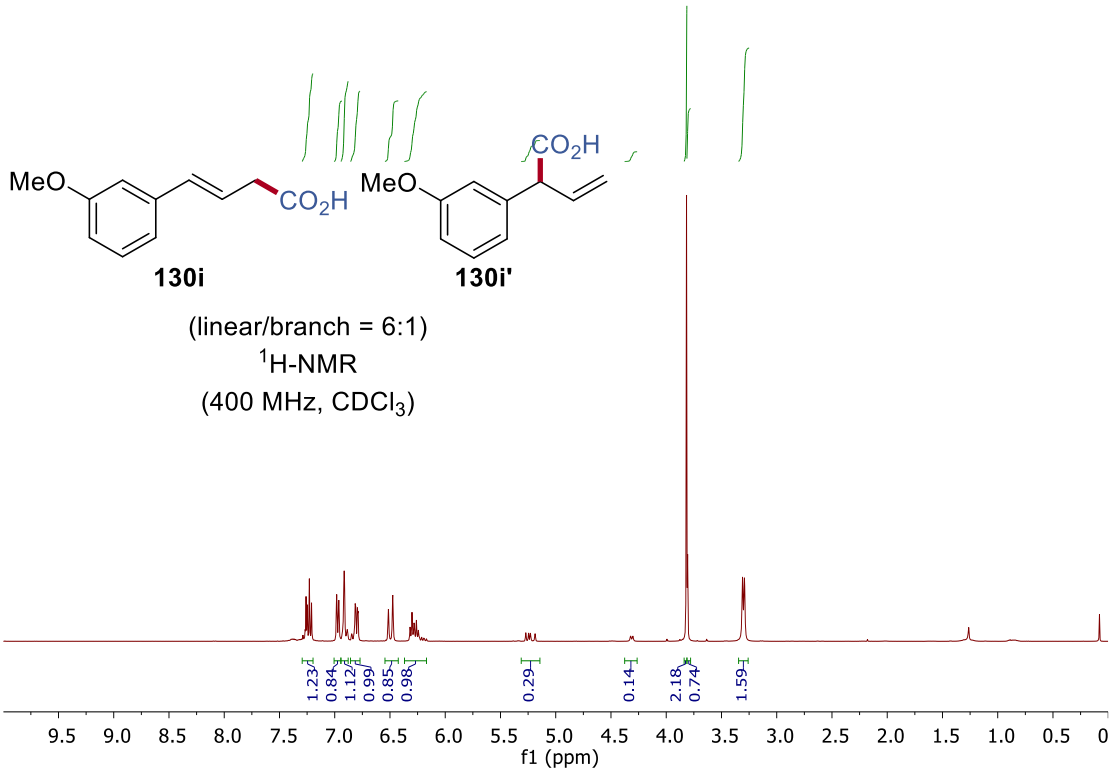
MeO
CO2H
MeO
CO2H
130i
130i'
(linear/branch = 6:1)
1H-NMR
(400 MHz, CDCl3)
1.23
0.84
1.12
0.99
0.85
0.98
0.29
0.14
2.18
0.74
1.59
9.5 9.0 8.5 8.0 7.5 7.0 6.5 6.0 5.5 5.0 4.5 4.0 3.5 3.0 2.5 2.0 1.5 1.0 0.5 0
f1 (ppm)

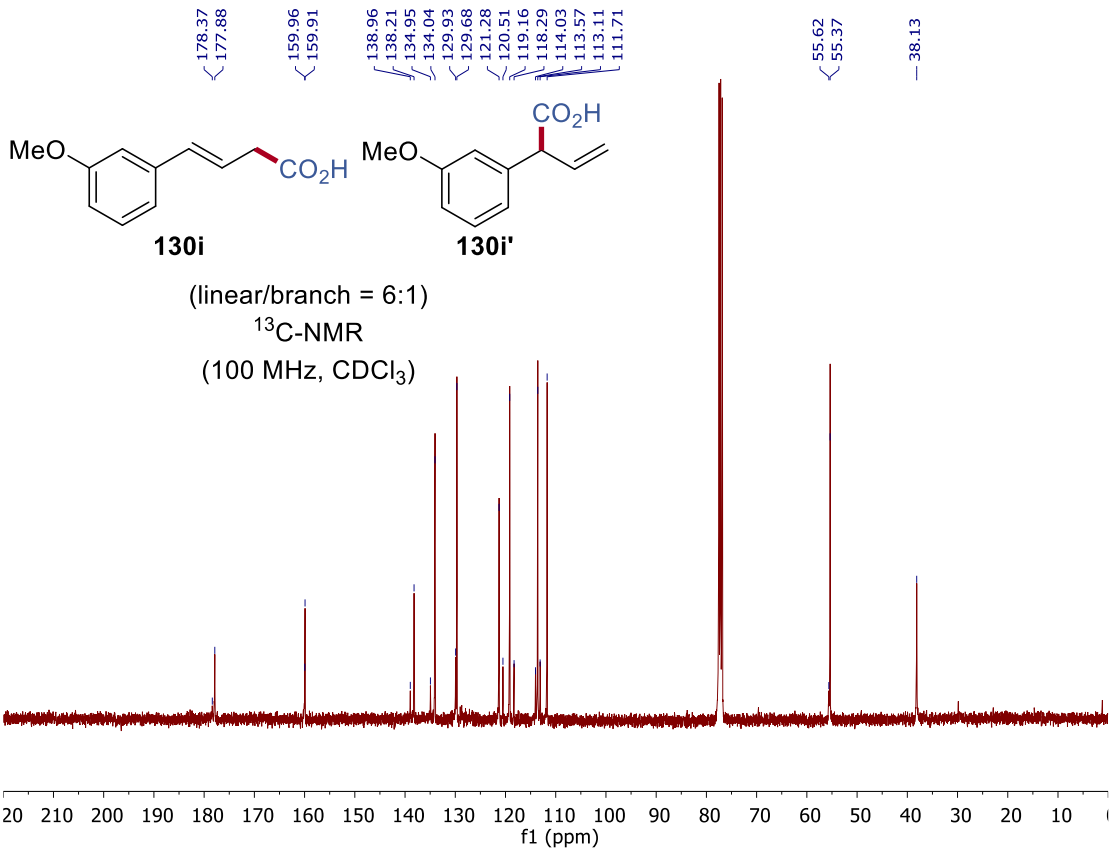
178.37
177.88
159.96
159.91
138.96
138.21
134.95
134.04
129.93
129.68
121.28
120.51
119.16
118.29
114.03
113.57
113.11
111.71
55.62
55.37
38.13
MeO
CO2H
MeO
CO2H
130i
130i'
(linear/branch = 6:1)
13C-NMR
(100 MHz, CDCl3)
220 210 200 190 180 170 160 150 140 130 120 110 100 90 80 70 60 50 40 30 20 10
f1 (ppm)

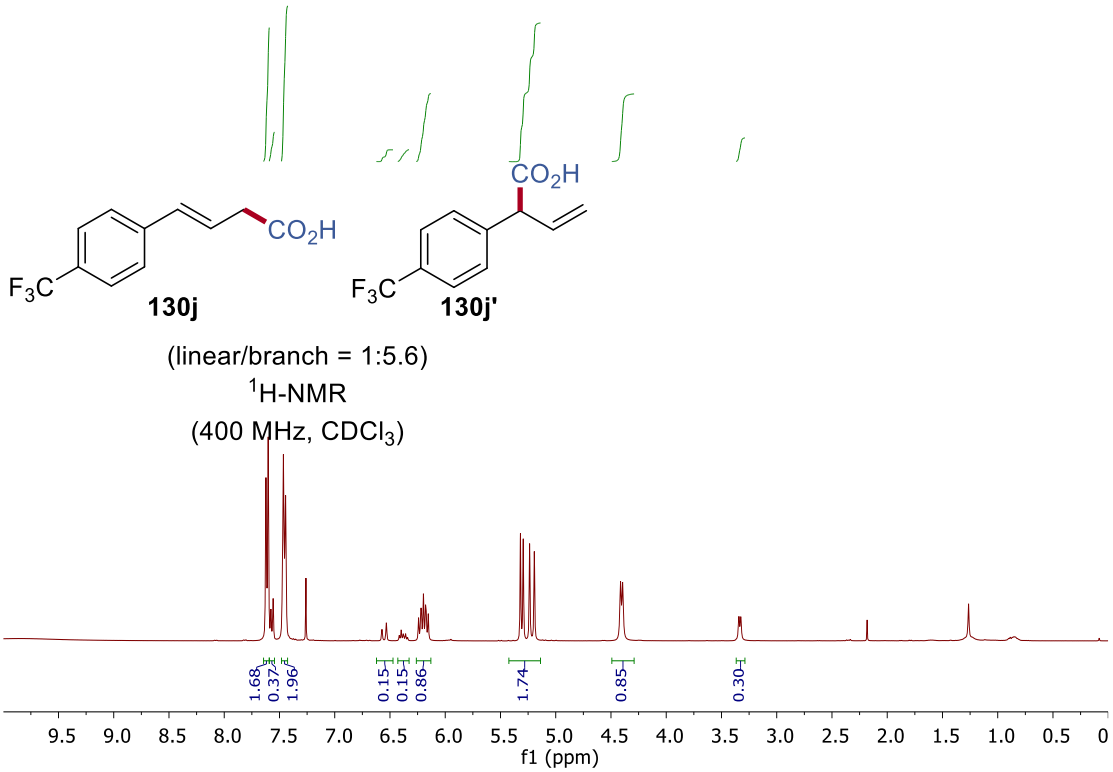
CO2H
F3C
130j
CO2H
F3C
130j'
(linear/branch = 1:5.6)
1H-NMR
(400 MHz, CDCl3)
1.68
0.37
1.96
0.15
0.15
0.86
1.74
0.85
0.30
9.5 9.0 8.5 8.0 7.5 7.0 6.5 6.0 5.5 5.0 4.5 4.0 3.5 3.0 2.5 2.0 1.5 1.0 0.5 0
f1 (ppm)

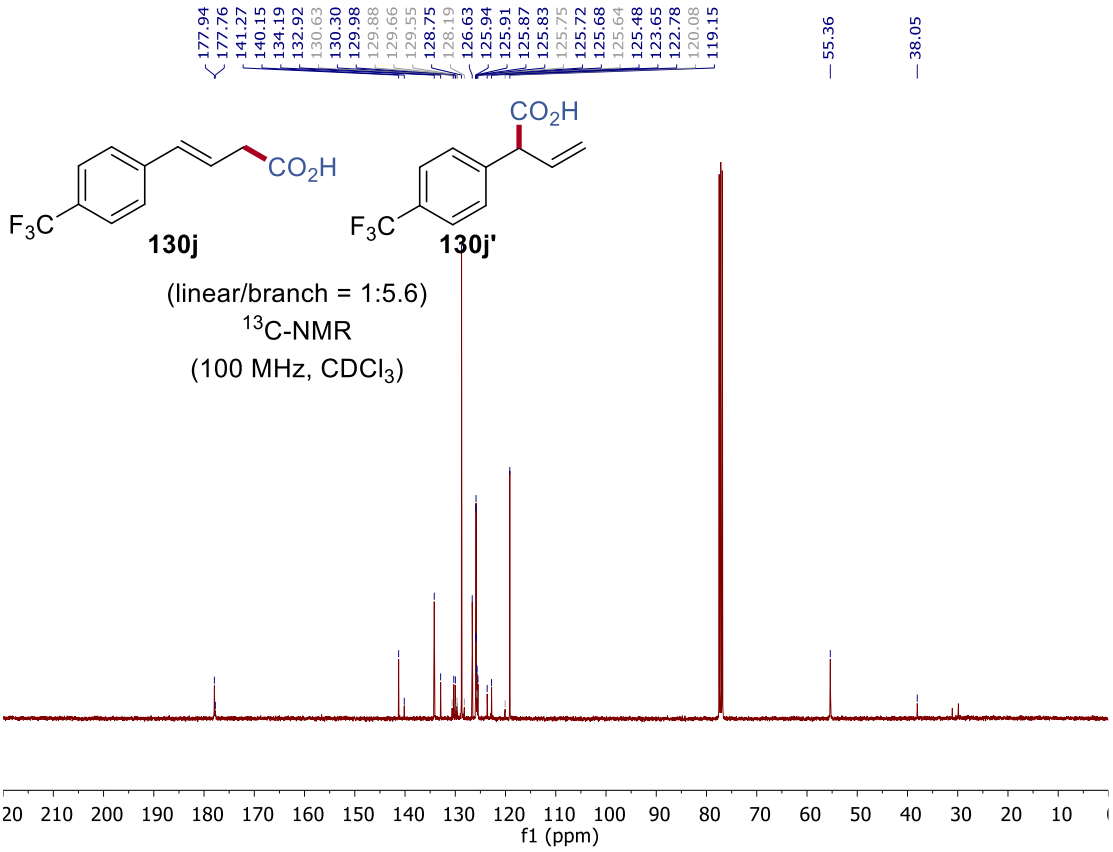
177.94
177.76
141.27
140.15
134.19
132.92
130.63
130.30
129.98
129.88
129.66
129.55
128.75
128.19
126.63
125.94
125.91
125.87
125.83
125.75
125.72
125.68
125.64
125.48
123.65
122.78
120.08
119.15
55.36
38.05
CO2H
F3C
130j
CO2H
F3C
130j'
(linear/branch = 1:5.6)
13C-NMR
(100 MHz, CDCl3)
20 210 200 190 180 170 160 150 140 130 120 110 100 90 80 70 60 50 40 30 20 10
f1 (ppm)

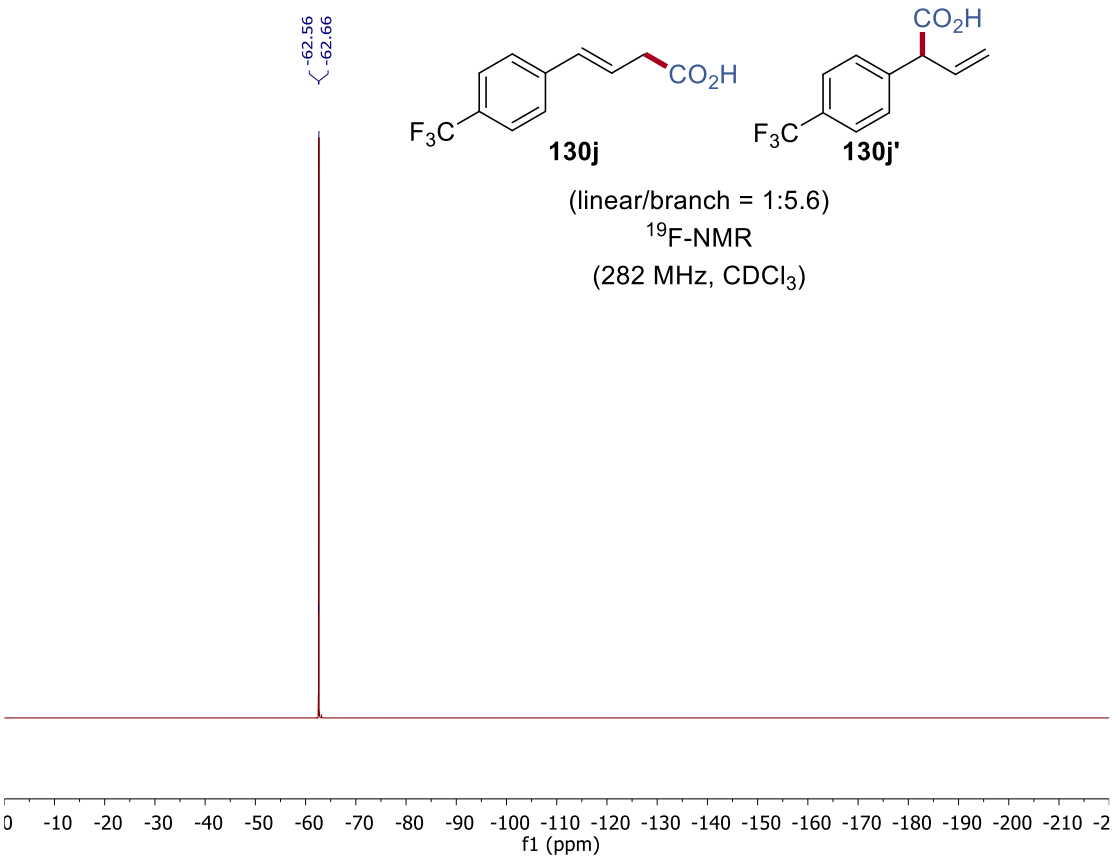

(linear/branch = 1:5.6)

^{19}F-NMR

(282 MHz, $CDCl_3$)

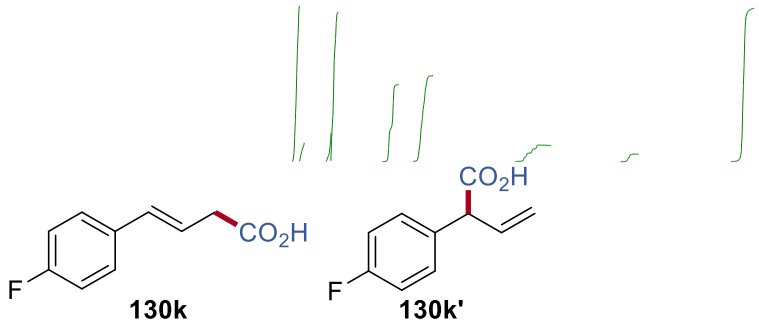

130k **130k'**

(linear/branch = 9:1)

^{1}H-NMR

(400 MHz, $CDCl_3$)

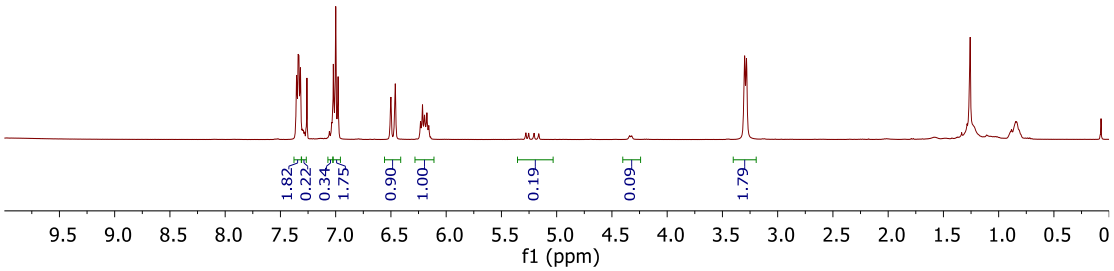

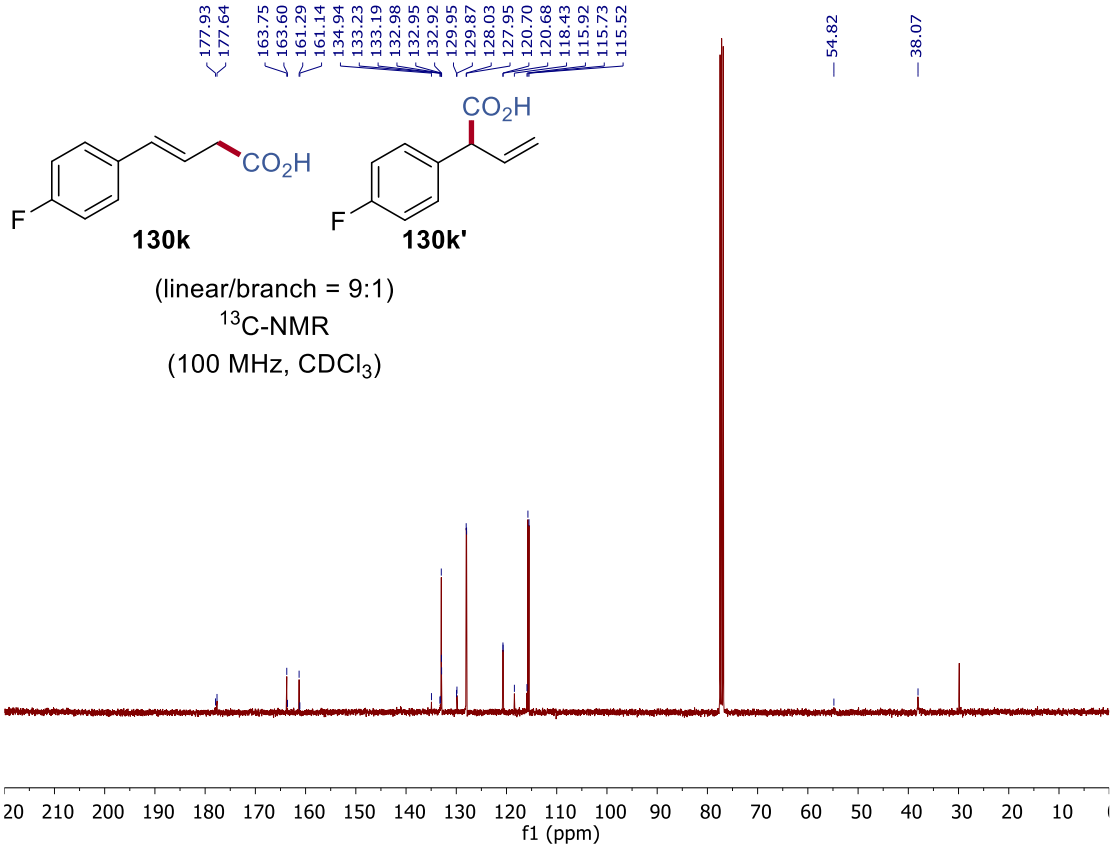

130k **130k'**

(linear/branch = 9:1)

^{13}C-NMR

(100 MHz, $CDCl_3$)

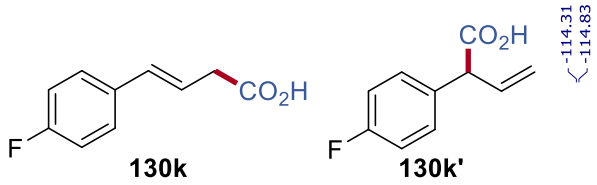

(linear/branch = 9:1)

^{19}F-NMR

(282 MHz, $CDCl_3$)

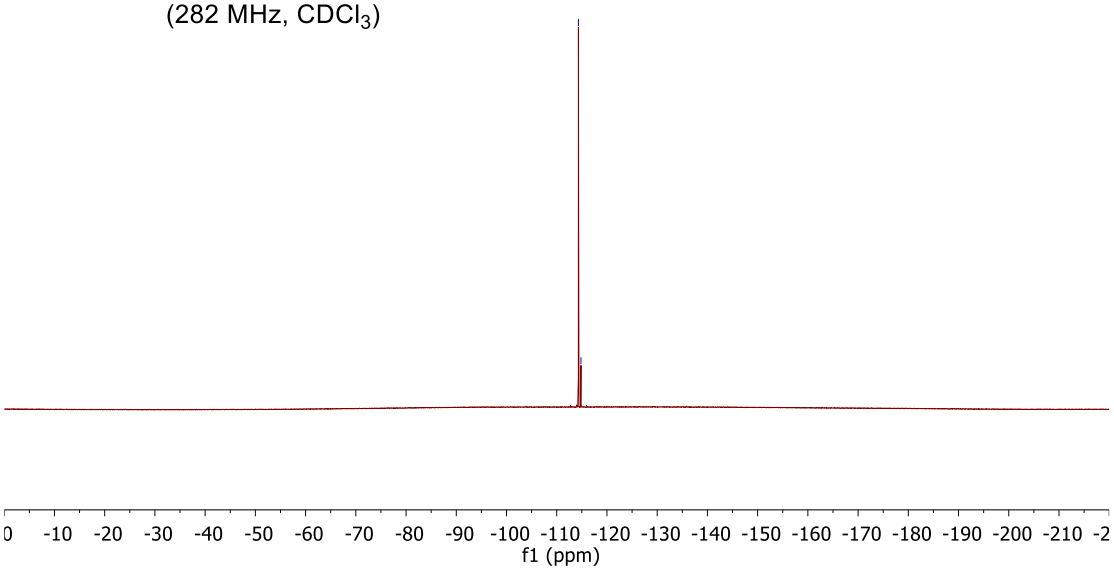

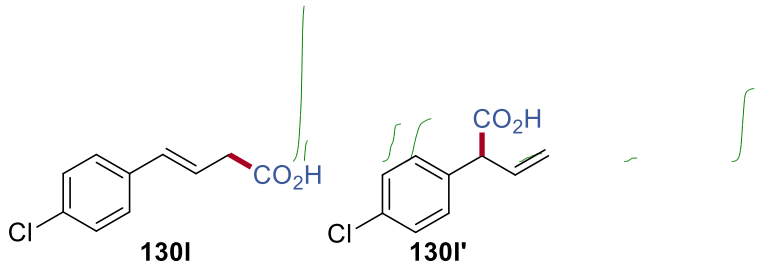

130l **130l'**

(linear/branch = 9:1)

^{1}H-NMR

(400 MHz, $CDCl_3$)

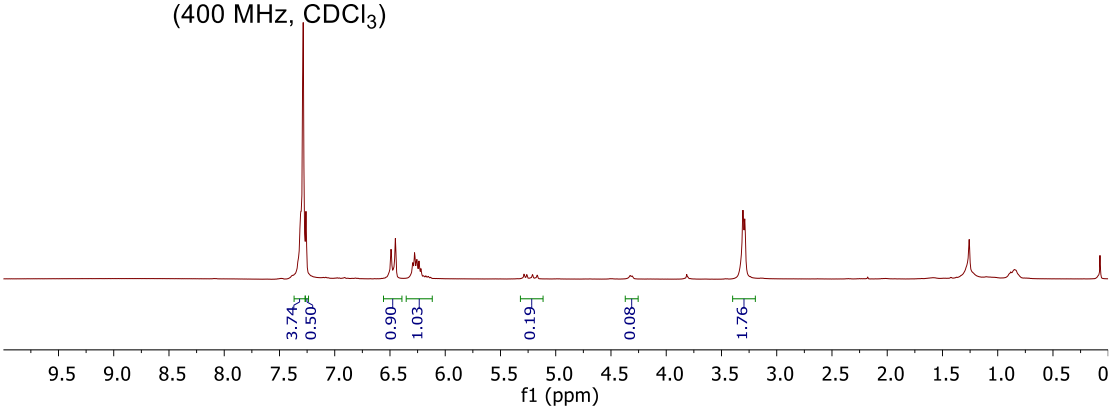

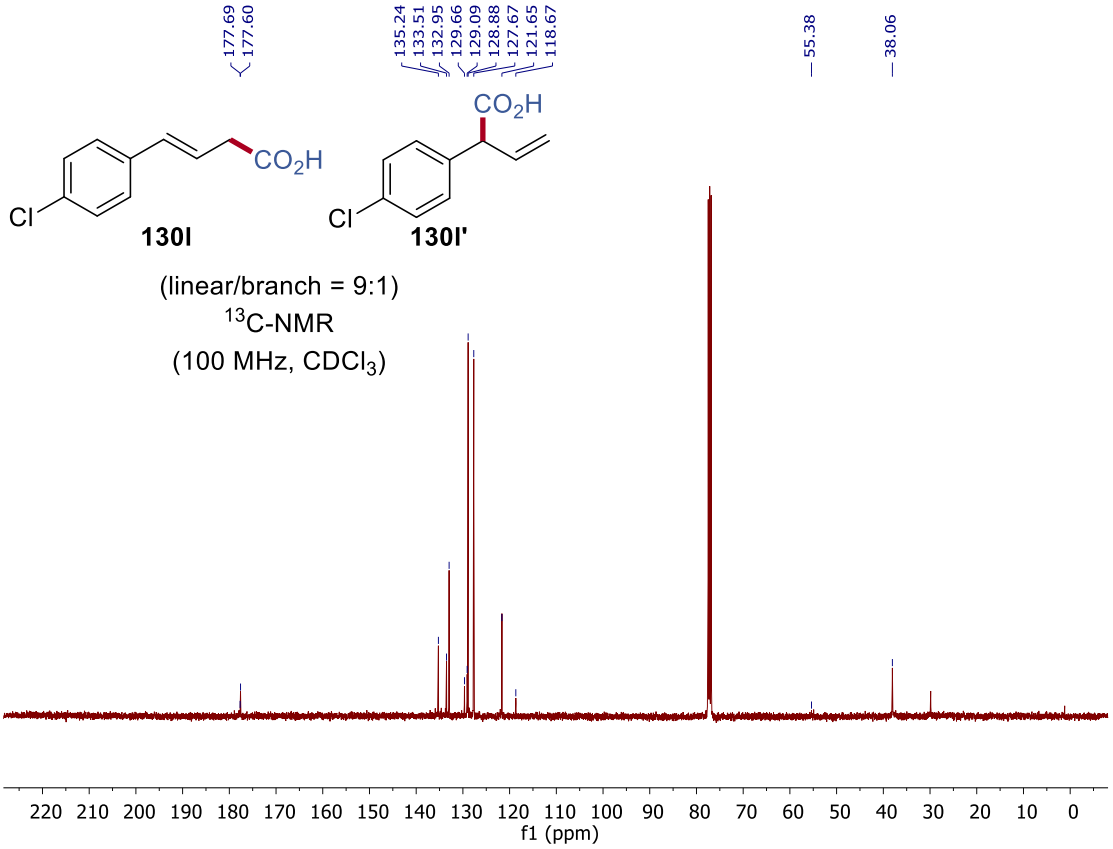

130l **130l'**

(linear/branch = 9:1)

^{13}C-NMR

(100 MHz, $CDCl_3$)

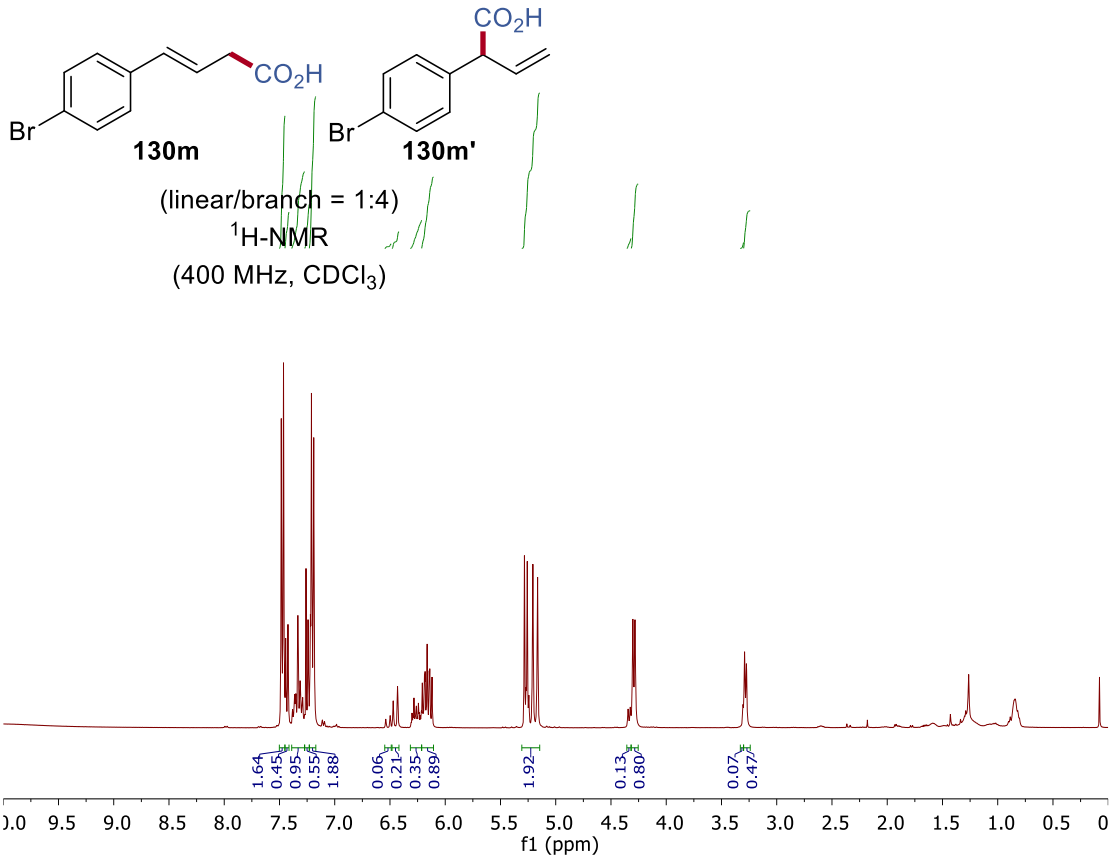
CO2H
Br
130m
CO2H
Br
130m'
(linear/branch = 1:4)
1H-NMR
(400 MHz, CDCl3)
1.64
0.45
0.95
0.55
1.88
0.06
0.21
0.35
0.89
1.92
0.13
0.80
0.07
0.47
f1 (ppm)

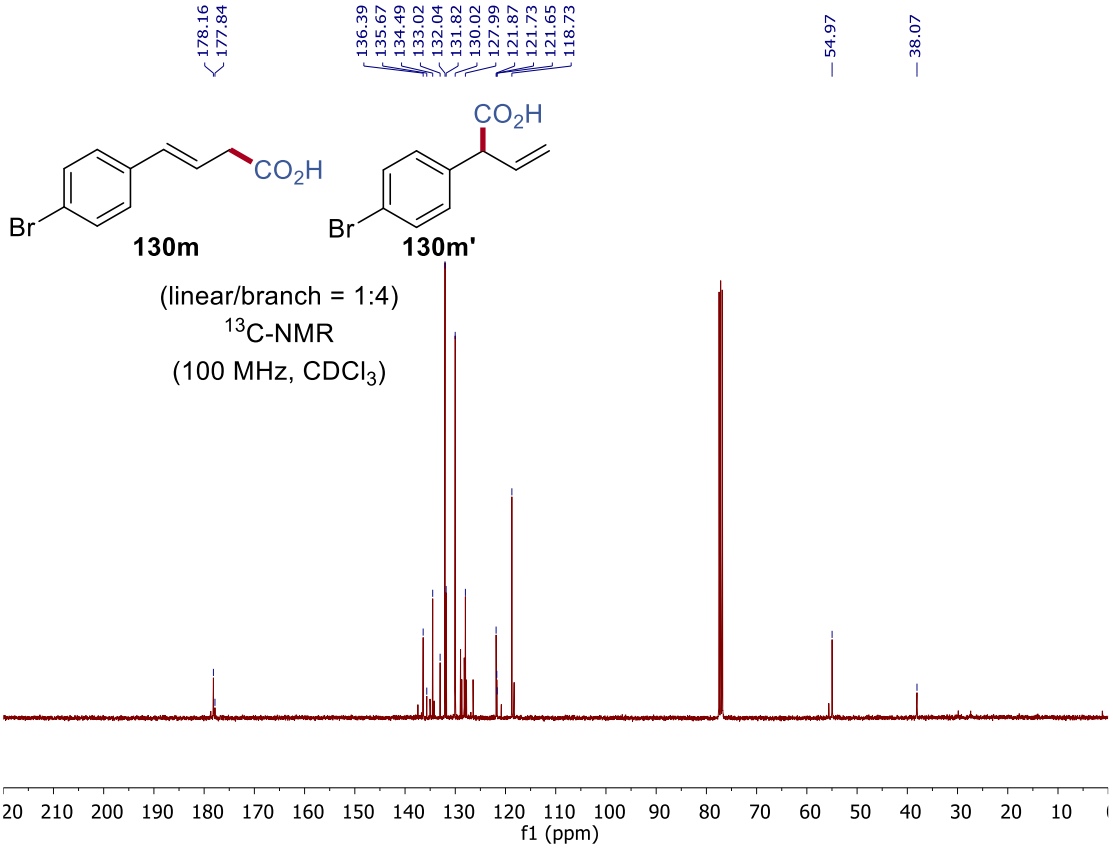
178.16
177.84
136.39
135.67
134.49
133.02
132.04
131.82
130.02
127.99
121.87
121.73
121.65
118.73
54.97
38.07
CO2H
Br
130m
CO2H
Br
130m'
(linear/branch = 1:4)
13C-NMR
(100 MHz, CDCl3)
f1 (ppm)

7.3 Electro-Reductive Nickel-Catalyzed Thiolations

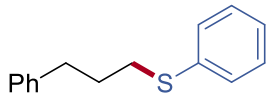

176aa

^{1}H-NMR

(300 MHz, $CDCl_3$)

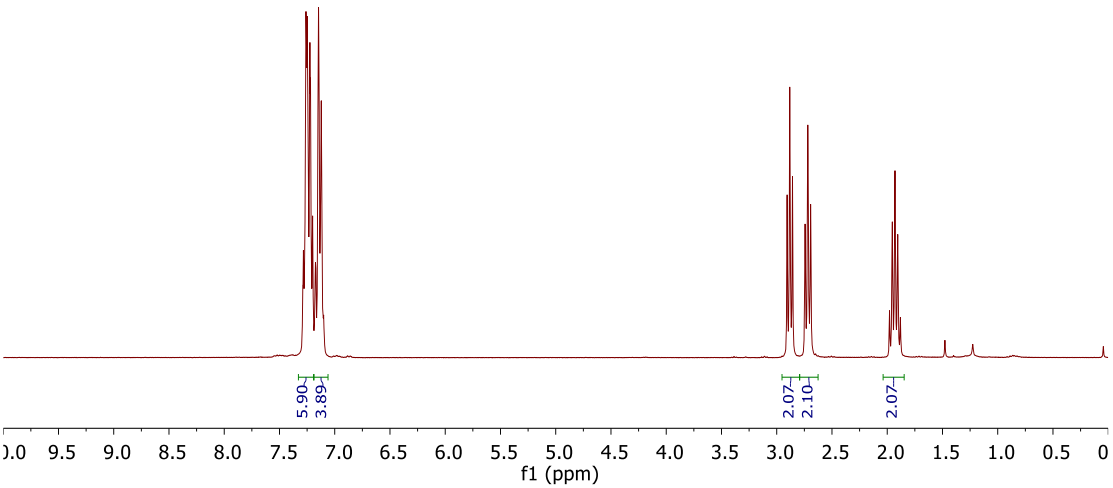

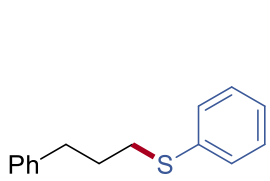

176aa

^{13}C-NMR

(75 MHz, $CDCl_3$)

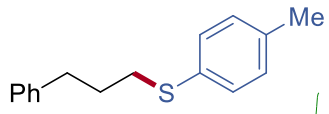

176ab

^{1}H-NMR

(300 MHz, $CDCl_3$)

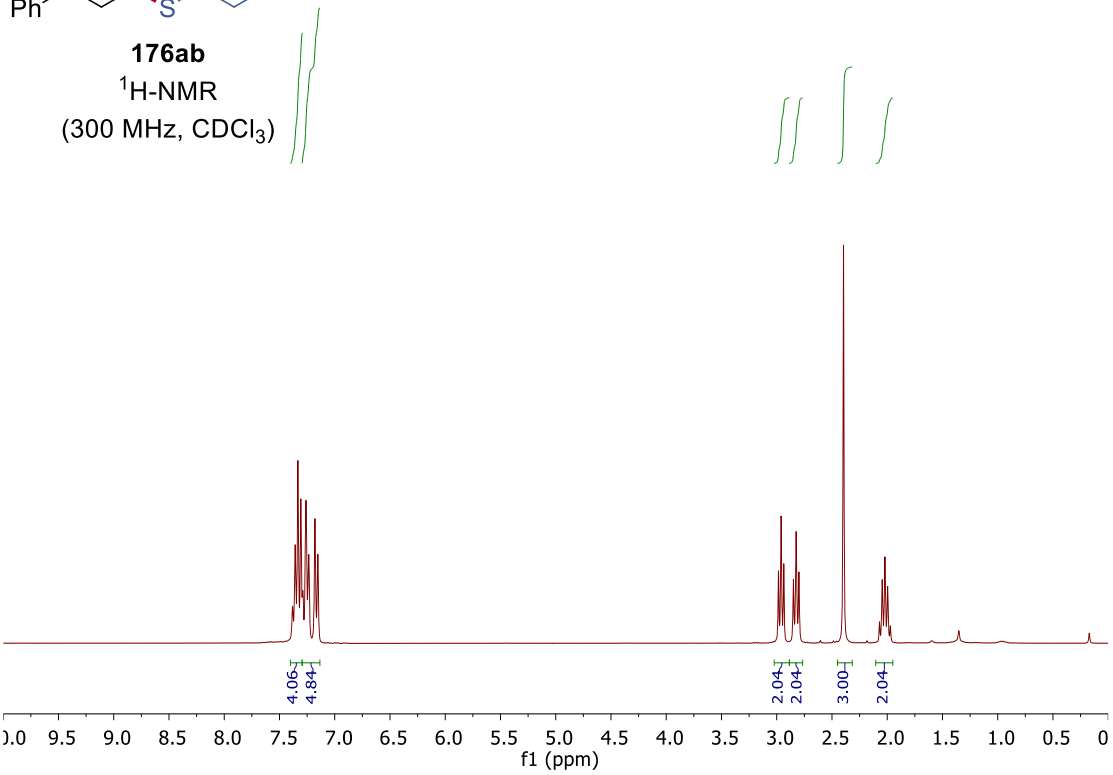

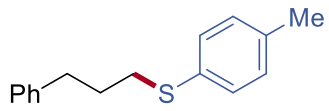

176ab

^{13}C-NMR

(75 MHz, $CDCl_3$)

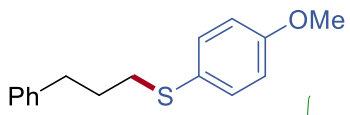

176ac

^{1}H-NMR

(300 MHz, $CDCl_3$)

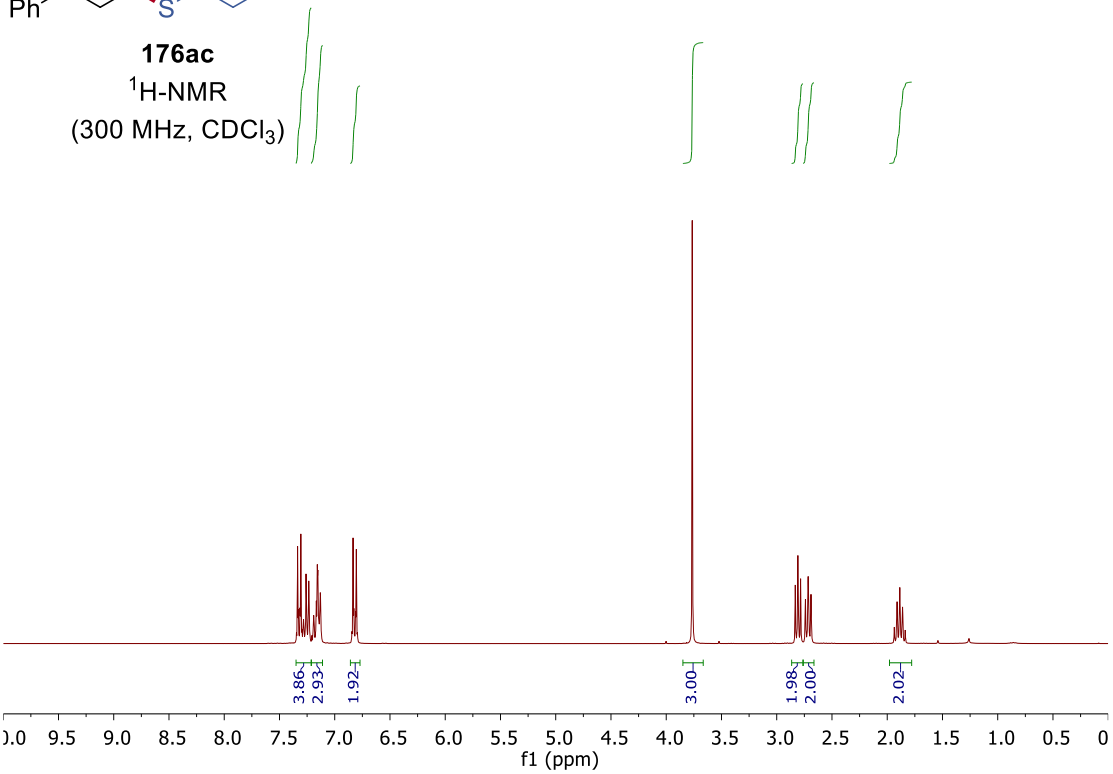

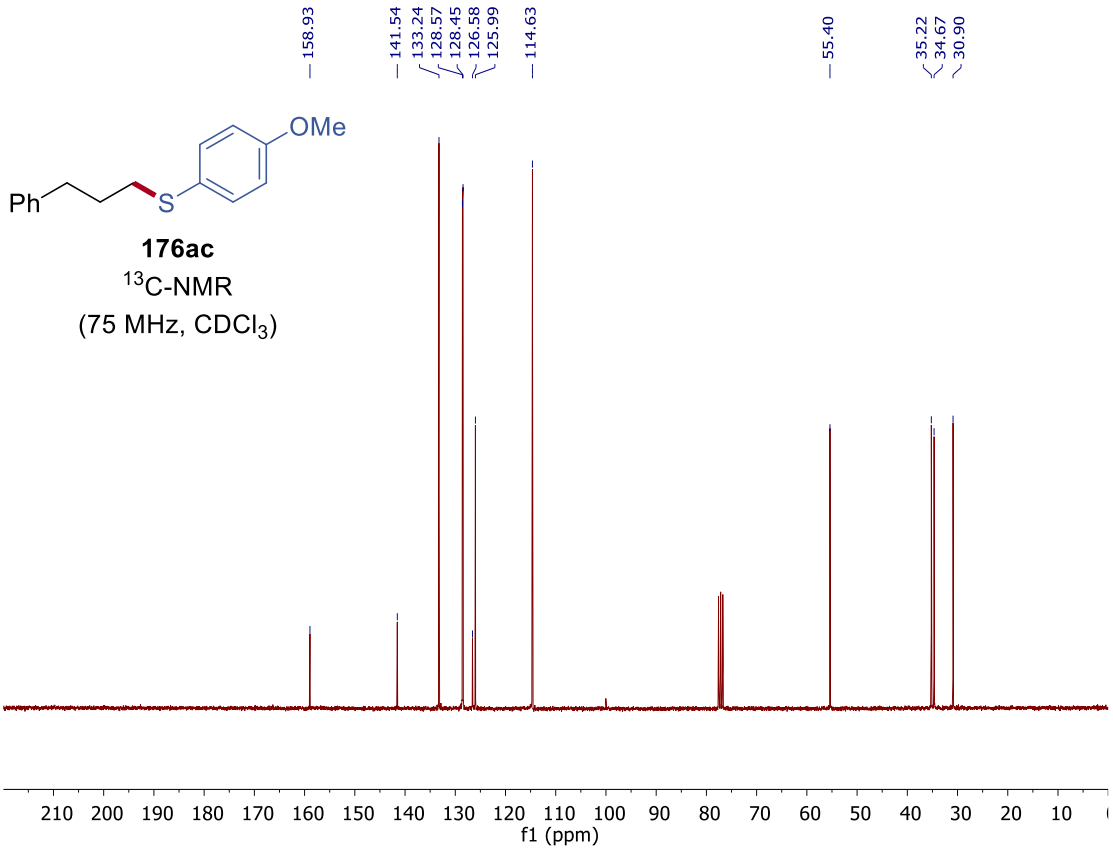

176ac

^{13}C-NMR

(75 MHz, $CDCl_3$)

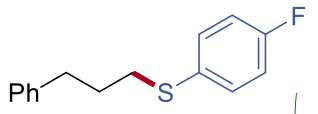

176ad

^{1}H-NMR

(300 MHz, $CDCl_3$)

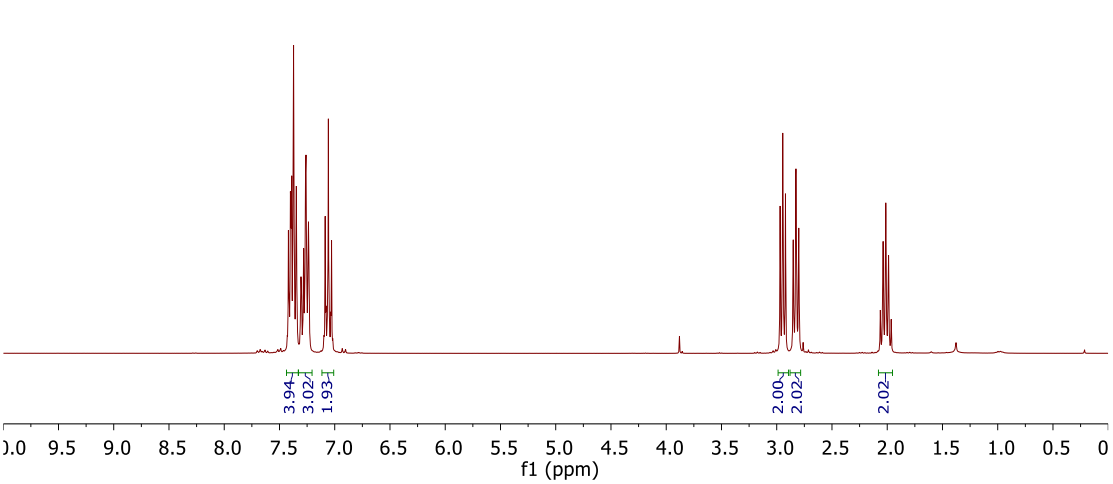

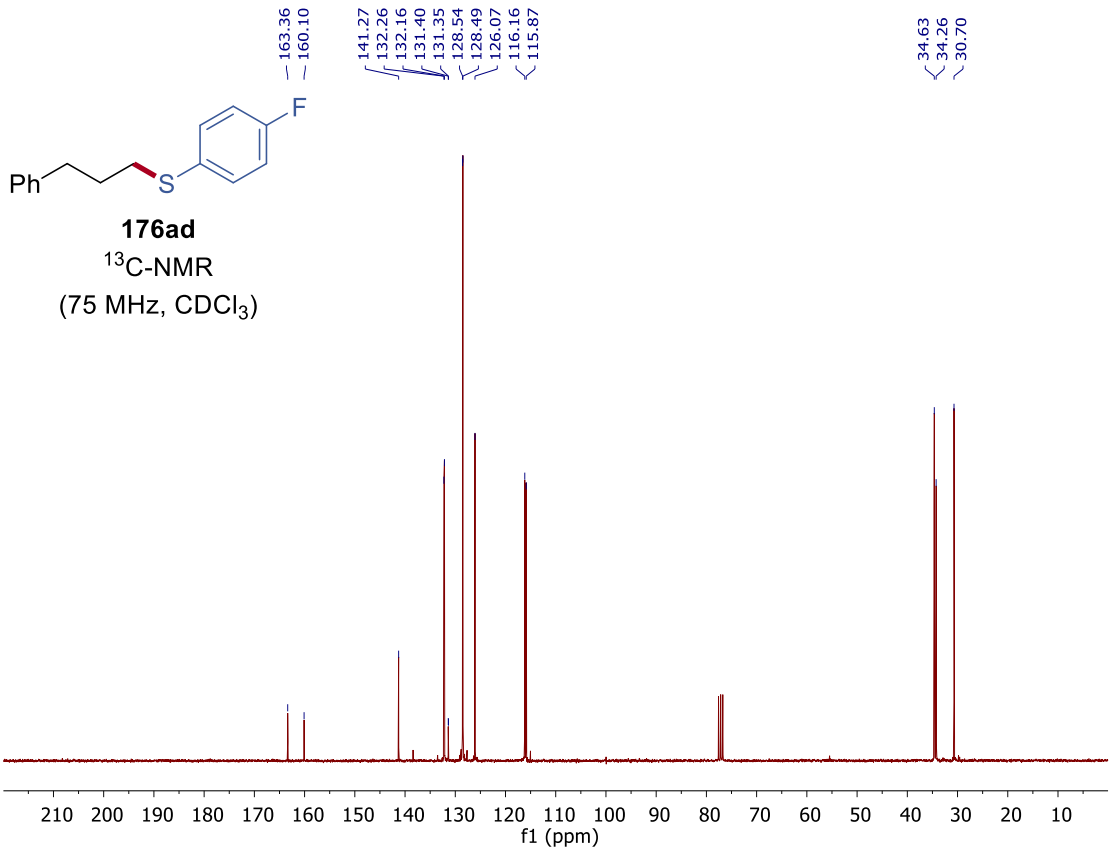

176ad

^{13}C-NMR

(75 MHz, $CDCl_3$)

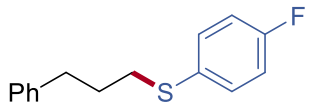

176ad

^{19}F-NMR

(282 MHz, $CDCl_3$)

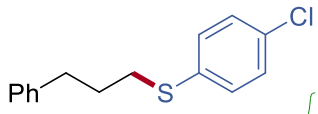

176ae

^{1}H-NMR

(300 MHz, $CDCl_3$)

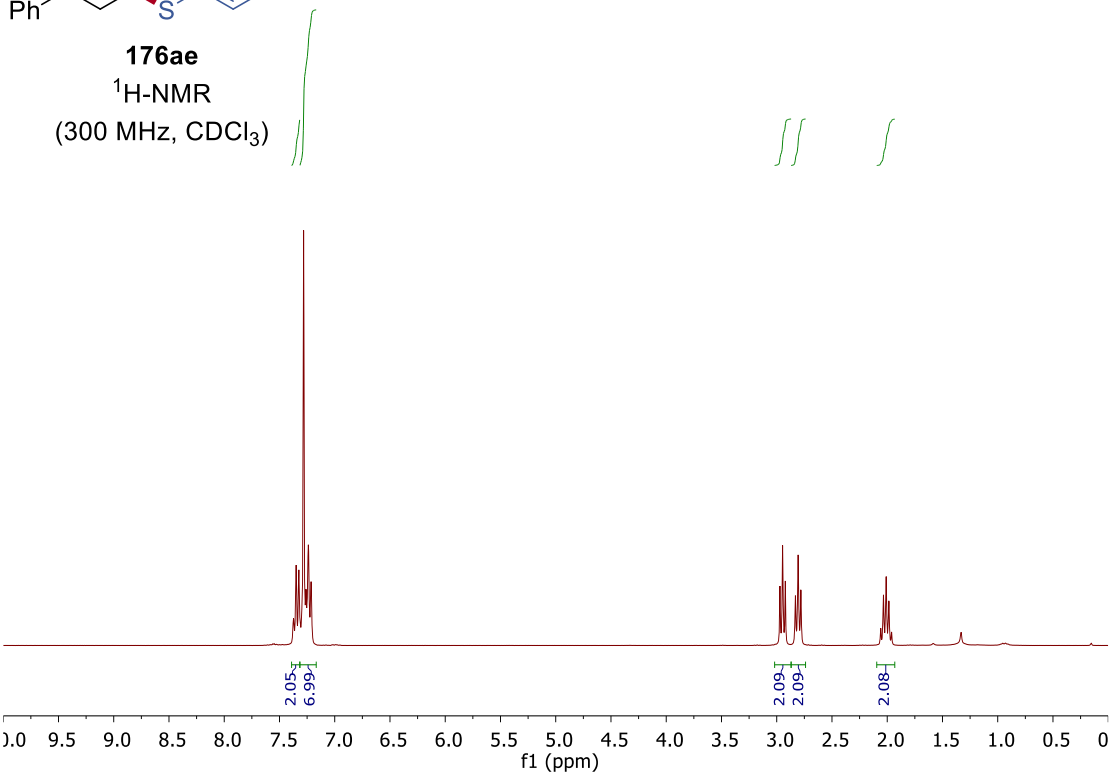

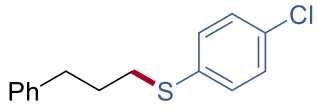

176ae

^{13}C-NMR

(75 MHz, $CDCl_3$)

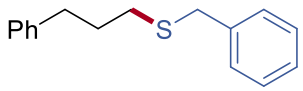

176af

^{1}H-NMR

(300 MHz, $CDCl_3$)

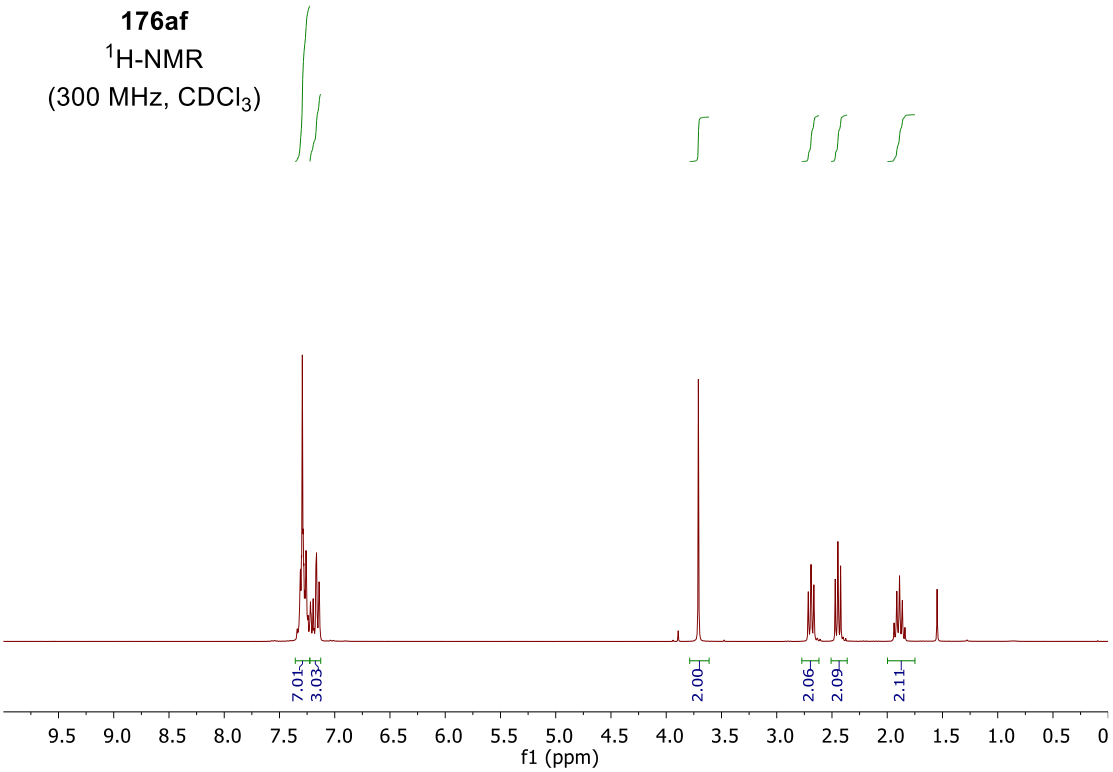

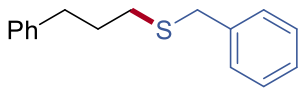

176af

^{13}C-NMR

(75 MHz, $CDCl_3$)

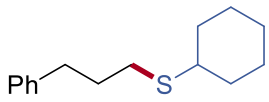

176ag

^{1}H-NMR

(300 MHz, $CDCl_3$)

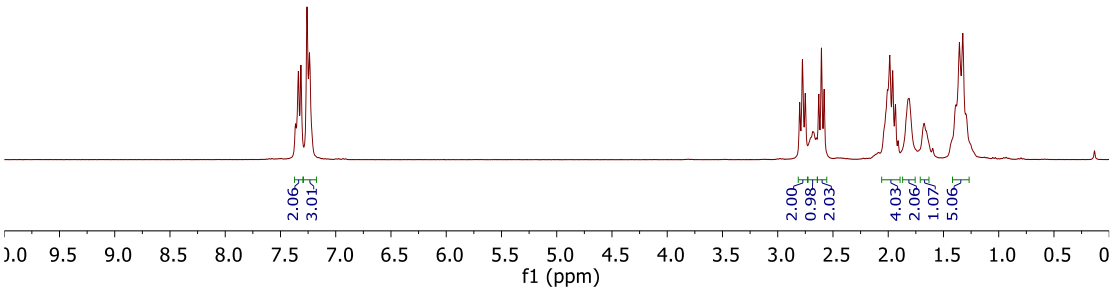

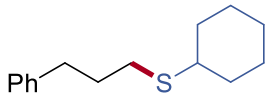

176ag

^{13}C-NMR

(75 MHz, $CDCl_3$)

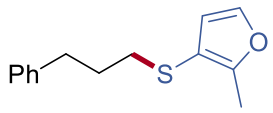

176ah

^{1}H-NMR

(300 MHz, $CDCl_3$)

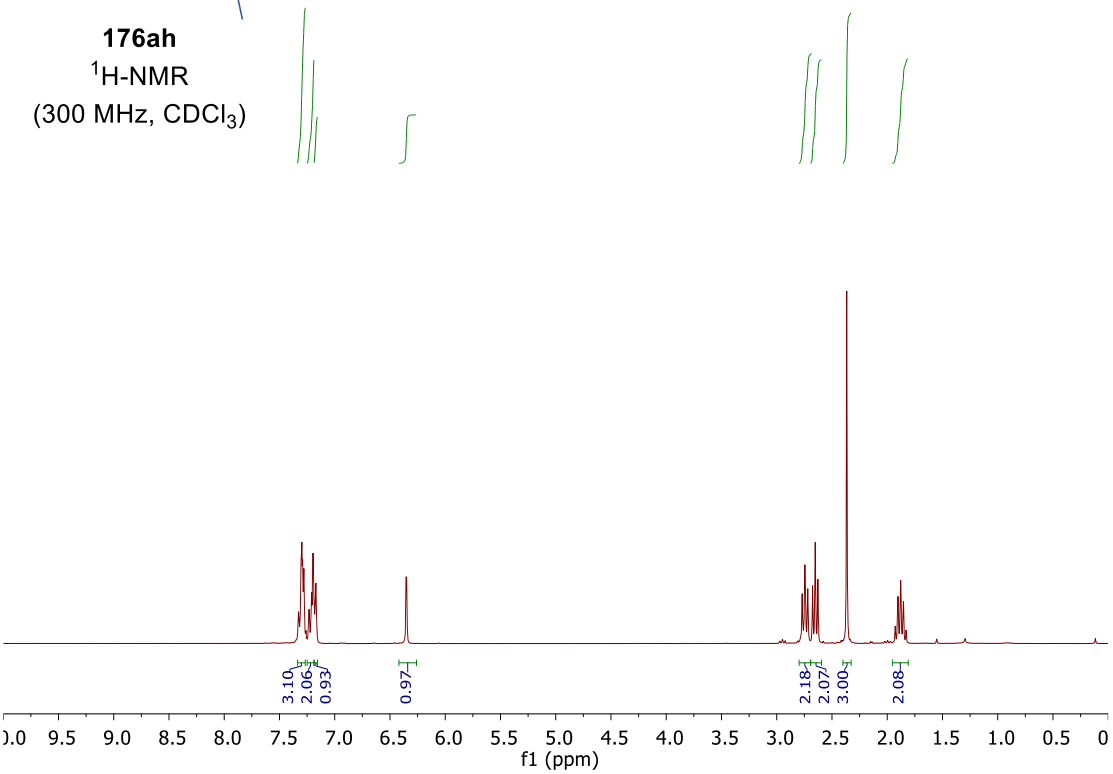

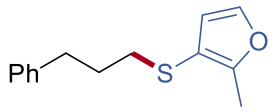

176ah

^{13}C-NMR

(75 MHz, $CDCl_3$)

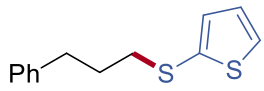

176ai

^{1}H-NMR

(300 MHz, $CDCl_3$)

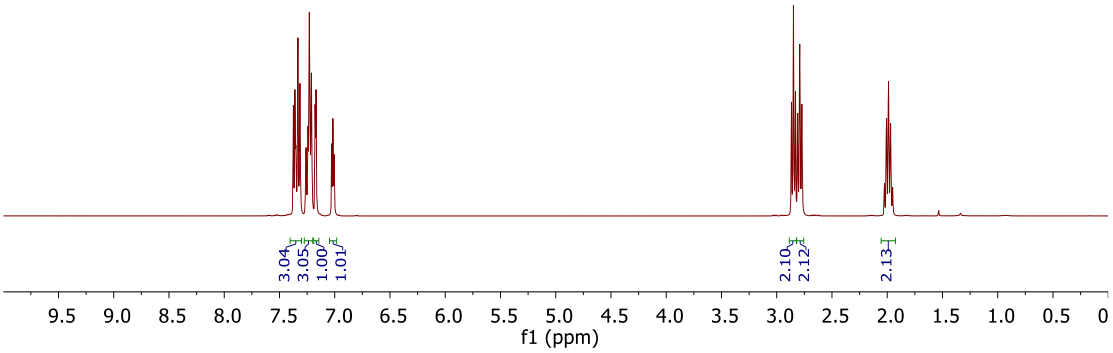

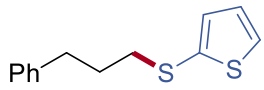

176ai

^{13}C-NMR

(75 MHz, $CDCl_3$)

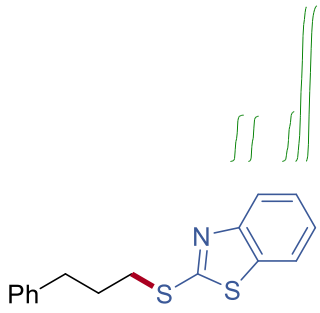

176aj

^{1}H-NMR

(400 MHz, $CDCl_3$)

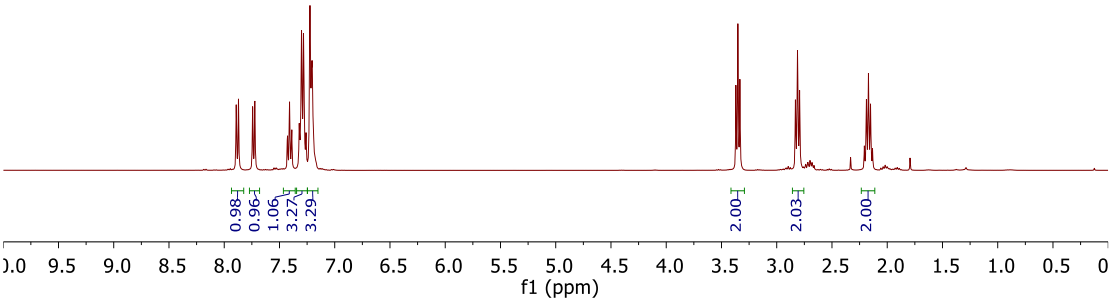

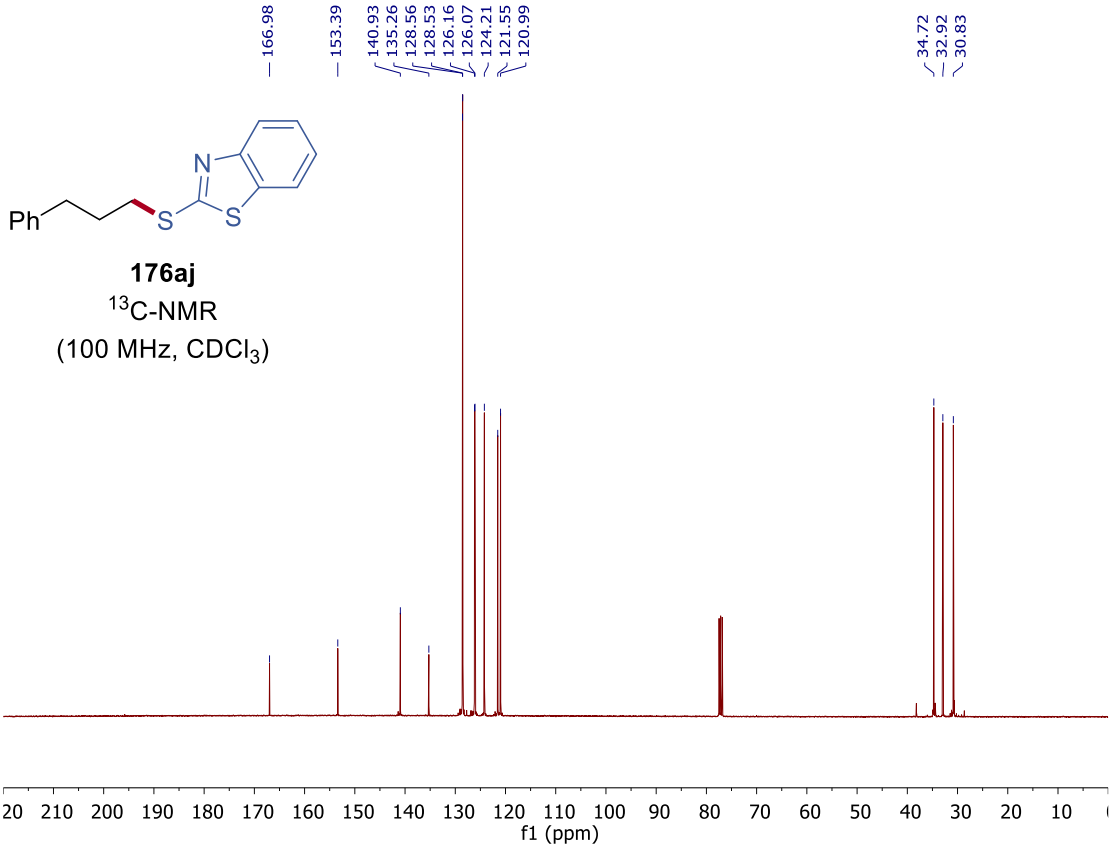

176aj

^{13}C-NMR

(100 MHz, $CDCl_3$)

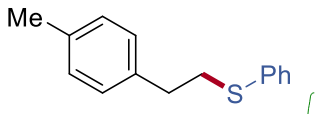

176ba

^{1}H-NMR

(300 MHz, $CDCl_3$)

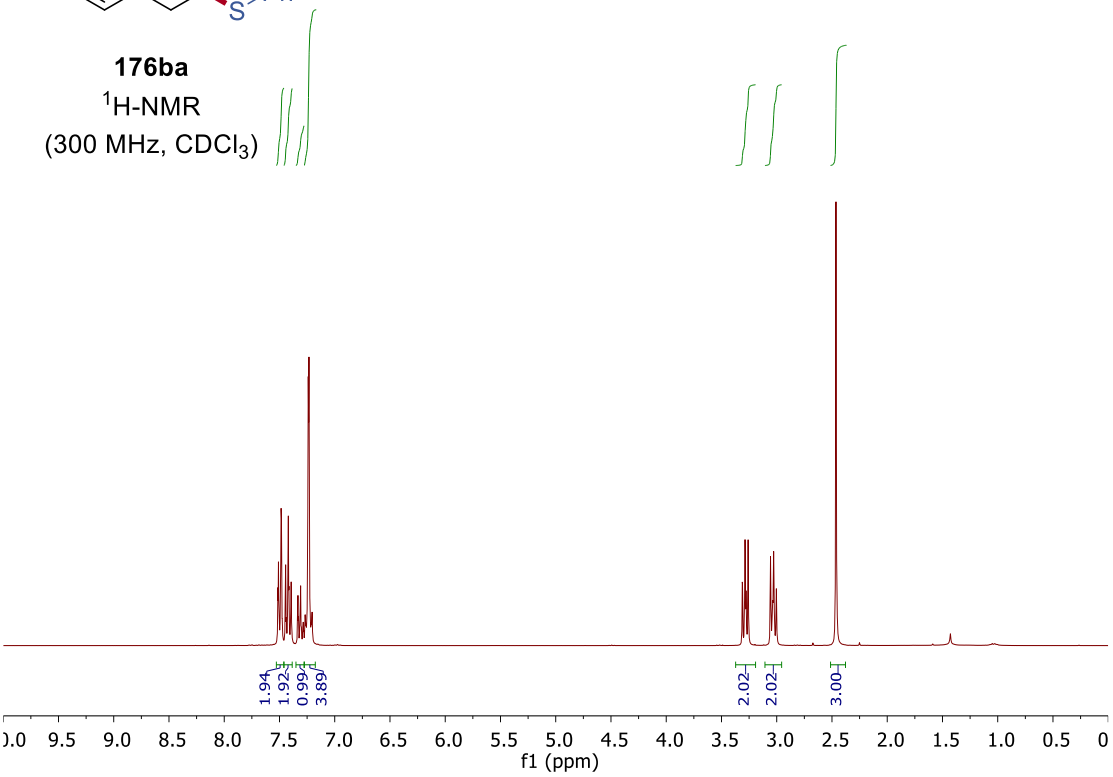

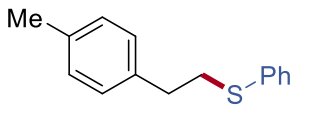

176ba

^{13}C-NMR

(75 MHz, $CDCl_3$)

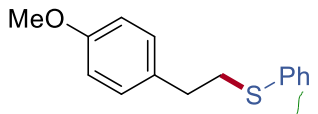

176ca

^{1}H-NMR

(300 MHz, $CDCl_3$)

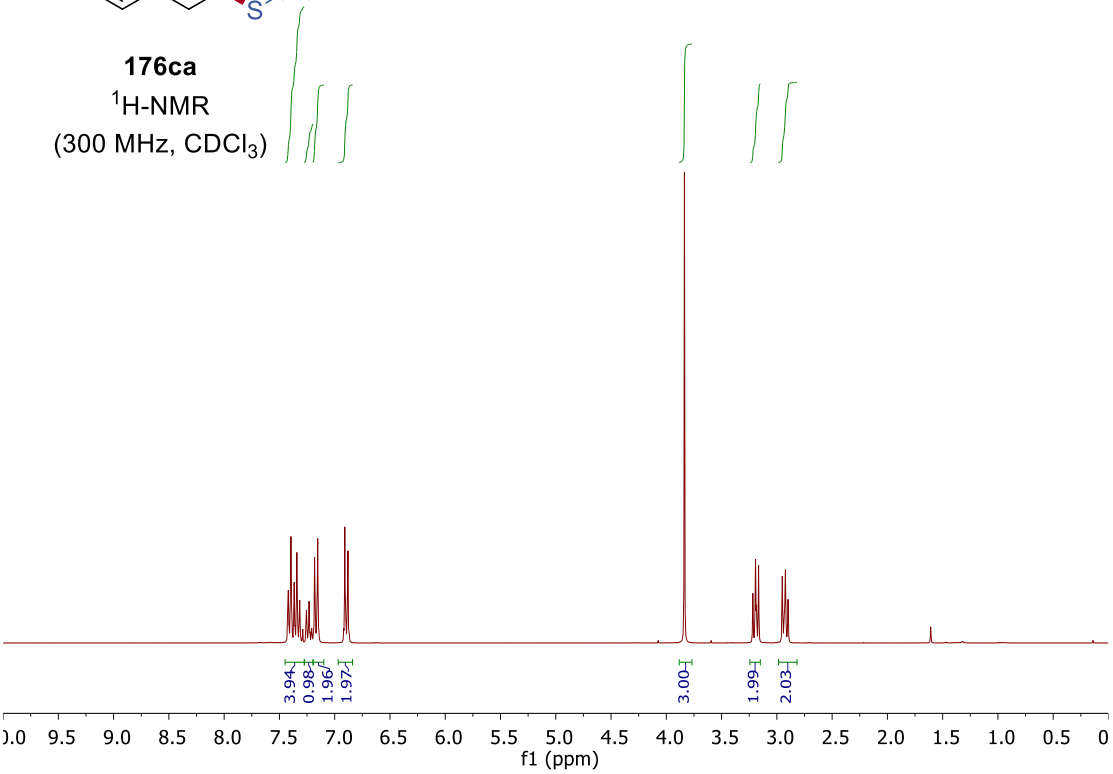

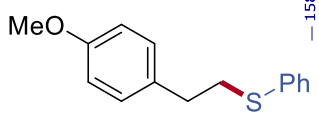

176ca

^{13}C-NMR

(75 MHz, $CDCl_3$)

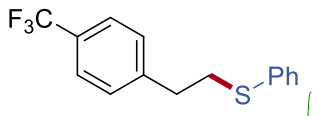

176da

^{1}H-NMR

(300 MHz, $CDCl_3$)

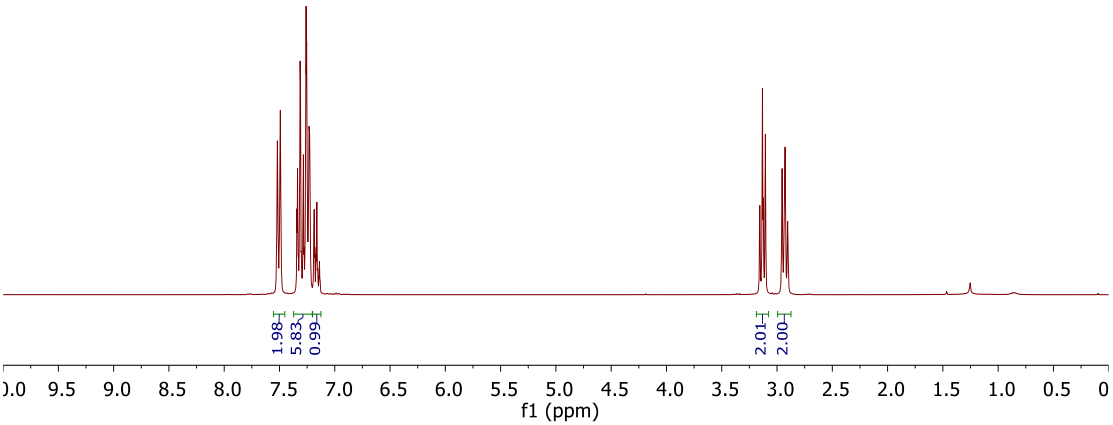

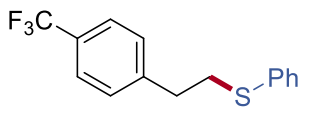

176da

^{13}C-NMR

(75 MHz, $CDCl_3$)

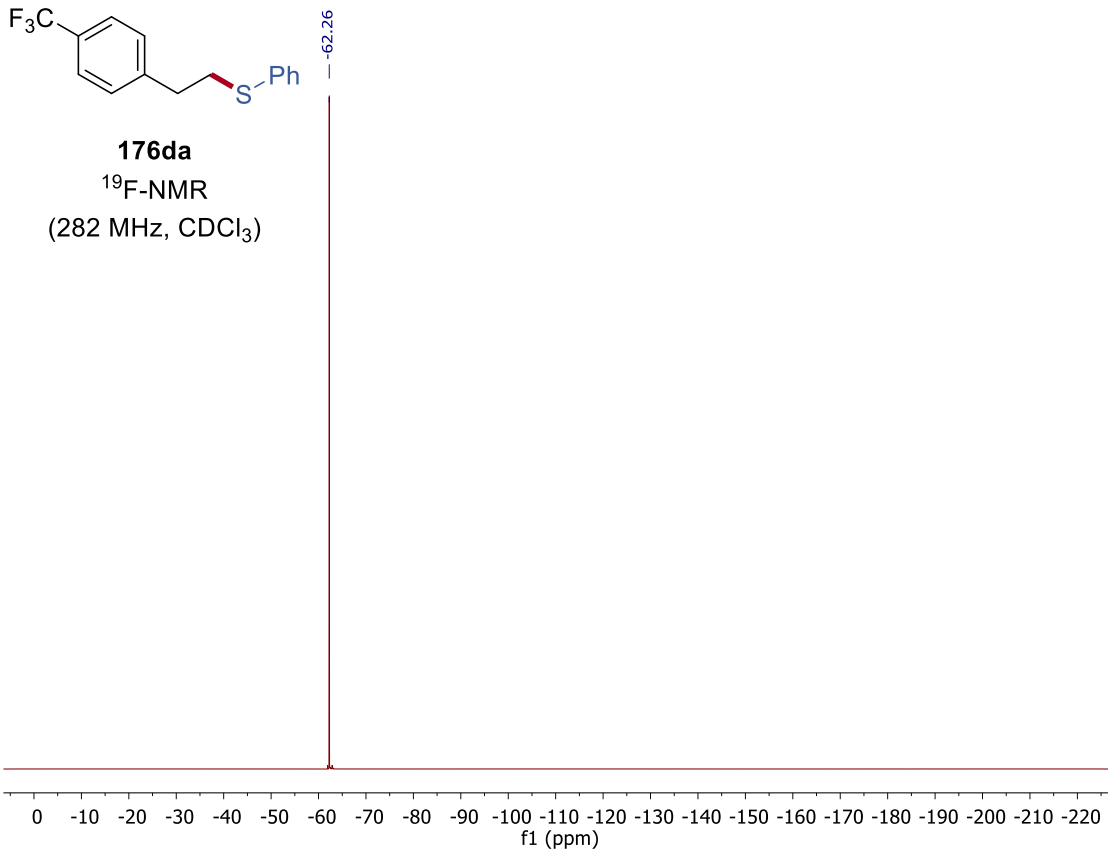

176da

^{19}F-NMR

(282 MHz, $CDCl_3$)

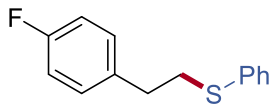

176ea

^{1}H-NMR

(300 MHz, $CDCl_3$)

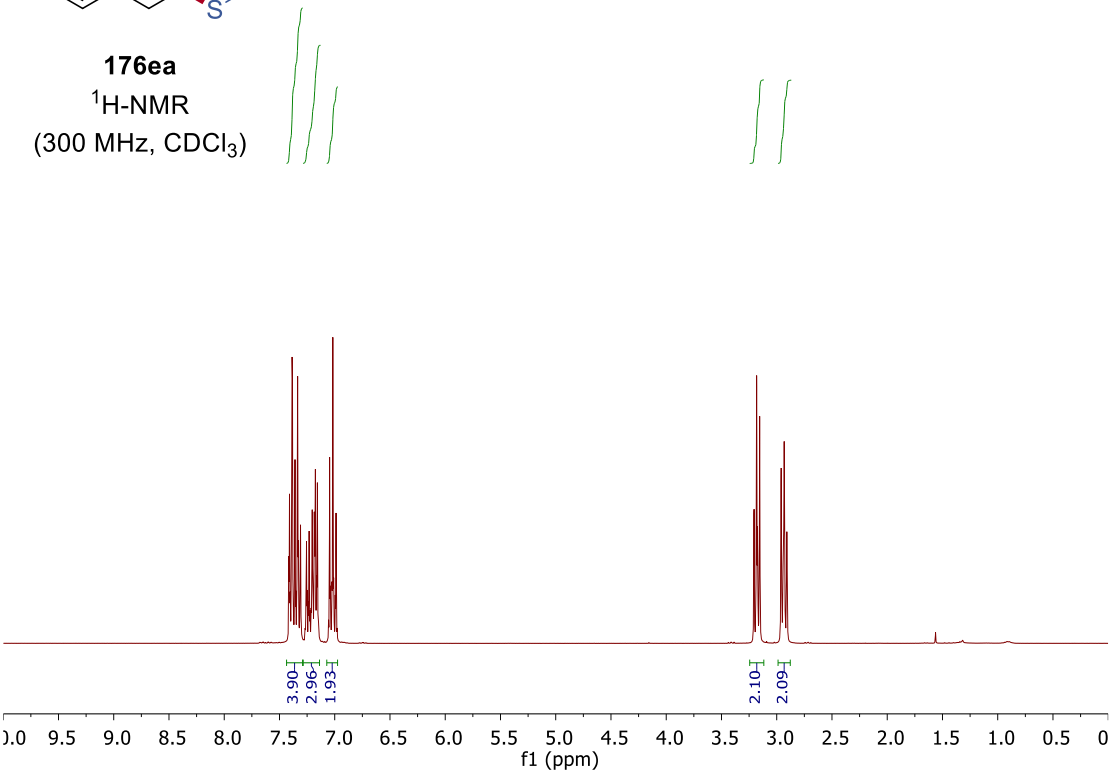

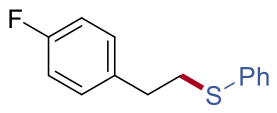

176ea

^{13}C-NMR

(75 MHz, $CDCl_3$)

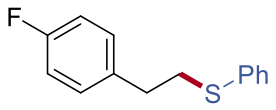

176ea

^{19}F-NMR

(282 MHz, $CDCl_3$)

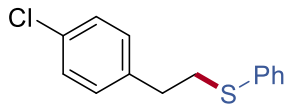

176fa

^{1}H-NMR

(300 MHz, $CDCl_3$)

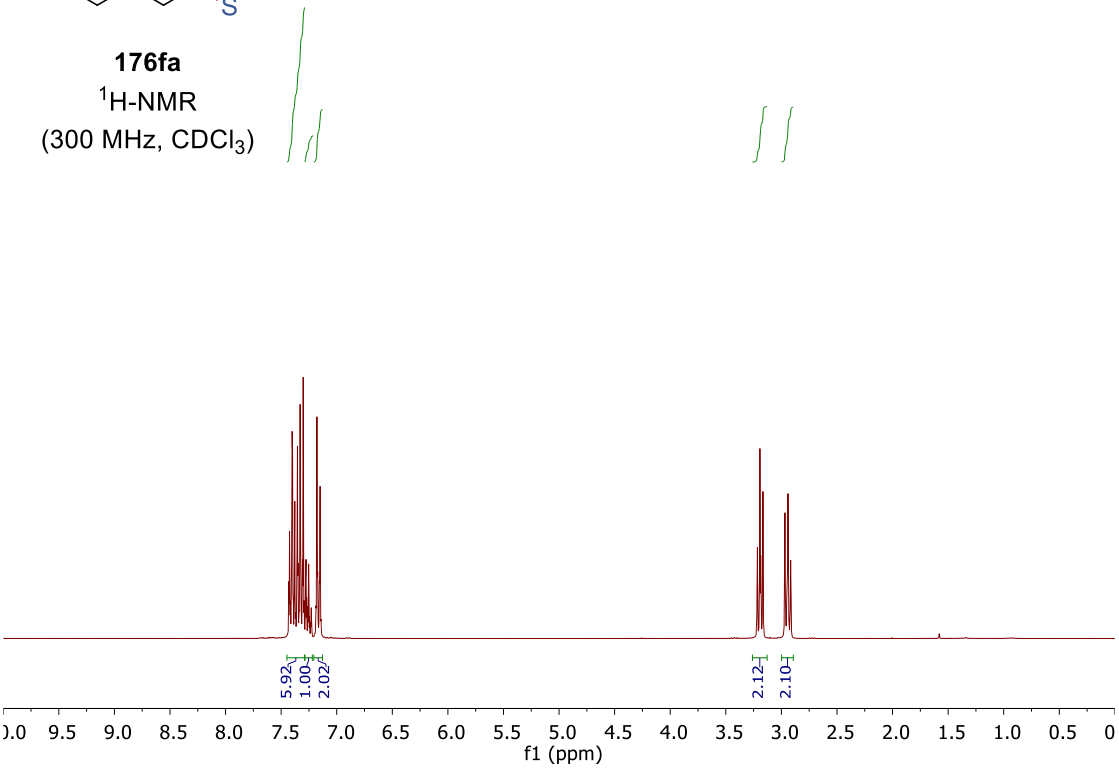

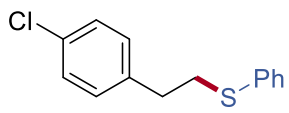

176fa

^{13}C-NMR

(75 MHz, $CDCl_3$)

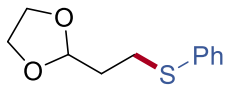

176ga

^{1}H-NMR

(400 MHz, $CDCl_3$)

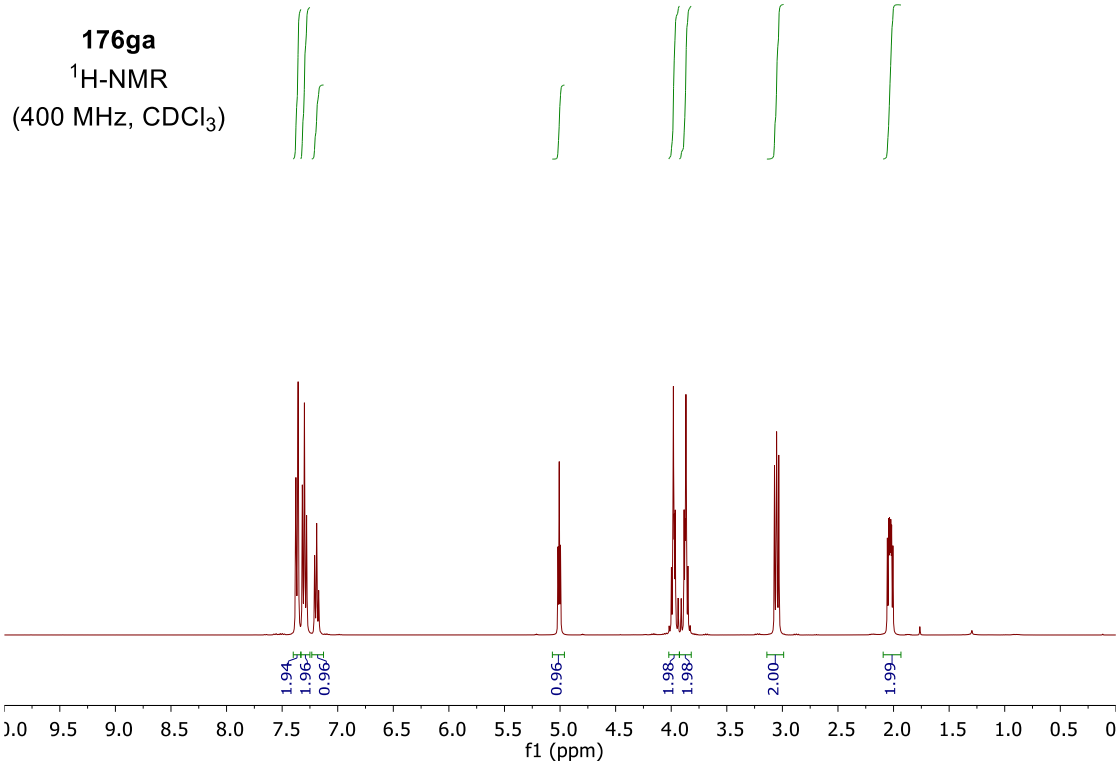

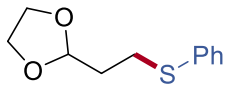

176ga

^{13}C-NMR

(100 MHz, $CDCl_3$)

176ha

^{1}H-NMR

(400 MHz, $CDCl_3$)

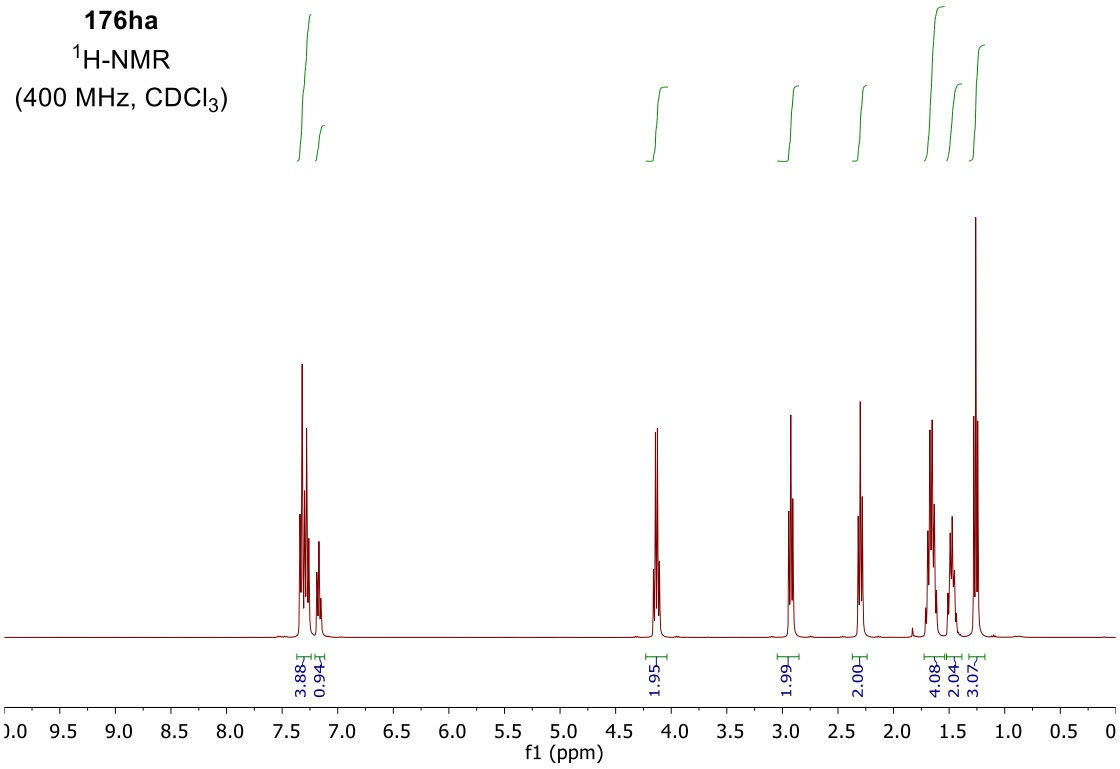

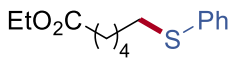

176ha

^{13}C-NMR

(100 MHz, $CDCl_3$)

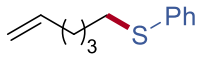

176ia

^{1}H-NMR

(400 MHz, $CDCl_3$)

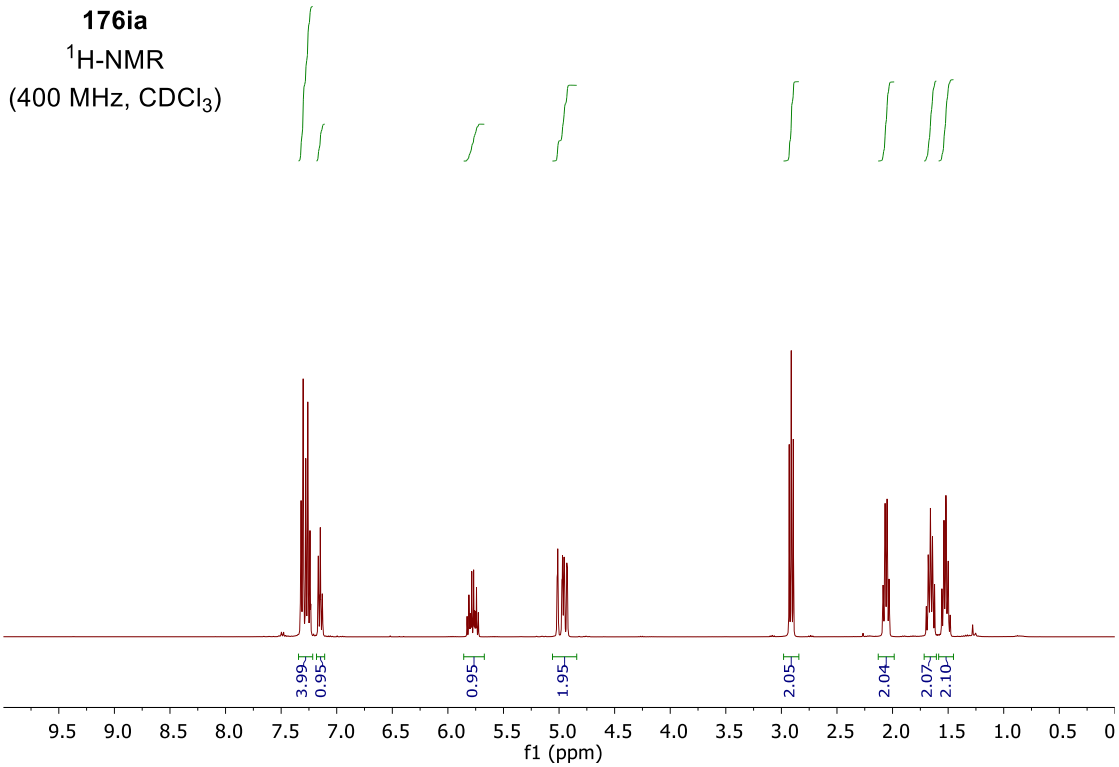

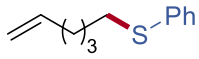

176ia

^{13}C-NMR

(100 MHz, $CDCl_3$)

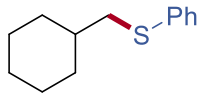

176ja

^{1}H-NMR

(300 MHz, $CDCl_3$)

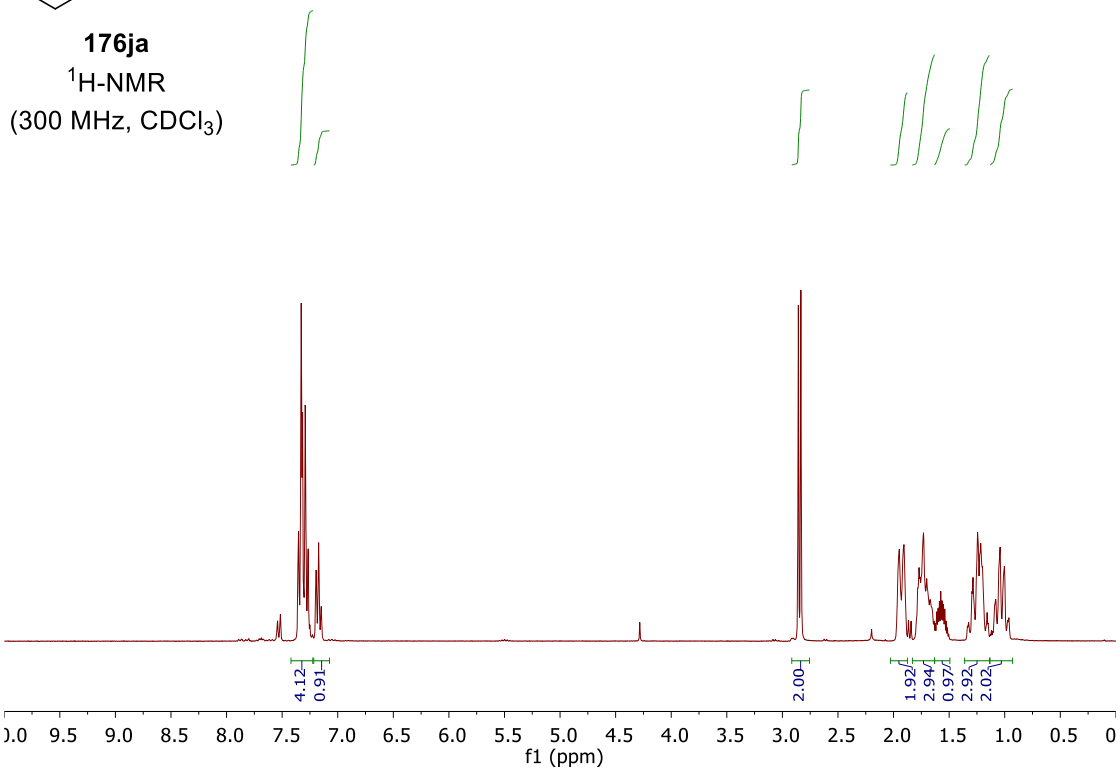

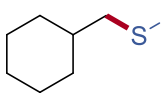

176ja

^{13}C-NMR

(75 MHz, $CDCl_3$)

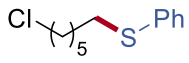

176ka

^{1}H-NMR

(400 MHz, $CDCl_3$)

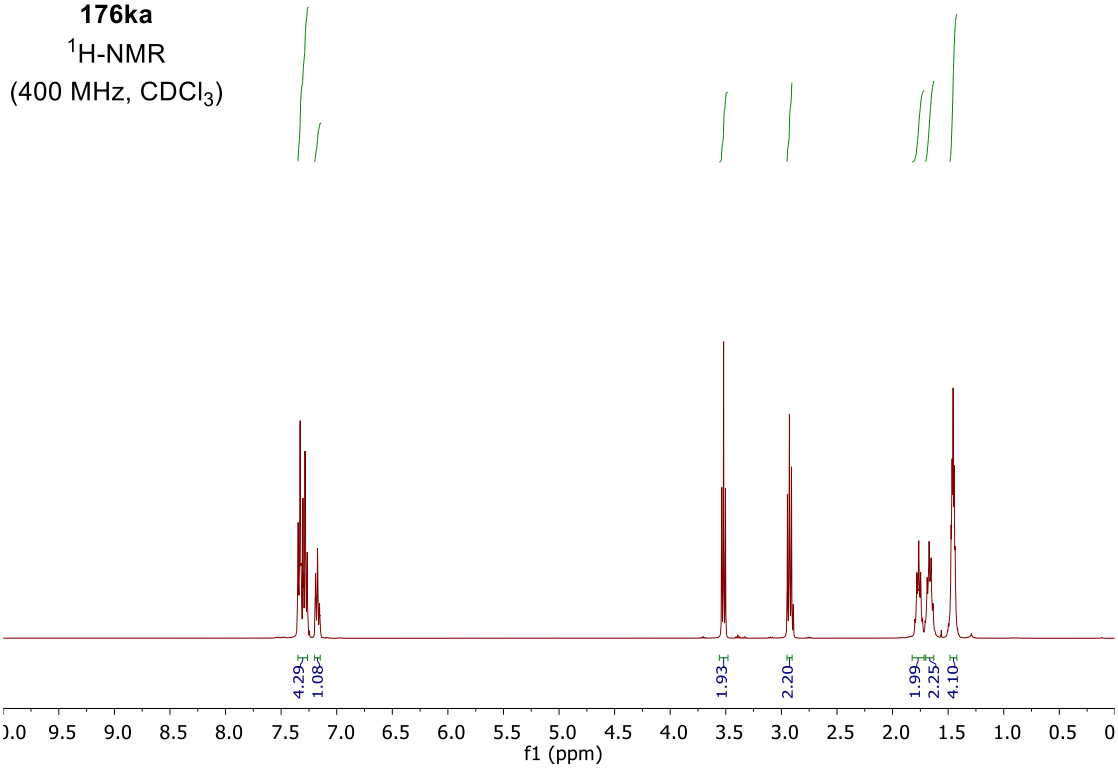

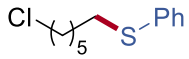

176ka

^{13}C-NMR

(100 MHz, $CDCl_3$)

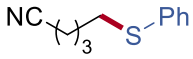

176la

^{1}H-NMR

(300 MHz, $CDCl_3$)

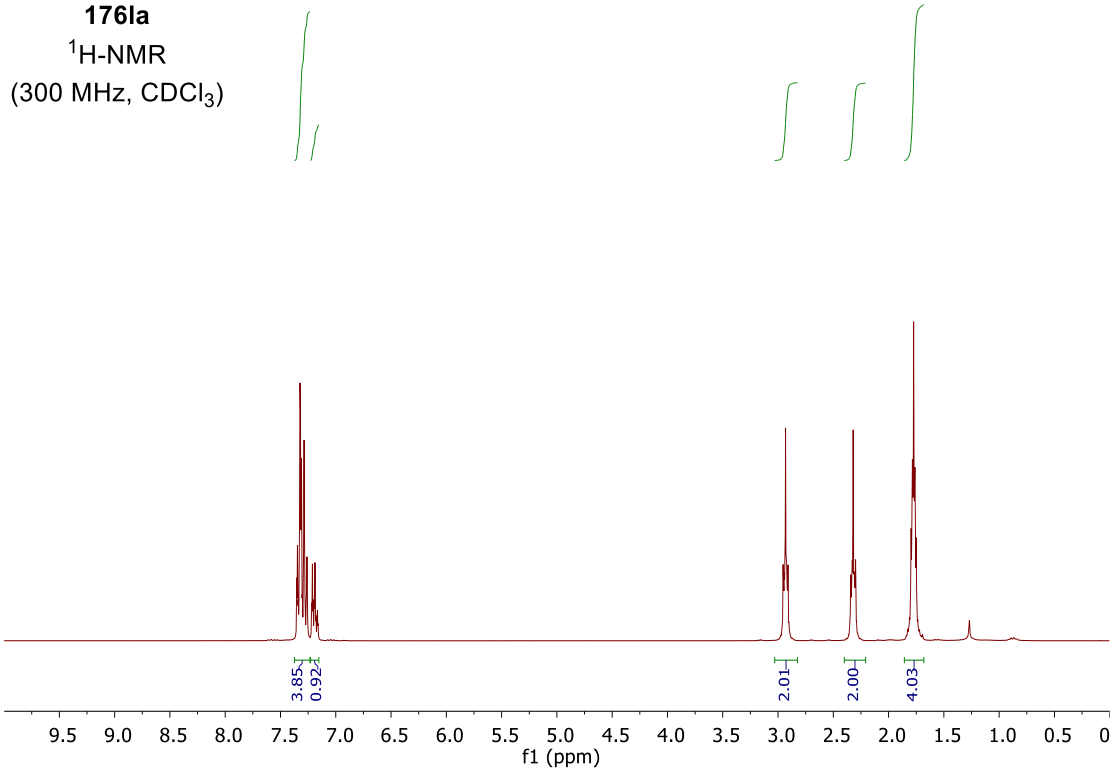

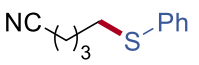

176la

^{13}C-NMR

(75 MHz, $CDCl_3$)

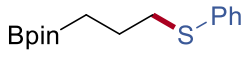

176ma

^{1}H-NMR

(300 MHz, $CDCl_3$)

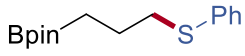

176ma

^{13}C-NMR

(75 MHz, $CDCl_3$)

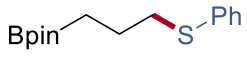

33.73

176ma

^{11}B-NMR

(96 MHz, $CDCl_3$)

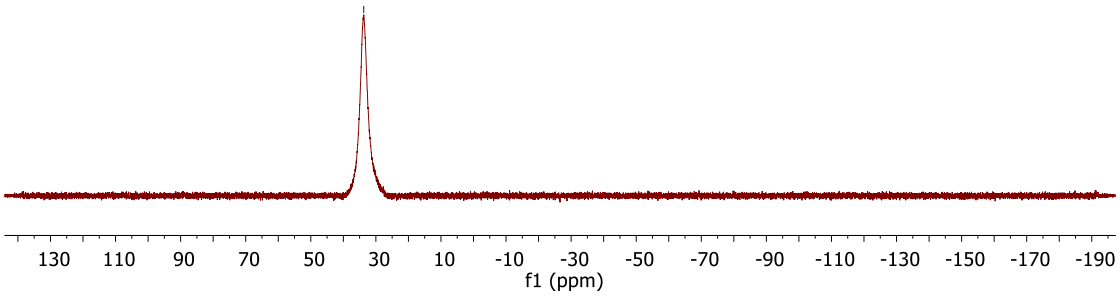

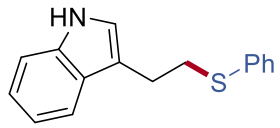

176na

^{1}H-NMR

(400 MHz, CD_2Cl_2)

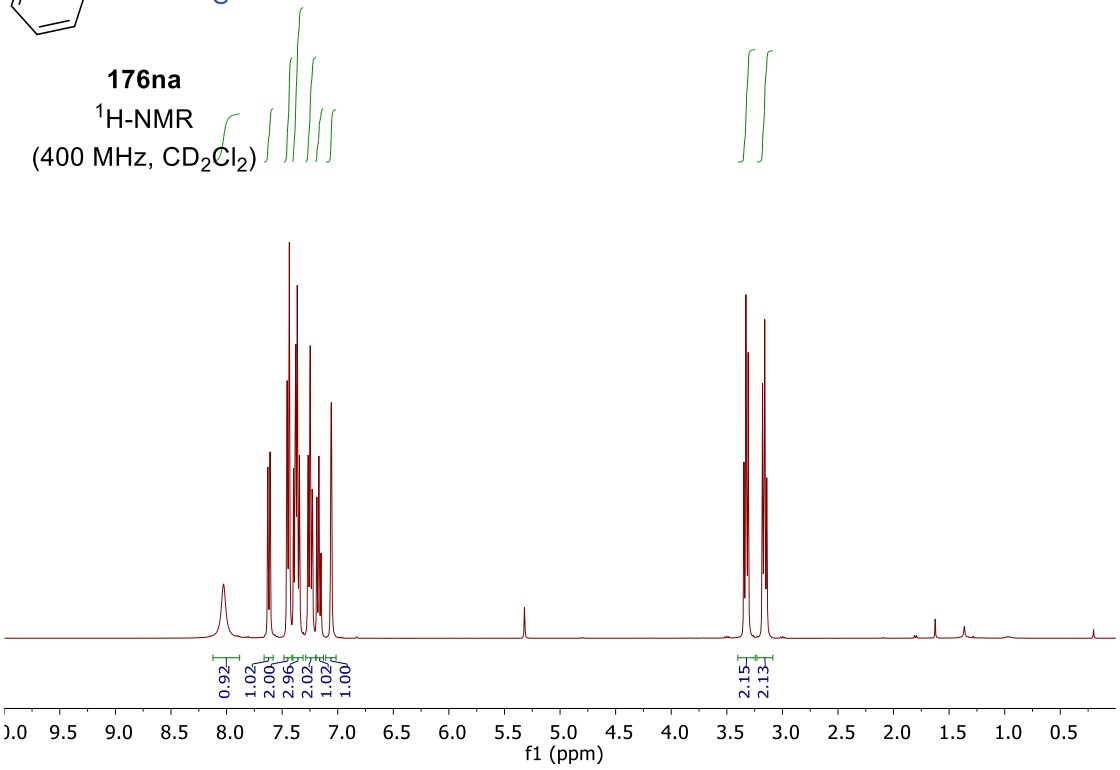

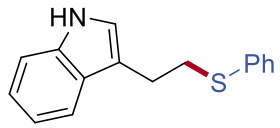

176na

^{13}C-NMR

(100 MHz, CD_2Cl_2)

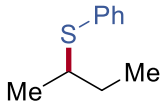

176oa

^{1}H-NMR

(400 MHz, $CDCl_3$)

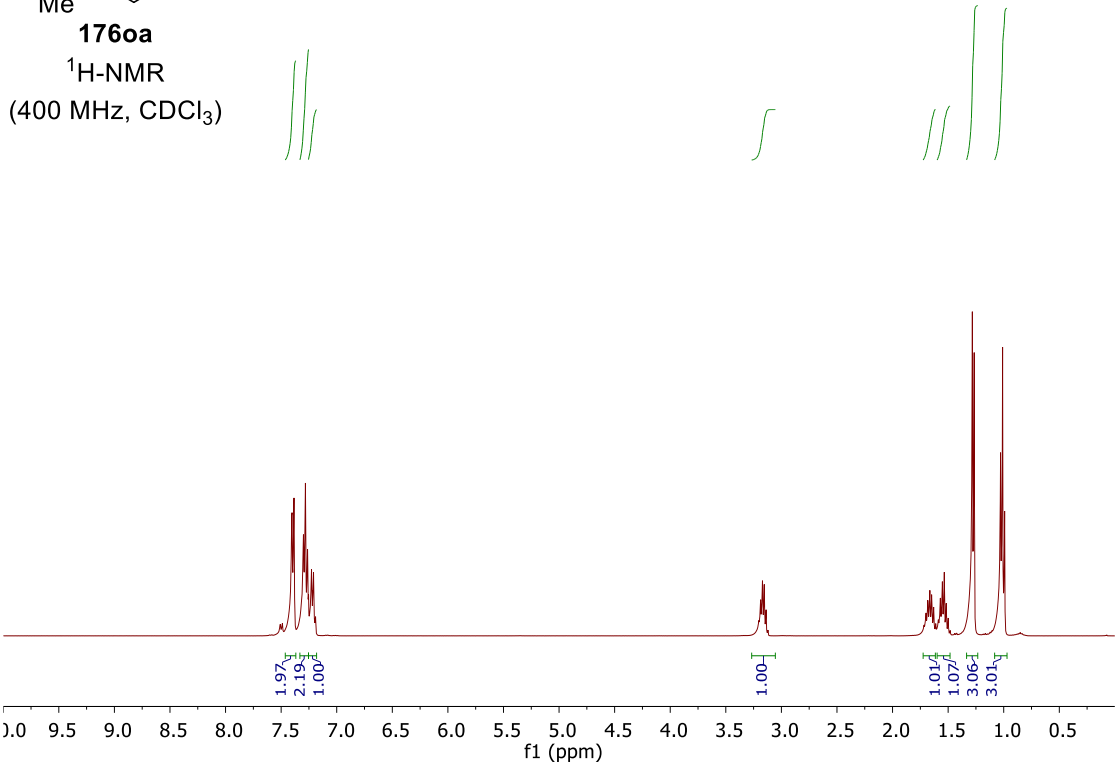

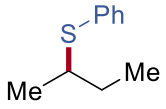

176oa

^{13}C-NMR

(100 MHz, $CDCl_3$)

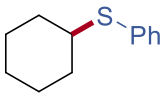

176pa

^{1}H-NMR

(400 MHz, $CDCl_3$)

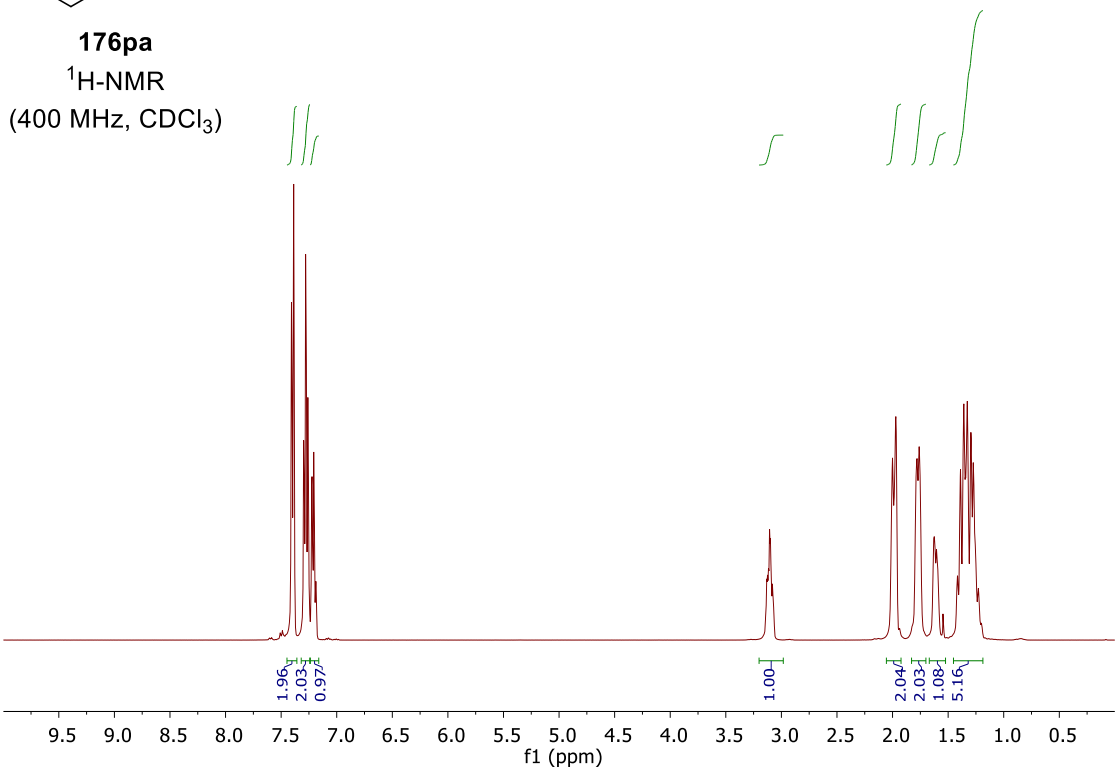

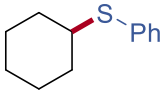

176pa

^{13}C-NMR

(100 MHz, $CDCl_3$)

Acknowledgement

It has been a very fruitful journey here in the Ackermann group which would have not been possible without the help of Prof. Dr. Lutz Ackermann. Hence, first and foremost, I would like to thank him for this opportunity and all the guidance that he has given me. It was definitely an empowering experience for one's knowledge in chemical research.

Second, I am thankful to my second supervisor Prof. Dr. Shoubik Das. His help and suggestions were indeed encouraging. I am also grateful to the other members of my thesis committee, Prof. Dr. Dr. h.c.mult. Lutz F. Tietze, Prof. Dr. Dietmar Stalke, Dr. Holm Frauendorf and Dr. Michael John.

Third, I would like to share my appreciation to a few of my co-workers whom I have either worked with or have had great discussions for ideas and thoughtful comments: Dr. Julian Koeller, Dr. Valentin Müller, Dr. João C. A. Oliveira, Dr. Cuiju Zhu, Dr. Youai Qiu, Dr. Mélanie Lorion, Dr. Fabio Pesciaioli, Dr. Thomas Müller, Dr. Ramesh C. Samanta, Dr. Shoukun Zhang, Dr. Torben Rogge, Dr. Lars H. Finger, Dr. Xuefeng Tan, Dr. Elżbieta Gońka, Dr. Joachim Loup, Dr. Nikolaos Kaplaneris, Dr. Tjark H. Meyer, Dr. Isaac Choi, Dr. Korkit Korvorapun, Leonardo Massignan, Alexej Scheremetjew, Agnese Zangarelli, Renato L. de Carvalho, Talita B. Gontijo and Anna Casnati.

Fourth, the thesis would not have been completed without the great help of many, namely: Dr. João C. A. Oliveira, Dr. Nikolaos Kaplaneris, Dr. Isaac Choi, Dr. Shoukun Zhang, Leonardo Massignan and Agnese Zangarelli.

Fifth, I am very much grateful to the permanent working staffs that have made the journey much smoother than it would have been; without their help, the working laboratory runs short of fuel: Gabriele Keil-Knepel, Stefan Beußhausen, Karsten Rauch and Bianca Spitalieri.

Sixth, I would like to give a toast to all the social events, abholung and the trip to Cuxhaven; they were often filled with fun and laughter. They made the PhD journey jaunty and lighter. As well as when season changes in Germany, I got to experience the different snippets of living here.

Seventh, to Oma Veronika Kramer and the Kramer family. I am indebted to all the support and help that all of you have given me before even stepping into Germany, as if I am one of your own. The entirety of this friendship transcended borders and cultures. On behalf of my family and myself, I dedicate this thesis and all the works in honour of that.

Last but not least, to the greatest mommy, daddy and sister. This voyage was made only plausible by you. I am very grateful for all the unconditional love, support and understanding that you have given me. I dedicate and share this achievement wholeheartedly to you.

"Reason is the slave of passion."

- Fyodor Dostoevsky